

ऋियं वै पृथ्वी भूतस्य प्रथमजा ।

This Earth, indeed, is the first-born among whatever exists.

- Shatpathbrahman, 14-1-2-10 -

शिला भूमिरश्मा पांसुः सा भूमिः संधृता धृता।
तस्यै हिरण्यवक्षसे पृथिव्या अकरं नमः ।।

Rock, stone, dust is this Earth; this Earth is held together firmly bound. To this golden-breasted Earth have I rendered obeisance.

- Atharvaveda, 12-1-26 -

DEDICATED TO

MY *"BAYKULEE"* - ARTEE

MY SON - SIMBA

MY PARENTS AND IN-LAWS

CHEMICAL STUDIES ON ORGANIC MATTER FROM PRECAMBRIAN ROCKS

by

SURESH N. KARKHANIS, B.Sc. (POONA), M.Sc.(BRISTOL), L.R.I.C., A.F.B.I.S., F.G.S., FELLOW OF THE ROYAL MICROSCOPICAL SOCIETY.

A Thesis Submitted for the Degree of
Doctor of Philosophy of the University of London

1976

Geology Dept.,
Imperial College,
LONDON,SW7 2BP,
England.

ABSTRACT

CHEMICAL STUDIES ON ORGANIC MATTER FROM PRECAMBRIAN ROCKS

As the title suggests this was not intended to be a study of a single area, but rather the chemical study of carbonaceous matter from four different sources of Precambrian sediments within the age group of 3.4×10^9 years to 2.0×10^9 years.

The areas under investigation were the Archaean Kromberg Formation of the Onverwacht Group of Swaziland and South Africa, the Kalgoorlie System, from Kalgoorlie, West Australia, and the Proterozoic Banded Iron Formations of the Hamersley Group, West Australia, and the South Alligator region of the Northern Territory, Australia.

The aim of the study was to gain a deeper understanding of the effects of incipient metamorphism on the carbonaceous matter in the rocks. As the study progressed, it was observed that in some samples, ordering of carbon, to the extent of graphitisation, has taken place, suggesting a high temperature thermal history. Graphite can be formed simply by heating carbonaceous matter to a high temperature under reducing conditions, or in the absence of oxygen. An estimate of temperature could not be obtained from the mineral assemblages in the rocks, and there is no geological evidence that these rocks have been subjected to very high temperatures. Some heating experiments were conducted under simulated geological conditions, to see if ordering of carbon can be achieved under comparatively low temperatures, possibly in the presence of the mineral assemblages found in Precambrian sediments.

The effect of metamorphism (heating) on carbonaceous matter is similar to the rank progression found in coals. As rank increases, the changes ultimately terminate in fully ordered crystalline graphite. This progression was studied by *X-ray diffraction*, and it was observed that low rank material has a very diffuse XRD pattern, and as the rank increases, the pattern alters towards graphite. Corresponding similar progressive increases were observed in crystallite sizes. At this stage, the *Electron Spin Resonance* (ESR) technique was introduced as a new approach to correlate the progressive changes. The results were encouraging and there exists a definite correlation between XRD data, crystallite size, ESR parameters, and H/C ratio.

Micropalaeontological investigations were also carried out using the *Scanning Electron Microscope* (SEM) on extracted carbonaceous matter and by examining thin sections in the light microscope, and some interesting observations were made. During the study of mineralogy of some carbonate rocks, *staining techniques* were used whereby ferroan carbonate was distinguished from normal carbonates. During this staining procedure, it was observed that some filaments were stained blue by potassium ferricyanide, which stains areas containing Fe^{2+} ions blue. These filaments were not otherwise visible during the optical microscope studies.

The filaments had been replaced by ferroan type calcite or dolomite, and therefore the external forms of fossil surfaces were preserved while the internal structures were destroyed. The fossils were preserved as moulds which could therefore be classified as an example of authigenic preservation. The filaments were attached to crystals of carbonates containing iron, and none were observed elsewhere in the rocks matrix, suggesting possible evidence for iron-precipitating microorganisms. The closely

morphologically resemble species of *Leptothrix* or *Sphaerotilus*. These results indicate the value of using staining techniques on carbonate rocks for obtaining micropalaeontological information.

ACKNOWLEDGEMENTS

There is a genuine feeling of inadequacy when I try to express my gratitude to someone who has been directing my research work during the last 2½ years. I would like to express my gratitude to Dr. Marjorie Muir for her encouragement and advice during the tenor of this work. As my supervisor, she has always made an effort to be available for consultation in spite of her frequent overseas commitments. Above all, she has shown me how to think independently, given a problem. This has been a major outcome and unique experience of this undertaking, which I undertook after a gap of 15 years. It has broadened the scope of my scientific capabilities.

I am further indebted to two other individuals, who are responsible in shaping up my future. It was Prof. Cyril Ponnamperuma of Laboratory of Chemical Evolution, University of Maryland, College Park, U.S.A., who urged me to begin my Ph.D. work at the Imperial College, London under Dr. M.D. Muir. In the light of my advanced age - I am in my early forties - his encouragement was particularly welcome. He used to say "It is never too late to acquire knowledge" and according to the Oriental Philosophy one should keep on doing his *"KARMA"*.

The other individual, to whom I am extremely grateful, is my wife Artee, who recognized, before I did, the valuable opportunity to broaden the scope of my career. She above all stood fast behind me through thick and thin by completely managing the family and financial obligations during my studentship. She has been a great source of encouragement through her frequent trans-Atlantic phone calls and to her I have dedicated this thesis.

There are many others also to whom I am indebted, particularly to Shabir Ali (Micro-palaentology) and my colleque Chris Peat, who spent considerable amount of their time in valuable discussion and made many useful suggestions relating to the work and organization of this thesis.

Many thanks to Prof.Janet Watson and Dr. G.P.L. Walker, F.R.S. for useful discussion in elucidating menerological aspects.

I am also grateful to my father - Dr. Karkhanis - who spent some of his time of his retirement and Bridge playing sessions deciphering my hieroglyphs and doing the rough typing of my draft manuscript.

I also thank Dr. Oduwolu and Dr. Sales of Inter Collegiate ESR Unit at Queen Mary College, London for the time and effort they took in trying to explain the author the ESR technique and its jargon.

I am also grateful to Dr. D.O. Hall of King's College, London for making available the samples from Kromberg formation, and to Mr. H.F. King, Mr. K.A. Plumb, Mr. J. Baldwin and Mr. B. McCrow and the Bureau of Mineral Resources, Canberra, without whose help none of the Australian smaples could have been collected.

Thanks are also due to Miss Mary Pugh of Geology, Royal School of Mines and Barry Foster of Mining Geology for donating the coal and mineral samples from their collections.

Many thanks are due to Ray Curtis, who made time available on X-ray diffraction unit in spite of his busy schedule, also to Bob Holloway for setting up P.T. experiments, to Paul Grant who showed the author how to twiddle the numerous knobs on the Stereo Scan Mark II A the X-ray micro-analyser and to a number of other members of the Geology Department, who

were always willing and available for assistance, and Mr. M. Rahman of Oil Technology Section, for carrying out C, H analysis on my samples.

I am also grateful to Dick Giddens for ably assisting me in his expert technical assistance in photography, which he managed to squeeze in between his "Cricket Talks".

I have also to thank Mr. Hunj, Ju-Jiang, Associate Professor, Department of Civil Engineering, Taiwan, University of Taipeh for assisting in translating Chinese literature written in Mandarin.

Lastly, I would like to thank Mrs. Ella Ng Chieng Hin of Cartography Room for her technical advice and Mrs. Carla L. Qamar-Luzac for typing the thesis.

TABLE OF CONTENTS

		Page No.
	Abstracts	i
	Acknowledgements	iv
	INTRODUCTION	*1 - 4*
CHAPTER - I		*5 - 21*
	INTRODUCTION	6
	Banding in Iron formation	7
	Chemistry of iron and silica	10
	Environments of deposition	11
CHAPTER - II	Materials and Methods	*22 - 80*
	A: GEOLOGICAL setting	
	a - Onverwacht Group	23
	b - Kalgoorlie	29
	c - South Alligator	32
	d - Hamersley	35
	B: Methods	
	Minerology	40
	X-ray diffraction (X.R.D.)	41
	Staining technique	41
	Chemical technique for separation of insoluble carbonaceous matter	51
	Carbon and Hydrogen Analysis	64
	Electron Spin resonance (ESR) technique	66
	X-ray microanalysis (X.R.M.)	78
	Crystallite size measurement (X.R.D.)	79

cont'd....

Page No.

CHAPTER - III — *81 - 91*

A: Metamorphism of Iron formation

1. Metamorphism of sulphide facies 82
2. " " oxide " 82
3. " " carbonate " 83
4. " " silicate " 84

B: Effect of metamorphism on carbonaceous matter 88

C: " " " " fossils 90

CHAPTER - IV — Micropaleontological Study — *92 - 119*

Previous Work

A. Swaziland sequence 94
B. Southern Cross. W. Australia 96
C. South Alligator 96
D. Hamersley. W. Australia 97

This Work

A. Kromberg formation 98
B. South Alligator 105
C. Hamersley region 108

X-ray microanalysis of fossil iron bacteria 118

CHAPTER - V — Discussion — *120 - 183*

A: Minerology

1. Kromberg formation 121
2. South Alligator 123
3. Hamersley 126

B: Insoluble carbonaceous matter

1. Kromberg formation 139
2. Kalgoorlie 141

cont'd....

Page No.

B. Insoluble carbonaceous matter (cont.)

3. South Alligator 141

4. Hamersley 142

C: ESR, chemical analysis and X-ray microanalysis 143

1. Kromberg formation 143

2. Kalgoorlie & Hamersley 149

3. South Alligator 150

D: 1. Artifacts during HCl/HF processing 151

D: 2. Synthesis of Abiogenic graphite 163

D: 3. Curtisite (Poly-aromatic hydrocarbon) 173

D: 4. Use of Carbonaceous matter as an metamorphic grade or palaeo-temperature 176

D: 5. Environment of deposition 180

Summary 184

Conclusion 186

APPENDIX *189-205*

Appendix I: Sample description 190

A. Onverwacht Group 190

B. Kalgoorlie 190

C. South Alligator 191

D. Hamersley 191

Appendix II:

A. Carbon isotopes studies by Infra-red spectroscopy 194

B. Possible use of Benzene Sulphonic Acid 202

cont.d.....

Page No.

Appendix III: List of publications 205

References *206 - 227*

INTRODUCTION

Sedimentary organic matter, although proportionately a very minor constituent of many rocks, is useful as an index of their degree of metamorphism. It has been known for several years that animal fossils occur in late Precambrian rocks (Glaessner, 1962, 1969) and micro-fossils, preserved as organic walled structures are known from rocks of many Precambrian formations (Tyler and Barghoorn, 1954; Barghoorn and Tyler, 1965; Barghoorn and Schopf, 1966; Schopf and Barghoorn, 1967; Schopf, 1968, 1970; Brooks and Muir, 1971; Brooks et al., 1973). Some authors have expressed doubts that the spheroidal and filamentous structures found in thin sections in the most ancient rocks are biogenic in origin (Engel et al., 1968; Nagy and Nagy, 1969; Schopf, 1975) and in many samples no structurally preserved organic matter (whether or not it represents the relict of early life) is preserved at all. Thus an alternative approach is required using organic geo-chemistry to try to identify in sedimentary organic matter the materials resulting from biological processes and their diagenetic and metamorphic alteration.

A literature survey shows that much work has been carried out on metamorphic rocks subjected to high temperatures and pressures. In contrast, little work has been done on sedimentary rocks subjected to mild metamorphism. According to Turner and Verhoogen (1960), "there must be a transition with increasing depth of burial between diagenesis and regional metamorphism". This transitional modification is referred to as incipient metamorphism.

Rocks subjected to incipient metamorphism have been neglected because they are difficult to study. This type of metamorphism leaves no minero-

logical imprints of specific nature and hence the recognition of degree of metamorphism becomes a formidable task. Sedimentary organic matter (carbonaceous matter) is of particular importance because it is a very sensitive indicator of incipient metamorphism. Thermal effects on organic matter are not reversible, will control the eventual fate of original organic substances and thus leave an imprint of thermal events on the rocks.

It is the purpose of this research to describe the effects of incipient metamorphism on carbonaceous matter by application of various chemical instrumental techniques, and to examine the highly altered organic matter for structurally preserved micro-fossils. The techniques used are evaluated and possible artefacts described.

The applications of organic metamorphism have been extensively studied by petroleum geologists in connection with oil and gas occurrence (Staplin, 1969), Bitterli (1963), Philippi (1957, 1965), Gutjahr (1966), Correia (1967) and Tissot et al. (1974). Recently Hood and Castano (1974) reviewed organic metamorphism and its application to studies of petroleum generation. Coals too, respond sensitively to changes in the environment, especially to temperature increases. (M. Teichmuller and R. Teichmuller (1966, 1968) and Kisch (1969, 1971). Coal and petroleum geologists have used various methods for characterization carbonaceous matter, such as chemical analysis for C-H-O composition, differential thermal analysis (D.T.A.), X-ray and electron diffraction, scanning electron microscopy, optical microscopy, vitrinite reflectance and occasionally electron spin resonance. Previously organic geo-chemical studies including C^{12}/C^{13} ratio, pyrolysis and ozonolysis have been carried out on rather few samples and in particular samples of Precambrian rocks.

Preliminary X-ray diffraction (X.R.D.) work on insoluble carbonaceous matter suggests a striking parallel between high grade carbonisation of coal and thermal effects on carbonaceous matter, which are characterized by means of studying the degree of ordering reflecting the crystallinity, which is a function of temperature. X-ray diffraction has been previously used to characterize carbonaceous matter by monitoring the (002) reflection of graphite French (1964), Landis (1971), McKirdy et al. (1975).

Methods of Study

In this work, X.R.D. was used to lay the foundation of this research. X.R.D. is a useful means of characterizing the degree of order in high carbon material (Ruland, 1968).

Electron spin resonance (E.S.R.) provides a measure of the number of odd electrons (spin density) present in the molecule. The odd (un-paired) electrons are produced when carbonaceous matter is heated, the peripheral -σ-(sigma) bonds are broken and there is an increase in the number of odd electrons. The possibility of using ESR was investigated on the basis of this theoretical property.

ESR had previously been used by Pusey (1973) to determine palaeo-temperatures of sediments. The number of free electrons has been related to palaeo-temperatures of coal Binder (1965), and to vitrinite reflectance values of coals affected by intrusion of sills (Crelling and Dutcher, 1968).

Microscopic observations (optical and scanning electron microscope (SEM) were also made in the investigation. Petrographic thin sections were studied to identify mineral assemblages and to evaluate the effect of carbonisation on the fossils. Parallel studies using the SEM were under-taken to investigate micro-palaentology.

The samples investigated were from the Archaean Kromberg Formation of the Onverwacht Group of the Barberton Mountain Land of South Africa, the Kalgoorlie System from Kalgoorlie, West Australia and the Proterozoic Banded Iron Formations of the Hamersley Group, West Australia and the South Alligator Region of the Northern Territory, Australia.

A total of 62 samples were investigated and they fell basically into the following sediments types, Cherts, Shales, Pyritic shales, Carbonaceous shales and Carbonate rocks. They ranged in age from 3.4×10^9 years to 2.0×10^9 years.

CHAPTER I

CHAPTER I

INTRODUCTION

The nomenclature of banded ferruginous cherty sedimentary rocks is very imprecise. For example, in the papers presented at the International Symposium on the Geology and Genesis of Precambrian Fe-Mn Formations and Ore Deposits held in Kiev, U.S.S.R. in 1970, the following terms were used by man contributors, which reflect the continuing controversy on the origin and hence generic aspects of ferrugineous rocks (Brendt, et al, 1972).

(i) Taconite: The term originated in the U.S. and followed by the U.S.S.R.

(ii) Itabirite: is a Brazilian term widely used in S. America and West Africa for oxide facies iron formation that has been metamorphosed to a degree that makes individual crystals of the rock megascopically distinguishable.

(iii) Jaspilite: is used in the U.S.S.R. for rock with iron present as hematite, magnetite, or martite and silica as "fine grained quartz-jasper or hornfels".

(iv) Ferruginous quartzite: is used in the Western World for rocks mainly detrital in origin. The rock may have the same chemical composition as iron formation, but the iron minerals could be clastic in origin.

(v) Iron Hornfels: Hornfels is the term used in the West for a 'fine grained' non-schistose metamorphic rock resulting from contact metamorphism. In the U.S.S.R. hornfels is used for fine grained rocks containing silicate and oxide facies of iron formation.

It may not have any relation to contact metamorphism but may have relation to regional and dynamic metamorphism. Iron hornfels in the U.S.S.R. is a coarse banded iron silicate-chert rock with fine grained quartz.

(vi) Banded hematite quartzite: is widely used in India and to some extent in Australia and represents oxide facies iron formation.

(vii) Iron Ore: This is a loosely used term in literature with economic implications.

However, James (1954) defined iron formation as follows: a chemical sediment, typically thin folded or laminated, containing 15% or more of sedimentary origin, commonly but not necessarily containing layers of chert. This definition is broad enough to encompass all the varieties of iron formation which have been mentioned above. As pointed out above, the various nomenclatures reflect the continuing controversy on the origin. The origin of iron formation is a controversial topic in itself and there are numerous hypotheses put forward e.g. magnatic, volcanic and even cosmic process. (See Alexandrov, 1973). However, significant numbers of research workers accept the origin of iron formation as chemical sedimentation. This origin accounts for the geo-chemical, minerological and sedimentological aspects. All these world wide formations were deposited between 3,800-1,500 million years ago (Goldich, 1973).

Banding in Iron Formation

Various explanations have been proposed for banding of different layers, and below is a brief review of different hypotheses:-

(i) Resulting from the leaching of iron oxides and silica at different pH ranges and in the presence of certain elements in solution, the banding of Si and Fe minerals was caused principally by selective weathering of the soil in different seasons: seasonal changes of temperature, caused the solutions transported to the basin of deposition to be composed almost exclusively of silica during warm seasons and chiefly iron oxide during cool periods of the year. (Alexandrov, 1955).

(ii) James (1954) postulated for his environment a restricted basin, which was separated from the open sea by thresholds that inhibited free circulation and permitted developments of abnormalities in oxygen potential and water composition could account for banded nature and he recognized oxide, carbonate, silicate and sulphide facies of iron formation, which, he thinks, reflect certain aspects of depositional environment and considers oxidation potential probably as major controlling factor.

(iii) Moore & Maynard (1929) indicated from their laboratory experiments that banding of iron-silica deposits could be due to differential rate of precipitation of iron and silica combined with seasonal changes causing varying quantities of the two materials to be brought into the basin of deposition at different periods throughout the year.

(iv) Oftedahl (1958) states that "the sharp & rhythemic banding which is frequent in iron formations may be due to periodic earthquakes governed bursts of iron bearing gases and the quiet giving of silicon bearing gases or hydro-thermal solutions in between".

(v) Woolnough (1941) explained banding as the result of pulsation in the amounts of silica and iron delivered to the basin.

(vi) Sakamoto (1950) postulated the mechanism of precipitation of iron and silica due to weathering under monsoonlike climatic conditions and periodic delivery of the iron and silica to basins which were wide but shallow and separated from the open sea by low barriers. He supposed that the iron was delivered to the basin by surface runoff during the wet season when the basin water was cool, acidic and oxidizing, and silica was delivered by the ground water to the basin during the dry season when the basin environment was warm, alkaline and less oxidizing. Briefly iron was precipitated during the dry season when the environment was less oxidizing and silica during the wet season.

(vii) On the basis of Eh, pH studies Krumbein & Garrels (1952) concluded that hematite is deposited at the oxidation-reduction-potential and pH values above a boundary which extend from an Eh of +0.16 and pH of 6 to a point at Eh -0.22 and pH of 9, that siderite is deposited below this boundary, but above a boundary from Eh -0.11 and pH of 6 to a point at Eh -0.31 and pH of 9; below this boundary pyrite is deposited. They concluded that the amount of a particular mineral that will precipitate will depend upon change in Eh and pH of the environment. They extended this work to the presence of calcium and concluded that calcite would deposit at pH greater than 7.8 through the entire range of Eh values. This led them to limit the field of deposition of iron-rich sediments to a pH range below 7.8.

(viii) Tyler & Twenfofel (1952) pointed out that sediments collecting in present dry lakes generally lack stratification, which they attributed to the activity of mud dwelling and mud eating organisms. The presence of lamination, they suggested, could be due to the absence of such organisms at that time.

(ix) Cloud (1973) suggested that episodicity of iron-rich bands may be due to cyclic changes in procaryotic population or rates of supply of ferrous iron or both.

Chemistry of Iron and Silica

Briefly in this section chemistry of Fe and Si in natural aqueous system will be discussed. The following section will show how these chemical properties of Fe & Si are incorporated in different models of disposition. A universal hypothesis for the source of iron and silica for BIF cannot be given. According to the literature survey various workers suggest either volcanic and/or weathering processes.

Most of the iron present in the marine environment where the pH is between 7.5 to 8.4, is in a particulate form both as ferrous and ferric. The total iron is generally in the range of 0.01-0.025 mg/l. (Cooper, 1935). Iron in ferric form is highly insoluble and in ferrous form it is highly soluble. Variation in redox potential and pH play an important role in forming various iron minerals found in BIF (Garrels and Christ, 1965). Cooper (1937) has shown that under reducing conditions at pH of 6 iron is 100,000 times more soluble than it is under oxidizing condition at a pH 8.5. This assures the marine environment of some concentration of iron.

Following the work of Krauskopf (1959) the chemistry of silica has been laid on a firm foundation. Silica concentration in sea water is in the range of 0.1-4 ppm in surface layers, but 5-10 ppm in the bottom layers. It is present in true solution as H_4SiO_4 and not colloidal silica.

The effect of pH on silicic acid or colloidal silica is that it usually gels more rapidly in the rage of pH 5 to 7 (Iller, 1955). Correns (1959) work suggests that solubility of silica decreases slowly with decrease in pH from 11 to 6.5 and it further decreases rapidly in the range of 6.5 to 4.5.

In modern times, precipitation of silica is brought about by silica secreting organisms like diatoms, radiolaria etc. But the organisms are thought not to be found in Precambrian times. So an alternative hypothesis for inorganic origin has to be sought. It is thought that to account for deposition of silica the seasonal changes in the environment played an important role. During Precambrian time possibly there was super saturation of silica due to leaching from the surrounding land and it remained persistently polymerized and precipitated as a consequence of near neutral to slightly alkaline pH of about 6.8-7.5 (Cloud, 1973). And the layers of iron were deposited during cold seasons overturn accounting for cyclic sedimentation.

Environment of Deposition

This section is an attempt to review the various models of the environments of deposition. No efforts will be taken to discuss the merits of any particular model. The discussion will be around the effect of Fe and Si precipitation. There is no shortage of proposed depositional models in the

literature. But none of the models individually have managed to satisfy successfully all the chemical, minerological, depositional diagnostic and/or physico-chemical constraints.

(1) Marine environment: James (1954) suggested deposition of iron formation took place in a restricted marine environment. This specific environment where basins were separated from the open sea by thresholds that restricted free circulation and permitted development of abnormalities in oxygen potential and water composition. These two conditions were suitable for iron deposits, but do not explain how banding originated.

According to Krumbein and Garrels (1952), the pH of the normal marine environment ranges from 8.4 at the top to 7.5 at the bottom; corresponding Eh ranges from +0.4 at the surface to +0.1 at the bottom. In a typical marine environment, there is an open circulation, the water is mildly alkaline and oxidizing throughout while in a restricted environment, the surface waters are alkaline and oxidizing but bottom waters may be reducing and acidic in reaction. They worked out the stability fields of pyrite-siderite-hematite which is reproduced in Figure (I)-1. The diagram shows that the form in which iron is precipitated is most strongly dependent upon oxidation reduction potential, Eh. This accounts for the different facies present in B.I.F. The major argument against this model is the virtual absence of calcium carbonate precipitates and abundance of ferrous carbonate. However, this is possible on theoretical grounds (using Krumbein and Garrels (1952) data). At pH 8.0 and Eh of about +0.2, the activity of Fe^{2+} and Fe^{3+} ions is about $10^{-10.5}$. The ferric hydroxide is the stable precipitate. In a restricted basin where the environment is more acidic and less oxygenated the pH would be 7.5 and Eh of -0.1 at which the activity of Fe^{+2} and

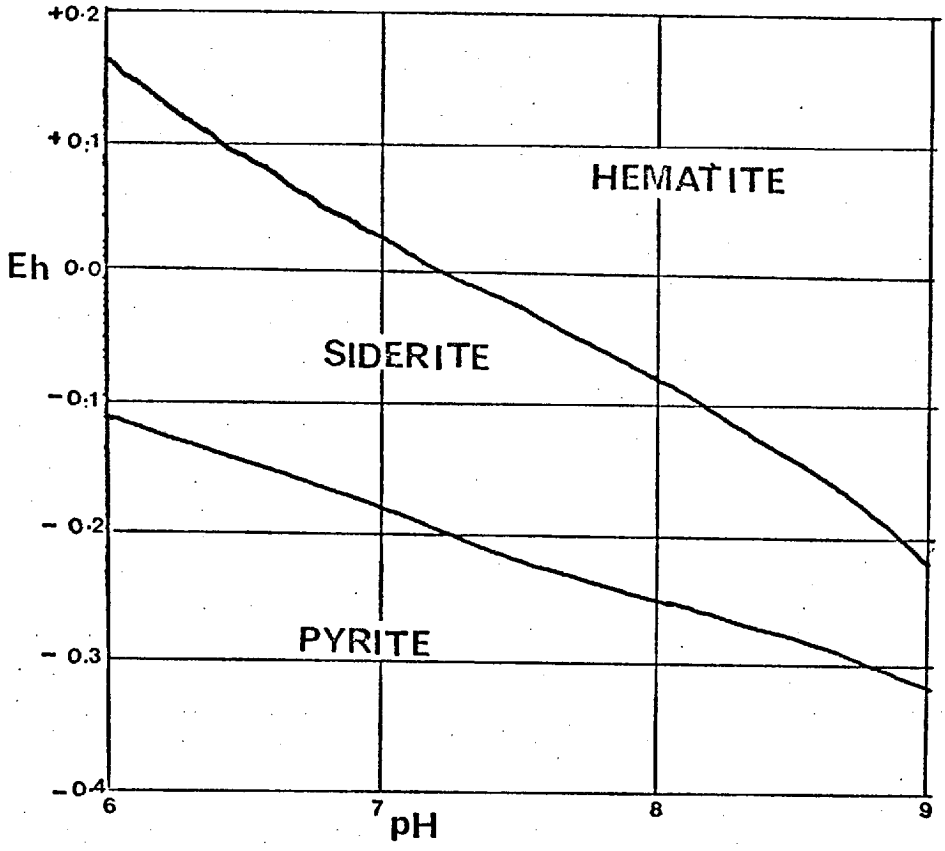


Figure-I-1 Stability fields of pyrite-siderite-hematite(After Krumbein and Garrels, 1952)The diagram emphasis the effect of oxidation-reduction potential, Eh on the precipitation of iron.

Fe^{+3} ions is about $10^{-4.7}$. And the stable iron mineral at these conditions is $FeCO_3$ (siderite).

The solution and precipitation of silica in sedimentary environments is not well understood. In the absence of suitable silica secreting organisms in the Precambrian basins, it is desirable to investigate the possibility of inorganic precipitation of silica. Iller (1955) showed that at the conditions which promote the gelling of silica, the silica can polymerize to form precipitates, and he reported that solutions of silicic acid (H_4SiO_4) or colloidal silica usually gel most rapidly within the range of pH 5 to 7. However, Krauskopf's (1956) own conclusion was that the solubility of amorphous silica is little affected by changes in pH in range 0-9 but increasingly rapidly as the pH rises to about 9.

To summarize, the effect of redox potential has a significant effect on the solubility and stability of iron minerals. The other factors that affect this are the pH of water and partial pressure of oxygen. It is interesting to note that modern marine environments, however, show no signs of iron concentrations comparable to that which would be necessary for the deposition of Precambrian iron formations.

(2) Freshwater environment of deposition: This is typical of the middle "Huronian" rocks of Lake Superior District. The region is assumed to be geomorphologically very mature. The climate varied from sub-tropical to warm temperate with moderate to high rain-fall. Variation in weather (colder and warmer) produced the alternate deposition, through weathering of iron and silica. The environment of deposition was a large and deep fresh water lake with relatively low organic activity. The lower water layer has

slightly reducing and acid conditions particularly in summer. This kept iron in solution in a reduced state. This condition was conducive to the deposition of silica. During the winter, the water environment was oxidizing and alkaline facilitating precipitation of a iron. The model satisfies the Eh and pH requirements for the stability fields of iron minerals. It may be said that several variations of the fresh water environments can satisfy this model.

(3) Lacustrine or closed basin environment: This is basically an extension of the fresh water environment of deposition proposed by Hough (1958). The most important feature of lakes is that thermal stratification which is due to variation in density of water with temperature. (Max. density at $4^{o}C$). The surface water, or epilimnion becomes warmed in spring and early summer and will overlie cooler and deeper water - the hypolimnion. The stratification is stable during the summer, but with the change in weather the whole column assumes a uniform temperature. The surface of the lake is in equilibrium with the atmosphere but the lower level (hypolimnion) is oxygen deficient. In this region there is a marked decrease in Eh during the period of stagnation. The upper layer (epilimnion) has suspended $Fe(OH)_3$, which will be reduced in the lower layer and go into solution and sink in the lower layer.

Silica is present in the lake waters as undissociated silicic acid. According to Krauskopf (1959), the silica content of rivers and ground water is less than 35 ppm SiO_2. The silica content increases in the hypolimnion during the period of stagnation. This is borne out by Tanaka's data (1953), which show that Si accumulated from 10 mg/l to 42.4 mg/l at a depth of 50 meters during the period of stagnation.

(4) Playa-lake complex depositional environment: This model proposed by Eugster (1973) can also be adapted to a marine environment after assuming that sea water is saturated with respect to amorphous silica. The environment for deposition is considered to be a barred or partially barred lagoon in arid climate. This model is based on the existence of a perennial lake occupying the centre of a broad basin. It could be over-flowing or closed. Climatic changes affect the lake level. On evaporation solids are precipitated (calcite). Carbonate muds may be washed into the central lake by seasonal storms. Magadiite or sodium silicate gels are considered the probable precursors for chert. Whenever oxygen is low, the iron is transported in solution. Whenever oxidizing conditions are available, Fe(ic) hydroxide is precipitated. The pH changes in the lake water would bring about precipitation of ferrous hydroxide, iron silicate and sodium iron silicate gels. These are considered possible precursors of hematite, magnetite, greenalite, stilpnomalene and riebeckite (Eugster and Ming Chow, 1973). They applied this model to the Green River formation, and extended this model to a marine lagoon model or to a normally barred lagoon with wide supratidal flats under the influence of continental waters. The basic assumption here would have to be that Precambrian sea-waters have to be near saturated with respect to amorphous silica.

(5) Laterite Weathering Model: This model is proposed by Lepp and Goldich (1964) to show the origin of Precambrian banded iron formation through chemical differentiation under an unoxygenated atmosphere. This sort of weathering is similar to lateritic weathering. Laterite profiles are highly permeable and resistent to erosion. Al, Ti and Fe(ic) ions are retained in the regolith but Fe(ous) iron, Ca, Mg and alkali metals are transported to the sea. They postulated that silica was largely deposited by replacement of primary carbonates.

(6) Hot Spring Analog: On the basis of similarities between stromatolites in the Yellowstone National Park and Gunflint stromatolites and comparison between silicification of the microbiota from Yellowstone with the Gunflint microflora, which according to Schopf (1970) has been rapidly encased in silica, Walter (1972) suggested a hot spring analog for the depositional environment.

(7) In trying to correlate the major geological episodes with the biological generation of O_2 and ferrous iron, Cloud (1972, 1973) suggested that during limited time extensive deposits of hematitic and magnetitic B.I.F. were deposited as follows:-

$$4\ FeO + \text{biol. } O_2 \text{ ..... } 2\ Fe_2O_3 \qquad (I)\text{-}1$$

$$Fe_2O_3 + C \text{ ..... } 4\ Fe_3O_4 + CO_2 \quad (I)\text{-}2 \quad \text{Perry et al, 1973.}$$

This accounts for the prevalence of magnetite and the variety of carbon in unaltered BIF. Iron oxidizing bacteria could also help to maintain low oxygen levels deriving energy from the oxidation of ferrous to ferric state. In the absence of silica secreting organisms a biological source of Si is ruled out and the hydroshere may have been saturated with monosilicic acid (H_4SiO_4).

According to Krauskopf (1956) the polymerization and precipitation of monosilicic acid to form SiO_2 is favoured with decreasing acidity of solutions to a neutral or slightly alkaline state. This will proceed at pH 6.8 to 7.5 while any carbonate compound will remain in solution as HCO_3^- ions and ferric oxide will be added intermittently. This episodicity of iron rich bands suggests cyclic changes in the procaryotic population or a rate of supply of ferrous iron or both.

(8) Volcanism and Geosynclinal Development: This was developed by Van Hise and Leith (1911) who state "The iron solution may have been transferred from igneous rocks to the sedimentary iron formation partly by weathering when the igneous rocks were hot or cold, but the evidence suggests that they were transferred partly by direct contribution of magmatic water from the igneous rocks or perhaps in small part by direct reaction of the sea waters upon the hot lavas.

However, there is much evidence opposing the theory of volcanism. In many parts of the world notably South Africa and South America, volcanism is lacking during the period of iron formation. In the case of the Huronian geosyncline the deposition of iron formation and volcanism coincide but according to the evidence outlined by James (1954) this relationship is purely accidental and structural, not chemical and by no means a necessary factor for precipitation of iron rich bands.

All these models mentioned above are equivocal in themselves. It seems, that modification to particular models has kept pace with parallel development in the research in other fields such as physical chemistry (Stability Constants, Equilibrium Constants, etc.). Every model contains valuable suggestions but none have yet successfully integrated chemical, minerological, depositional, and diagenetic constraints (Eugster, 1973).

The Playa-lake model suggested above is quite versatile as it incorporates all the latest physico-chemical data such as stability constants, equilibrium constants, Gibbs Free Energy values etc. and with little modification it could be adopted for marine lagoon models or barred lagoon models for continental waters. Also with numerous occurrences of evidences of life in the Precambrian, the model suggested by Cloud is worth consideration.

FIGURE: 2 Various depositional models are shown in Figure 2 a,b,c,d for comparision .They reflect a parallel development of collection of physico-chemical data.

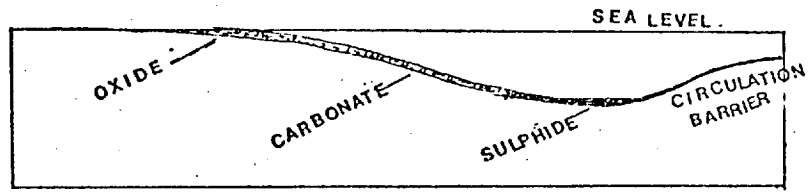


Figure-I-2a : Depositional zones in a hypothetical restricted deep basin in which iron compounds are being precipitated (after James, 1954).

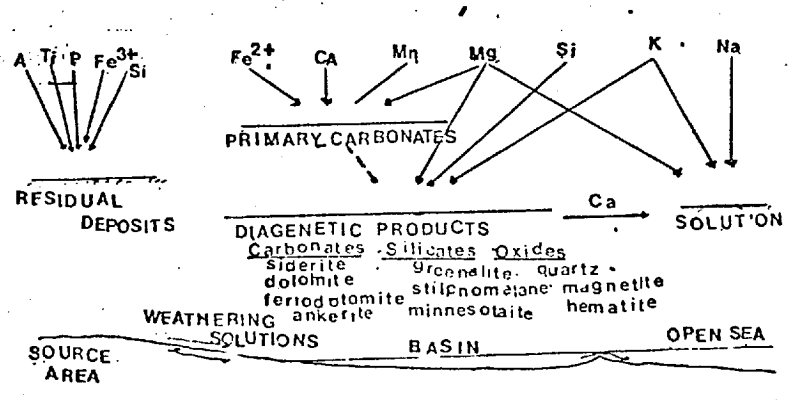
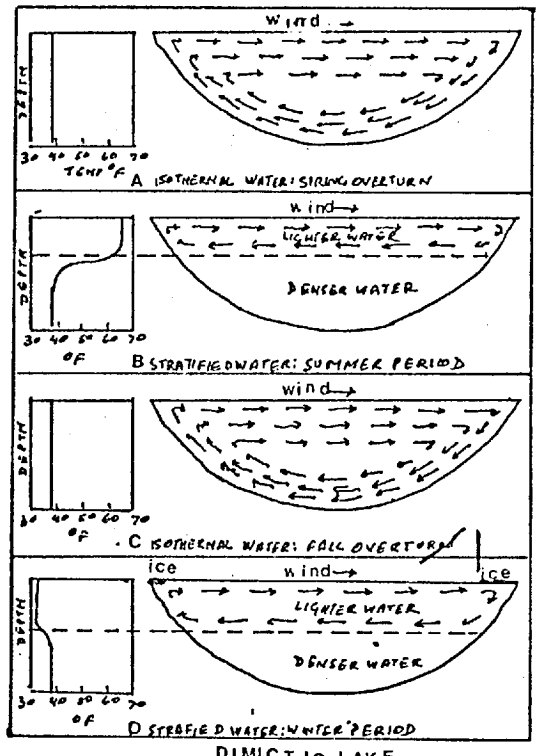


Figure-I-2b : Lateritic weathering model showing chemical differentiation to produce Precambrian Iron formation under an atmosphere lacking free Oxygen.Under these conditions the Eh-sensitive elements, Fe and Mn accompany Si.(after Lepp and Goldich).



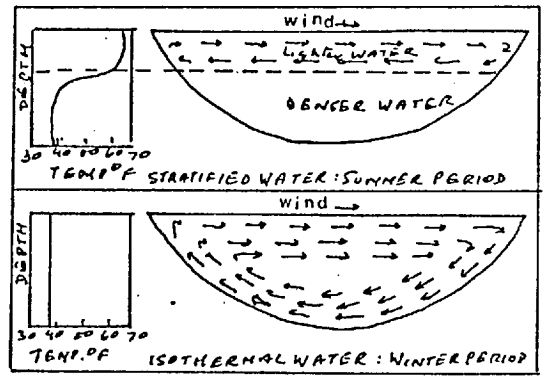


Figure-I-2c

Left hand figures: The annual temperature cycle in dimictic lake of temperate zone.

Right hand figures: The annual temperature cycle in monomictic lake of sub-tropical or warm temperature zones (after Hough, 1958).

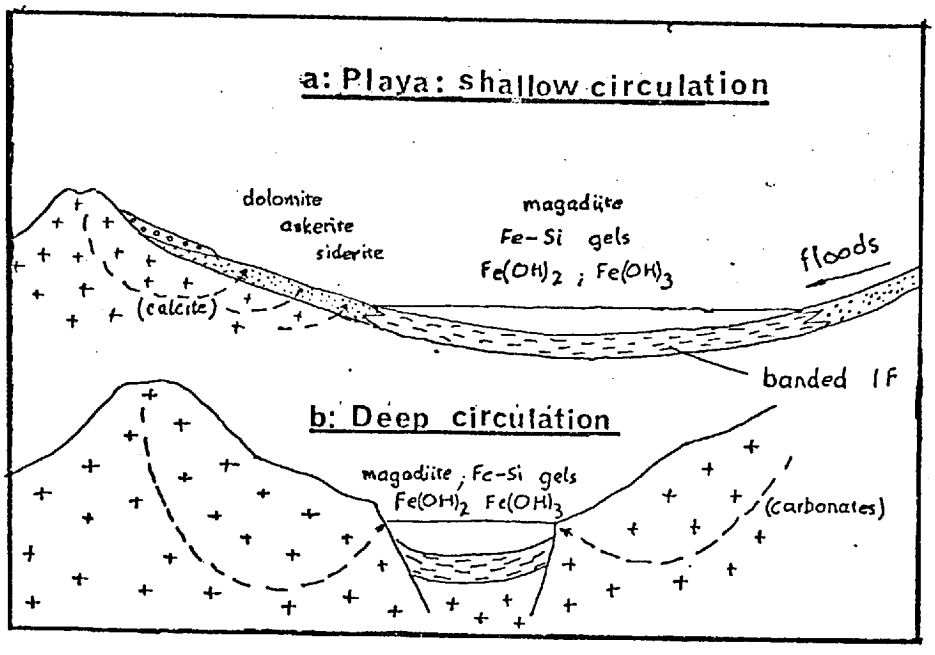


Figure-I-2d : Playa-lake model for banded iron formation.
(after Eugster and Ming-chou, 1973)

a) Shallow circulation with playa fringes.
b) Deep circulation (no playa fringes).

However, the most obvious conclusion is that Precambrian iron formations are diversified in origin and may not fit a single depositional model.

Various models are shown in Fig. (I) 2 a-d for comparison. Comparison of these models reflect parallel development in the collection of physico-chemical data. As soon as such a data is made available the previous model is modified. Even at this stage no single model could fit the depositional model.

CHAPTER II

CHAPTER II

MATERIAL AND METHODS

In this chapter, original techniques are briefly described and the observations and data obtained by earlier published techniques are tabulated, and as far as possible grouped together, according to geographic locality. Interpretations will be discussed in a later chapter and occasionally will be based on an interplay of various techniques.

The samples were collected from the Hamersley basin and Yilgarn Block, W. Australia, Barberton Mountain land, South Africa and the South Alligator River, Northern Territory, Australia. A brief summary of the geological setting, lithology and the age of the rocks will be given here for each area.

The data and other pertinent information on individual samples is listed in Appendix I.

A. Geological Setting:-

a. ONVERWACHT GROUP, SWAZILAND SUPERGROUP:

The rocks of Barberton greenstone belt are collectively referred to as the Swaziland Supergroup (Fig. (II) - 1a).

The lower volcanic succession has been termed as the Onverwacht Group while the overlying sedimentary assemblages have been referred to as the Fig Tree Group and the Moodies Group (Fig. (II)-1b).

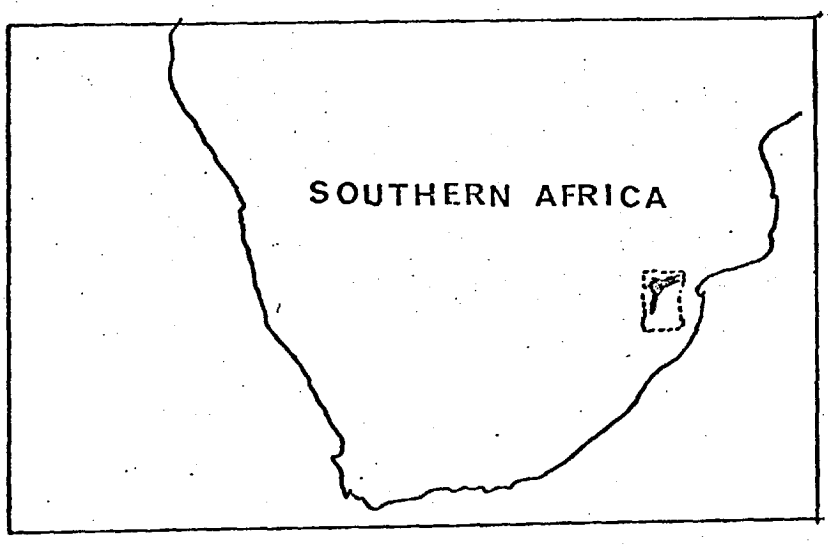


Figure-II-Ia-Locality Map for
Swaziland Sequence

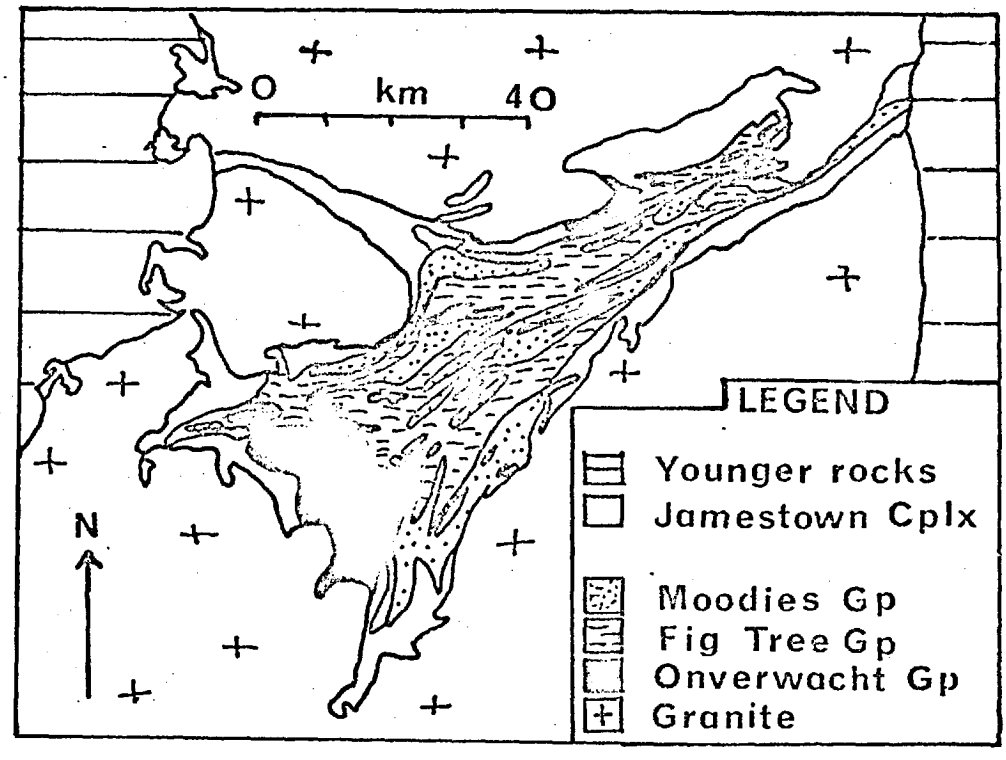


Figure--II--1b

Important rock formations of the Barberton Mountain Land of the Eastern Transvaal.

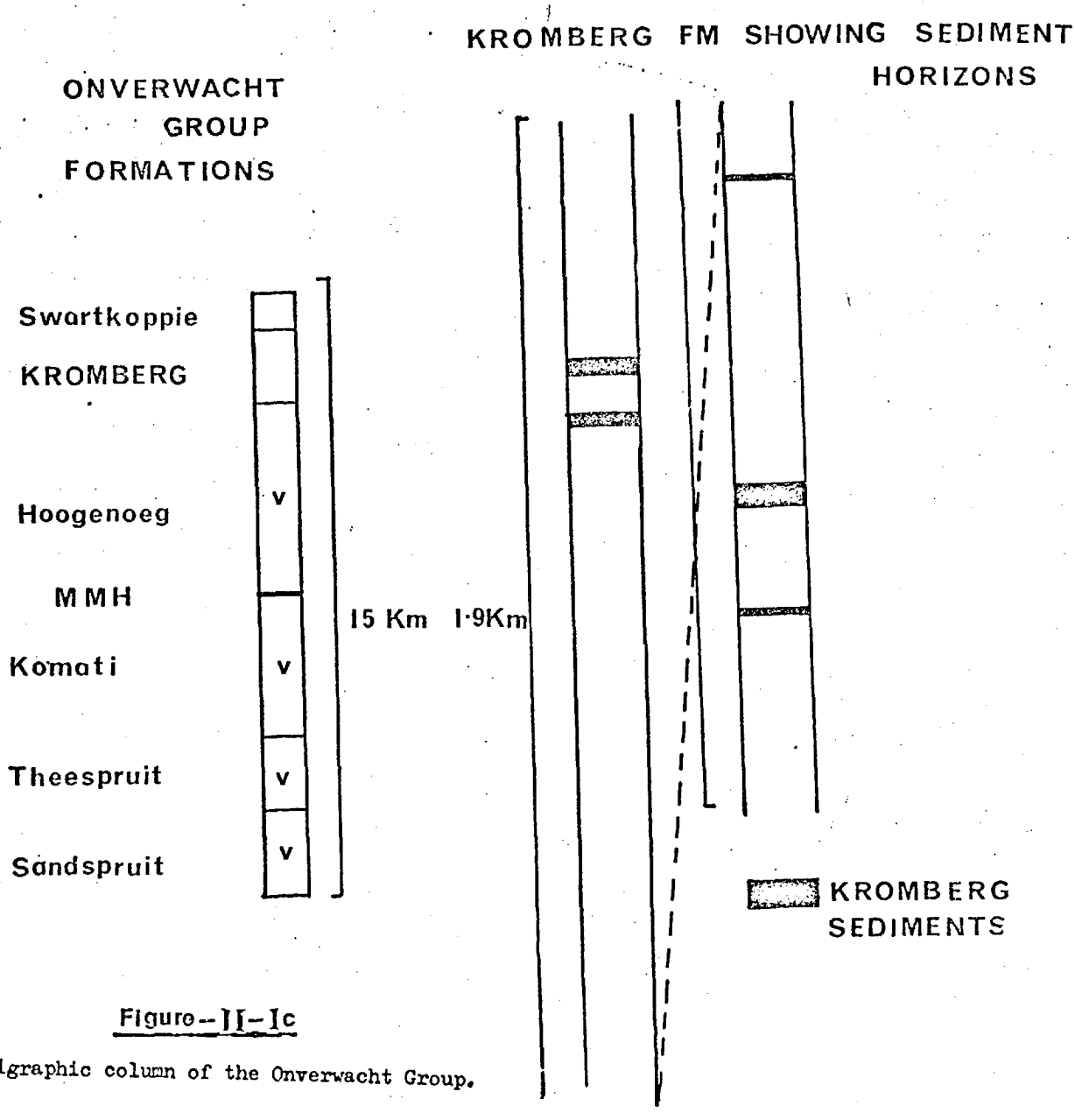


Figure-II-1c

Stratigraphic column of the Onverwacht Group.

The Onverwacht Group which is the oldest of the strata, is approximately 10,665 m. The Fig Tree series has a thickness of approximately 15,235 m that mainly dip in a vertical direction and have been folded about a number of major axis.

The lower formations of the Onverwacht Group are Sandspruit, Theespruit and Komati Formations and they are about 2,124 m, 1,889 m and 3,504 m thick respectively. The Sandspruit is the lowest formation and may lie on granite basement.

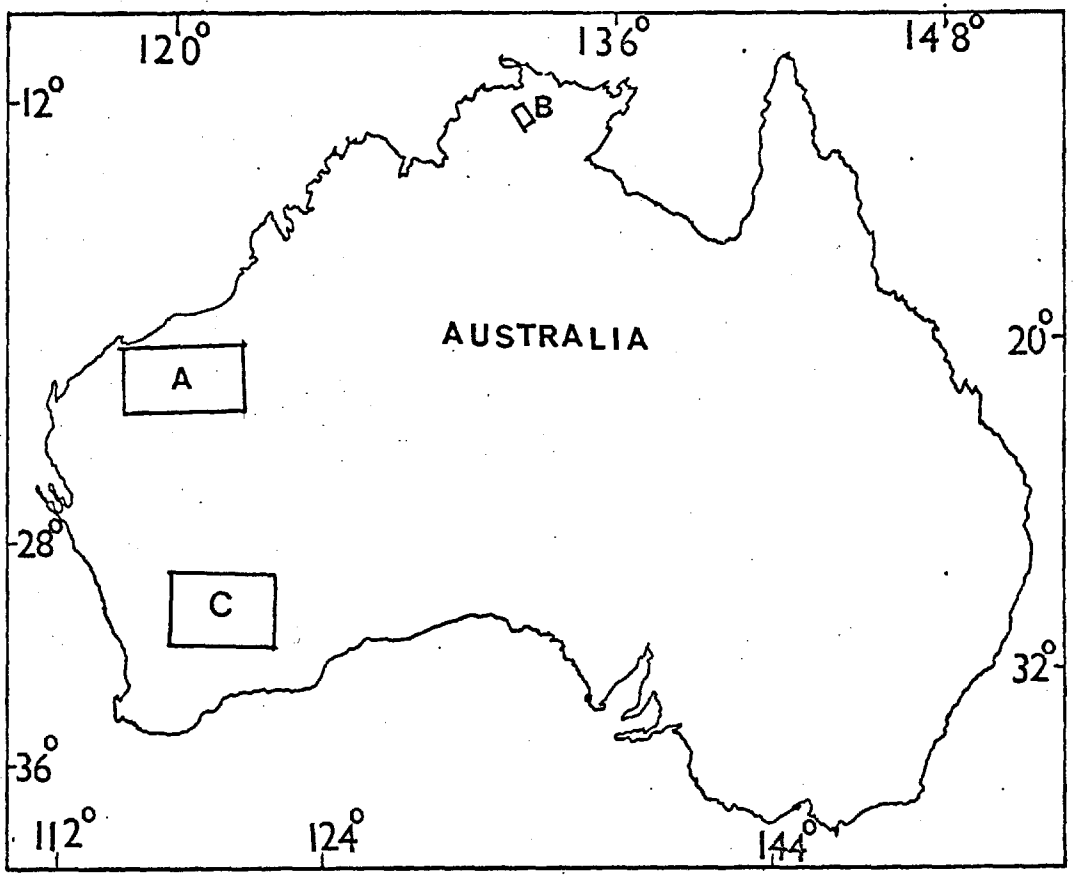
The three upper formations are confined to the Southern and Central portions of the Barberton belt and are known as, from the base to the top the Hooggenoeg, Kromberg and Swartkoppie Formations. They have the thickness of about 4,845 m, 1,920 m and 9,141 m respectively (Fig.(II)-1C). The Middle Marker Bed is situated just below Hooggenoeg Formation and shows a concordant Rb-Sr age of 3.35×10^9 years (Hurley, 1972).

The samples were collected from Kromberg formation along the Komati River adjacent to J.C.I. Camp (See Appendix I for details).

The Onverwacht succession consists of both acid and basic rock types. The acid assemblage is considered entirely extrusive and consists of quartz and felspar porphyries while the basic assemblages are described as being composed mainly of massive fine-grained andesitic lavas in which flow layers and amygdales are visible (Viljoen and Viljoen, 1969).

Massive tholeiitic lavas are the main rock type encountered with Kromberg Formation from which most of my samples are taken. Well-developed pillow structures are particularly well-exposed in the vicinity of the Komati River in the Komati Gorge.

Figure--II-2a Locality Map



A - Hamersley Group

B - South Alligator River Valley

C - Kalgoorlie

The other rock types in the Kromberg Formation are mafic pyroclasts comprising mainly of ash and tuff zones and agglomerates. A number of felsic lava zones and ultra-mafic horizons are present within the formation. Chert horizons are wide-spread in the Kromberg Formation and the main rock type is in most cases black carbonaceous chert with minor interlayers of carbonates.

Elemental analyses and mineral analyses of rock types show that the Onverwacht is mostly composed of α-quartz and various other less abundant mineral types. The Onverwacht cherts contain less carbonate (0.05%) than the Fig Tree cherts (1.58%), but the organic carbon content in the Onverwacht sample (0.24%) is similar to that in the Fig Tree (0.24%) (Brooks, 1971).

The Onverwacht Group is mined for gold, Chrysotile, barites and some base metals.

b. KALGOORLIE:

Three samples of archaean metasediments from two localities near Kalgoorlie (near Bulong and near Southern Cross) in the Yilgara Block of Western Australia (Fig.(II)-2a,(II)-2b). Many of the rocks in this area are metavolcanic rocks (Fig. II. 2c) but cherts and jaspers occur in the metasediments. The Mungari Beds from which the samples are taken, contain abundant phyllites, schists, and other fine grained metasediments and cherts and banded iron formations as well as metavolcanics. The so-called Kalgoorlie system is intruded by microcline-oligoclase granites which have been dated by Rb-Sr methods at 2,612 ± 13 m.y.old.* One of the samples (PM 5) was taken from the Evelyn Molly Prospect, 17 Km South of Southern

*Glikson (1971)

Figure II-2b :Geological sketch map. The framed area represen
the COOLGARDIE-KURRAWANG sequence.
(20 miles = 32 km). after A.Y.Glikson,1971.

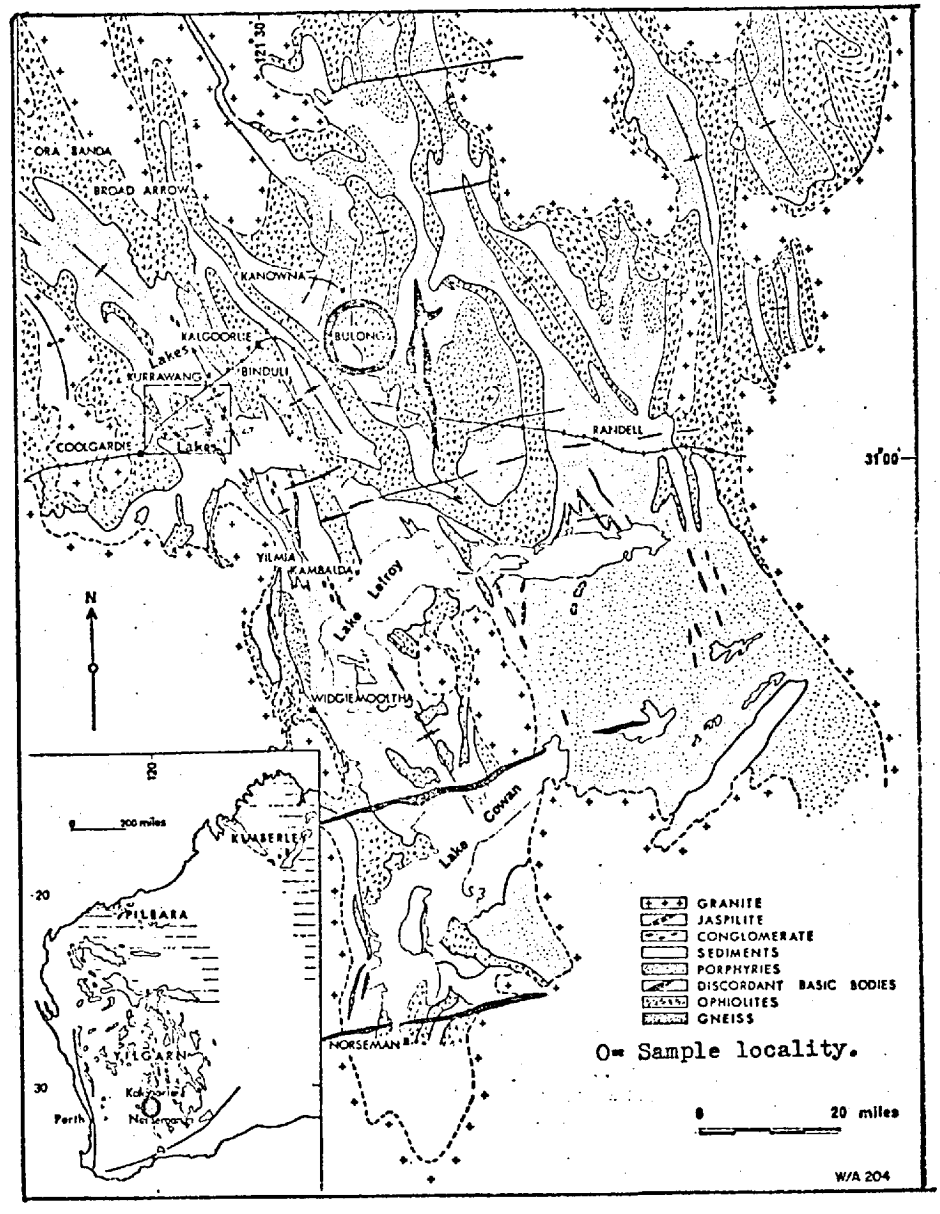


Fig. (II) 2c. Stratigraphy of the ARCHAEAN of the Kalgoorlie/Coolgardie Region. (Simplified after Glikson, 1971).

	Main Rock Types	Thickness
KURRAWANG BEDS.	Mainly meta-greywackes and meta conglomerates.	2,500 m
MUNGARI BEDS.*	Meta-sediments and meta-volcanics.	10,300 m
COOLGARDIE OPHIOLITES	Meta-volcanics.	6,560 m

* Samples from the Gunga meta-argillites at the base of the Mungari Beds.

Cross (W.A.- See Fig. (II) 2b), from which ferruginous micro-fossils have been reported (Marshall, May & Perret, 1964). These have been subsequently been shown to be late weathering artefacts (Muir et al, 1974). The Kalgoorlie/Coolgardie region is a mining centre, initially gold mining and now nickel.

c. SOUTH ALLIGATOR RIVER:

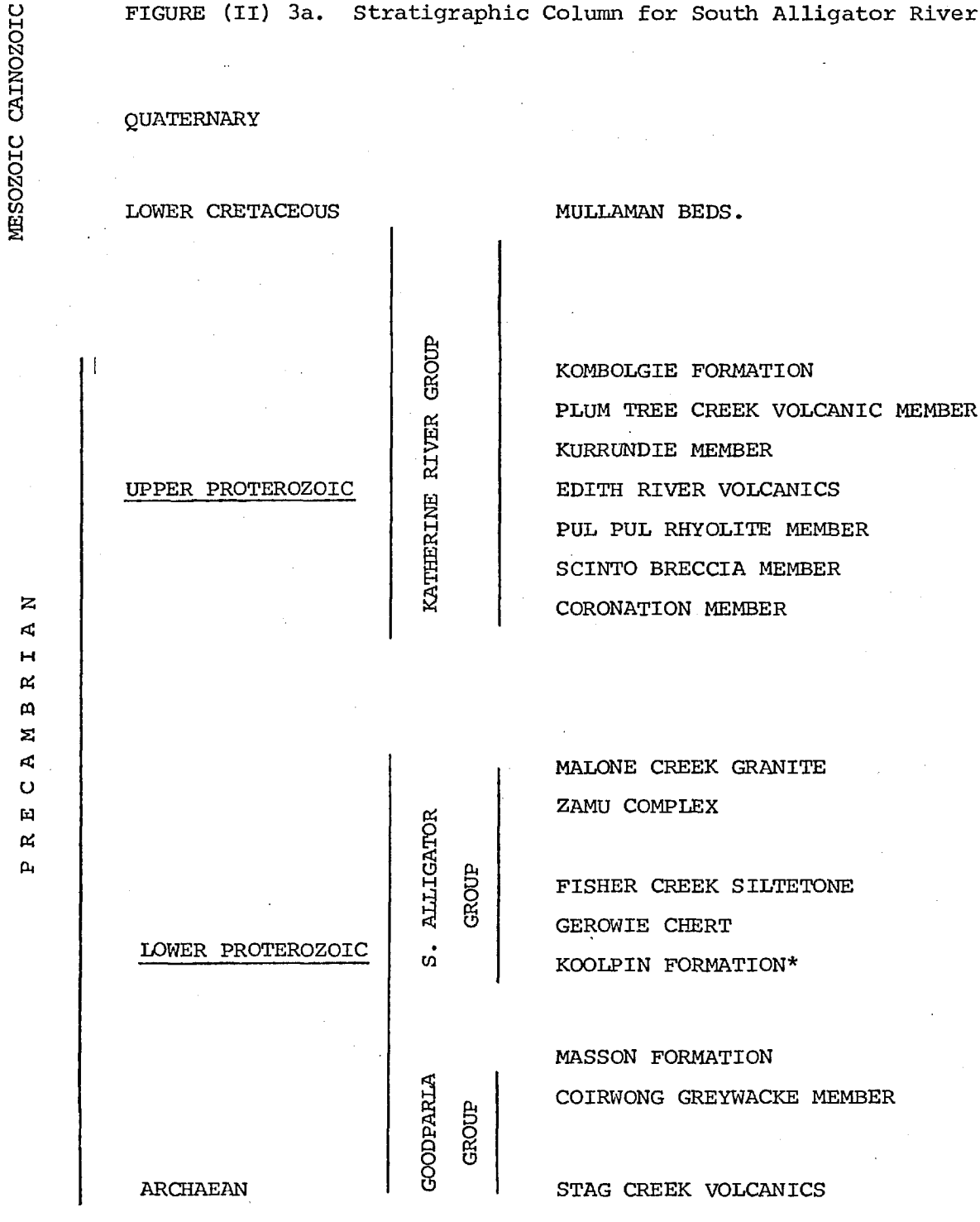
South Alligator Group together with Goodparla Group and one formation of Finnis River Group are regarded as Lower Proterozoic. Figure (II)-2a shows the locality map.

The South Alligator Group has been sub-divided into three formations - The Koolpin, Gerowie Chert and Fisher Creek Silt stone having a thickness of about 914 m, 914 m and 5180 m respectively (Fig. (II) 3a).

The samples were collected from the Koolpin formation (See Appendix I for details). The lithology of the Koolpin Formation is summarized below (Walpole et al, 1968) (Fig. (II) 3b).

This formation comprises of banded iron formation, inter-bedded carbonaceous shale and cherty ferruginous siltstone with restricted lenses of dolomite including a stromatolitic dolomite at the base. The carbonaceous shales are in places pyritic and contain lenses and nodules of chert. The essential minerals are quartz and sericite with kaolinite, siderite, chlorite and hematite being locally important. The area is mineralised and contains pitchblende, uranite, torbanite, chalcocite, eskobornite, galena and other base metal sulphides. It has been mined at Rockhole, Teagues Prospect, and El Sharana for uranium minerals.

FIGURE (II) 3a. Stratigraphic Column for South Alligator River Samples.



*Samples taken from here.

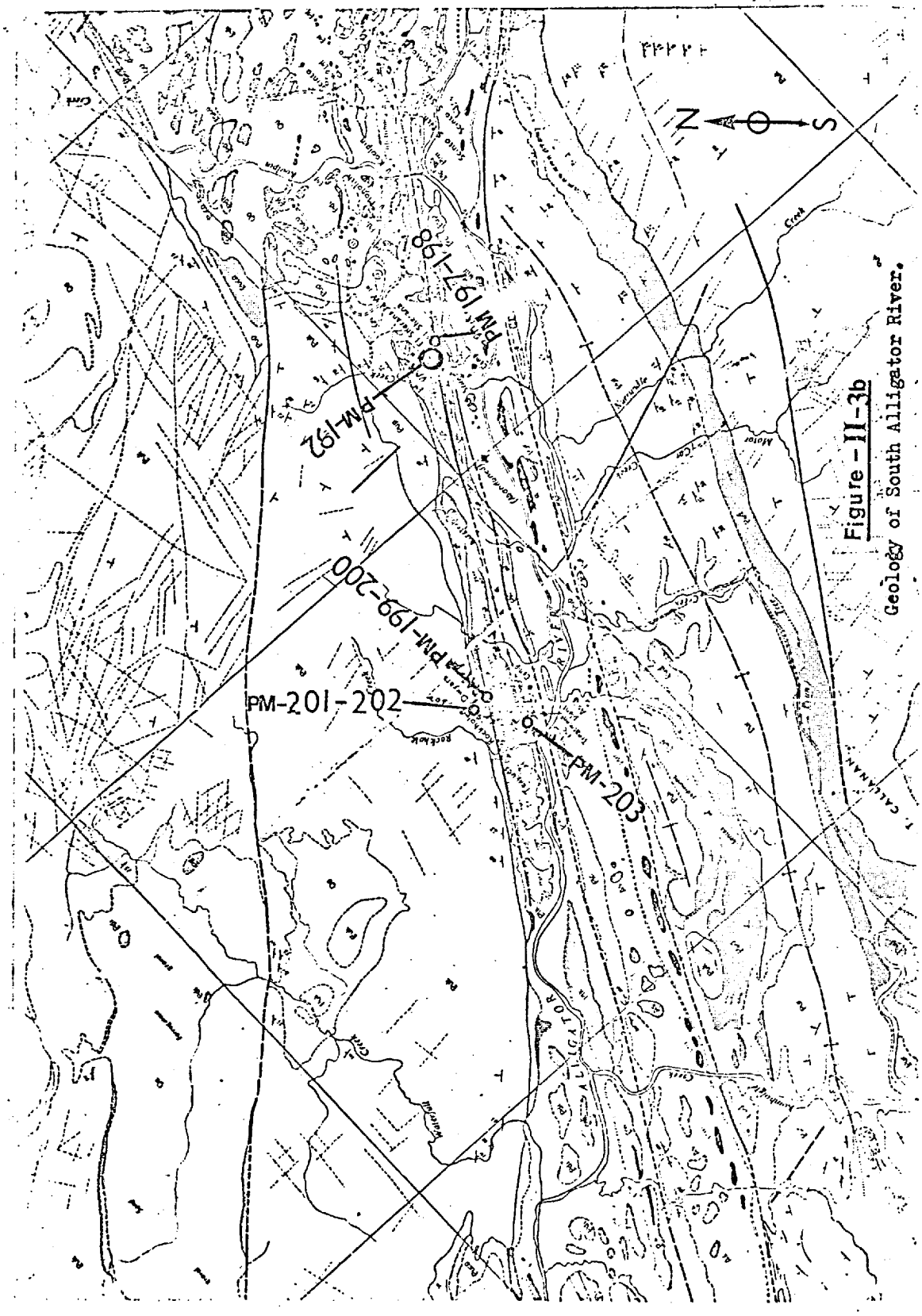


Figure - II-3b
Geology of South Alligator River.

d. HAMERSLEY:

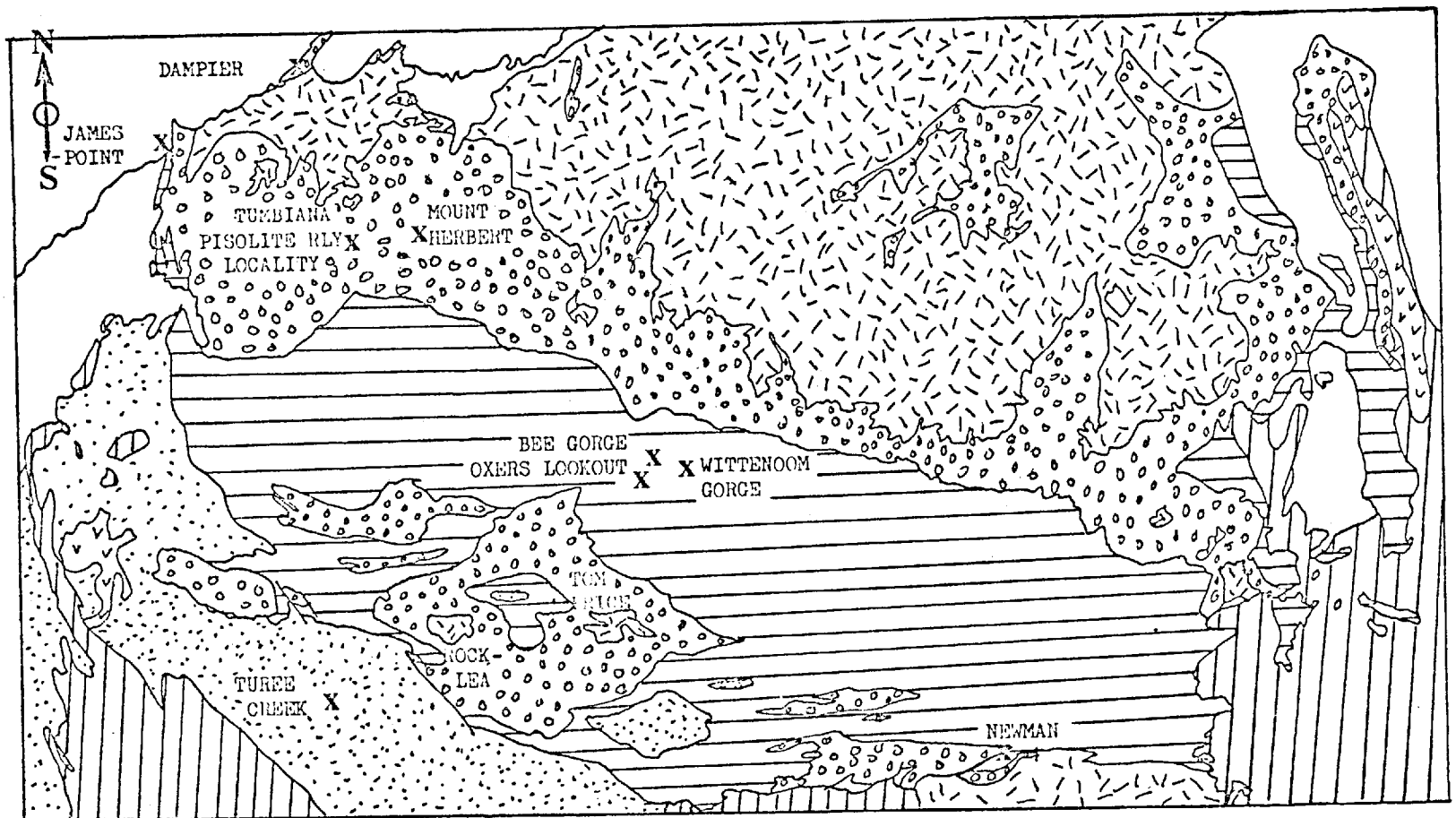
The Hamersley range lies on the W. Coast of Australia between latitude $21^{o}30'$ and $23^{o}30'$S and longitudes $116^{o}00$ to $120^{o}30'$E. The Province is delimited by the extent of an eliptical basin 160 x480 Km., in which the lower Proterozoic Hamersley Group sediments and volcanic were deposited. Fig.(II)-2a shows the locality of the basin and Fig.(II)-4a shows the extent of the depositional basin for the Mt. Bruce Supergroup (Trendall & Blockley, 1970) and Fig.(II)-4b shows the stratigraphic column of Hamersley Group (Trendall & Blockley, 1970).

The Hamersley basin itself is an ovoid depositional basin about 500 Km long and 200 Km wide with a West-North-Westerly elongation. The Mount Bruce Supergroup consists of three main divisions: at the base is the Fortescue Group followed confirmably with the Hamersley Group and above it with some local discontinuity, the Wyloo Group, and sample localities are shown in Fig.(II) 4c.

The Fortescue Group has a maximum thickness of 4,350 m. and consists largely of basic lava, pyroclastic rocks, sandstone and shale. The Hamersley Group is about 2,500 m thick with abundant iron formation. The Wyloo Group has a thickness of 9,500 m and consists of clastic sediments with thick local developments of dolomite and basalt.

Rb-Sr ages for the inter-layered volcanics of Mt. Bruce Super Group indicate that the deposits were formed between 2.2×10^{9} and 2.0×10^{9} years ago (Crompston and Arriens, 1963).

The Hamersley region was first exploited for the gold in the West Pilbara Goldfield, but more recently blue asbestos mining was operated



GENERALISED REGIONAL GEOLOGICAL MAP OF THE HAMERSLEY REGION, W.A. Scale 1:2,500,000. (after TRENDALL & BLOCKLEY, 1970)

Figure-II-4a

WYLOO GROUP

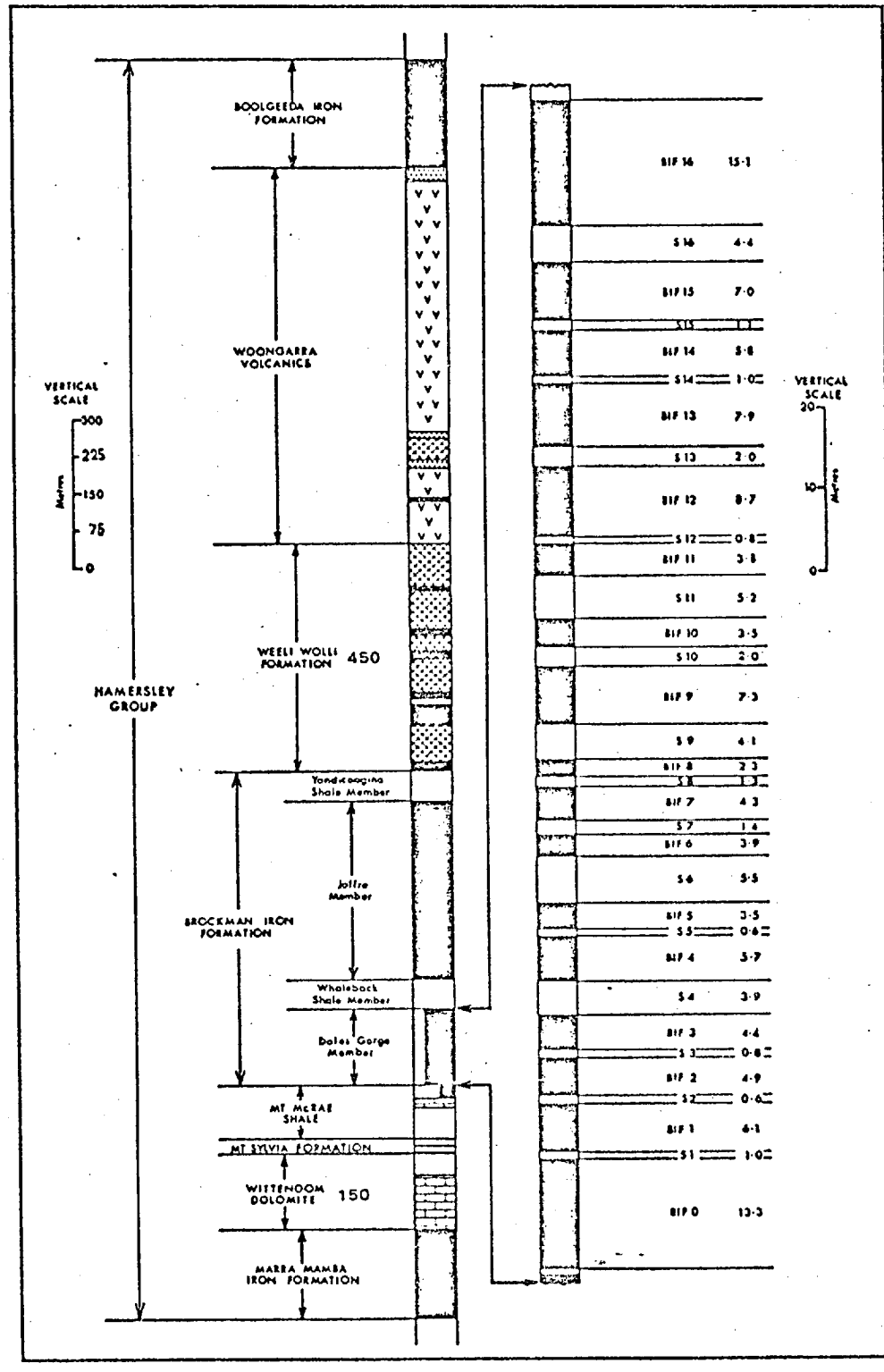
ARCHAEAN

PROTEROZOIC GRANITE

FORTESCUE GROUP

BANGEMALL, BRESNAHAN, MOUNT MINNIE & MANGANESE GROUPS

HAMERSLEY GROUP

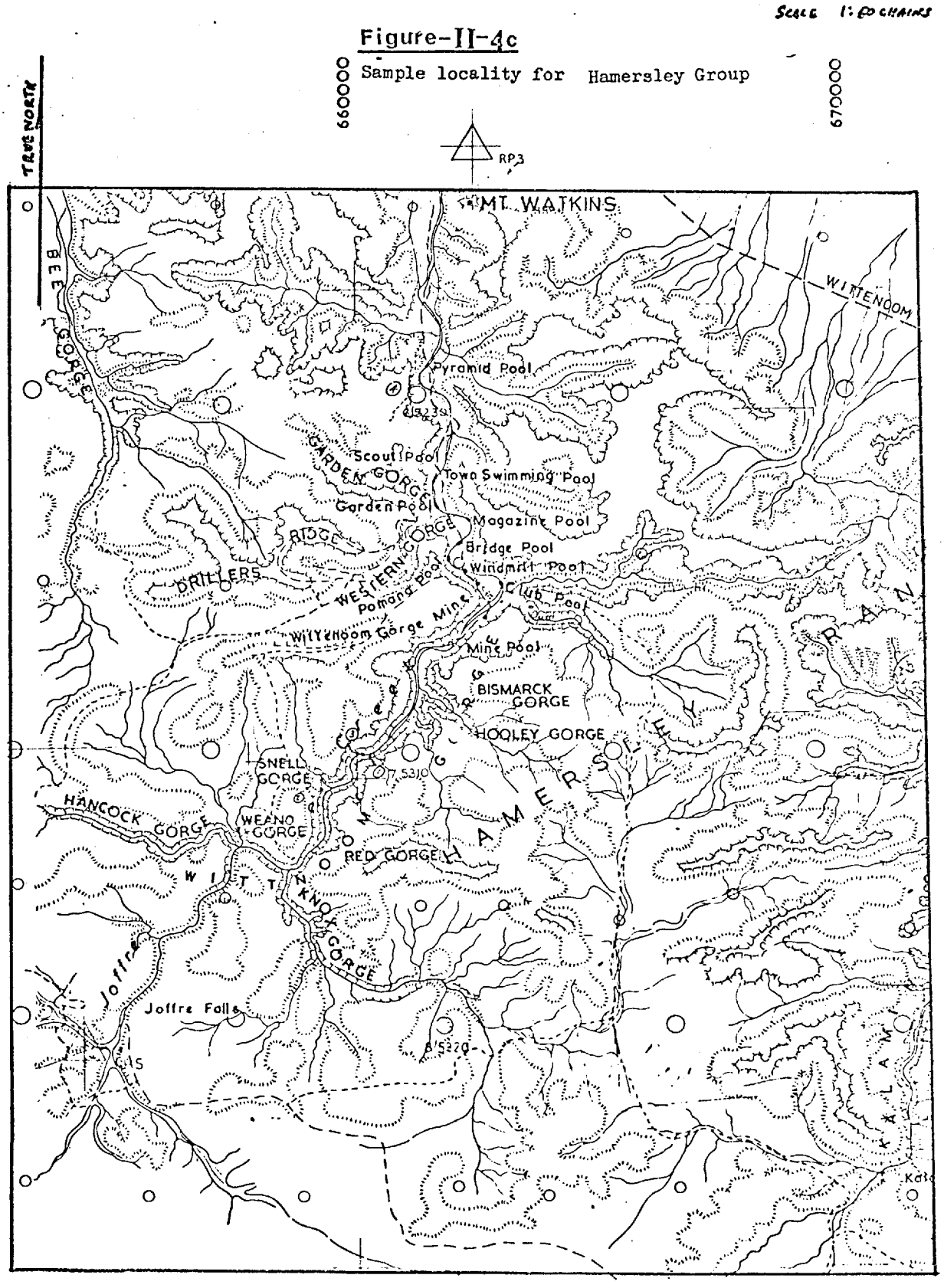


Figure

Fig 4 b Stratigraphic column of the Hamersley Group, and internal details of the Dales Gorge Member of the Brockman Iron Formation.

Figure-II-4c

Sample locality for Hamersley Group



and and presently iron mining is a major industry. Some small base metal prospects are likely to be mined and there is a thriving minor industry polishing semi-precious stones including jasper, tiger eye etc.

B. METHODS

In this section the techniques will be described following brief introduction and the data obtained by each technique will be tabulated and the results will be discussed in the next chapter.

The samples, collected by various people from the previously mentioned areas, basically fall into the following categories.

1) Cherts
2) Shales
3) Pyritic Shales
4) Carbonaceous Shales
5) Carbonate bearing rocks

This range of rocks was investigated for their minerology by X-ray diffraction supplemented by thin section petrographic studies in the laboratory. In some instances chemical staining techniques were used to differentiate limestones and dolomites especially the ones which carry a small portion of ferrous iron in their crystal lattice.

The X-ray diffraction (X.R.D.) and the staining technique (S.T.) will be briefly described below.

Mineralogy:- About 50.G. of the rock sample was crushed in a "Tema" swing Mill crusher equipped with a tungsten carbide crushing mortar to a reasonable size. The final powdered sample was prepared by grinding in an agate pestle and mortar to pass -200 mesh.

The powdered sample was mounted in an aluminium cavity mount.

X-RADIATION PROCEDURE

The samples were X-rayed on a standard Phillip's Wide Angle X-ray diffractometer with proportional counter using CoK_{α} radiation at 38 kV and 24 mA. Scanning speed was $1^{o}2\theta$ per minute and the chart speed was ½ inch per minute providing $1^{o}2\theta$ per inch print out for all samples. The scanning was done from 5^{o} to $70^{o}2\theta$. The rate meter and the time constant were generally 400 cps f.s.d. and 2 respectively. Whenever scanning speed was 2^{o}/min., divergent, scatter, and receiving slits were 1^{o}, 1^{o}, and 0.006 inch respectively.

The quartz which is always present in the sample, served as an internal standard for the exact measurement of the peak location.

Table (II)-(1) lists the strong X-ray lines used for identification of the minerals encountered. And the minerals identified for each rock sample are listed in table (II)-(3a, b & c) for each area.

STAINING TECHNIQUE

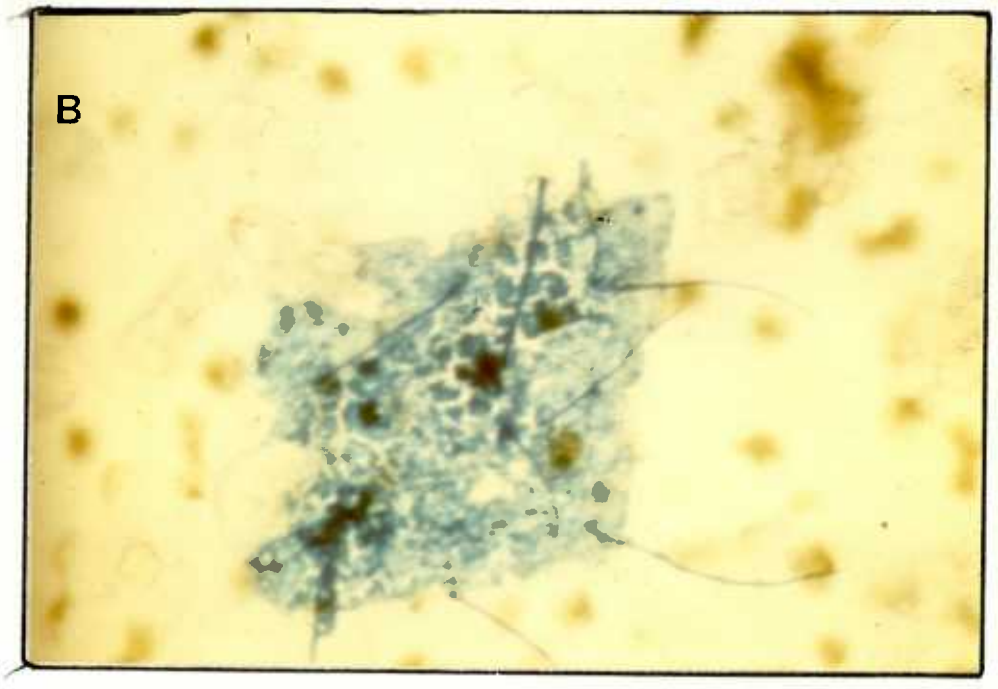
Various carbonate minerals were identified by staining over a set period of time with Alizarin red S (A.R.S.) and potassium Ferricyanide (P.F.). This technique is commonly used as a routine method by sedimentary petrologists and is of considerable importance in limestone petrology.

During staining it was observed in a few slides, that fossils were clearly distinguished from carbonate matrix. This clear-cut difference is shown in Figure (II)-5a, which is a thin section prior to staining and Figure (II)-5b, the same section after staining. The fossils are prominently displayed and are a characteristically attached to a carbonate mineral (Ferroan dolomite).

Figure--11--5



A-- Thin section of PM-24 (Hamersley) showing DOLOMITE rhomb, before staining (X Nicols).



B-- After staining-the filaments are distinctly visible. The blue colour is due to ferrous iron .

TABLE (II).1. Strong X-ray reflections of minerals in Precambrian sediments from Australia and South Africa.

Mineral	hkl	d(Å)	2θ (degree)	INT	Mineral	hkl	d(Å)	2θ (degrees)	INT
Quartz	101	3.34	31.1	10	Ankerite	104	2.90	36.0	10
	100	4.25	24.35	6		113	2.20	48.0	6
	112	1.817	59.03	5		018	1.81	59.3	6
					Dolomite	211	2.88	36.3	10
Hematite	104	2.69	38.8	10		332	1.801	59.6	6
	110	2.51	41.8	8		321	1.784	60.2	6
	321	1.697	63.6	7	Siderite	211	2.80	37.3	10
						332,321	1.737	62.05	8
						110	3.60	28.8	4
Magnetite	113	2.53	41.55	10	Glauconite		10.1	10.2	10
	333	1.611	67.55	8			2.59	40.4	10
	004	2.09	50.7	7			4.53	22.8	8
Goethite	110	4.18	24.75	10	Greenalite	201	2.59	40.8	10
	130	2.69	38.8	8		001	7.12	14.45	8
	111	2.44	43.05	7		002	3.56	29.1	8
Calcite	211	3.05	34.1	10	Chamosite	001	7.06	14.6	10
	220	1.922	55.5	7		002	3.53	27.4	10
	321	1.877	56.95	6		201	2.46	42.65	9
Stilpnomelane	001	11.9	8.6	10	Chalco-	112	3.03	34.4	10
	003	4.04	25.6	5	pyrite	024	1.854	57.7	8
	004	3.03	34.4	3		132	1.591	68.4	6
Minnesotaite	002	9.53	10.8	10	Uraninite	113	1.647	64.35	10
	202,204	2.52	41.6	7		111	3.15	33.0	7
	004	4.77	21.65	1		022	1.926	55.4	6
Riebeckite	110	8.40	12.25	10	Muscovite	002	10.0	10.3	10
	310	3.12	33.3	6	(2M1)	006,024	3.35	31.0	10
	151,331	2.73	38.2	4		202	2.56	40.9	9
Marcasite	020,110	2.70	38.7	10					
	211	1.755	61.35	9					
	110	3.43	30.3	6					
Pyrrhotite	102	2.08	51.0	10					
	101	2.65	39.5	6					
	110	1.728	62.4	5					

As far as the writer is aware, this is an original observation and has not been reported in the literature in the context of preservation of fossils. It is, therefore, my intention to introduce this technique as routine in micropalaeontological work. The technique is briefly described herein (For details, refer to Dickson, 1965, 66).

Staining with A.R.S. (0.2g per 100 c.c. of 1.5% HCl) differentiates calcite from dolomite. Different solubilities of carbonate minerals in dilute hydrochloric acid cause the difference in surface topography of thin section. Calcite is more soluble than dolomite. The stain imparts no colour to dolomite while calcite is stained pink to red.

Next, the section is stained with P.F. (0.2g per 100 c.c. of 1.5% HCl which produces Turnbull's blue in the presence of ferrous iron. This way ferroan calcite and dolomite can be distinguished. Adhesion of the stain is very weak, so extra care is necessary in the last stage to avoid touching of any surface of the section.

From the micropalaeontological stand-point the potassium ferricyanide stain was more useful and specific. As mentioned previously, P.F. reacts with ferrous iron to give deep blue-Turnbull's blue- precipitate of Ferrous ferricyanide as per following re-action:

$$3FeCl_2 + 2K_3Fe(CN)_6 \text{ .....} Fe_3\{Fe(CN)_6\}_2 + 6KCl \text{ .....Eq. (II) 1}$$

The detailes stages of the procedure are shown in Table (II) 2

TABLE (II) 2. Staining Technique

Step	Procedure	Time	Carbonate	Result
I	Etching		Calcite	Considerable etch
	1.5% HCl	10-15 sec	Ferroan Calcite	
			Dolomite	
			Ferroan dolomite	Negligible etch
II	Staining			
	0.2g A.R.S. per 100 c.c. of 1.5% HCl	30-45 sec.	Calcite	Very pale pink-re
			Ferroan calcite	Very pale pink-red, pale blue-dark blue if superimposed, give mauve-purple royal blue
	2.0g P.F. per 100 c.c. of 1.5% HCl		Dolomite	No colour
	Mixed in ratio A.R.S. : P.F. = 3:2		Ferroan dolomite	Pale, deep turquoise depending on ferrous iron
III	0.2g A.R.S./100 c.c. of 1.5% HCl	10-15 sec	Calcite	Pale-pink-red
			Ferroan calcite	
			Dolomite	
			Ferroan dolomite	No colour

Following the use of strong X-ray reflections (Table (II) 1) and the staining technique (Table (II) 2), the mineralogy was determined and the results are tabulated in table (II) 3a, b & c for all the three areas.

TABLE (II) 3a. Onverwacht Mineralogy

S. No.	Type	X-ray Diffraction	
		Whole rock mineralogy	Acid insoluble matter
K-1A	Carbonaceous Chert	Q., Chlo., Clay fraction	Hump (i) 4.49Å-3.06Å, gra., Traces of R., Pyr., Marc.
K-3	Carbonaceous Chert	Q., Chlo., Clay fraction, Ferroan dolo., Pyr.	Gr.(R), R, Pyr, Mar, Ti(II)O., (Sod., Al, Silicate hydrate) and some U.I.P.
K-4	Chert	Q., Chlo., Clay Mineral?	Bimodal Hump (i) 4.49Å-3.06Å, (ii) 2.201-2.006Å
K-6	Chert	Q., Chlo., Clay fraction, Calc. and ferroan carbonate in cracks & veins	Traces of gr., R, Py., Marc, (Sod. Al. Silicate hydrate) Pot. fluosilicate hydrate)
K-7	Chert	Q., Chlo., Clay fraction, Cal. (Ferroan)	Bimodal Hump 4.49-3.06Å, 2.201Å-2.006Å
Hall-1	Carbonaceous Chert	Q., Chlo., Clay fraction	Bimodal Hump (i) 4.49Å-3.06Å. (ii) 2.201Å-2.006Å, gr.? R, Py., Marc., (Sod., Al, silicate, Hydrate and Magn. fluoride)
Hall-$1^{W/L}$	Carbonaceous Chert	Q., Chlo., Py.	Bimodal Hump (i) 4.49Å-3.06Å, (ii) 2.201Å-2.006Å possibly pure "kerogen" deduced from X.R.D. Analysis
Hall-2	Carbonaceous Chert	Q., Chlo., Clay fraction, Py.	Bimodal Hump (i) 4.49Å-3.06Å (ii) 2.201Å-2.006Å possibly pure "kerogen" deduced from X.R.D. Analysis.

TABLE (II) 3b South Alligator, Australia Mineralogy

S.No.		X-ray Diffraction	
		Whole rock Mineralogy	Acid insoluble matter
PH-192	Black cherty Shale	Q., Clay Mineral	Bimodal hump i) 4.49Å-, 3.06Å, ii) 2.201-2.006Å, gr., R., Tr. of pyr.
193	Black Shale	Q., Clay Mineral	(Pot. fluosilicate) and some U.I.P.
194	Black Chert	Q., Clay Mineral	Sp., Pyr., hump in the region 4.49-3.06Å
195	Black Shale	Q., Chl., Musco., Mont., Cu-sulphide	Hump in 4.49-3.06Å region, gr.? Sp. (Mg. fluosilicates) and some U.I.P.
196	Black Chert	Q., Clay Mineral	Hump 4.49Å-3.06Å, gr. Py. and some U.I.P.
197	Volcanic Rock	Q., Chlo., Musco., H., Mont., Cu-sulphide	Sp., Pyr., R., H. (Hieritite)
198	Chert Jasperlite	Q., Clay, Traces of H.	Hump 4.49-3.06Å, gr., (Hieritite) U.I.P.
199	Black Shale	Q., Clay., Chlo., Mart., Galena? Cu-suphides	(Hieritite) & some U.I.P
200	Black Shale	Q., Clay, Chlo., Mart., Galena? Cu-sulphides	(Hieritite)
201	Coal	Q., Clay, Chlo., Mart., Traces of Galena & Cu-sulphides	Hump 4.49-3.06Å, gr Hieritite, Traces of H.
202	Pitch Blende	Q., Gth., Mart., Uran., Arsenopyrite? Eskbornite, Cu-sulphides and some U.I.P., possibly secondary uranium minerals.	Bimodal hump (i) 4.49Å-3.06Å (ii) 2.201Å-2.06Å, gr.? & some U.I.P.
203	Cherty Shale	αFe_2O_3, Q., Clay mineral, Sid., 9th, Arag? Chamo, Chlo., Pyr? Traces of Marc., Eskbornite, Cu-sulphides.	Hump 4.49Å-3.06Å, Traces of H. and some U.I.P.

TABLE (II) 3c Hamersley Mineralogy

S.N.	Type	X-ray diffraction Whole rock Mineralogy	Acid insoluble matter
PM- 1	Banded chert	Q, H, Chlo?	Gr. (R), R, Pyr.
3	Chert	Q, Traces of Mont, Chlo.	
5	Banded Ferruginous chert	Q, H, Traces of clay Mineral	H, Pyr, Marc, Chrom, (MgFS)
9	Calcite	Cal, Trace Ferroan Cal.	
		traces of clay minerals	*
11	Brownish Shale	Q, Dolo, Cal?	(K_2SiF_6 Hieritite)
12	Glassy chert	Q, Ferroan dolo, sid, traces of clay	*
13	Calcite	Ferroan Cal., Traces of Q, Ferroan dolo & clay mineral	*
			(Amorphous carbon (hump)
14	"	Same as PM-13 ——→	R, Pyr. (K, Na, Mg, fluosilicat- K, Ca fluosilicate hydrate)
15	Finely banded chert	Q, Traces of Cal, dolo., Pyr., Clay min.	Pyr. & Marc.
17	Massive BIF	Q, Traces of clay, Ferroan Cal., Py. & H., Trace of M.	*
19	Sideritic chert	Q., Traces of Ferroan Cal., & dolo., & Chl.?	Rutile & Amorphous carbon hump
21	Banded chert	Q., Cham., Siderite, Traces of M.	*
23	Cherty BIF	Q., Rieb., Traces of H., Ferroan dolo., Croc., Traces of cal.	*
24	Shale	Q., Ferroan dolo., Siderite, Traces of Cal. Hydrobiotite?	*
25	Chert	Q., Traces of Ferroan dolo & other carbonates & traces of ankerite	*
28	Chert	Q., Sid., Ferroan dolo.	*
30B	Chert?	Q., Minn., Sid., Traces of Ferroan dolo., & Pyr.	*
31	Chert?	Q., Stilp., Min.? Traces of Gth	Pyr.
36	?	Q., Gth., Pyr., & Traces of M.?	Pyr.

cont'd..(Table (II) 3c)

continuation TABLE (II) 3c

S.N.	Type	X-ray diffraction Whole rock Mineralogy	Acid insoluble matter
PM- 38	Banded Chert	Q., Traces of clay Ferroan carbonate	Pyr., Marc. (Sod., Mag., fluo-silicates)
39	Shale	Q., Gth., & traces of other carbonates	*
40	BIF	Cal., Traces of Q., Ferroan dolo., Chamo?	*
43	Core Sample	Q., Sid., Stilp?	*
44	" "	Q., Rieb., M., Traces H., Mart.	*
45	" "	Stilp., Traces of dolo., Pyr., Green	Pyr.
46	" "	Stilp., Pyr., dolo., Traces of Green	Pyr.
47	Shale	Traces of Q., Ill, Pyrrh., Chamo, Cal. & Traces of Chalco	Pyr., Gr., Sulphur
48	Banded dolomite Chert	Q., Cal., Traces of Pyrrh. Chamo.?	Same as above (Calcium fluoride)
49	Banded sulphide bearing rock	Q., Cal., Traces of Pyrr., Chamo., Chalco.	Gr., R., Pyr., and possibly sulphur.
50	Shale	Q., Cal., Chem., Ill and clay mineral, Mica?	Hieritite & some Chalco
51		Chlo?	
52	Shale	Q., Traces of clay? Dolo-chlo. & some unidentified minerals	Same as above

KEY

Q	=	Quartz	R	=	Rutile
H	=	Hematite	Gth	=	Goethite
M	=	Magnetite	Chlo	=	Chlorite
Cal	=	Dolomite	Green	=	Greenalite
Sid	=	Siderite	Chamo	=	Chamosite
Ank	=	Ankerite	Musco	=	Muscovite
Pyr	=	Pyrite	Mont	=	Montemorillonite
Marc	=	Marcasite	Ill	=	Illite
Pyrrh	=	Pyrrhotite	Gr	=	Graphite (hexagonal)
Chalco	=	Chalcopyrite	Gr. R_2	=	Graphite (Rhombohedral)
Chrom	=	Chromite	*	=	Insufficient residue
Rieb	=	Riebeckite	( )	=	Synthetic mineral
Minn	=	Minnesotaite			after 1 NHCl, 40% HF
Stilp	=	Silpomelane			treatment
Croc	=	Crocidolite	Mart	=	Martite
Sp	=	Spinel	MgFS	=	Magnesium Fluosilicate
			U.I.P.	=	Unidentified peaks
			Kerogen	=	Totally demineralized

Chemical Technique for the Separation of Insoluble Carbonaceous Matter (Kerogen) from the Rocks

The present investigation was mainly based on Kerogen. This is the residue which is normally dark brown to black amorphous polymeric material which acquires the structural characteristics of graphite on thermal degradation. Often it forms a sort of bluish or black gluey or rubbery material of repulsive sort. Pirie (1965) referred to that as "the black gunk which unskilled chemists get when they are trying to make something, the text books say they ought to get ..... the stuff they throw down the sink". "GOO" is often used instead of "GUNK" in English literature, and it seems that the mere sound of these words indicates the chemists' distaste. As a passing reference, the author would like to point out with due respect to the reader that it seems the word "GOO" has a root in the Marathi language, which is one of the major languages of the Indian Sub-continent - happens to be the writer's mother tongue. It literally means "Shit". It seems that the word is a contribution to the English vocabulary from British Colonial times.

The study of kerogen particularly from rocks with low carbon content is important, since it is likely to be present as indigenous organic matter and not as a contaminant.

In general, carbonaceous matter in sedimentary rocks responds sensitively to changes in the environment especially temperature changes.

The isolation of insoluble carbonaceous matter (kerogen) from its mineral matrix without fractionating or chemical alteration of the kerogen is a very difficult proposition and further problems are perhaps due to the difficulties involved in recovering small amounts of insoluble matter.

Physical and chemical methods for isolating kerogen from mineral matter has been discussed by Forsman (1963), Robinson (1969) and Saxby (1970) has reviewed the chemical methods for isolation of kerogen in sediments.

In the present work, the technique adopted by palaeontologists is used: 10g of sample being grounded to -200 mesh size and then treated with INHCl to remove Ca & Mg. This was followed by HF treatment leaving the samples over-night on a boiling water bath to remove silicates and alumino-silicates. More basic rocks form insoluble fluorides of the type $MgAlF_5H_2O$, $NaAlF_4 . XH_2O$ and probably $Fe^{2+}(AL, Fe^{3+})\ F_5 . XH_2O$ (Langmyhr and Kringstadt, 1966). Experience from silicate analysis showed that if a strong complexing agent like 2.5% boric acid is added to the solution, the formation of the insoluble fluorides and fluorosilicates is prevented. Hot INHCl treatment for 24 hours gives similar results (French, 1964). This treatment also prevents the formation of gel during the dissolution of silica by hydrofluoric acid.

In the case of chert samples, if the samples contain finely divided silicious particles, HF treatment will generate heat (exothermic reaction) and this will cause the macerate sample to boil and overflow. This can be minimized usually by diluting the original 40% HF. Once the original heat of reaction of HF has been dissipated, HF concentration can be safely increased and treatment continued in a boiling water bath. Insoluble residues are not allowed to evaporate to dryness, as this will cause the re-crystallization of insoluble fluorides.

Complete silicate solution is rarely practicable. As mentioned above certain insoluble fluorides are found, though their formation can be prevented by addition of INHCl, e.g. Hieretite (K_2SiF_6) sometimes appears in organic concentrates after HF treatment, but can be removed by boiling 10% HCl and

Figure--II 6

X.R.D. traces showing the importance of removing the QUARTZ (101) reflection to see the GRAPHITE (002) reflection.

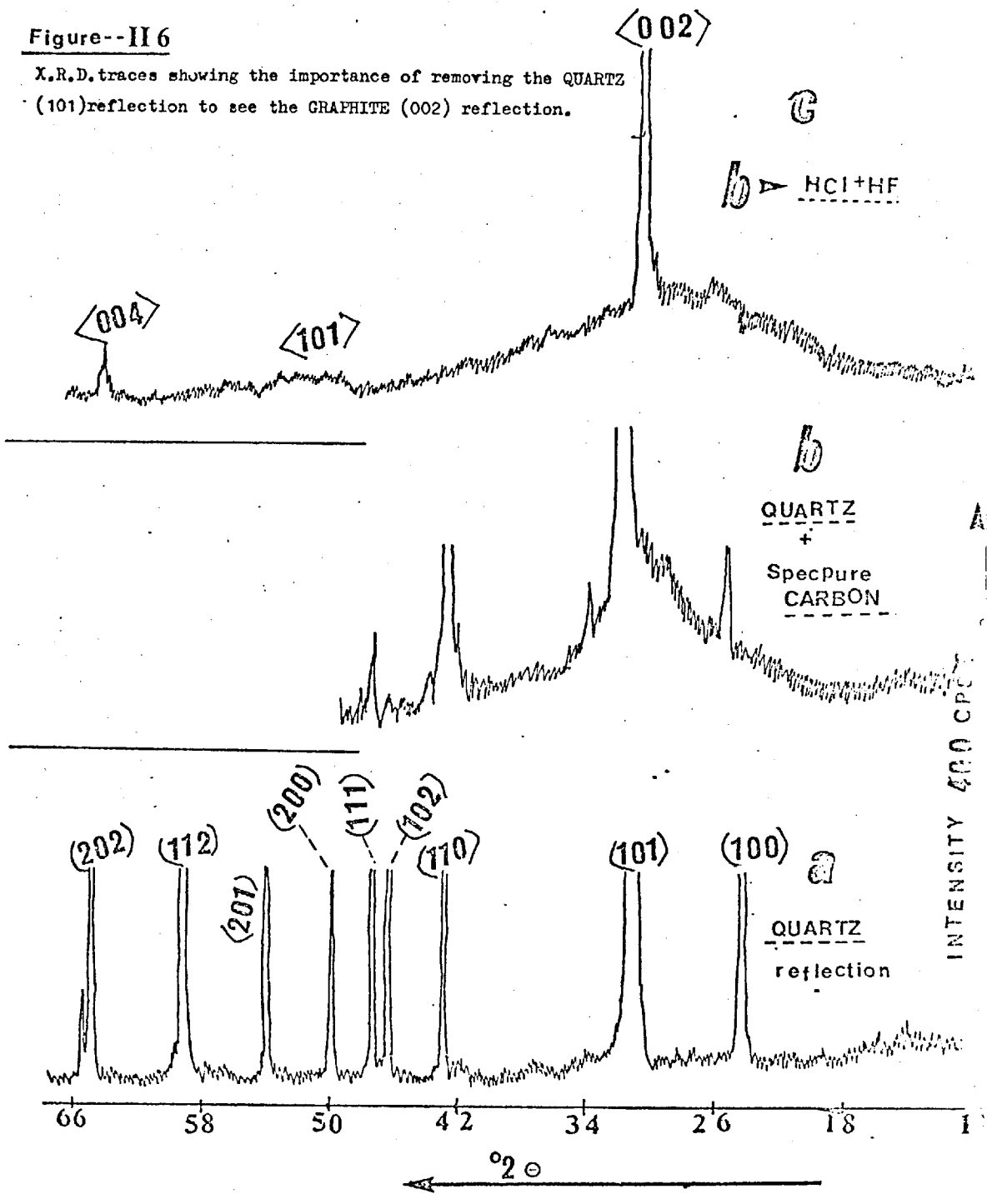


Figure--II--7

Scanning Electron Microscope photograph of (flaky) carbonaceous matter.



boiling water treatment during filtration. Other aspects of formation of insoluble fluorides and fluoro complexes will be discussed later (see also Karkhanis, in Precambrian Research, 1976, in press).

The main objective is to 1) try to keep the insoluble fluorides to a minimum and 2) to remove quartz and thereby the strong *(101)* quartz peak which masks any graphite *(002)* reflection (see fig. (II).*6*). No further demineralization was attempted as this would have required drastic conditions which would have altered the kerogen.

In summary the 1 N HCl and 40% HF treatment will remove most of the carbonates, sulphides, basic or amphoteric oxides or hydroxides as follows at a boiling water bath temperature.

In Hydrochloric Acid

$CaCO_3 + 2H^+ \ldots\ldots\ldots Ca^{2+} + H_2O + CO_2$ .....Carbonates Eq. (II) 2

$Zn5 + 2H^+ \ldots\ldots\ldots Zn^{2} + H_2S$ .....Sulphides Eq. (II) 3

$Fe(OH)_3 + 3H^+ \ldots\ldots\ldots Fe^{3} + 3H_2O$ .....Hydroxides Eq. (II) 4

Pyrite (FeS_2) is slightly soluble in dilute HCl depending upon its particle size.

40% Hydrofluoric Acid

$SiO_2 + 4HF \ldots\ldots\ldots\ldots SiF_4 + 2H_2O$

$SiF_4 \underset{\ldots\ldots\ldots}{\text{excess HF}} H_2SiF_4$ .....Silica Eq. (II) 5

The carbonaceous residues thus obtained were dark or black under optical microscope and flaky appearance under the scanning electron microscope {Fig. (II). 7}. The residues were dried in the oven under 50°C and weighed. The table (II). 4 below show the percentage recovery.

TABLE (II) 4. % Recovery of Insoluble Carbonaceous Matter

HAMMERSLEY		SOUTH ALLIGATOR		ONVERWACHT	
Sample No.	% I.S.C.M.	Sample No.	% I.S.C.M.	Sample No.	% I.S.C.M.
PM-1	0.125	PM 192	-	K-1A	0.31
3	-	3	0.03	K-3	3.80
9	-	4	-	K-4	0.80
12	-	5	6.63	K-6	0.23
14	-	6	0.26	K-7	0.18
17	-	7	0.02	HALL-1	0.17
19	0.016	8	0.79	HALL-1W/L	1.07
21	-	9	15.90	HALL-2	0.16
31	-	200	14.66		
38	0.55	1	8.12		
47	7.41	2	0.501		
48	7.59	3	0.24		
49	8.65				

Key: I.S.C.M. = Insoluble Carbonaceous matter.
- = Unrecoverable amount.

The X-ray diffraction results on insoluble residues from the three areas are summarized in Table (II) 3a, b, c in the previous section. The X-ray diffraction traces of final insoluble residues on the Onverwacht samples are described in detail below.

The traces of the Onverwacht Insoluble residues (Figure (II) 8) indicate the presence of pyrite, marcasite and zircon and there is a sharp peak at 2θ value of 32.1° corresponding to d spacing of 3.24 Å, suggesting rutile can also survive this treatment. There are other peaks showing the presence of unidentified inorganic minerals. The strong (101) quartz

peak is totally absent from these residues and therefore could not mask any graphite reflections.

The carbonaceous residues had dark or black colours with a shiny flaky appearance under the optical microscope. Some portions of this material were mounted on glass slides as smear mounts (Grinding was avoided as this sort of mechanical treatment produces a rhombohedral modification of graphite as consequence of translation or gliding of the layer plane. This accounts for the quality of X-ray traces). They were studied using a Phillip's diffractometer with vertical goniometer (CO-radiation at 38kV, 24mA and proportional counter) running continuously from 2 to 74°. The output was recorded on a chart recorder. The X-ray pattern is shown in Fig. (II) 8 shows that the material is carbon with some graphite. The values of graphite indices are given in Table (II).5.

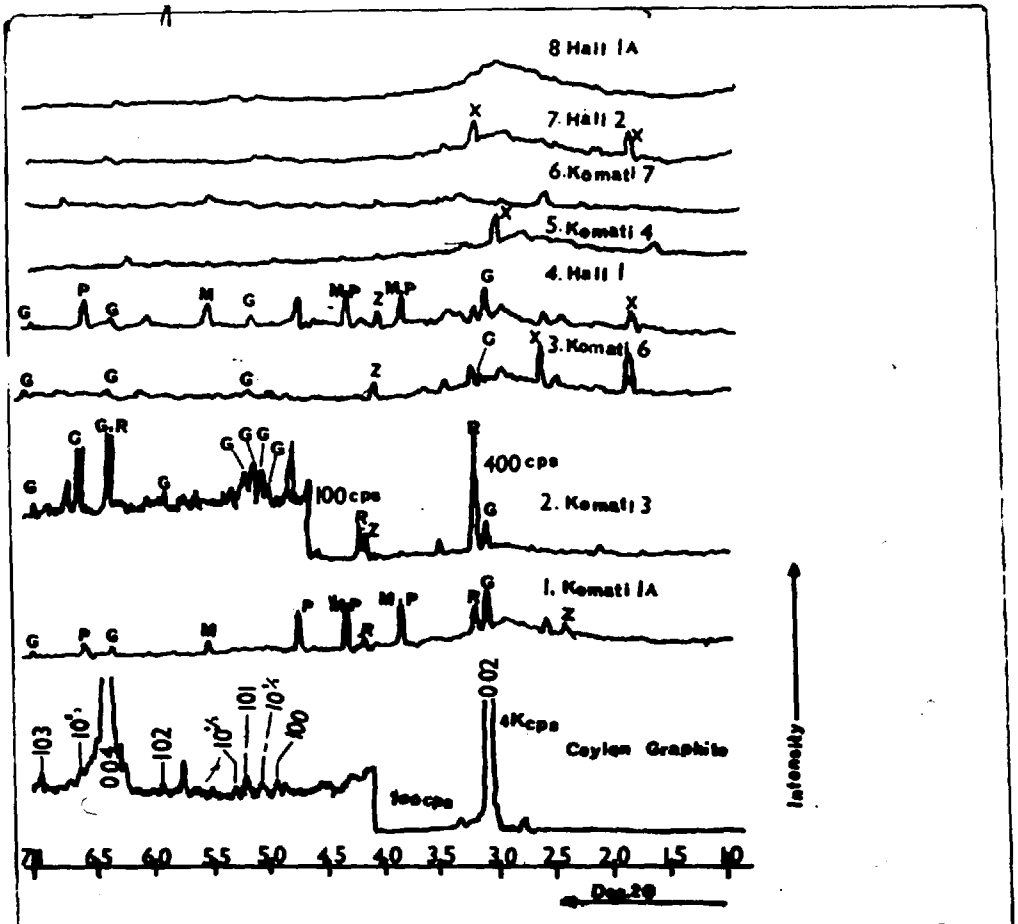
TABLE (II).5. Tabulation of all Possible hkl Reflections for graphite (space group P63/mmc) between 4° and 70°using Monochromatic Co-Kα Radiation.

Indices	*d* values and corresponding 2θ degrees for graphite		Relative Intensities
	d(Å)	2θ (deg)	
002	3.36	31.05	10.0
100	2.13	49.70	1.0
$10^{2}/3$†	2.087	50.80	1.0
101	2.033	52.25	5.0
$10^{4}/3$†	1.961	54.35	0.5
102	1.800	59.65	0.5
004	1.678	64.50	8.0
$10^{8}/3$†	1.627	66.75	0.5
103	1.544	71.00	1.0

* 2θ and *d* values from Berry and Thomson (1962)

† *d* values for rhombohedral form indexed with reference to cases of hexagonal form (Lipson and Stokes, 1942-43).

Figure --II--8



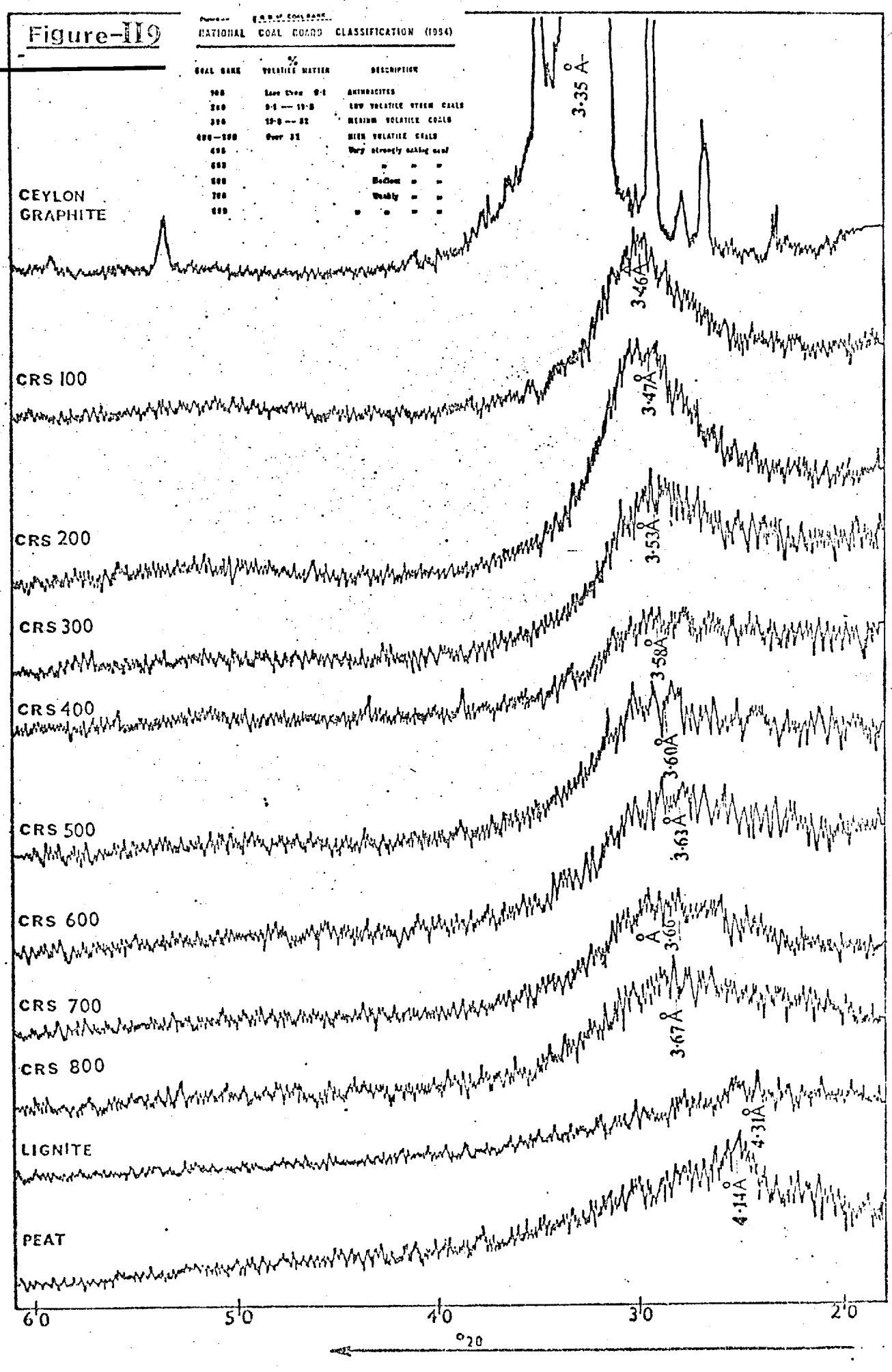
X-ray diffraction traces showing the occurrence of graphite in the Kromberg Formation of the Onverwacht. The reflections are indexed with reference to the structure of Ceylon graphite (Hamilton et al., 1970). The peaks designated *G*, *R*, *M*, *P* and *X* represent graphite, rutile, marcasite, pyrite and unknown, respectively.

Figure -- X.R.D of COAL RANK

NATIONAL COAL BOARD CLASSIFICATION (1964)

COAL RANK	% VOLATILE MATTER	DESCRIPTION
100	Less than 9·1	ANTHRACITES
200	9·1 --- 19·5	LOW VOLATILE STEAM COALS
300	19·6 --- 32	MEDIUM VOLATILE COALS
400—900	Over 32	HIGH VOLATILE COALS
400		Very strongly caking coal
500		" " "
600		Medium " "
700		Weakly " "
800		" " " "

Figure-II9

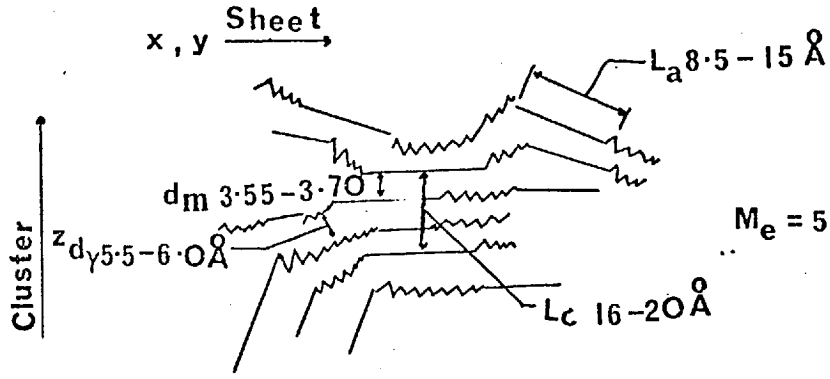

NATIONAL COAL BOARD CLASSIFICATION (1954)
% VOLATILE MATTER
DESCRIPTION
CEYLON GRAPHITE
CRS 100
CRS 200
CRS 300
CRS 400
CRS 500
CRS 600
CRS 700
CRS 800
LIGNITE
PEAT
3·35 Å
3·46 Å
3·47 Å
3·53 Å
3·58 Å
3·60 Å
3·63 Å
3·60 Å
3·67 Å
4·31 Å
4·14 Å
6·0
5·0
4·0
3·0
2·0
°2θ
INTENSITY 400 CPS

French (1964) classified the degree of Crystallinity of organic matter on the basis of graphite *(002)* reflection and his scheme is used here. Traces 7 and 8 and to a lesser extent 5 and 6 show the broad peak indicative of asphaltic material (van Krevelen, 1961; Weiler, 1963) which according to the classification of Landis can be described as graphite-*d*(Landis, 1971). Traces 1,2,3,4 show sharper *(002)* reflections though the intensity is much lower with reference to normal Ceylon graphite. Trace 2 shows extra weak reflections at $2\theta = 50.8^{\circ}$, 54.35° and 66.8°. These reflections indicate the presence of small amounts of rhombohedral modification in otherwise normal hexagonal graphite (Lipson and Stokes, 1942-1943). The reflections are also in Ceylon graphite which is sheared and they were indexed as ($10^{2}/3$, $10^{4}/3$ and $10^{8}/3$) with reference to the axis of the hexagonal form (Hamilton et al., 1970).

The coal samples of various ranks (from lignite through anthracite) were treated according to the above procedure and then X-rayed. The X.R.D. traces are shown for comparison purposes (Figure (II) 9)

Comparison of Figure (II) 8 and Figure (II) 9 show that there is a striking parallel between carbonisation of organic matter and coal dispersed in sediments during incipient metamorphism.

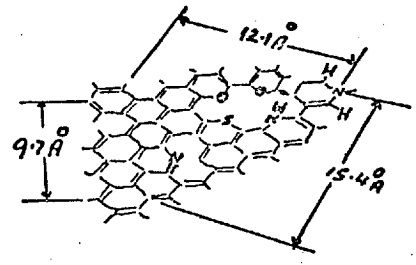
Extensive studies by Yen, (1972) have shown that the structure of kerogen is similar to the structure of asphaltine. Numerous aromatic benzene type rings lie in the same plane to form a sheet-like structure. Several of these sheets produce a basic kerogen molecule on polymerization. The heteroatom (O, S and N) produces dislocation in the otherwise perfect structure. Paraffin chains may be attached to this molecule and geothermal events can crack the chains (Fig. (II) 10). This leaves unpaired



represents the zig-zag configuration of saturated carbon chain or loose net of naphthenic rings

represents the edge of flat sheets of condensed aromatic rings

A Cross-sectional view of an asphaltene model based on X-ray diffraction.



B Numerous aromatic, benzene type rings in the same plane to form the asphaltic sheet having defective centers (gaps & holes), which are sites for the unpaired spins.

Figure-II-10

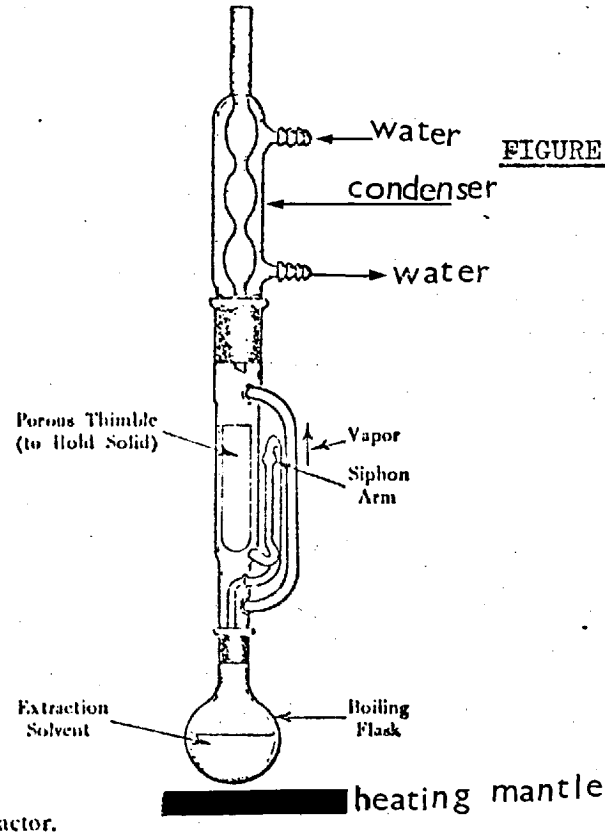


FIGURE:---- II-11

Soxhlet extractor.

electrons behind as organic free radicals which are believed to be stable through geological time.

In the past, several investigators have carried out studies on free radicals and transition metal ions associated with carbonaceous matters in natural carbons and coals of various ranks, using the technique of Electron Spin Resonance (Ubersfeld, 1954; Retcofsky, 1968; Duschiene,1961). All of these early studies were confined to measurements of Spin concentrations, the *Lande' g* factor and ESR Spectral widths. As mentioned earlier, there is a striking parallel between carbonisation of coal and dispersed organic matter in sediments and efforts were directed to a study of ESR absorption on insoluble carbonaceous residues from the Kromberg formation of the Onverwacht Group. This work was further extended to co-relate ESR parameters such as spin concentration, line widths and *g*-value with *(002)* X-ray diffraction peak for carbon and H/C atomic ration.

Isolation of carbonaceous matter from the mineral matrix was carried out as described earlier, with slight modification which is described below. About 20g of sample previously crushed to -200 mesh in a 'Tema' swing mill was shaken in a separating funnel with carbon di-sulphide and benzene separately to remove sulphur and soluble organic matter including any superficial contamination from long storage and handling. Later each sample was extracted by an all open Soxhlet extractor (Fig. (II) 11), using benzene-methanol solvent (Azotropic mixture 3:1) for 10-12 hours. The residue from the thimble was treated with ^{1}NHCl and 40% HF described earlier and ESR measurements carried out.

Carbon & hydrogen analyses were also carried out as below:-

Carbon and Hydrogen Analysis

The model 240 PERKIN-ELMER Elemental Analyser was used to determine the carbon and hydrogen contents of carbonaceous matter. The instrument detects and measures the combustion products (CO_2 H_2O). Combustion occurs in pure oxygen under static conditions and the products are analysed automatically in a self-integrating steady state, thermal conducting analyzer, and results are recorded in bar graph form on 0-1 mV recorder.

Helium is used as a carrier gas to carry combustion products from the combustion train through the analytical system to the atmosphere. The combustion train and analytical system are shown in a simplified configuration in Figure (II) 12. Combustion occurs under static conditions in an excess of oxygen at about 950°C.

The detector outputs were calibrated using known standards for normal C and H determination Acetanilide (C_6 H_5 NHCO.CH_3) (C-71.9%, H-6.71%, N = 10.36% was used as a standard.

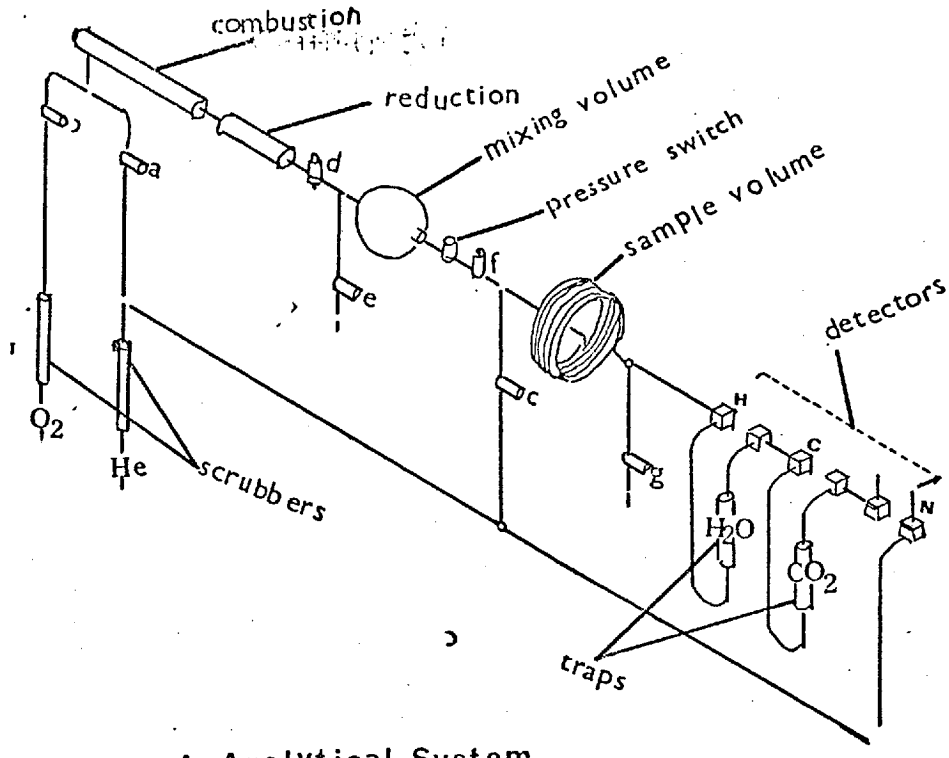
Samples are weighed in platinum boats between 1mg-3mg range. The following table shows elemental composition (C & H) for the three locations.

TABLE (II) 6. Carbon & Hydrogen Analysis

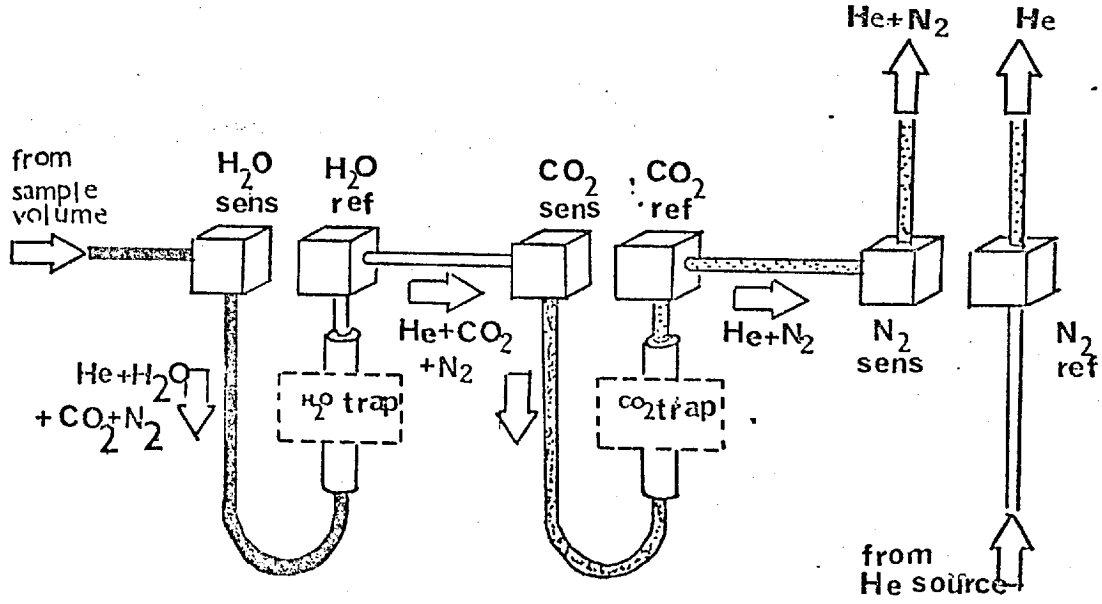
Sample No.	% Element		
	C	H	
KROMBERG Formation			Note
K-1A	73.44	2.53	
K-3	43.36	2.10	Samples K-3 and
K-4	62.66	1.46	HALL-1: show lower
K-6*	49.09	7.16	carbon content.
K-7	74.77	2.00	The remainder could
HALL-1	46.07	1.14	be the contribution
HALL-2	91.17	1.16	from pyritic sulphur.
HALL-1/WL	85.17	1.19	

*filter paper contamination

Figure-II-12 Analytical System for C,H analysis.



A--Analytical System
&
Combustion Train



B-- Detector Flow Diagram

Continuation ..... TABLE (II) 6

Sample No.	% Element C	% Element H
HAMMERSLEY & KALGOORLIE		
PM-1	98.02	1.05
PM-38	52.24	2.91
PM-47	12.49	0.96
PM-48	4.29	1.32
PM-49	7.15	1.20
SOUTH ALLIGATOR		
PM-196	74.26	1.52
198	4.34	2.45
199	14.56	1.16
200	11.55	0.98
201	52.06	0.78
202	81.42	1.45
203	66.01	2.13

ELECTRON SPIN RESONANCE (ESR) TECHNIQUE

By virtue of its intrinsic angular momentum, an electron behaves like a tiny bar magnet. The basic phenomenon of ESR technique is the *ZEEMAN* effect. By placing a paramagnetic sample such as organic free radicals or transition metal ions in a static field, the spin magnetic moments of the unpaired electrons are forced to align with or against the external field, the energy E between two spin states being given by the equation AYSCOUGH, 1967.

$$E = g\beta Ho \quad \ldots\ldots\ldots\ldots \quad \text{Eq. (II) 6}$$

where g = Spectroscopic splitting factor which approximates to 2.

β = Bohr magneton (factor converting angular momentum to magnetic momentum)

Ho = applied magnetic field.

KEY

k -- klystron
c -- cavity
cd--crystal detector
rl--resistive load
tp--tuning probes
ti--tuning iris
pa--pre-amplifier
aa audio amplifier
r--recorder

mc--modulating coil
em--electromagnet
a --attenuator
kps--klystron power supplies
afc.sg--automatic frequency control,sweep generator
afc.d--automatic frequency control,discriminator
apsd--audio phase-sensitive detector
mfg--modulating field generator
mfpsd--modulating field phase-sensitive detector
mfa--modulating field amplifier

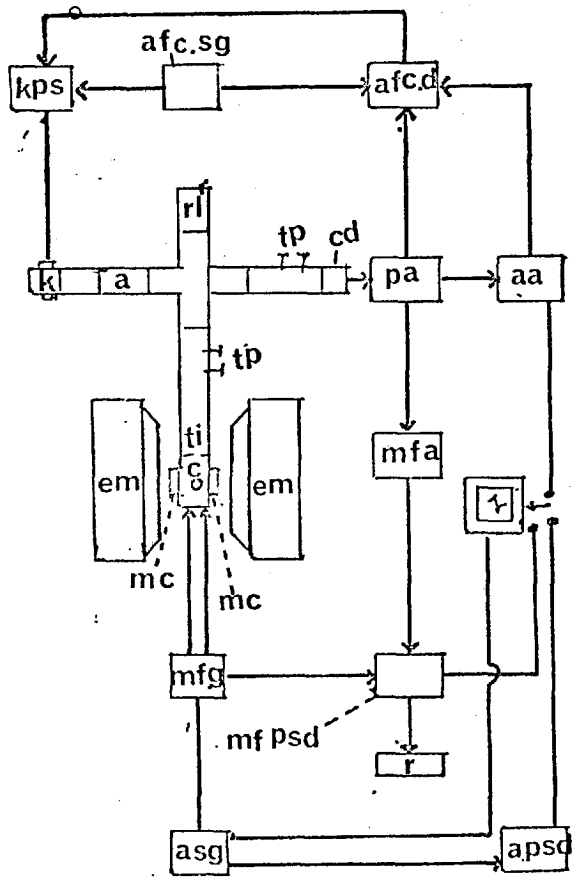


Figure--II-13 BLOCK DIAGRAM OF ELECTRON SPIN RESONANCE EQUIPMENT.

When the sample is irradiated with electro-magnetic energy, electrons in a lower energy state absorb energy and jump to a higher state if the frequency of the radiation (V_o) satisfies equation (II) 7

$$h\nu_o = g\beta H_o \quad \ldots\ldots\ldots \quad \text{Eq. (II) 7}$$

where h = Planck's constant.

The measurements were made with "Decca X3 employing Newport 11 inch magnet, type M4x" which was equipped with two modes of detection at 33cps. The magnetic field range is 0-13,000 gauss (i.e. g-value down to 0.5). Microwave radiation of 9,270.288 ± 0.002 was used. All measurements were made at room temperature on solid samples. A block diagram of ESR equipment is given in Fig. (II) 13.

All the ESR parameters were measured against a known amount of *1 -1' diphenyl-2-picrylhydrazyl* (DPPH) standard which has one unpaired electron per molecule and a molecular weight of 394 giving it 1.53×10^{21} spins/gm. (394g contain 6.025×10^{23} spins $\therefore$ 1 gm = 1.529×10^{21} spins). DPPH and the unknown spectra were scanned alternatively. The *g* value of DPPH was taken as 2.0037, the free electron value.

The first attempt the ESR spectrum was run on the powdered rock sample. The spectrum is shown in Fig. (II) 14. This is an example of inter-action between nuclear spin and magnetic moment, which gives this sextet of hyper-fine splitting.

This approach was aborted, as can be seen the areas of the spectrum we are interested in show overlap of various lines in the region of free radical absorption (around 3300 gauss and $g \simeq 2.0$)

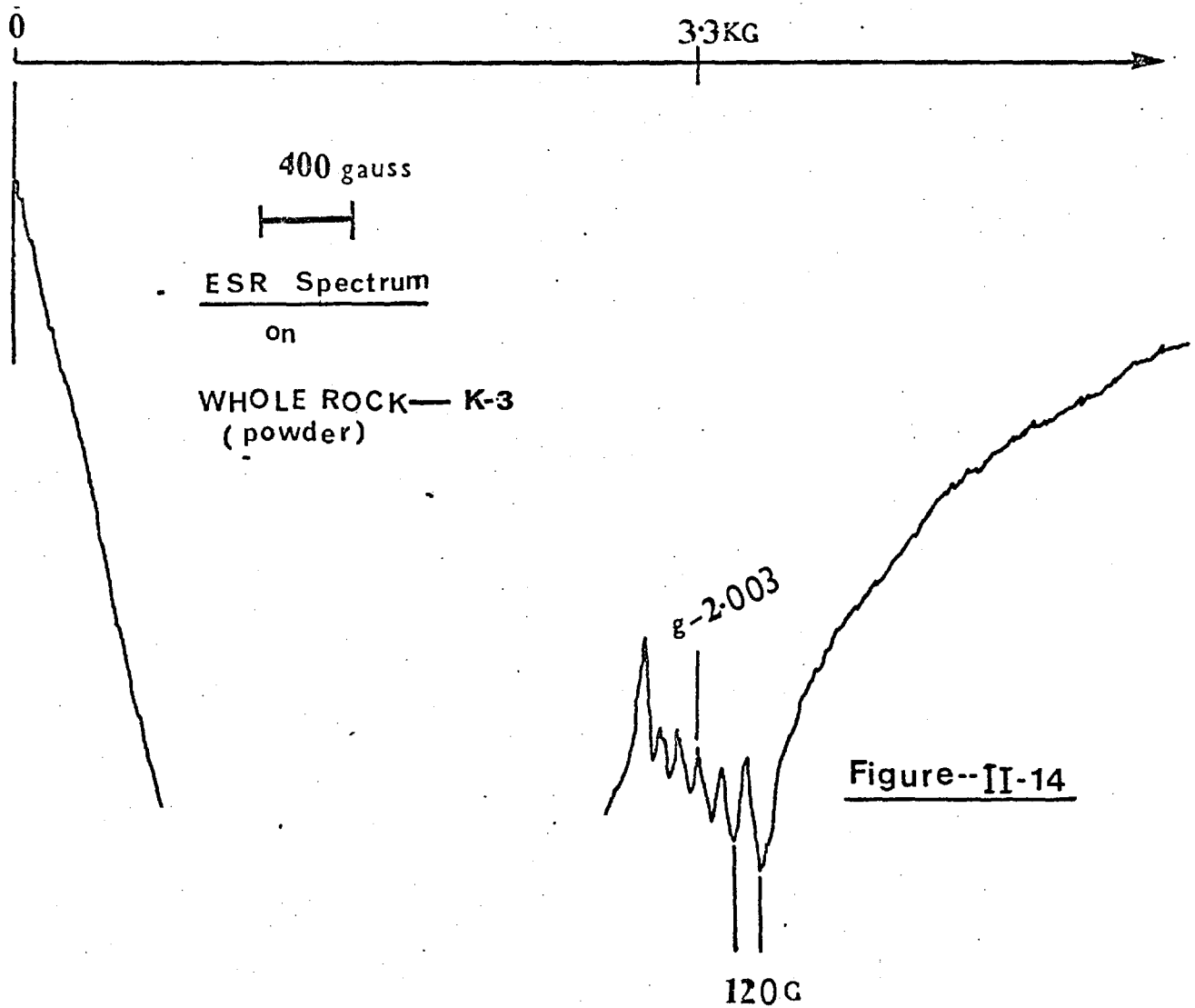
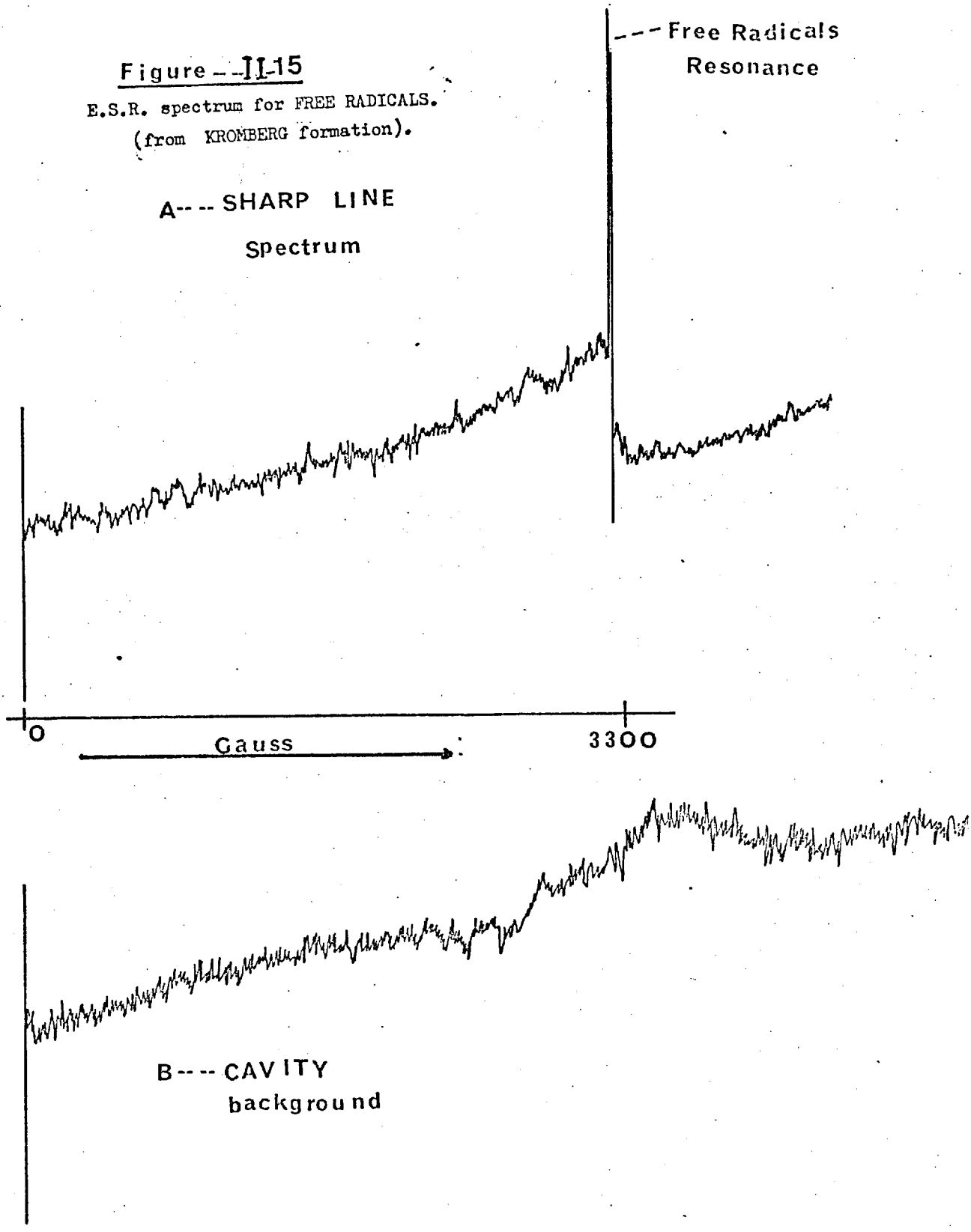


Figure--II-14

E.S.R. spectrum of the Mn^{2+} ion. The six components expected from Mn^{55} nucleus, the nuclear spin of which is 5/2.

Figure -- II-15

E.S.R. spectrum for FREE RADICALS.
(from KROMBERG formation).



However, the assignment of the spectrum was carried out as follows:- This is a spectrum typical of transition elements, which have $3d^n$ electrons in their outermost shell (n = 1 to 9).

The six equidistant lines with separation of 120 G. belong to the ion with a spin of (2I + 1 = 6) = $^5/_2$.

Only three elements give this type of spectrum

Isotope of Ti^{3+} - Ti^{47}

Fe^{3+}

and Mn^{2+}

The natural abundance of Ti^{47} is around 5% and one can only seen Ti^{47} lines if the spectrum is run at He temperature.

Fe^{3+} ion has an absorption in the region of 4.2 *g* i.e. around 1640 Gauss. So this spectrum was assigned to Mn^{2+} ion which has I = $^5/_2$, and the theoretical splitting distance of (60-90 gauss) is within experimental value of 120 gauss obtained here.

As mentioned previously, this exercise was not worthwhile. So the spectrum was run on carbonaceous matter.

The typical ESR spectrum for carbonaceous matter is shown in Fig. (II) 15a. For free radicals, these are generally symmetrical, narrow single line devoid of any fine structures. Fig. (II) 15b is a spectral contribution from cavity background. For *free radicals*, resonance occurs at about 3350 gauss. Line width was calculated for the spectrum as shown by the construction in Fig. (II) 16. The *g*-values were calculated from Eq. (II) 7. For spin concentration, the derivative peak height of the signal was normalised to unit length of sample in the 3mm diameter 'Spectrosil' quartz sample holder and then calibrated against a known amount of DPPH.

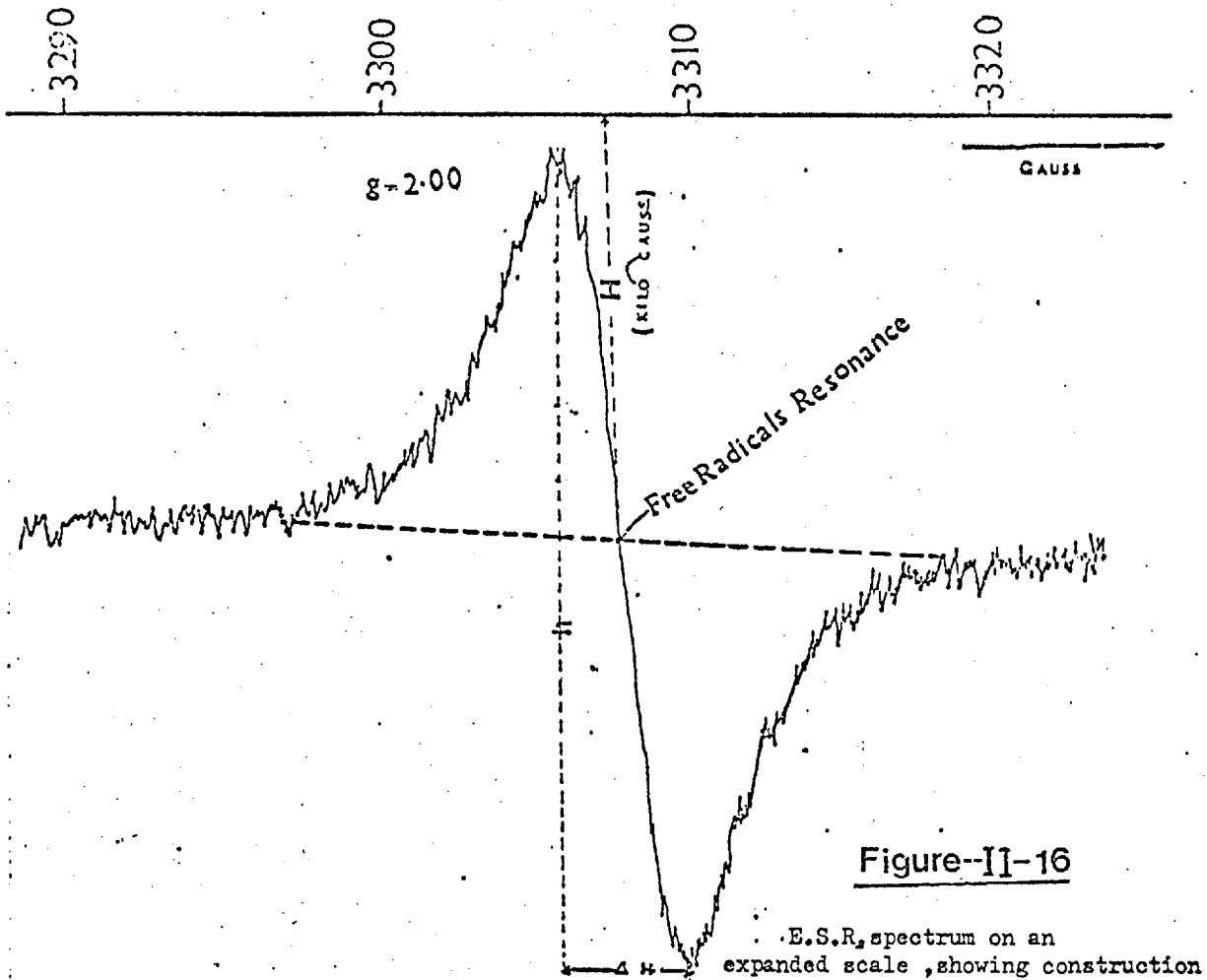


Figure--II-16

E.S.R. spectrum on an expanded scale, showing construction for various ESR parameters.

A serious problem in determining integrated absorption area from ESR curves, is the complication introduced by the line shape. Where the line shape is not simple, the wings of the ESR curve become lost in the noise. This can be corrected by measuring separately the contribution by the wings under increased gain and modulation amplitude. The ESR spectra for the Kromberg formation were not complicated but the ones for the Hamersley and South Alligator samples were somewhat complicated and separate re-runs were done on some of them.

A typical spectrum for a sample from the Kromberg formation run on an expanded scale is shown in Fig. (II) 16. These were generally symmetrical, narrow, single lines devoid of any fine structure. Various ESR parameters and H/C atomic ratios are shown in Table (II) 7.

TABLE (II) 7. ESR Parameters*

Sample No.	Free radicals spin/g x 10^{15}	Line width ΔH gauss	*"g"* value	H/C Atomic ratio
H1W/1	1.87	2.4	2.00177	0.17
H2	2.09	2.7	2.00186	0.15
K6**	4.76	6.2	2.00166	-
K7	5.23	3.6	2.00177	0.32
K1A	6.78	3.7	2.00174	0.41
H1	7.14	4.0	2.00201	0.30
K4	9.43	3.5	2.00192	0.28
K3	9.47	4.1	2.00195	0.58
DPPH Std.	1.53×10^{21}	0.17	2.00237	-

* Average of two determinations.

** Sample K6 was contaminated with filter paper during filtration.

As mentioned earlier, the ESR spectra for Australian samples were complicated. Two such spectra are shown in Fig. (II) 17 and 18 and the ESR data is summerized below in Table (II) 8.

TABLE (II)-8. ESR Data for Carbonaceous Matter from Australian Samples.

KALGOORLIE & HAMERSLEY

S.No.	Free radicals spin/g x 10^{15}	Line width ΔH gauss	"g" value	H/C ratio
PM-1	5.28	very narrow	2.00462	0.13
19	1.78	" "	2.00662	n.d.
38	1.94	" "	2.00662	o.92
47	10.02	140	∿2.00662	3.70
48	Intense peak	Broad		2.09
49	49.12	224	∿2.00662	3.77

SOUTH ALLIGATOR

S. No.	Free radicals spin/g x 10^{15}	Line width ΔH gauss	"g" value	H/C ratio
*PM-193	2.196	<28	2.00662	n.d
PM-194	Insufficient sample		-	n.d.
PM-195	No signal	-	-	n.d.
*PM-196	1.89	<28	2.00662	0.25
PM-197	No signal	-	-	n.d.
*PM-198	- -	-	-	6.77
*PM-199	0.383	∿200	2.00662	0.96
*PM-200	0.426	∿192	2.00662	1.02
*PM-201	0.067	∿160	2.00662	0.18
*PM-202	0.586	∿310	2.00662	0.21
*PM-203	2.11	28	2.00662	0.39

* Additional feature g = 3.31

n.d. not determined (insufficient sample).

Figure-II-17

Hamersley E.S.R

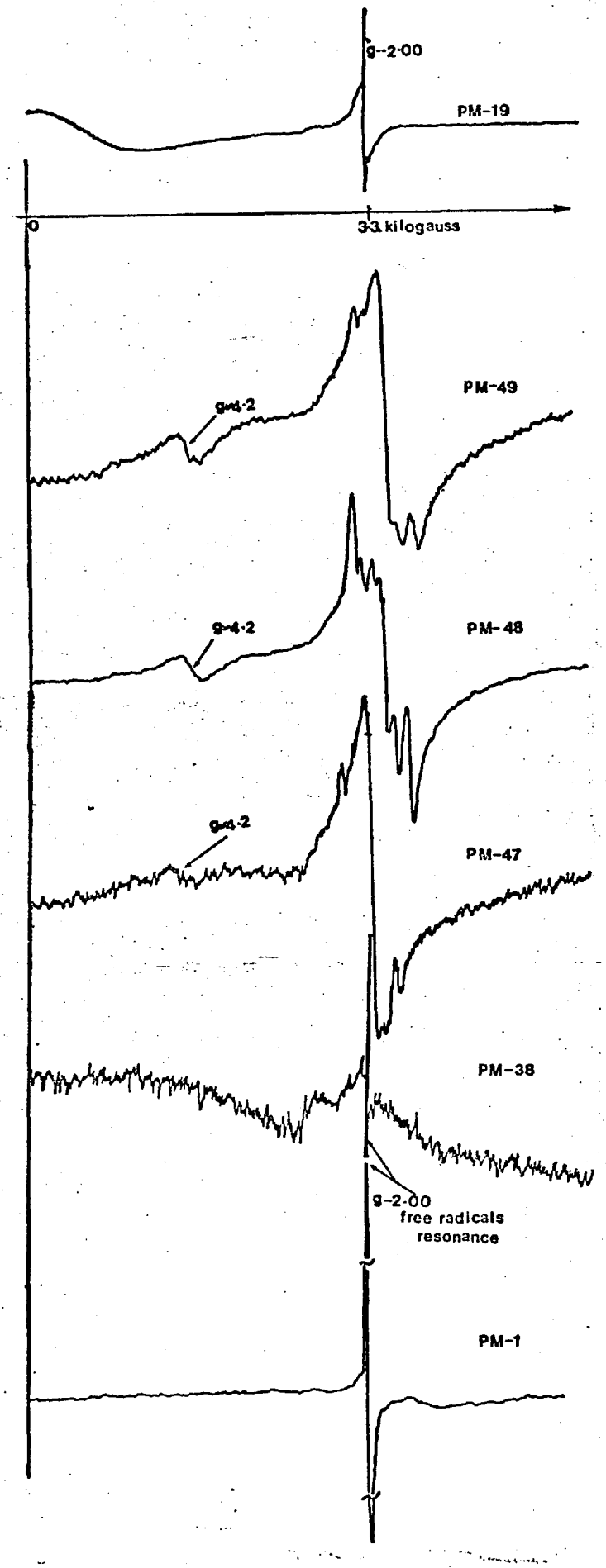


Figure--II--18

South Alligator----a

E.S.R

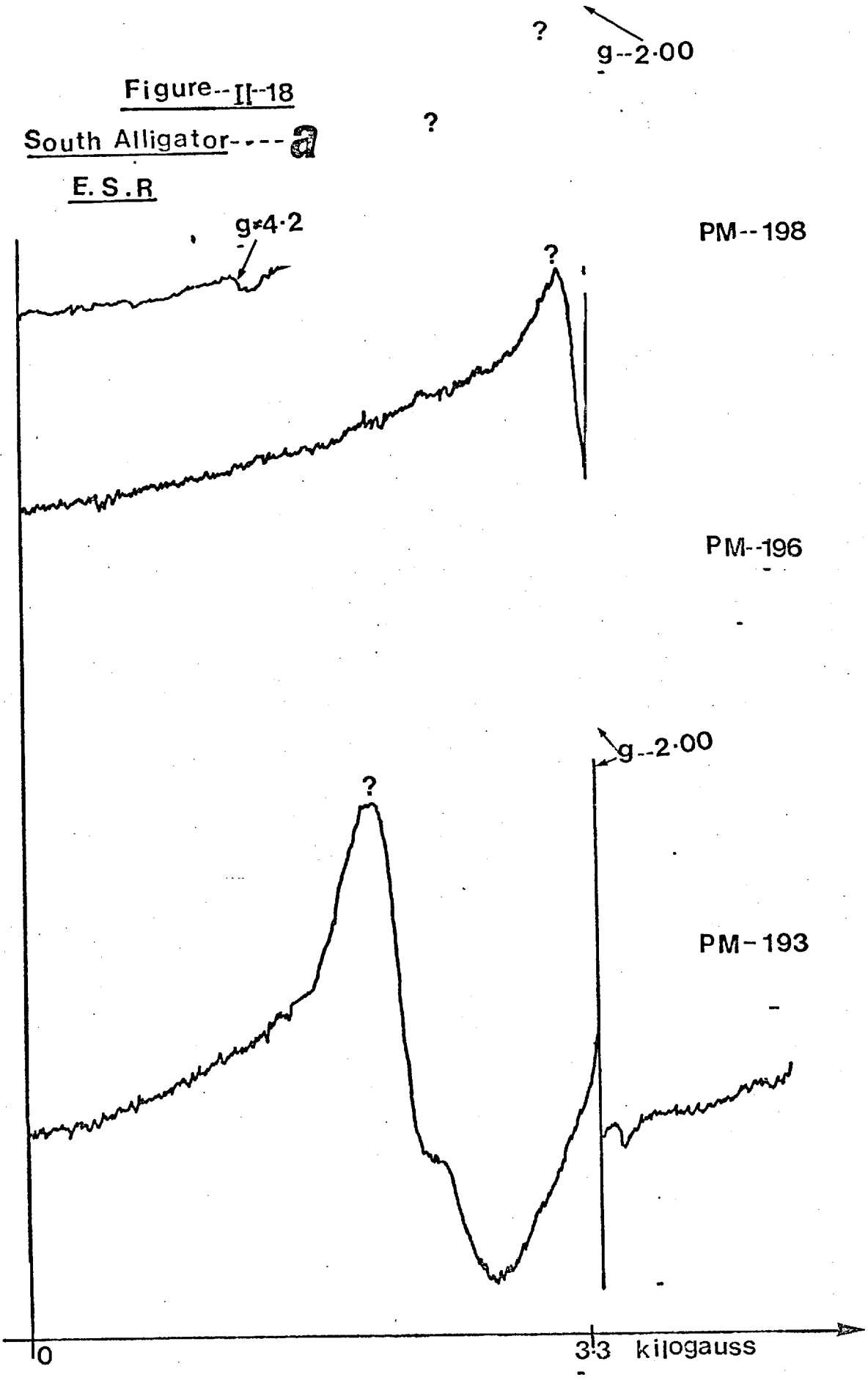
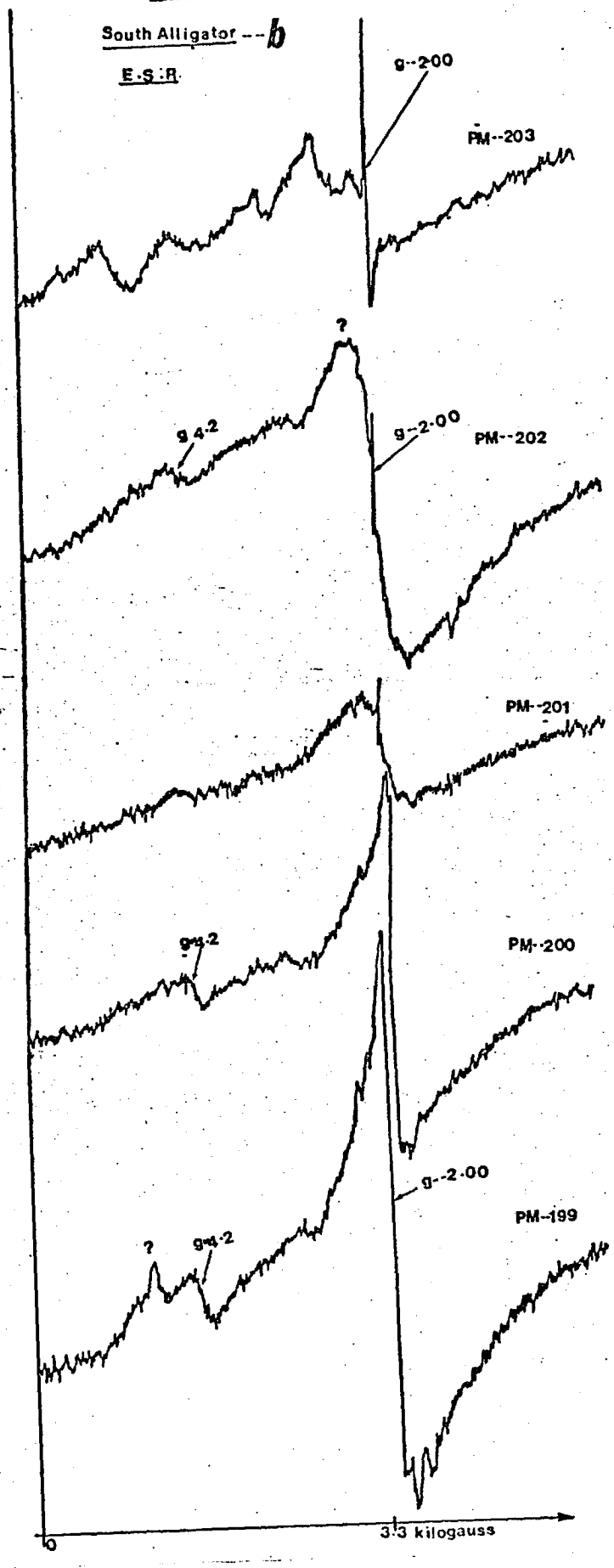


Figure-II-18


South Alligator --- b
E.S.R.
g--2·00
PM--203
?
g 4·2
g--2·00
PM--202
PM--201
g=4·2
PM--200
g--2·00
PM-199
?
g=4·2
0
3·3 kilogauss

From the spectra Fig. 17 and 18, there is a definite evidence of more than one type of absorption. The main features of the spectrum are the 'g' values at approximately 4.2 and 2.0 and occurs almost in all the analysed samples of these areas.

For some of the spectra, the "quantum-mechanical perturbation" theory approach is necessary, which the author feels less competent. Hence the empirical approach was considered for the assignment of the spectra. Some of the insoluble carbonaceous matter was analysed by X-ray micro-analysis (described below). Table (II) 9 shows the trace analysis for Australian samples. The analysis shows the presence of paramagnetic elements.

X-ray micro-analysis (XRM)

The micro-analysis was carried out on insoluble carbonaceous matter using ORTEC solid state Si(Li) energy dispersive X-ray micro-analyzer attached to a Stereoscan IIA. The out-put from the spectrometer is displayed on the cathode-ray tube of Northern Scientific Econ II Multi-channel analyzer. Line scans were recorded by chart recorder.

All specimens were glued on Al stub with 'Durofix' and coated with carbon to increase the conductivity between the specimen and the stub.

Qualitative elemental analysis is given in Table (II) 9 Also included H/C atomic ratio for Australian samples

TABLE (II) 9. X-ray Micro-Analysis & H/C Atomic Ration for Carbonaceous Matter from Australian Samples.

	Fe	Cr	Cu	V	Ti	Mn	Si	Ca	Pb	U	H/C
Pm- 1	++	+	-	-	+	-	-		-	-	0.13
19	++	+	-	-	-	-	+	+	-	-	-
38	++	+	-	+	-	Tr	+	+	-	-	0.67
47	++	-	-	-	-	Tr	+	+	Tr	?	0.92
48	++	-	-	-	-	-	-	+	Tr	++	3.70
49	++	-	-	-	-	-	-	+	Tr	++	2.09

Continuation .....TABLE (II) 9.

	Fe	Cr	Cu	V	Ti	Mn	Si	Ca	Pb	U	H/C
PM-195	++	-	-	-	+	-	-	-	-	-	-
196	++	-	TR	-	+	-	-	-	-	-	0.25
198	++	-	TR	-	+	-	-	+	-	-	6.77
199	++	-	-	-	-	-	-	-	-	-	0.96
200	++	-	-	-	-	-	-	-	TR	-	1.02
201	++	-	-	-	+	-	-	-	TR	+	0.18
202	++	-	-	-	+	-	-	-	TR	+	0.21
203	++	TR	-	-	-	-	-	-	TR	TR	0.39

\+ - represent the peak height of 1 square on the oscilloscope screen.

++ - " " " " " 2 " " " " "

TR - Barely visible peak over the background

? - possibly present.

Extension of X-ray Diffraction (XRD) to the measurement of crystallite Size of Carbonaceous Matter.

Preliminary data by XRD, ESR and Chemical analysis showed a systematic change (to be discussed later), and the XRD work was further extended to measure the crystallite size of carbonaceous matter from the Kromberg formation and sample PM-1 from Archean (Bulong near Kalgoorlie, W. Australia).

The Scherrer equation (1918) gives the relation between crystallite size and the breadth of diffraction peaks. The equation is expressed as:-

$$D = \frac{K\lambda}{B \cos \theta} \qquad \text{(II) 8}$$

where D = crystallite size in Å perpendicular to the diffracting planes

K = Constant (0.7 - 1.7) assumed to be 1.0 in this case.

λ = Wave-length of X-radiation in Å

B = Width of the diffracting peak at half height in terms of 2θ converted to radians

θ = Bragg angle at the maximum.

It is necessary to point out that the results are only relative as no correction factors were applied for diffracting wave-lengths of $K_{\alpha 1}$ & $K_{\alpha 2}$ X-radiation and for line broadening due to the instrumental factors.

In the present case the major error would probably result from drawing the base line on the XRD traces. The simplifying assumption is made that the crystallite would approximate a cylindrical shape (similarity with carbon residues of coals and carbon blacks), therefore the *(001)* planes representing the peak can be used for estimating the height of the cylinder: that is the *C*-axis of the crystallite the *(1oo) (oko)* planes representing poles can give an average value for the diameter of this hypothetical cylinder.

Table (II) 10 shows the crystallite size in Å for the insoluble carbonaceous matter from the Kromberg Formation and sample PM-1 (Kalgoorlie) for comparison.

TABLE (II) 10. Crystallite Size for Insoluble Carbonaceous matter from Kromberg Formation.

Sample No.	Crystallite size Å
K-1A	480.46
K-3	1093.43
K-4	310.19
K-6**	-
K-7	19.31
HALL-1	530.53
HALL-2	21.23
HALL-1 W/1	24.16
PM-1	304.60

** Sample contaminated with filter paper during filtration.

CHAPTER III

CHAPTER III

A. METAMORPHISM OF IRON FORMATION

The purpose of this chapter is to evaluate the significance and role of metamorphism in BIF and to recognize the consequent changes in the minerology of the iron formation. This will be discussed with special reference to four major sedimentary iron-rich facies and examples will be cited from the literature and previous work. James (1954) had delinated four sedimentary facies on the basis of the dominant iron minerals. They are sulphide, oxide, carbonate and silicate facies. The effect of metamorphism on organic matter and delination of organic facies will be discussed later.

1. Metamorphism of Sulphide Facies:- This facies is composed of finely banded rock or slate with variable amounts of pyrite, mostly concentrated in layers.

Effect of metamorphism

(i) The grain size of pyrite generally increases with increasing grade of metamorphism (James, 1954) e.g. Wabush iron formation (Klein, 1964).

(ii) Pyrrhotite will be formed rather than pyrite, under high grade metamorphic conditions (Gundersen & Schwartz, 1962), e.g. Biwabik iron formation (French, 1968).

2. Metamorphism of Oxide Facies:- This facies consists mainly of finely banded mixtures of chert, quartz or jasper, magnetite or hematite and at certain times hydrous iron oxides. The unmetamorphosed Sokoman iron formation in West Central Labrador contains rocks of this type (Perrault, 1955). These rock types are also described by James (1955) and French (1968) in Biwabik

Iron formation and by Trendall & Blockley (1970), for the Hamersley Group.

Effect of metamorphism

(1) Recrystallization of chert and iron oxide takes place with marked increase in grain size of quartz.

(ii) Average grain size of quartz is less than 0.1 mm for low grade metamorphism.

(iii) Average grain of quartz is 0.1 mm to 0.22 mm for higher grade metamorphism.

Similar results were reported by Gross (1961) for the iron formation of Labrador Trough, Canada and by Dorr (1964) for Minas Gerais, Brazil.

3. Metamorphism of Carbonate Facies

This facies consists of carbonates (such as siderite, ferroan dolomite-ankerite series and calcite) and banded mixtures of chert or quartz and lesser amounts of magnetite and primary iron silicates. Examples of these are found in rocks described by James (1954) from Lake Superior iron formations. Also French (1968) reported rocks consisting of siderite and ankerite from metamorphosed cherty taconite from Biwabik Iron formation.

The Hamersley Group in W. Australia contains rocks with bands of siderite or ankerite in more or less unmetamorphosed iron formation. Trendall and Blockley (1970) and this work.

Effect of metamorphism:- (Medium to High grade)

(i) Original carbonates still present, indicating that the chemical potential of CO_2 was very high e.g. North Michigan Formation

(James, 1955). Biwabik formation zone 3 (French, 1968).

(ii) a. If the chemical potential of CO_2 is low, new silicates will form according to the following simplified reaction:-

$$Ca(Fe,Mg)(CO_3)_2 + 2SiO_2 = Ca(Fe,Mg)Si_2O_6 + 2CO_2 \qquad \text{Eq. (III) 1}$$

↑ Ferroan dolomite ↑ Clinopyroxene

b. If H_2O is present chemical potential is high, the silicates will be formed according to the following reaction:-

$$5Ca(Fe,Mg)(CO_3)_2 + 8SiO_2 + H_2O \rightarrow Ca_2(Fe,Mg)_5Si_8O_{22}(OH)_2 + 3CaCO_3 + 7CO_2 \qquad \text{Eq. (III) 2}$$

↑ Ferroan dolomite ↑ Actinolite

$$8(Fe,Mg)CO_3 + 9CO_2 + H_2O \rightarrow (Fe,Mg)_7Si_8O_{22}(OH)_2 + (Fe,Mg)SiO_3 + 8CO_2 \qquad \text{Eq. (III) 3}$$

↑ Siderite ↑ Grunerite ↑ Orthopyroxene

(iii) Oxidation of iron carbonates to form Magnetite:-

$$6FeCO_3 + O_2 \rightarrow 2Fe_3O_4 + 6CO_2 \qquad \text{Eq. (III) 4}$$

An example is found in low grade metamorphic parts of the iron formation of the Lake Superior region (La Berge, 1964).

4. Metamorphism of Silicate facies:- This is the most complex facies. It consists of hydrous iron silicates, calcite, siderite, dolomite ankerite series, chert or quartz and iron oxides mainly magnetite. The quartz-silicate assemblages are interbanded with quartz-carbonate-magnetite horizons.

Effects of metamorphism:-

During progressive metamorphism:-

(i) Various stages of dehydration takes place provided the original silicate facies contain mainly greenalite, minnesotaite or stilpnomelane.

(ii) Decarbonisation and dehydration takes place if carbonates are present.

Figure (III) 1 shows schematic diagrams for the changes during progressive metamorphism (Klein, 1973).

The simplified chemical equations for these cahnges are given below:-

(a). $(Fe,Mg)_6Si_4O_{10}(OH)_8 + 4SiO_2 \rightarrow 2(Fe,Mg)_3(Si_4O_{10}(OH)_2 + 4H_2O$

Greenalite — Minnesotaite

Eq. (III) 5

(b). $(Fe,Mg)_3Si_4O_{10}(OH)_2 \rightarrow (Fe,Mg)_7Si_8O_{22}(OH)_2 + 4SiO_2 + 4H_2O$

Minnesotaite — Grunerite

Eq. (III) 6

(c) $2(Ca,Na,K)_4(Al_2Fe_{35}Mg_9)(Si_{63}Al_9)(O,OH)_{216} \cdot nH_2O =$

Stilpnomalane

$\sim 11(Fe,Mg)_7Si_8O_{22}(OH)_2 +$

Grunerite

Eq. (III) 7

$\sim 3(Ca,Ma,K)_{2.6}(Mg,Fe,Al)_5(Si,Al)_8O_{22}(OH)_2 + \sim 26SiO_2 + 44H_2O$

Hornblende

(d) $4(Fe,Mg)_3Si_4O_{10}(OH)_2 + 2Ca(Fe,Mg)(CO_3)_2 + SiO_2 =$

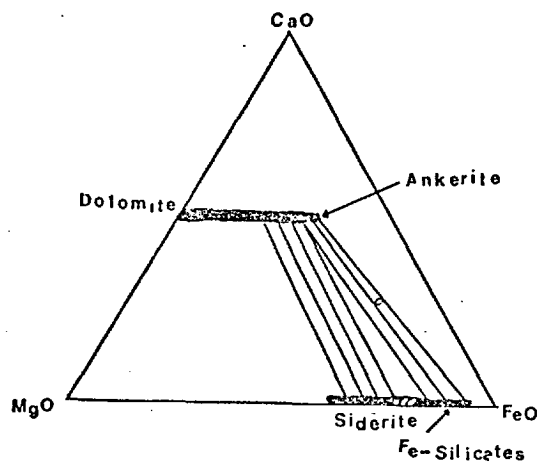
Minnesotaite — Ferrodolomite

Eq. (III) 8

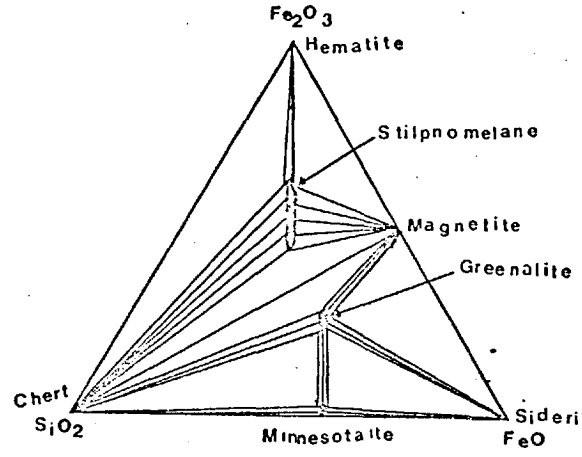
$(Fe,Mg)_7Si_8O_{22}(OH)_2 + Ca_2(Fe,Mg)_5Si_8O_{22}(OH)_2 + 2(Fe,Mg)SiO_3 + 4CO_2 + 2H_2O$

Grunerite — Ferroactinolite — Orthopyroxene

Examples of these reactions are found in Bewabik iron formation of Zone I and Zone III (French, 1968).



A

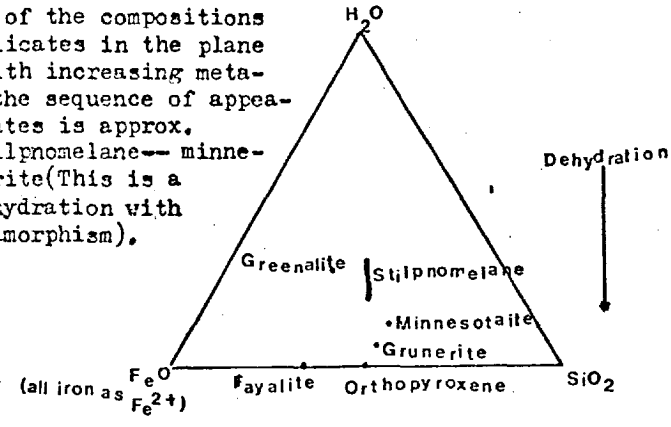


B

A:Schematic diagram for assemblages in unmetamorphosed quartz-silicate iron-foration, in the system FeO-MgO-CaO-SiO_2-CO_2 .(H_2O and CO_2 are considered as perfectly mobile components.

B:Schematic diagram for assemblages in unmetamorphosed quartz-silicate iron-formation in the system FeO-Fe_2O_3-SiO_2-H_2O-CO_2.(H_2O and CO_2 are considered perfectly mobile components.
The consideration of the Fe^{3+} component allows for the schematic delineation of the compositional fields of several of the primary or diagenetic iron silicates.

C:Representation of the compositions of the iron silicates in the plane FeO-SiO_2-H_2O.With increasing metamorphic grade the sequence of appearance of silicates is approx. greenalite--stilpnomelane-- minnesotaite--grunerite(This is a sequence of dehydration with increasing metamorphism).



C

Figure-III-1 Schematic diagrams showing the changes during progressive metamorphism.
(After Klein,1973)

The above discussion summarizes three types of mineral assemblages in different grade of metamorphism. Table (III) 1 below, reproduced from French (1973), summarized the following observations:-

(1) Primary assemblages made up of quartz (chert), siderite, greenalite, and hematite with minor amounts of chlorite and magnetite.

(2) On low grade metamorphism the assemblages consist of siderite, ankerite, calcite, quartz and possibly magnetite.

(3) For low grade metamorphism approximating to chlorite stage, development riebeckite, stilpnomelane, minnesotaite are probably from earlier primary or secondary minerals.

TABLE (III) 1. Mineral Assemblages in Diagenetic and Low Grade Metamorphic Iron Formation (Adapted from French, 1973).

Pressure & Temperature Condition	Original Material	Diagenetic		Low grade Metamorphic
		Primary	Secondary	
Temperature	< 100°C	100-150°C	150-200°C	200-350°C
Pressure	< 100 b	1Kb	1-2Kb	2-5Kb
	Magadiite Na-Si gel	Chert	Quartz	Quartz
	$Fe(OH)_3$ $Fe(OH)_2$	Hematite Magnetite(?)	Hematite Magnetite	Hematite Magnetite
	$FeCO_3$	Siderite	Siderite	Siderite
	$(Fe,Mg,Ca)(CO_3)_2$		Ankerite	Ankerite
	(gels)			Magnetite Minnesotaite Stilpnomelane Riebeckite
	Fe-Si gel Greenalite(?)	Greenalite Chamosite(?)	Greenalite(?) Chamosite Chlorite	Chamosite(?) Chlorite Magnetite Minnesotaite Stilpnomelane Riebeckite
	Volcanic glass Clay minerals (Na,K)-Fe-Si gel	Montmorillonite Illite glass	Montmorillonite Illite Chlorite Stilpnomelane(?)	Chlorite Stilpnomelane Riebeckite

B. EFFECT OF METAMORPHISM ON CARBONACEOUS MATTER

Most of the organic debris that has come to rest on earth is found in sediments. Hunt (1962) analyzed 100 rock speciments collected from various formations from major sedimentary environment. Shales average 2.1%, carbonates 0.29% (Gehman, Jr., 1962) and sandstone, 0.05%. Using these data, Weeks (1958) reported the total organic matter entrapped in sediments as approximately 3.8×10^{15} metric tons with 3.6×10^{15} metric tons in shales. This organic matter is mostly found in a finely disseminated state associated with fine grained sediments. Igneous rocks contain five percent of carbonaceous matter.

The carbonaceous matter in rocks is not easily characterized because of inherent analytical difficulty and therefore has been given less attention than it deserves. However, the point in favour is the stability of individual organic compounds under diagenetic condition, which is very high for some of them, for example, Amino acids are stable over million years under low temperature conditions. This is reflected from experimental work done by Vallentyne (1957), Conway and Libby (1958) and Abelson (1959). Small amounts of combined sugars (0.1-10ppm) have been reported by Palacas (1959) from ancient sediments as old as Precambrian. Lipids and related compounds also appear to be stable (Degens, 1967).

Petroleum geologists have developed a new concept of organic facies, and have used organic matter in sedimentary rocks as an indication of the degree of metamorphism.

The three organic facies that develop with increasing temperature/time are defined by Staplin et al. (1973).

(1) Immature facies with abundant methane, trace quantities of C_2-C_{14} hydrocarbon and a C_{15}+ fraction containing non-hydrocarbon compounds.

(2) The mature facies consists of a complete spectrum of hydrocarbon (C_{15}+)

(3) The metamorphic facies consists mainly of methane and traces of heavier hydrocarbons, and practically no non-hydrocarbon material in the C_{15}+ fraction (indicating thermal destruction).

The three facies are summarized in Table (III) 2 below.

TABLE (III) 2. Thermal Facies

Metamorphic Facies	Gas C_1-C_4	Gasoline C_4-C_7	Kerosene C_8-C_{14}	Heavies C_{15}+	Solids Kerogen
Immature	Mainly C_1	Lean	Lean	Rich	Faint Yellow
				Mainly hydrocarbon	Yellow
Mature	Mainly C_2-C_4	Rich All components	Rich	Rich-both hydrocarbons & non-hydrocarbons	Yellow Brown
Metamorphosed	Mainly C_1	Lean absent	Lean absent	Lean-mainly hydro-carbons	Brown-black Black

During low grade metamorphism, the carbon content of carbonaceous matter increases gradually with a corresponding rise in rank. This process is termed "Coalification". On the other hand if the process is rapid, and carbonaceous matter is rapidly heated and charred, the process is termed "Carbonisation". Sometimes these two terms are misleading as some authors use them as if they are synonymous (McIntyre, 1972).

In both processes, there is a cleavage of molecular bonds, which eliminates the lower molecular weight compounds and proceeds towards an enrichment of carbon content. Carbon-dioxide and methane are the initial

products that are first eliminated. Ultimately the reaction ends in formation of graphite (for coalification) and amorphous carbon (coke) (for carbonisation). Coke can ultimately be converted to graphite if high enough temperatures are available.

The effect of low grade metamorphism on carbonaceous matter is coalification - gradual change in the rank via slow maturation. This can either be caused by (i) heat or (ii) Shear. The rhombohedral modification of hexagonal graphite, observed in the Onverwacht is believed to be due to Shear in the Kromberg formation Karkhanis (1975).

C. EFFECT OF METAMORPHISM ON FOSSILS (Fossil Diagenesis and its Preservation)

Apart from odd laboratory simulated experiments (Oehler and Schopf 1971) there is not much known about the effect of metamorphism on fossils. Considerable amount of information, however, is available, primarily on pollen and spores (Gray and Boucot, 1975) and coal (Teichmuller and Techmuller, 1968), (Sen Gupta, 1975).

It is, however, true that most Precambrian fossils so far investigated and previously reported do not possess any hard (mineral) parts in their structure, and the whole entity can be regarded as carbonaceous organic matter. As such for all practical purposes, it can, therefore, be investigated as any other carbonaceous matter for example "coal". The comments from section IIB are equally applicable.

In the course of fossil diagenesis sometimes the organic substances are replaced by inorganic substances both of which may subsequently be destroyed. This process is known as leaching diagenesis (Thenius, 1973). If

some of the original structure is retained, a complete substitute of original remains by infiltering water is secondarily filled by crystals to form a pseudomorph.

Fossilization results in quite a different state of preservation. Most important agents are carbonates mainly in the form of Calcite and dolomite and sometimes silica. Sometimes they are converted into pyrite or marcasite. A minor occurrence in fossil diagenesis is the limonitization - by iron hydroxide, which may be in the form of brown iron stone and conversion to sulphates, phosphates and sometimes gluconites (Thenius, 1973).

CHAPTER IV

CHAPTER IV

MICROPALAEONTOLOGICAL STUDIES

In attempt to detect microfossils in the samples, Optical microscopic studies were made on petrographic thin sections and acid resistent (INHCl, 40% HF) insoluble organic residue. The insoluble residues were further examined in detail by S.E.M.

In this section various occurrences of cellularly preserved micro-organisms previously reported from the Precambrian will be listed and the assemblages of structurally and organically preserved organisms that were observed during this work will be reported. Wherever possible photographs of present day micro-organism or distinct entities or 'types' of existing microscopical organisms will be shown for comparative purposes.

No attemp will be made to discriminate specimens from particular strata or sequences. The procedure adopted here will be listing of micro-fossils from the whole locality (for previous work) and for this work, it will be restricted to the area of sampling. For example, Swaziland sequence (for previous work) and Kromberg formation (This work).

TABLE (IV) 1. Micropalaeontologic Occurrences in

(A) Swaziland Sequence Barberton mountainland, South Africa.

Name	Description	Size	Shape	Stratography	Affinity	Rock Assemblages	Reference
Organized elements	Well developed micro-structures with tear marks	6-20μ	Spheres with 'double walls'	Through the Onverwacht Group	Do not meet the criteria for biological origin	Argillaceous chert and carbonates	Engel et al. (1968) Nagy & Nagy (1968-69)
Archae-sphaeroids barbertonen-sis	Unicellular, isolated organic sphaeroids	Av.dia. 19μ	Sphaeroid	Fig Tree Group	Blue-green algal group chroococ-cales	Black chert facies	Schopf and Barghoorn (1967)
Eobacterium isolatum	Irregular filamentous organic structures	Av.length 0.55μ	Rod-shaped	Fig Tree Group Barberton	Bacterium like	Chalcedonic black chert	Barghoorn and Schopf (1966)
Type-A	Opaque, egg-shaped, hollow	20-60μ	Globular	Fig Tree series	Resembles cysts of flagellets	Chert	Pflug (1967)
Type-C	Sphaeroidal cork-screw like contorted threads	20-30μ	Filamentous	Vicinity of Sheba Gold Mine	Nostocalean blue-green algae	Shales & Cherts	" "
Type-B,D,E	are structures observed in maceration and they are questionable whether the forms have retained the vestiges of the original shape of organism or whether they have formed under inorganic conditions in a fracture.						" "

continued.....

TABLE (IV) 1.A. (Continuation)

Name	Description	Size	Shape	Stratigraphy	Affinity	Rock Assemblages	Reference
-	Alga-like form	< 30μm	-	Fig Tree Group	-	-	Engel et al. (1968)
-	Roughly sphaeroidal with small dimple or depression	15-20μm	Sphaeroidal	Kromberg, Swartkoppie	Biogenic	Chert	Brooks & Muir (1971)
-	-	20-50μm	-	Fig Tree Group	-	Chert	Dungworth & Schwartz (1972)
-	Hollow filamentous	4-8μm	Filamentous	Theespruit	Biogenic	Chert	Brooks, Muir & Shaw (1973)
-	Complex forms sphaeroids single or paired filaments (segmented or non-segmented)	3-7μm 1-3μm dia. 25-42μm long	Sphaeroid Septate & non-septate filaments	Kromberg	Biological possibly comparable with remains of organisms in modern laminated mats	Carbonaceous	Muir & Hall (1974)

This table is incomplete without these references cited.
The first reference is a review paper Schopf (1975). The second reference Muir & Grant (1976) gives the micropalaeontological evidence from Onverwacht Group and the third reference Muir et al. (1976) discusses the criteria for biogenicity for these fossils.

TABLE (IV).1

(B). Southern Cross - Western Australia.

Name	Description	Size	Shape	Stratigraphy	Affinity	Rock assemblages	Reference
R. Series	Basiliform object about 2.3x3.1μ with further elongation with central construction	2.3 dia.	Spheres	Archaean	Biological affinity	Fine-grained quartzite associated with banded iron formation	Marshall et al. (1964)
Y. Series	Double budding pyriform or peg top shape rod with clubbed ends with pairs of lateral buds on one side K-shaped tetrad pyriform lobes, sometimes hexads, decads and later multiple buds.	0.6-0.8μ		Archaen	Biogenic, iron oxidizer?	Quartzite	"
M. Series	Consists of yellow core lacking the symmetrical lobulate structure filamentous and sphaeroids	8μ across		"	Biogenic	"	"
				Tertiary or more recent contamination	Biogenic		Muir, Hamilton et al. (1974)

(C) S. Alligator: No microfossils have previously been reported from this area.

TABLE (IV) 1.

(D). Hamersley - Western Australia

Name	Description	Size	Shape	Stratigraphy	Affinity	Rock Assemblages	Reference
Laberge's Type C	Thick-walled, rugose and internally chambered	12-25μ in diameter	Sphaeroidal	Brockman iron formation	Organic origin	Chert matrix	Laberge (1967)
Laberge's Type D	Outer walls thinned and reticulate surface	15-25μ in diameter	"	Wittenoom gorge	"	Chert and Jasper layer	"

Edgel (1964) has reported fossil calcareous algal growths, such as stromatolites and onkolites and some possible medusoid impressions. He has placed emphasis on the possible significance of calcareous algae for stratigraphic correlation. He provides evidence for the occurrence of algal growths from Brockman iron formation and possibly for the Wittenoom dolomite.

PLATE--IV--1

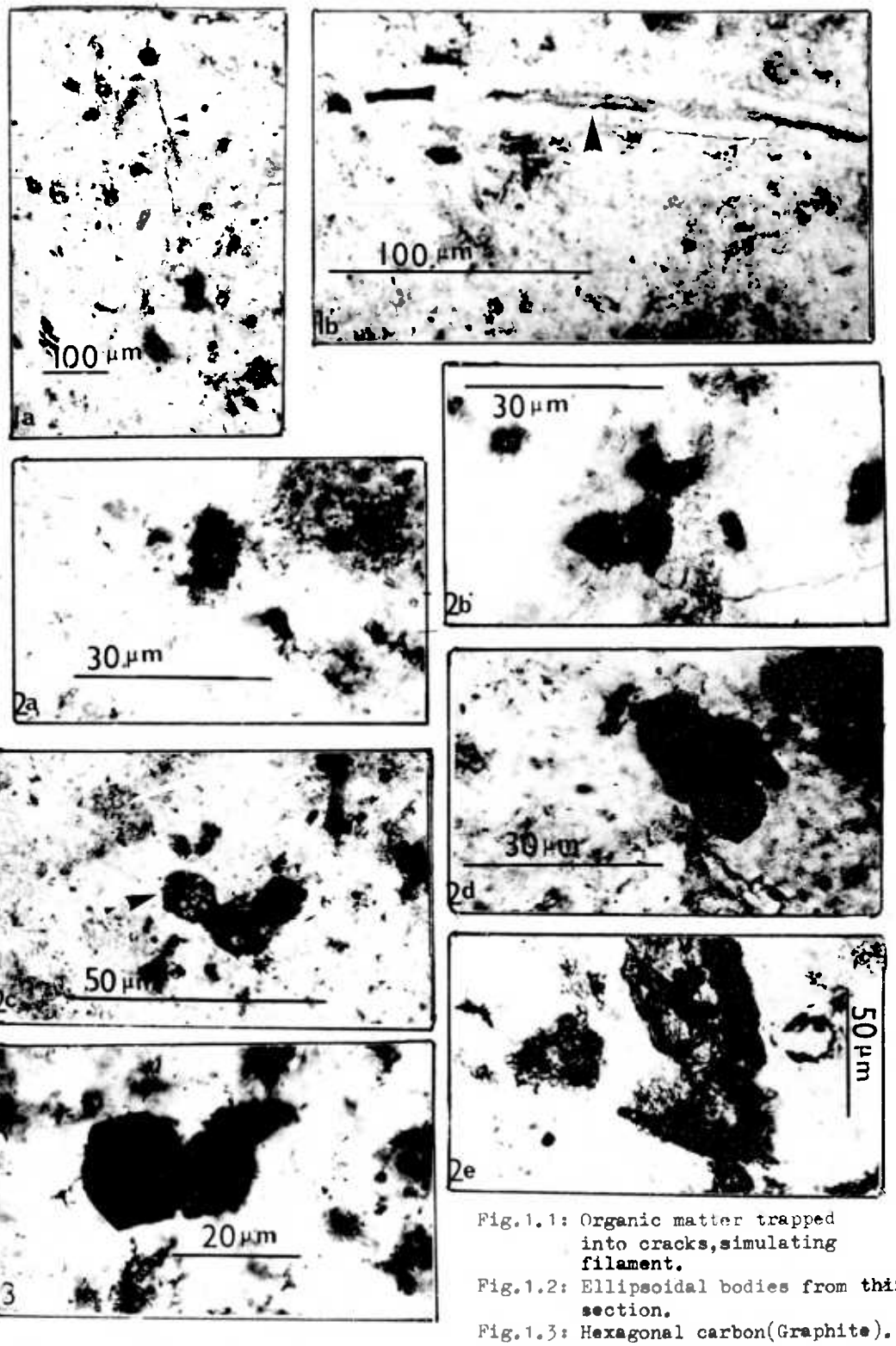


Fig.1.1: Organic matter trapped into cracks, simulating filament.

Fig.1.2: Ellipsoidal bodies from thin section.

Fig.1.3: Hexagonal carbon(Graphite).

THIS WORK (Micropalaeontological investigation)

A. Kromberg Formation:-

Microscopic examination of thin sections from this formation showed that the rocks indicate some porosity. This was very evident for Sample Hall-1, which showed numerous cross-cutting fissures. Some of the fissures were found to be filled with organic matter, appearing deceptively like filaments. Also crack fillings are planar features but filaments are not. Plate (IV) (1) 1a, b is such a false filament (arrow). Hence care is necessary in discriminating contamination and artefacts. In the present work, the thickness of the structure was applied to discriminate between real filaments and false ones. Examination of a number of thin sections showed that real filaments were much wider than fals filaments from cracks and fissures.

Plate (IV) 1, 2a, b, c, d and e all show ellipsoidal bodies observed in thin sections. The blackness of the organic matter indicates the amount of carbonisation and mineralisation where present. 2a is a single ellipsoidal body resembling somewhat Globular Type A microfossil of Pflug (1967). In 2c, d, and e, it seems that the individual ellipsoidal bodies are united to form a chain. 2c shows a fine quartz inclusion (arrow) giving a reticulate appearance. The other two bodies are highly carbonised. 2e shows four such bodies attached end to end to form a beaded filament, which is also highly carbonised and pyritized. It seems that (2e) is an example of pressure solution and force of crystallization. Similar example has been sited from P.M.17 (Hamersley). See Plate (V) (8) 1.

Plate (IV) (1) 3 shows -two hexagonal structures- the one larger has a perfect six-sided outline and the smaller has also six-sided morphology in this section {H-1(4)}. In view of the fact that X.R.D. on the in-

PLATE - - IV-2

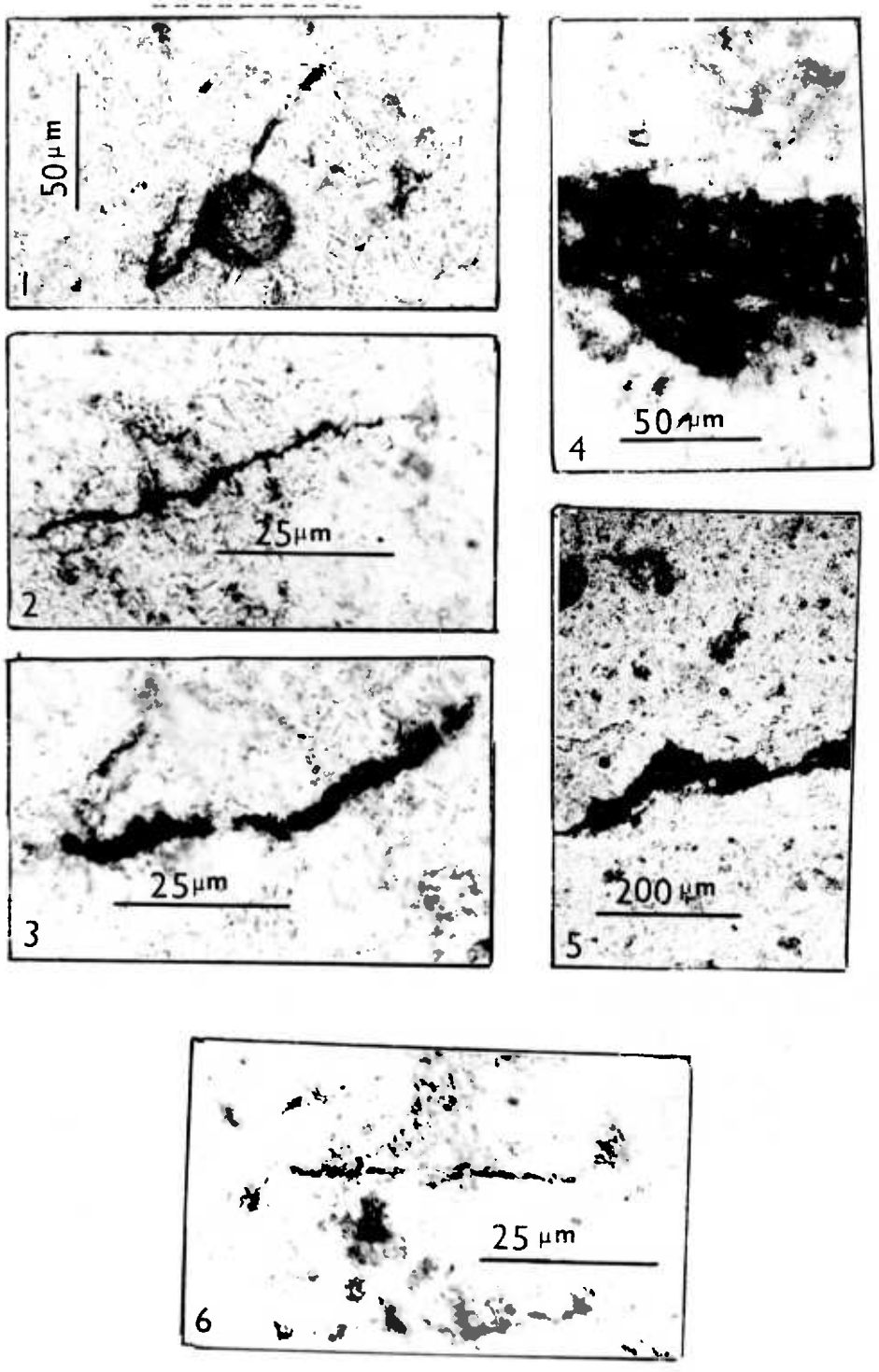


Fig.2.1,2&3: Fossils resembling Type 'D' of Pflug.
Fig.2.4 : Algal mat.
Fig.2.5 &6 : Example of fracture filling by organic matter.

PLATE---IV-3

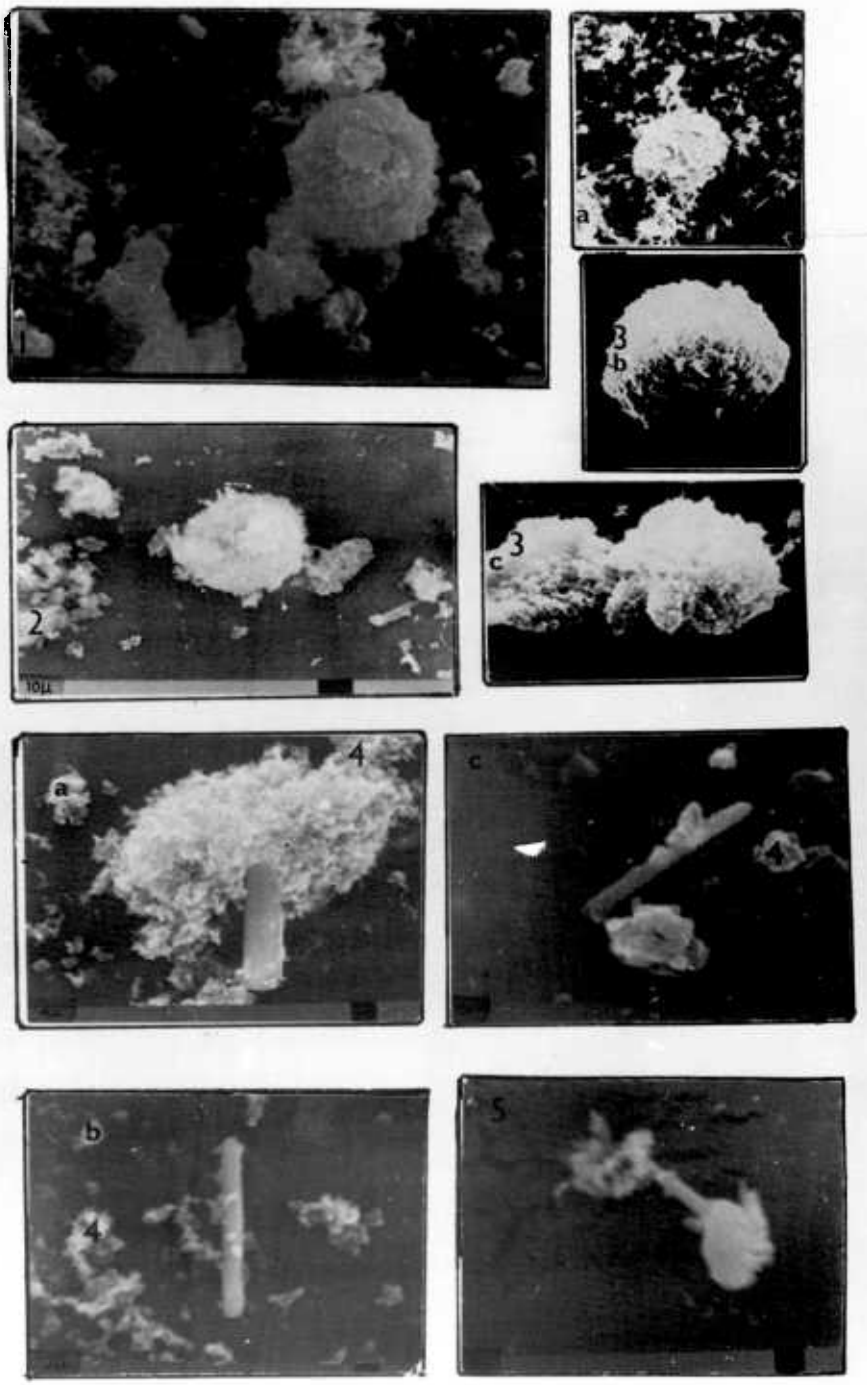


Fig.3.1 &2:Sphaeroidal objects from Kromberg formation (S.E.M.).
Fig.3.3 :Sphaeroidal object from Swartkoppie formation.(from Brookes and Shaw(1973) with kind permission from the publishers.
Fig. 4 :Fluffy organic matter from Kromb erg formation.
Fig. 5 :Filament attached to the oval body.

soluble carbonaceous matter in this sample showed well-ordered graphites peak (See Fig. (II) 8 trace 4). It could be concluded that this is carbonaceous matter, which has been carbonised to graphite.

Pl. (IV) (2) 1, 2 and 3 resemble filamentous type D bodies of Pflug (1967. The only difference worth noting is that his observations were made for macerated preparations, while here the filaments are show in thin sections. P. (IV) 2, 4 shows a structure formed of individual filaments to those in Fig. (1), (2), (3). It is possible that the individual filaments lined parallel to each other, wall to wall, produce a form 'mat'.

Note the difference in Fig. (5) and Fig. (4). In Fig. (5) the organic matter has entered in the fractures and occupies space in the matrix. The organic matter has been compressed against the walls of the fractures giving the basic appearance of a filament or a mat, whereas in Fig. (4), one can see distinctly individual filaments.

Pl. (IV) (2) 6 is a further example of narrow fracture filling, which simulates filamentous structure. In this case the organic material is squashed in quartz (chert matrix) infillings.

The insoluble organic residues from all these samples were mounted on a stub and examined by S.E.M. 600.

Pl. (IV) (3), Fig. 1 and 2 shows sphaeroidal objects comparable with the specimens illustrated by Brooks and Muir (1971). (Fig. 3a, b, c) for the Onverwacht chert and Schopf (1970) for the Bitter Springs formation.

Pl. (IV) (3), Fig. (4) shows filaments which is cylindrical and covered with fluffy organic matter. One such isolated filament is shown in Fig. (4) b, c. Fig. (5) shows another such filament attached to an oval body.

PLATE IV-4



Fig.4.1: Eobacterium isolatum.

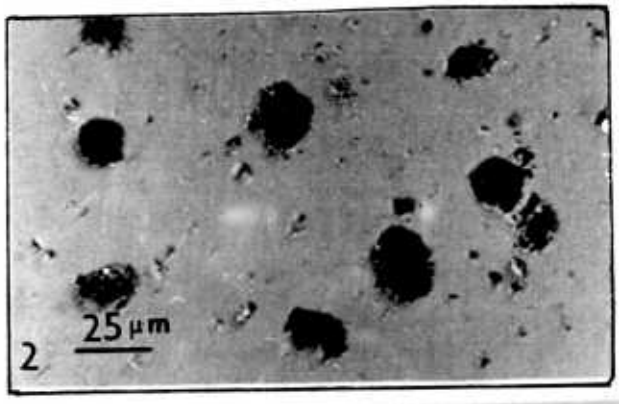


Fig.4.2:Structures formed in maceration technique.

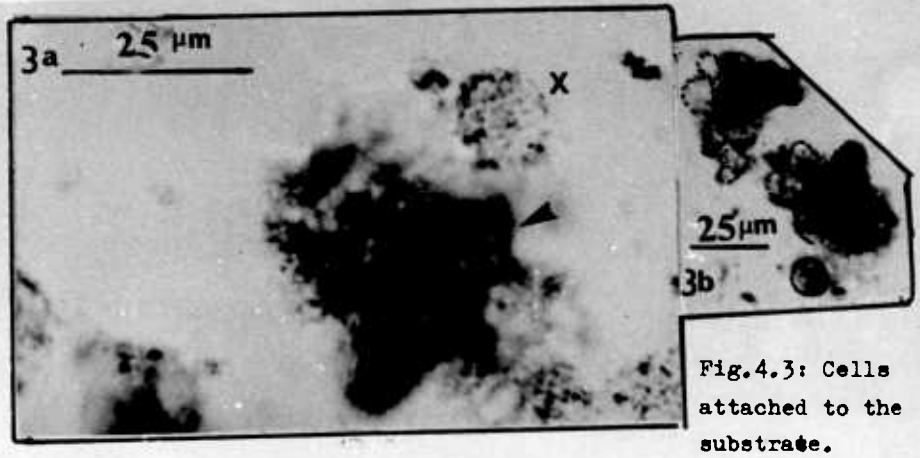


Fig.4.3: Cells attached to the substrate.

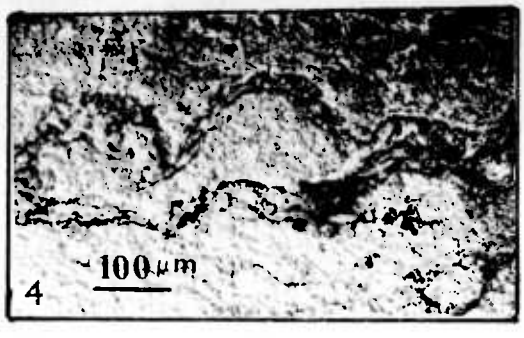


Fig.4.4.Microstromatolite?

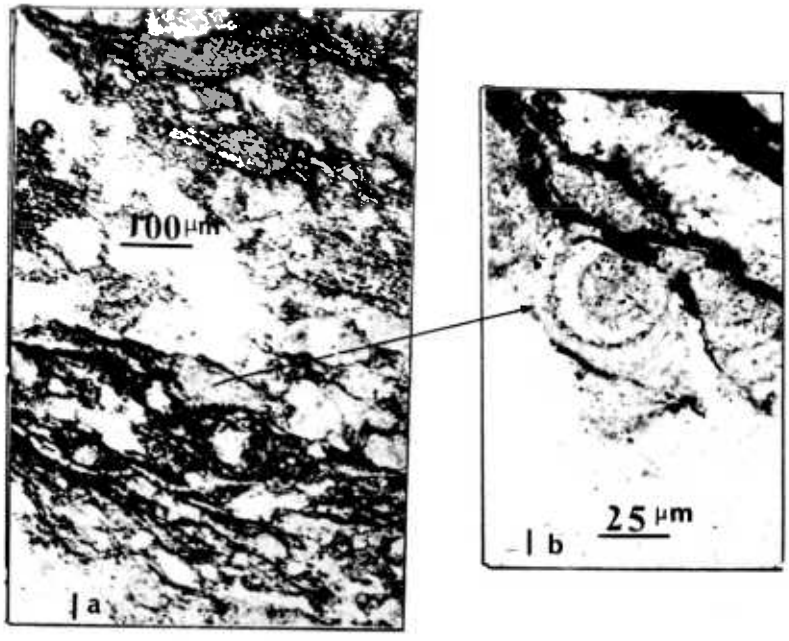


Fig.5.1a Algal mat showing onkolite.
Fig.5.1b Onkolite under high power (×100).



Fig.5.2 : S.E.M.photograph showing septate filament.



Fig.5.3: Vacuoles or pockets of traps possibly for oil bearing material?

Pl. (IV) (4), Fig. (1) looks like a flattened bacterium like cell interpreted here as *Eobacterium isolatum*. The specimen is comparable to the specimen illustrated by Barghoorn and Scopf (1966) from the Fig Tree.

Pl. (IV) (4), Fig. (2) shows a number of sphaeroidal structures produced by maceration technique.

In Pl. (IV), Fig. (3a) such a single cell marked 'X' is seen and the area marked by an arrow shows the number of cells, which, when seen at different focii, appears to consist of numerous individual cells bunched together. Fig. 3b is a tracing showing details of cells and their organisation. Muir & Grant (1975).

Pl. (IV), Fig. (4) is a layer of algal mat observed in this sections. The fine grain quartz and some iron minerals (opaque) are trapped between some layers. Could this be a *microstromatolite?*

B. South Alligator

Plate (IV) (5) 1 is a photograph of thin section PM-196 revealing algal mat in which there are a few occurrences of concentric bodies like *onkolites*. There are numerous bodies like this. Under high power, concentric layers are distinctly seen (Photograph 1b). The whole structure looks mucilaginous and possibly contains some minute sand grains (photograph (1b). The minerolo- of this sample is quite simple-quartz and minor amounts of clay minerals.

Pl. (IV) (5) 2 is a scanning electron micrograph of an acid resistant residue of PM-200 showing a filament with distinctly visible speta.

PM-203 has a layer algal mat with numerous pockets or vacuoles (see Arrow), which are possibly the traps for oil bearing material (Photomicrograph 3).

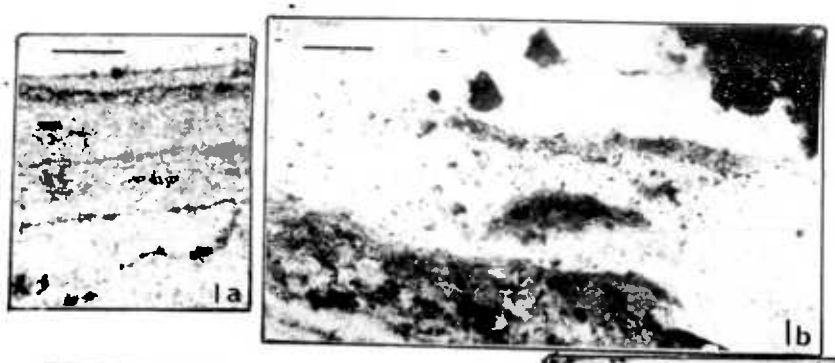
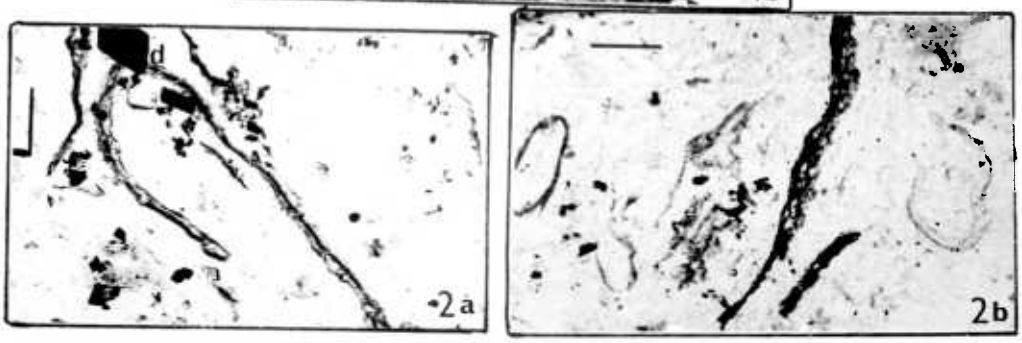
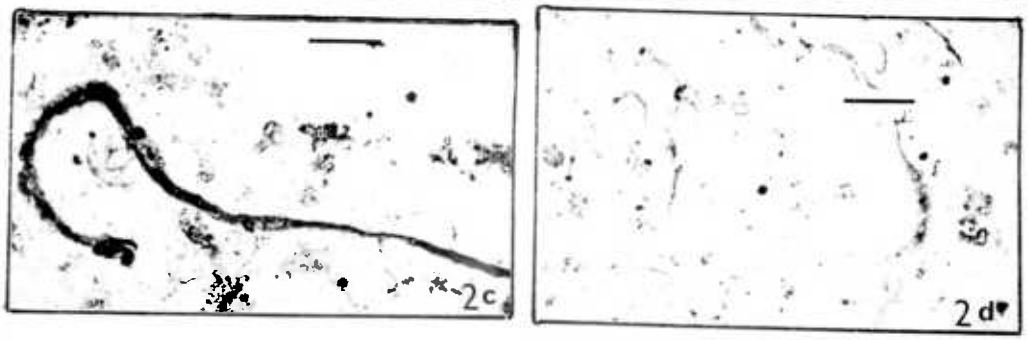
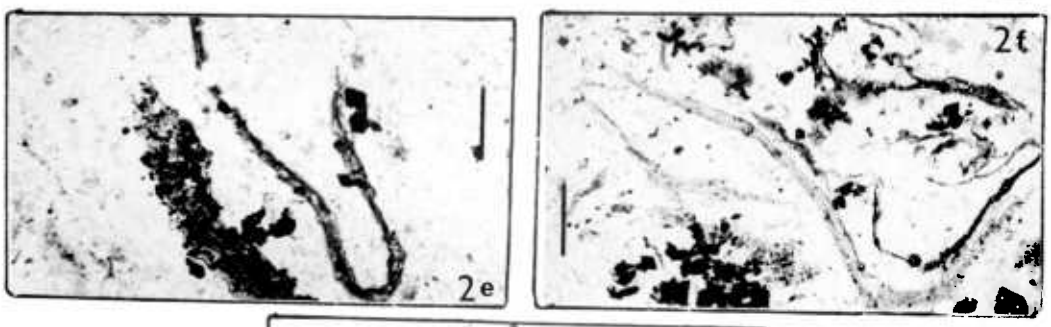
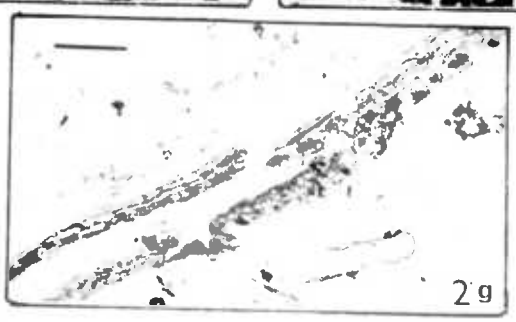


Fig.6.1:Stratified Algal mat.





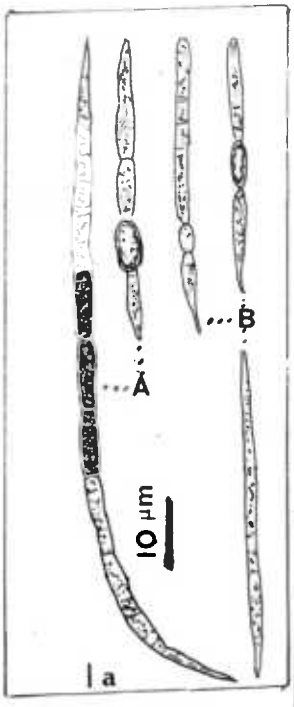


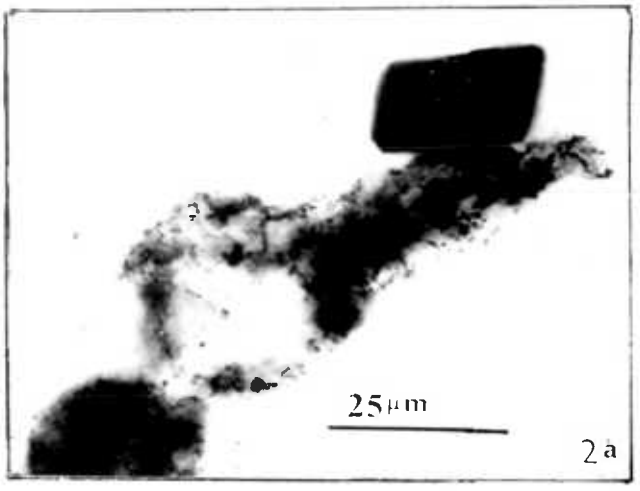


Scale Bar = 100μm

Fig.6.2 :Petrographic thin section of PM-38 showing high energy environment of deposition.

PLATE--IV--7





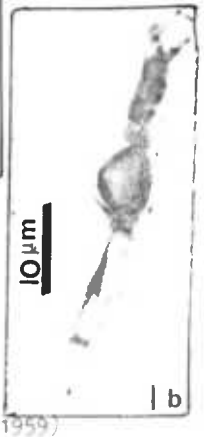




Fig.7.1a(A) : Raphidiopsis mediterranea

7.1a(B) : Raphidiopsis indica. (after Desikachary, 1959)

Fig.7.1b: Petraphera vivescenticulata.

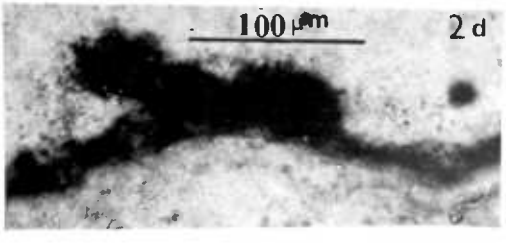


Fig.7.2a,b,c,d : Akinete like structures.



Fig.7.1b: (after Nagy, 1974).

C. Hamersley Region

Stromatolites have previously been reported, Edgell (1964), Walter (1971). Many samples show stratified algal mats. This is particularly prominent in the petrographic thin section PM-38, which is shown in Pl. (IV) (6) 1a, b. In this same section, individual filaments are commonly seen separated. The curly appearance and irregular spread of these filaments indicate that the original environment of deposition was very high energy environment with high degree of water agitation and turbulence (Fig. (2) a-g). The section gives an appearance of a "burial ground" (Fig. (2) d). Fine filaments are seen in better preserved condition and they resemble the recent species of cyanophytes. *Raphidiopsis mediterranea* and *Raphidiosis indica* Pl. (IV) (7) 1 (A) & (B), respectively described by Desikachary (1959) and Nagy (1974) have described well-preserved fossil remnants of filamentous blue-green algae from dolomitic limestone from Transvaal Sequence of South Africa. She proposed the name *Petraphera vivescenticule* (Fig. (1) b) having an akinete like structure. The photomicrographs (Fig. (2) a, b, c, d) show such a filament with akinete structure, which shows differential mineralization. The cell like structure which resembles akinetes has a red-coloured mineral enclosed which could probably be an iron mineral.

I think these are the individual members of the filaments which are collectively laid down to form the lamination or the algal mat.

The other interesting observations were made as an outcome of staining technique for determining the various carbonate rocks from this region. The following discussion is pertinent to PM-9 and PM-24 where fossils were observed and identified as iron bacterial resembling modern species of *Sphaerotilus* These were found as casts or moulds (Karkhanis, 1976).

Conclusive evidence for microbial participation in the genesis of the massive sedimentary iron formations from the Precambrian is fragmentary. Structures resembling fossilised bacteria have previously been reported, and they tend to resemble modern iron bacteria such as *Sphaerotilus*, *Gallionella* and *Metallogenium* (Tyler and Barghoorn, 1954, Cloud, 1956). The atmosphere at that time is believed to have been almost devoid of oxygen and highly reducing (Cloud, 1968). The concentration of atmospheric oxygen was probably between 0.0001 and 0.001% Present Atmospheric Level, and may have remained at this level for 2×10^9 years after the emergence of algal photosynthesis (Berkner and Marshall (1965).

The fossils described in this paper were found during a study of the mineralogy of the Lower Proterozoic Brockman Iron Formation, Hamersley Group, of Western Australia (ca. 2×10^9 years old) Compston and Arriens, 1968). Two specimens (PM-9 and PM-24) collected from the Whaleback Shale Member, at Wittenoom Gorge, W.A., were identified as dolomitic chert by X-ray diffraction. Optical microscopy showed the presence of fibrous stilpnomelane, and the staining technique suggested by Dickson (1965) distinguished the dolomite as ferroan.

The weakly acid solution of potassium ferricyanide (P.F.) was used to stain petrographic thin sections (0.2 g P.F. in 100 ml. of 1.5% HCl) Dickson (1965). The section was first cleaned with 'Teepol' to remove all grease or immersion oil, dipped in a beaker containing the above stain, and allowed to react for 45 to 60 seconds. The slide was then removed, and immediately rinsed with distilled water. The stain is on the surface of the minerals in the form of a precipitate, and may easily be destroyed if touched. Thorough washing with water is necessary to remove all the acid, otherwise carbonate crystals (especially calcite) would dissolve. Care is also requi-

PLATE--IV--8

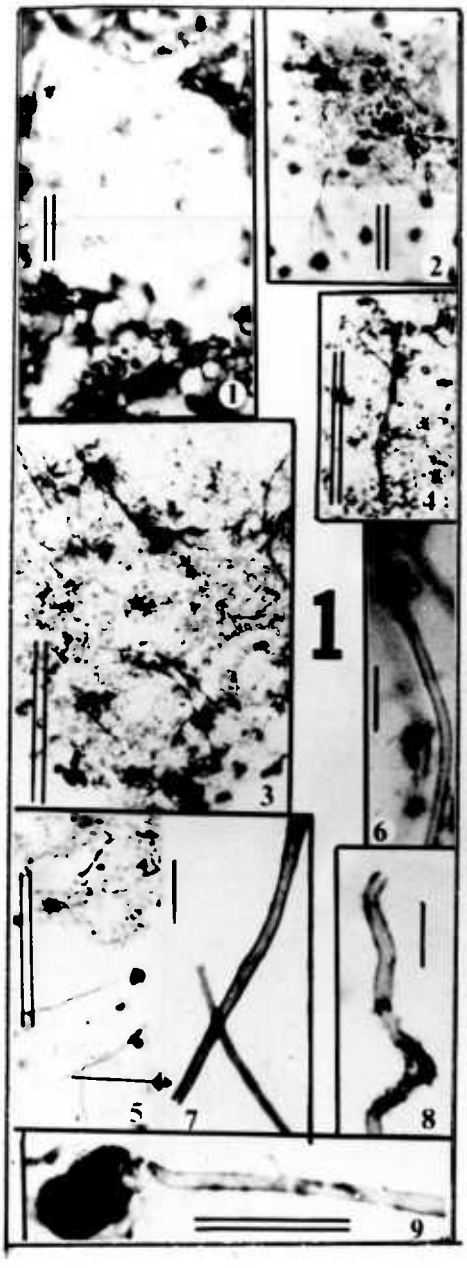




Fig.8.1.1: Dolomite rhomb prior to staining under Xnicols.

1.2: Dolomite rhomb after staining showing filaments on the surface of the crystal.

Fig:1 Single bar = 10 μm

Double bar = 100 μm

Fig.8.1.3&4: show filaments on the surface of the crystal, some of the filaments are attached to the rounded bodies.

1.5: Filament detached from the crystal during coverslip mounting.

1.6: Modern specimen of Sphaerotilus from Silwood Lake, Berkshire.

1.7: Same filament in 5 at higher magnification.

1.8: Isolated filament for comparision with Fig.6.

1.9: Rounded body to which the filament has been attached, mainly composed of ferrous iron.

Fig.8.2.S.E.M. photo of beaded filament from PM-24 after maceration.

red in the use of water, as prolonged contact of the precipitate with water renders it soluble.

Potassium ferricyanide reacts with ferrous iron to give a deep blue - *Turnbull's blue* - precipitate of ferrous ferricyanide as shown:-

$$3FeCl_2 + 2K_3Fe(CN)_6 \longrightarrow Fe_3\{Fe(CN)_6\}_2 + 6KCl \quad \text{..... Eq. (IV) 1}$$

During this study of the carbonates, it was observed that some ferroan dolomite crystals showed filamentous structures on or near the surface of the crystals Pl. (IV) (8) (1) 2, 3, 4, 5. They were stained deep blue, showing the presence of ferrous iron. The morphology of these filaments resembling the modern iron bacterium *Sphaerotilus*. Almost all the filaments are to be found attached to or lying on the surface of ferroan dolomite crystals, and each filament is filled with ferroan carbonate. No filaments are found in the rest of the matrix of the rock. The length of the filaments, on average, is 100 μm, and the fossils show no apparent morphological distortion, except that some of them have been broken during coverslip mounting. Many of the filaments appear to be attached to a round body mainly composed of ferrous iron, judged from the intensity of the staining Pl. (IV) (8) (1) 9.

Before staining, the filaments in the slide were invisible Pl. (IV) (8) (1) 1. This may mean that they were preserved as carbonate moulds formed during early diagenesis. This is an example of an *authigenic* preservation process (Schopf, 1975), involving early cementation in soft sediment, usually by iron and carbonate compounds - in this case, *ferroan dolomite* - preservation of structures of delicate shape and form.

Isolated filaments Pl. (IV) (8) (1) 7,8 were obtained when mounting the coverslip. A drop of glycerine was applied to a thoroughly water washed, stained slide, in order to preserve it for a longer period of time. The slide was then warmed to make the glycerine less viscous and the coverslip put in place. During this operation, some of the filaments became detached from the substrate and moved away to a new position free of the matrix.

The fossil material was compared morphologically with modern species of *Sphaerotilus*, collected from water samples from Silwood Park Lake, Ascot, Berkshire, England. A few drops of stain were allowed to react with the modern sample, and a similar colour change was observed Pl. (IV) (8) (6) 6. The morphological agreement is self evident when Pl. (I) (8) (1) 6. (modern bacteria) and Pl. (IV) (8) (1) 7, 8 of the isolated fossil filaments are compared. Somewhat similar structures have been detected preserved in haematite and chert of Tertiary age, Muir et al. (1974), and from other Precambrian iron formations from Canada, Barghoorn and Tyler (1965), and from Western Ausralia, Walter (1975). It has been suggested that these other structures, Muir et al. (1974), Barghoorn and Tyler (1965), Walter (1975) represent the remains of fossil iron bacteria, and, on the grounds of strong morphological similarity of the stained ferroan dolomite filaments, both with these and with modern *Sphaerotilus*, I suggest that the structures revealed in the present work represent the remains of Precambrian iron bacteria. It might be argued that these tabular structures have formed as the result of boring by algae and fungi, but one would expect boring algae and fungi to be gerally distributed throughout the rock. However, this can be ruled out in the present case, because the filaments are invariably associated only with the ferroan dolomite crystals, and are *not* generally distributed. Furthermore, algal and fungal filaments are generally much larger, and may often be septate. Septa were not observed in my material. If the structures represent borings, then a trail of mucilaginous material

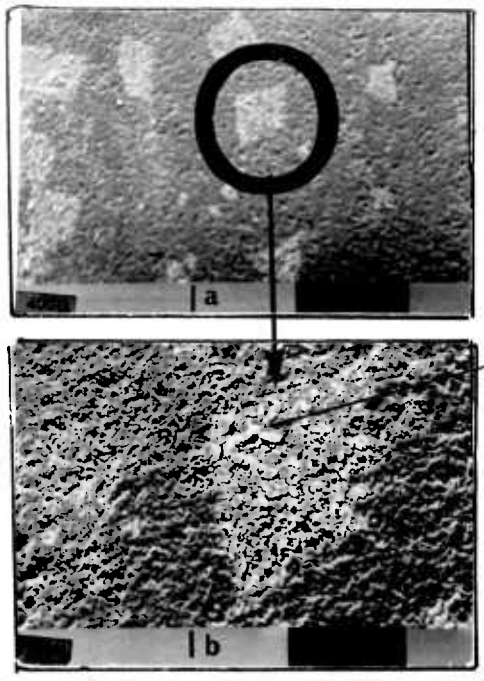




Fig.9.1a:S .E.M.photograph showing Ferroan dolomite rhomb.

1b:Higher magnification of fig.1a.Note the Atomic Number effect in 1a.The filament is is seen at the surface on the surface of the crystal in1b.

1c:Filament in(1b) at higher magnification,showing tubular structure(casting).

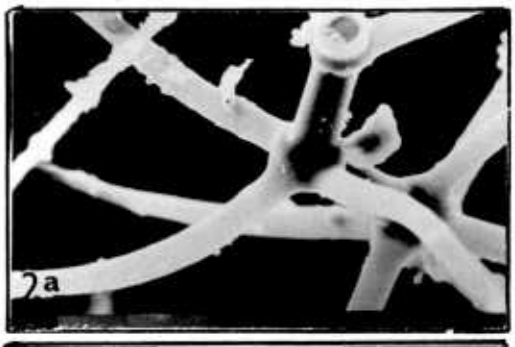
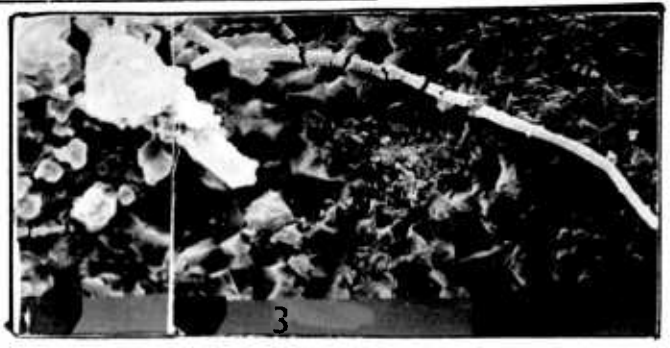




Fig.2a:Air-borne contamination found embedded in the glue.

2b:Higher magnification of (2a).

2c:Composite S.E.M.photo. of of the round body to which the filament is normally attached.(Compare with PlateIV-8-1.9).



might be expected around the filaments. None have been observed, and no trails or 'borings' (if such they are) appear to connect up the individual and spatially isolated ferroan dolomite crystals. It should also be noted that if the filaments do represent the remains of iron bacteria, that present day examples are always associated with clots of colloidal iron hydroxides, and it might be suggested that the ferroan dolomite crystals represent the diagenetic products of such clots.

Statements have been made in the past that 'bacteria do not have hard parts that can be fossilised, so there is little to be learned directly about their evolution' Breed (1975). In view of the application of this staining technique to carbonate rocks, this statement probably must be modified. Also the technique, or similar methods, must be extended to other forms of preservation, such as in pyrite, in limonite, in phosphate, in silica, and in calcite. As well as providing evidence for the presence of iron bacteria in ancient rocks, the technique offers the possibility of discovering previously undetectable microfossils from many different sedimentary environments in the Precambrian that are at present considered to be barren.

This work was extended to acid insoluble matter and its examination under the scanning electron microscope (SEM). It was not possible to obtain any filament from Plate (IV) (8) (1), with the exception of one beaded filament as shown in Pl. (IV) (8) (2). Possibly because of inherent composition (iron carbonate), the filaments may not have survived the acid treatment. Consequently this SEM work was further extended by taking a peel of the section. The peel was then mounted on the Aℓ stub by double sided sellotape and the staining was done as described previously. Some encouraging results were obtained. The results will be discussed at the end of this chapter with reference to Plate (IV) 9 and 11.

PLATE IV-10

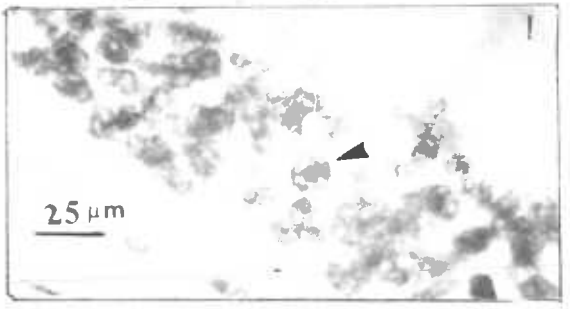


Fig.10.1:Thin section of PM-31 showing spherical structures pigmented by hematite to red colour.

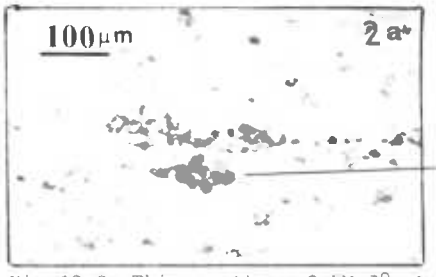


Fig.10.2a:Thin section of PM-38 showing small black specks.



Fig.10.2b:Black specks under high magnification, Mn bacteria resembling Metallogenium personatum.

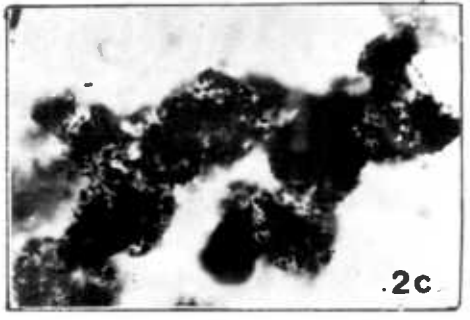


Fig.10.2c: Black specks from Cooley Dolomite of the McArthur Group.

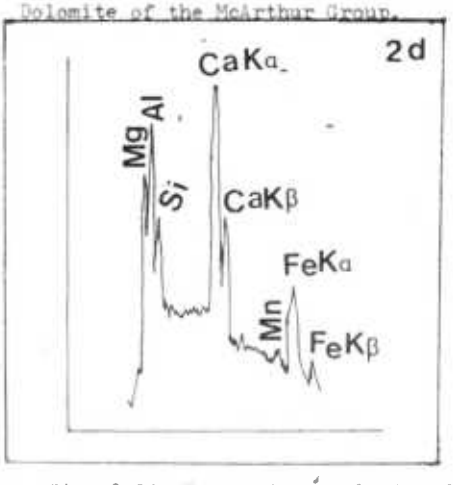


Fig.10.2d: X-ray microanalysis of fig.2c.(after Muir et al.1974).

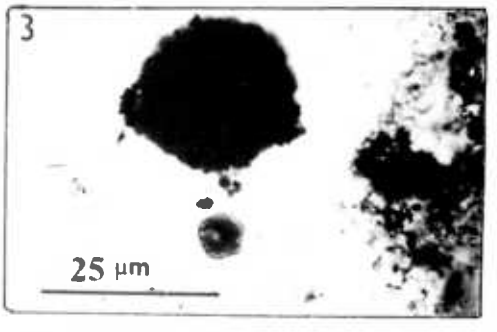


Fig.10.4.3:PM-38 thin section showing circular cell with reticulate double wall.The cell resembles Huranospora microreticulata.

The other various structures that were observed from Hamersley Region are described below. No difinite interpretations are offered.

Some spheroidal and elliptial structures are found as pockets in the bedding-Section PM-31. The rest of the matrix is hematite or goethite. Under high power these spherical structures look pigmented by hematite to red colour. In some structures, the centre is nearly pigmented to red colour and the structure also shows circular cell wall (Arrow, Pl. (IV) (10) 1). There is no organic matter visible in the petrographic thin Section. Red pigment is exclusively due to hematite and/or goethite.

It may be that these are relicts of microfossils. Microfossils can be preserved in a number of ways. Algal filaments and spore like bodies pigmented by hematite were found preserved and described by Barghoorn and Tyler (1965).

Pl. (IV) (10) 2a,b is a thin section of PM-38. No features are distinguishable. Small black specks are lumped together, the outline which is circular is distinctly observable especially in the high power photomicrograph (Pl. (IV) (10) 2b. Similar material was investigated by Muir et al. (1974) from Cooley Dolomite of the McArthur Group, N.T. Australia (Pl. (IV) (10) 2C shows morphological resemblance between these structures. They also show strong resemblance to the manganese depositing bacterium *Metallogenium personatum* Perfil'yev (1961). Fig. 2d is an X-ray spectrum of (2c).

This interpretation is reinforced when insoluble carbonaceous residue was examined by X-ray microanalysis, which showed presence of Mn (see Table (II) (8)).

Pl. (IV) (10) 3 is of PM-38 thin section which shows a circular cell with thick reticulate double wall. These structures are not very abundant. Only half a dozen cells were observed scattered throughout the section, which were highly carbonised and no internal differentiation was possible. This solitary better preserved cell much more resemble *Huraniosporamicro-reticulata* (Barghoorn, 1966). Similar structures have been described from the Amelia Dolomite, McArthur Group (1600 m.y.old) by Muir (1974).

X-Ray Microanalysis - PM-24 (Hamersley) Iron Bacteria

The filaments (PL IV-9) being very brittle, their mounting on the Aℓ stub was not very successful. The petrographic thin section was then mounted in the "Lakeside 70C" themo-setting resin. Hence this time it was easier to remove the peal of the section from the glass slide, on warming gently on the hot plate. Such a peal was mounted on a double sided sellotape and thence on the Aℓ stub. The stub was then immersed in the staining solution and the section stained as described previously. The filaments were visible. Pl. (IV) (9) 1a and b are the SEM photographs of the carbonate crystal under investigation. The filament is distinctly visible even at lower magnification (Fig. 1a).

Photographs 2, 3 and 4 from Pl. (IV) 11 are the distribution micrographs for Si, Ca and Fe respectively of the same field shown in Pl. (IV) (11) 1.

As far as the filament and the matrix is concerned, there seems to be very little difference in composition. It seems Fe, Ca are the major elements of the matrix and the filament, showing the complete replacement of the filament body with ferroan carbonate. The outline of the filament is still vaguely visible showing minor difference in the ultimate elemental composition of the filament walls with respect to Fe.

The elemental distribution (not shown here) of the round body (Pl. (IV) (9) 3) is presumed to be rich in total iron, the major component of which being ferrous iron. (inference-staining technique - intense blue colour).

PLATE - IV-11

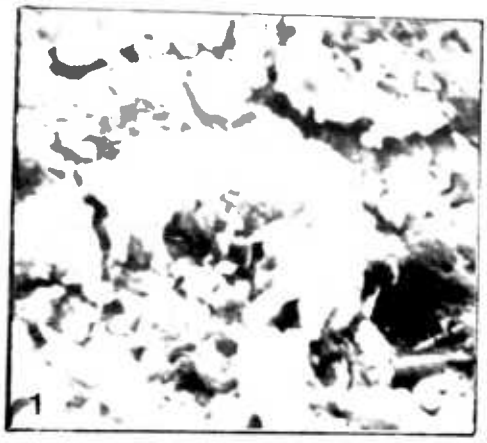
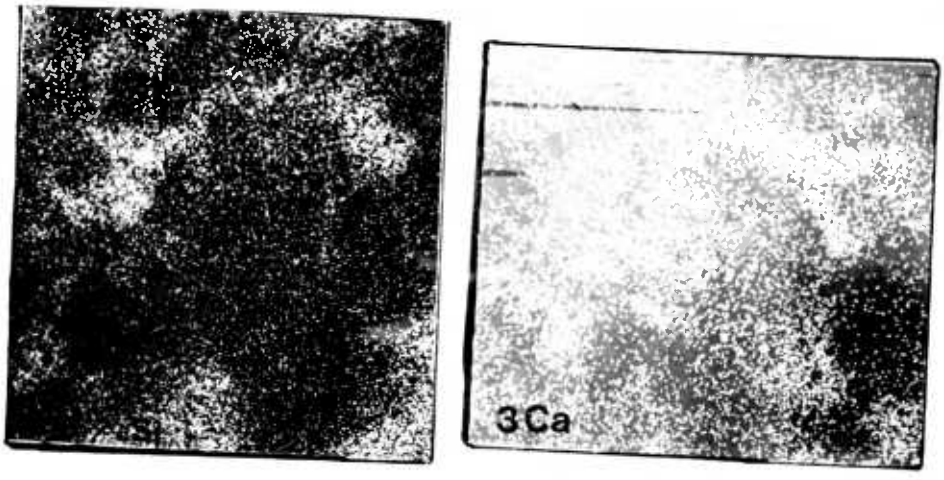


Fig. 1: S.E.M. photograph of the filament that has been analysed. Higher magnification (X1500) photo of the filament in Plate (IV).9.1b.



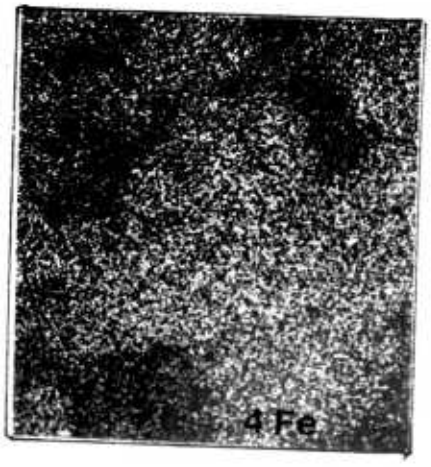


Fig. 2: Si Kα distribution micrograph of the field in Fig. 1. (2.5 K cps.).

Fig. 3: Ca Kα distribution micrograph of the field in Fig. 1. (200 cps.)

Fig. 4: Fe Kα distribution micrograph of the field in Fig. 1. (700 cps., 100 sec. exposure).

CHAPTER V

CHAPTER V

DISCUSSION

As mentioned before minerological and petrological examinations were undertaken on polished sections. All the samples were analysed by X.R.D. to identify the major minerals. Carbonates were identified by staining techniques as described previously.

A. MINEROLOGY

A-1: Kromberg Formation

The minerology is reported in Table (II) 3a and the samples were mostly cherts and carbonaceous cherts. The principal mineral is α-quartz. Pyrite and carbonate are minor components and chlorite is present in all the samples.

The thin sections showed that some of the samples have fractures and fissures. This is particularly prominent in HALL 1 (Pl. (IV) 1). The cracks and fissures are frequently filled with disseminated carbonaceous matter - giving a deceptive appearance of filaments (micro-fossil). While interpreting organic geochemical results, this fact should be borne in mind in order to decide if material is indigenous or not.

Examination of the thin section H-1 W/L showed one peculiar structure, which looked like a hollow spherule or ovoid (Pl. (V) (1) 1A. This body under high power appeared to be filled with needle-like (acicular) crystals probably composed of quartz, Pl. (V) (1) 1B. Only one occurrence of this type of structure has been noted, and no definite inference will be offered.

PLATE---V--1

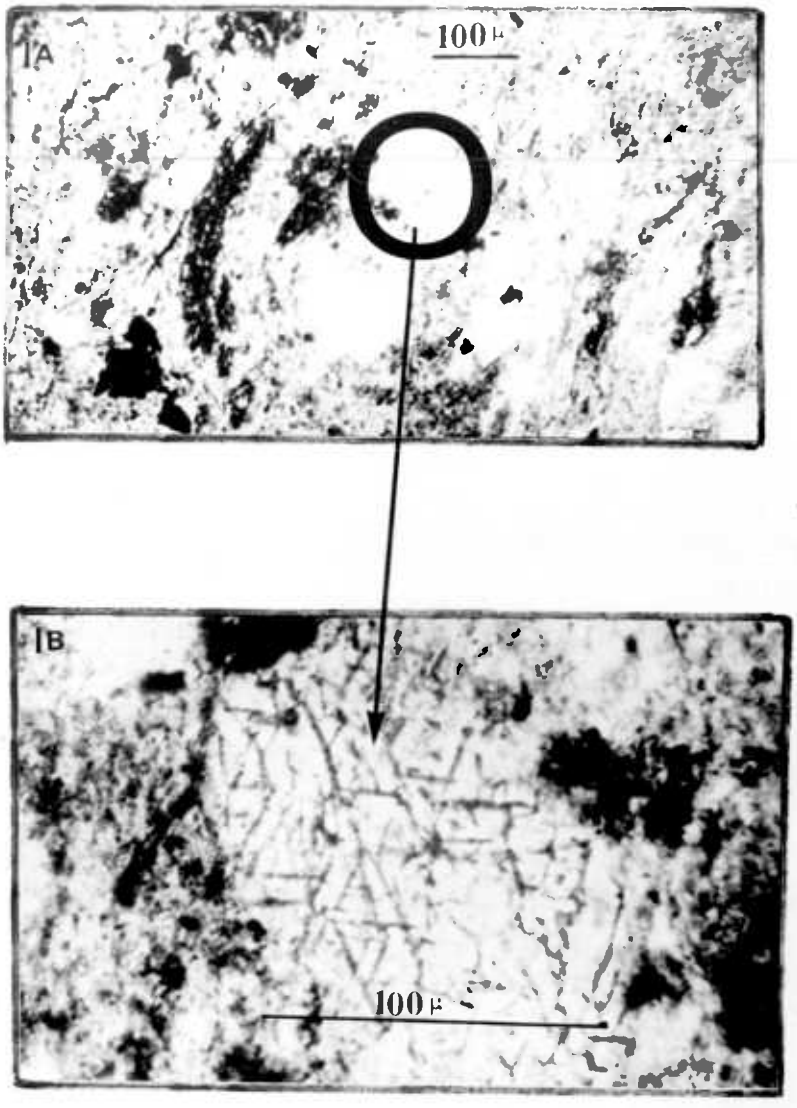


Fig:1.1A:Thin section of H-1 W/L(Kromberg) showing cavity filled with needle-like crystals(possibly Quartz?) The cavity adjacent to it is void.
Fig:1.1B: Higher magnification (x40) ,showing the needles.

A-2: South Alligator River

This area has been extensively studied and mapped by the Bureau of Mineral Resources (Walpole et al., 1968) and several other geologists. This area is closely associated with uranium mineralization. Ayers & Addington (1975) carried out geological and petrographic studies on the acid volcanic rocks and carbonaceous shales of the Koolpin Formation. In this thesis work, the carbonaceous shales from the Koolpin Formation were x-rayed for minerological studies. The minerals are listed in Table (II) 3b. The essential minerals were quartz, siderite, hematite, chlorite, uraninite and pitchblende. This author also confirms the presence of eskebornite, chalcopyrite, pyrite and marcasite as minor accessory minerals. I also suspect the presence of very minor quantity of gold in the organic residue.

PM-202 contains massive hematite, which is shown in PL (V) 2.1 and PL (V) 2.2 is a photomicrograph of sample PM-203, which shows hematite pseudomorphs after siderite. The original siderite seems to have been altered or replaced by hematite (shows typical blood-red colour). When there is a complete material exchange while maintaining the external form, the pseudomorph is classified as a *Pure Displacement Pseudomorph* (Niggli, 1920; Glover & Sippel, 1962).

X.R.D. showed traces of siderite and aragonite (?) (See Table (II) 3b). This texture is connected to siderite, because in thin section it shows a platy habit. The thin sections perpendicular to the bedding plane showed that pseudomorphs were of the same shape and size. This leads to the conclusion that the starting mineral has to have a platy habit. And siderite satisfies this criterion.

PLATE--V--2

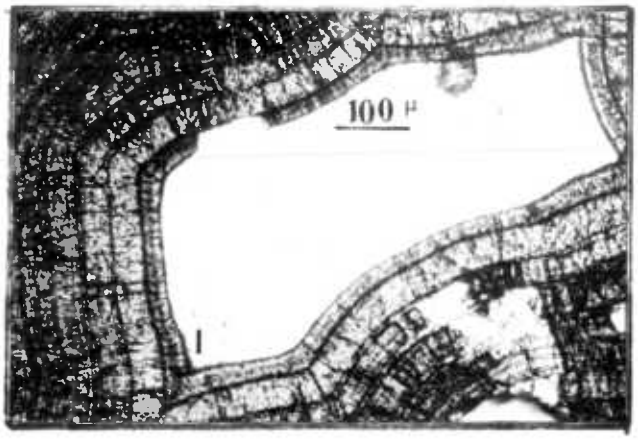


Fig 2.1:Thin section of PM 202(South Alligator) showing massive hematite-blood red colour inthin section.

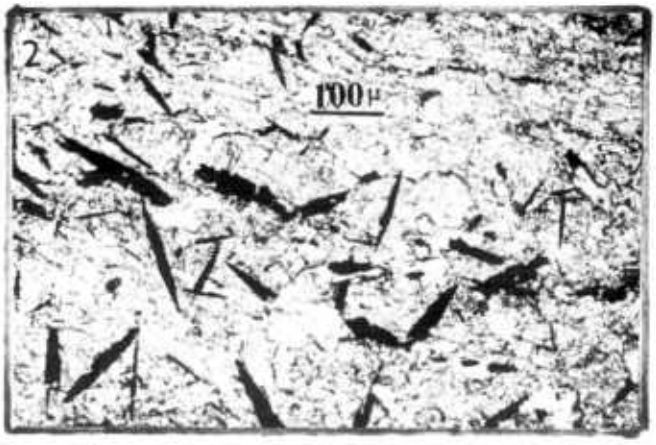


Fig 2.2:Thin section of PM-203(South Alligator) showing hematite pseudomorphs after siderite.This is an example of Pure Displacement Pseudomorph.

Plate- V 2



Fig.2.2A:Thin section of PM-203(South Alligator). A3,A4,A5 & A6 are the areas analysed by X-ray Microanalysis.(See the text for elemental analysis).

If siderite is oxidised, then it is converted to hematite. The supply of oxygen is maintained by breakdown of original hematite, which is buried under the over-burden of sediments.

The following equations will supplement this argument.

$$Fe_2O_3 \longrightarrow 4Fe_3O_4 + O_2 \qquad \text{---------- Eq. (V) 1}$$

(Original hematite)

$$FeCO_3 + O_2 \longrightarrow 2Fe_2O_3 + 4CO_2 \qquad \text{---------- Eq. (V) 2}$$

(Siderite) (oxidation) (hematite pseudomorph after siderite)

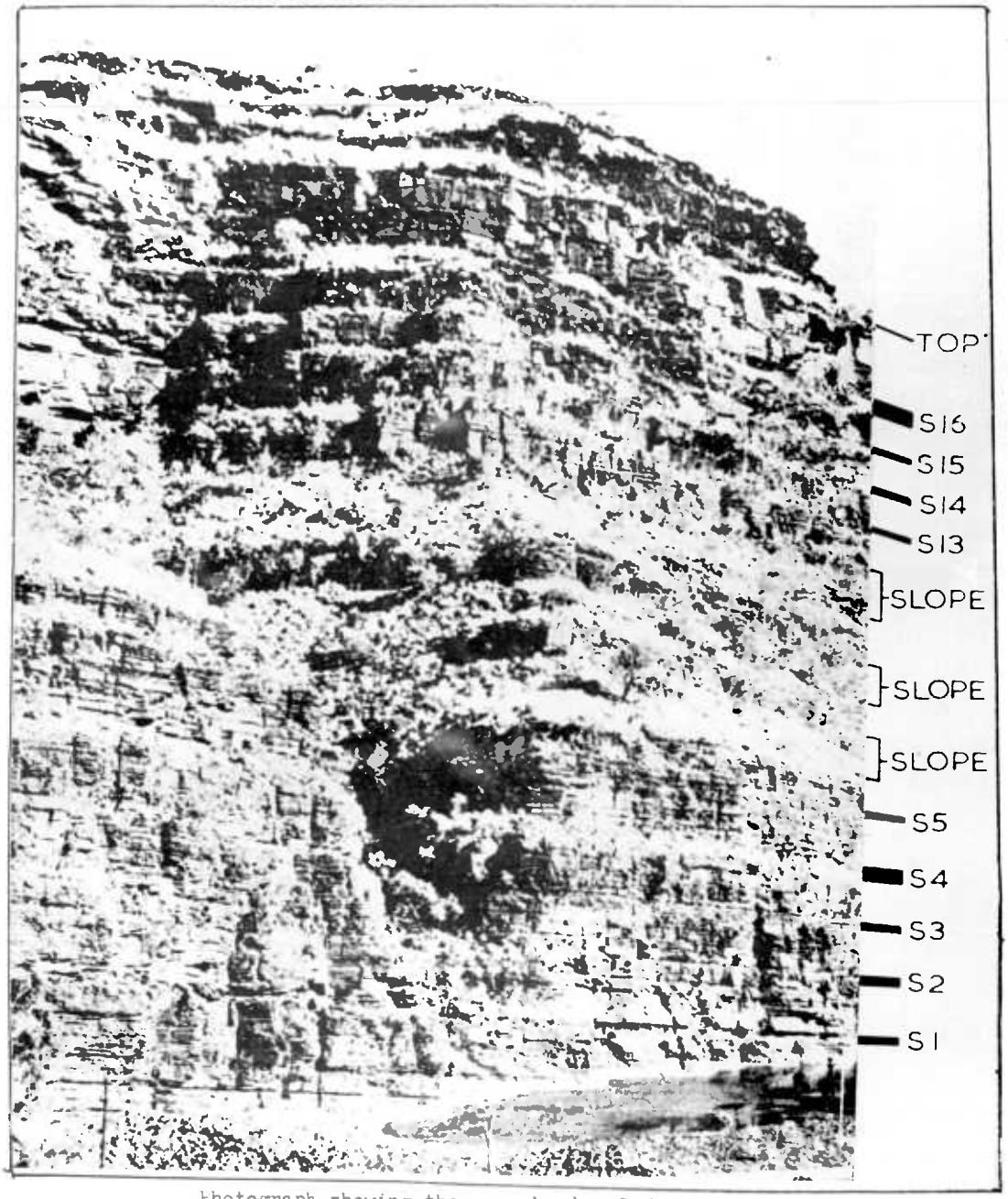
The other possibilities are minnesotaite or gypsum. But these are ruled out on the basis that (1) their absence in the thin sections even in minor amounts and (ii) minnesotaite has needle-shaped habitat though gypsum is platy (See the revised interpretation at the end of section A).

A-3: Hamersley Group

The lithologies of the iron formations have been described in detail by Trendall & Blockley (1970). They are typically finely banded (except for the Boolgeeda Formations) and chert bands alternate with iron-rich bands, the latter being called 'chert matrix' by Trendall & Blockley (1970). In the Dales Gorge Member, there are three distinct scales of banding (Trendall, 1965): *macro-banding, meso-banding and micro-banding.* A brief description of these various forms of banding follows:-

Macro-banding is the name given to the major alternations between the two contrasting lithologies of the Members. Macro-bands of B.I.F. are numbered from *BIF0* to *BIF16* and they are made up of iron formations and

PLATE--V--3



Photograph showing the macrobands of the Dales Gorge Memberat Wittenoom Gorge.(With the kind permission of Director,Geological Survey of Western Australia).

alternate with "shale" horizons, *S1* to *S16* which are generally thinner and consist of shale, chert and siderite. The macro-band sequence and thicknesses are shown in Fig. (II) 4b and the field expression of macro-banding appears as in Plate (V) 3 (after Trendall & Blockley, 1970).

Meso-banding is the name given to the banding of a scale, which shows a succession of internally consistent bands of different composition with an average thickness of less than an inch. Mesobands in the Dales Gorge Member consist of stilpnomelane, carbonates or riebeckite.

Micro-bands are defined by alternations of regular laminae with thicknesses of 0.2-2mm. They contain most commonly either hematite, ankerite, siderite or stilpnomelane. These laminae are usually visible to the naked eye.

According to this classification, the samples are categorized as shown in Appendix I.

Following the X.R.D. data available from Table (II) 3c, it is convincing and evident that the most abundant mineral by far for samples from the Dales Gorge Member (S.No.PM-9 to PM-21) representing the S-15 and S-16 shales and BIF 16 of Trendall is finely crystalline quartz. Some of the cherts have a fine mosaic of quartz with average grain diameter of 5 to 40 microns, which concurs with Trendall's observations. His petro-fabric analysis of 200 grains of a single chert meso-band from the Dales Gorge Member gave an average diameter of about 30 microns.

In some samples after quartz, next in abundance are the carbonate minerals. They are differentiated into calcite, dolomite, ankerite and siderite on the basis of X.R.D. identification. Some of the calcite and

PLATE---V-4

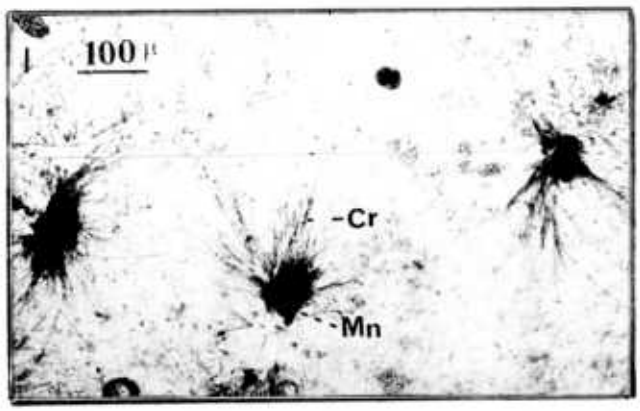


Fig 4.1:Thin section of PM-17(Hamersley)show CROCIDOLITE, (Cr) attached to magnetite(Mn).

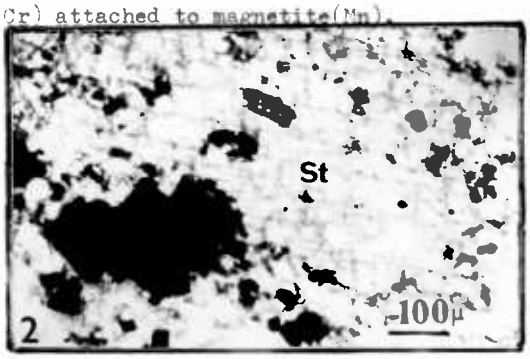


Fig 4.2:Thin section of PM-23(Hamersley) showing characteristic mesh of of STILPNOMELANE(St), (light green colour in thin section).



Fig.4.3: Thin section of PM-43(Hamersley),showing band of STILPNOMELANE(St)in chert matrix. Pleochroic green in thin section.

dolomite are ferroan type distinguished on the basis of the staining technique described in Chapter II.

PM-9 and PM-24 have particularly abundant dolomite rhombs, and some of these are hollow. A ferroan dolomite composition is indicated on the basis of potassium ferricyanide staining, which imparts a blue colour to Ferrous iron. These two samples contain iron precipitating bacteria possibly of the type resembling modern *Sphaerotilus* (Discussed in Chapter IV).

PM-17 is a massive B.I.F.16 and contains hematite, which is sub-hedral to eu-hedral. The sample contains traces of pyrite, which was only doubtfully detected by X.R.D. (below detection limits) but was confirmed when acid insoluble matter was X-rayed. This implies that pyrite was concentrated in the acid insoluble matter. Because of its scarcity, it is impossible to describe its texture or other characteristics, except for one pyrite grain, which showed movement in the matrix (Discussed later in this chapter).

The other mineral not detected by X.R.D. was later identified as crocidolite by optical microscopy. The crocidolite fibres are very weakly diffracting and seem to be amorphous to X-rays. Grubb (1971) did some experiments using gels. He obtained a fibrous phase of crocidolite, which was synthesised at temperatures between 110°C to 350°C, and identified this phase by Infra Red (I.R.) absorption. Crocidolite in PM-17 appears to be more or less evenly and closely spaced out among the chert and seems to be attached to magnetite, Pl. (V) (4) 1, giving it the appearance of a *'beetle like structure'*. Magnetite seems to serve as a point of nucleation for these fibres, which look like whiskers. This relationship between crocidolite and magnetite supports the claim of Celliers and Genes (1964) that magnetite plays an important role in nucleation and growth of

PLATE---V--5

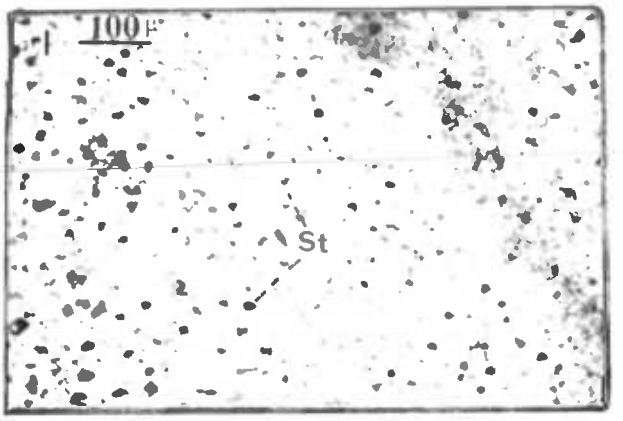


Fig.5.1:Thin section of PM-24(Hamersley) showing corona texture of STILPNOMELANE(St).The texture suggests a product of "quench" reaction.

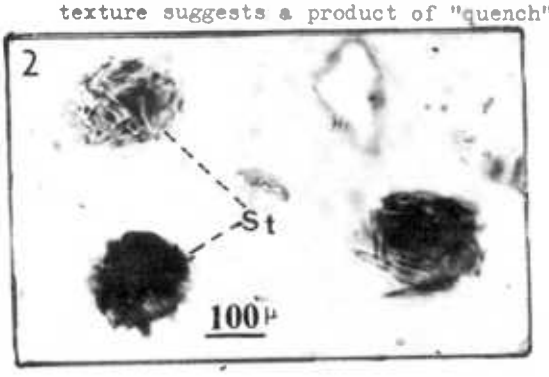


Fig.5.2Higher magnification(X100)of individual spherule formed of cross fibres,some are brown andfew are green in transmitted light.

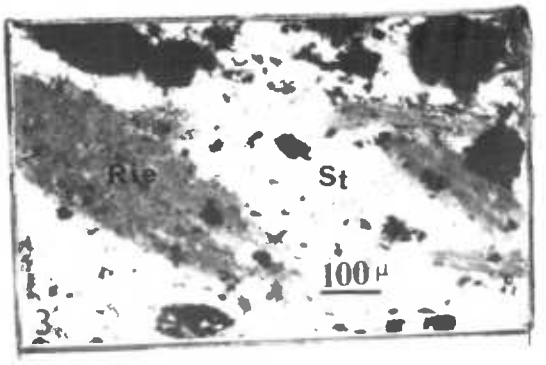


Fig.5.3: Ribbon-like platy blue mineral associated with stilpnomelane(St)Pseudomorphed after fine RIEBECKITE(Rie).

crocidolite. Crocidolite which is a fibrous polymorph of riebeckite, also occurs in sample PM-23. It mostly appears as a cross fibre vein around pyrite crystals Pl. (V) (6) 1. This observation is contrary to what Grubb (1971) reported. He observed cross fibre veins of crocidolite filling fractures around magnetite screens.

In PM-17 all the major facies (carbonate, sulphide, oxide, silicate) of iron formation as described by James (1954), can be found. Other minerologically interesting features were varieties of stilpnomelane. Grubb (1971) recognized three different forms of this mineral.

In PM-23, Pl. (V) (4) 2, the characteristic mesh of stilpnomelane can be seen, which has a light green colour and in the section elsewhere, it is being replaced by fibrous crocidolite and platy riebeckite.

Pl. (V) (4) 3 is a photomicrograph of PM-43. In this sample, stilpnomelane appears as a band in a chert matrix and consists of a strongly pleochroic green and brown variety with a super-imposed schistocity. According to Grubb (1971), this is a product of increased diagenesis. The third variety is from sample PM-24. The small spherule or corona texture is present in the entire section Pl. (V) (5) 1. Under high magnification Pl. (V) (5) 2, (X100), every spherule is seen to be formed of cross fibres and some of the spherules under transmitted light are brown and a few are green.

The other associated mineral is ferroan dolomite in a quartz matrix. The texture of this section (PM-24) suggests that it is a product of a "quench" reaction. The process of crystallization has been arrested in 'time', at an early stage of crystal development.

PLATE---V--6

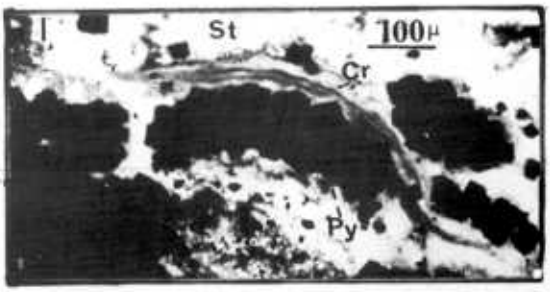


Fig.6.1:Thin section of PM-23 (Hamersley) showing CROCIDOLITE(Cr),a fibrous polymorph of Riebeckite(Rie).It is appearing as cross fibre vein around pyrite(Py) crystals.

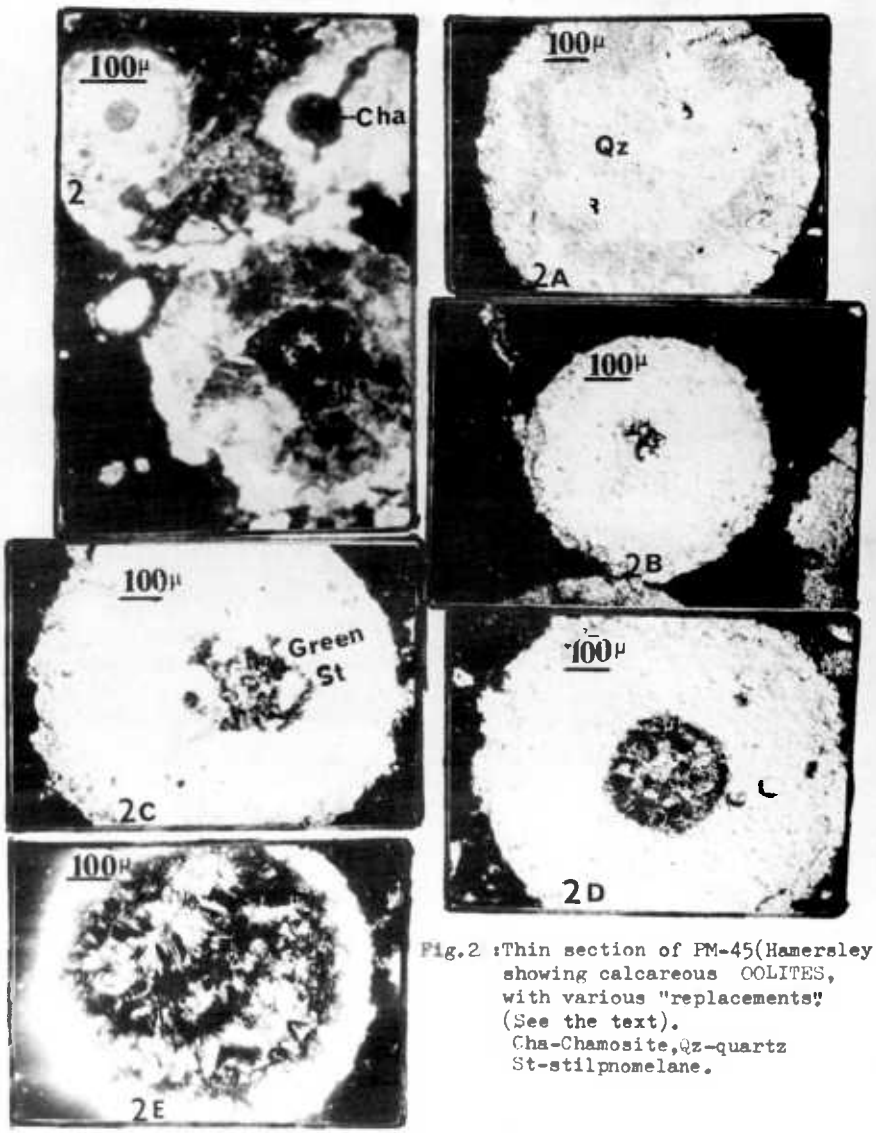


Fig.2 :Thin section of PM-45(Hamersley) showing calcareous OOLITES, with various "replacements" (See the text).
Cha-Chamosite,Qz-quartz
St-stilpnomelane.

A ribbon-like platy blue mineral, (PM-23), Pl. (V) (5) 3 is occasionally found associated with stilpnomelane. This could be pseudomorphed after fine riebeckite (Grubb, 1971).

The sample PM-45 contains sphaeroidal bodies Pl. (V) (6) 2 composed of concentric arrangements of various "replacements". Starting from outside the replacement proceeds through quartz (Fig. 2A) and ultimately ends in a massive chamosite crystal (Fig. 2). There are various opinions about the origins of these sphaeroids. According to Trendall (1970), they seem likely to be filled in by gas bubbles entrapped during collapse. Laberge (1966) suggests they could be of volcanic origin. A closer examination of thin section shows that the sphaeroidal cavities are replaced by quartz (fine grains), stilpnomelane and greenalite Pl. (V) (6) 2A,B,C,D and E. At some places, internal replacement has ended in a massive chamosite crystal. There are also traces of carbonates (dolomite) and I, therefore, think that they were originally calcareous oolites, which have become ferriferrous oolite under diagenetic replacement. Chemositic oolites have been forming at least for the last 2×10^9 years (Wagner, 1928) and ferriferrous oolites have formed as recently as Early Jurassic, Latal (1952).

In the lower Proterozoic Gunflint Formation of Ontario, Canada, layers of greenalite in some siliceous ooids have also been reported (Dimroth and Chauvel, 1973).

It is possible that in the sedimentary environment, if solute-rich waters are drained laterally through carbonate ooids, these ooids will be replaced by chamosite (ferrous, aluminium-rich septa-chlorite) if the original water is aluminium-rich or by greenalite (ferrous alumium-poor septa-chlorite) or chert if alumium poor.

PLATE-V-7

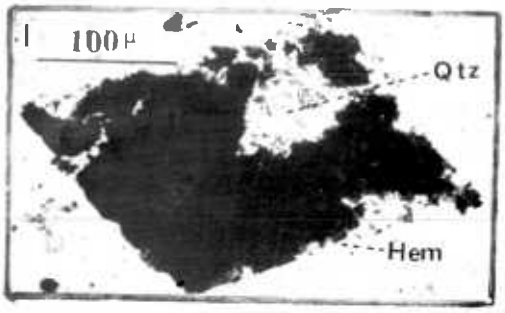


Fig.7.1:Thin section of PM-38, (Hamersley)showing textural variety of hematite.(Hem).



Fig.1.A,B,C;show partial to complete replacement by quartz(Qtz).







Fig.1.D,E.Similar texture, as aabove from PM-17. (XNicol).

PLATE--V--8

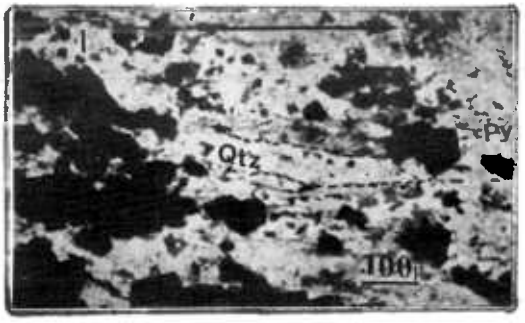


Fig.8.1:Thin section of PM-17(Hamersley)showing an example of PSEUDO-FOSSIL,where pyrite crystal(Py) seems to have moved (dashed line)Trail mainly composedof quartz-Qtz. Arrow indicates the direction of the flow.
(Compare the similar phenomenonin PLATE(IV)(1).2e, from Kromberg formation).

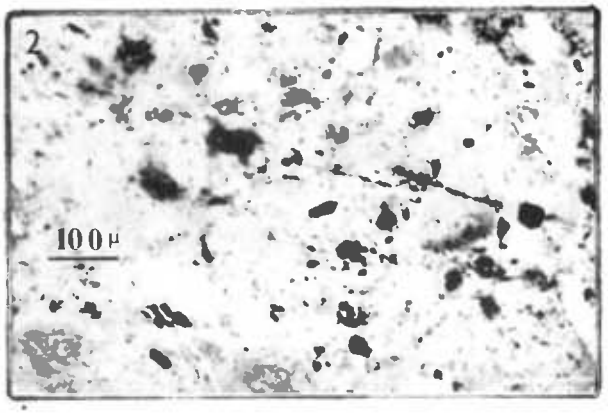


Fig.8.2:Thin section of H-1(Kromberg)showing dessiminated organic matter.

This view-point needs further re-assessment and this could be done by proper sampling for sedimentary environmental studies.

Section PM-38 contains examples of textural variety of hematite. The term cellular hematite is taken from Trendall (1972), who noted a similar variety from B.I.F.14 macro-band of the Dales Gorge Member, which he assigned to secondary weathering.

Pl. (V) (7) 1 is a photomicrograph of this kind of texture. The difference between this example and the one reported by Trendall (1972) is that in my material there is partial or occasionally complete replacement by quartz (Fig. 1 A,B,C), while in Trendall's example the crystals are pitted with small rounded holes filled with quartz. Similar textures were found in PM-17 (Fig. 1 D,E) and have been reported by Spencer & Percival (1952), and Percival (1967) from India and the Hamersley ranges.

PM-17 is a massime banded iron formation (B.I.F.16). The matrix is mainly composed of quartz and hematite. Pyrite and magnetite are trace components and there are occasionally minor amounts of silpnomelane. The thin section when examined optically, showed the appearance of flow in one direction, Pl. (V) (8) 1 (arrow). The direction of flow is deduced from a pyrite crystal, which seems to have moved from its original position to a new location. The trail or appendage as marked in Figure is mostly composed of quartz (chert) with some disseminated pyrite crystals along the line. Similar *'Pseudo-fossils'* were observed by Tyler and Barghoorn (1962) from the lower algal zone of the Gunflint Formation, Canada and the Biwabik Formation of Minnesota. They assigned this phenomenon to a combination of pressure solution and force of crystallization of quartz or carbonate.

It is interesting to note that the example cited here shows that the phenomenon can operate in the absence of appreciable amount of organic matter.

Similar phenomenon has been observed from Kromberg Formation. See Plate (IV) (1) 2.e. The filament (beaded) is pyritized and moved to position. The movement is distinctly visible. This sample contains appreciable amount of organic (dessiminated) matter. Plate (V) (8) 2.

Followed from Section A-3:

These hematite plates (PM-203) were analysed by X-ray microanalysis (by Mr. V. Belmer, Edax International, The Hague). Plate (V) (2) 2A shows the points of analysis and table (below) shows the corresponding elemental analysis (corrected for mass absorption). The ananlyses show the presence of Ca and S in the crystal lattice. In the light of this new evidence the previous interpretation need to be modified. It seems that these pseudomorphs are after gypsum. The sequence could therefore be

Gypsum ⟶ Siderite ⟶ Hematite

The X-ray microanalysis of Hematite pseudomorphs from PM-203 (S. Alligator pitchblende)

Element	Analytical Line	Analytical Location Percentage, %			
		A_3 (Part)	A_4 (small) part	A_5 (Blade)	A_6 (Matrix)
Fe	K	34.620	45.746	98.012	51.150
Si	K	29.161	26.156	0.578	34.105
Al	K	5.264	2.386	0.500	2.981
S	K	3.971	1.911	0.146	0.273
Cl	K	15.769	7.483	0.499	-
U	M	1.154	0.566	-	-
Ca	K	6.253	1.966	0.263	6.667
Mg	K	3.805	13.782	-	4.316
Mn	K	-	-	-	0.505

B. INSOLUBLE CARBONACEOUS MATTER

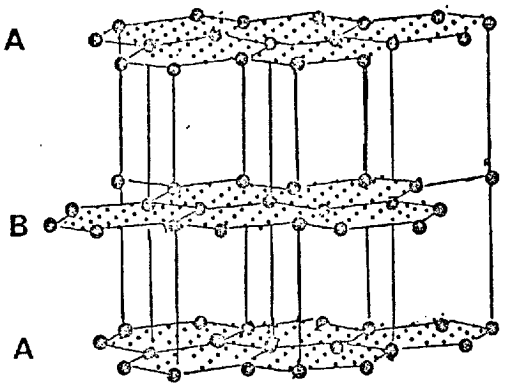
B-1: Insoluble Carbonaceous Matter from Kromberg Formation

The X.R.D. traces of the final insoluble residues are shown in Figure (II) 8 in Chapter II. The specific conditions for the formation of graphite in these samples are still unknown. The original carbonaceous material may have had a sedimentary origin or may represent juvenile carbon extruded with tholeiites. Oehler et al. (1972) considers their average $\delta^{13}C$ value of -15.8°/oo in carbonaceous chondrites and suggest that this can be interpreted as evidence for non-photosynthetic plants in the lower Onverwacht; in the manufacture of cast iron excess carbon separates as flakes from the melt to form a solid solution known as *"Kish"* graphite (Ubbelohde and Lewis, 1960).

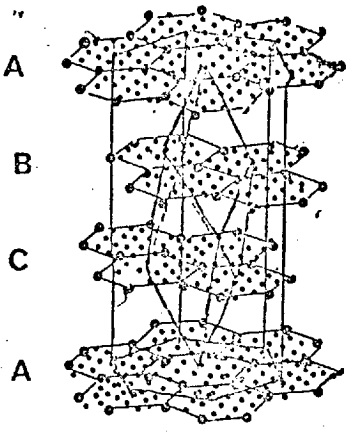
Normally under laboratory conditions, graphite would be formed by simply heating carbonaceous matter to a high temperature under a reducing atmosphere. Although graphitic material is present, there is no geological evidence that these rocks have been subjected to high temperatures; the possible temperature range compatible with experimental data on the stability of greenschist-facies minerals is 300-500°C (Fyfe et al., 1958). Hamilton et al. (1970) have shown that plant structures can be perfectly preserved as graphite. Another condition that might favour the formation of graphite in nature under far less drastic conditions is *Shear*, which would deform the graphite crystals to produce the *rhombohedral* form (Freise and Kelly, 1963). Rocks of the Onverwacht series in the Komati valley are sheared (Visser, 1956).

With respect to the quality of the X-ray traces, it was previously mentioned that the portions of the material were mounted on the glass

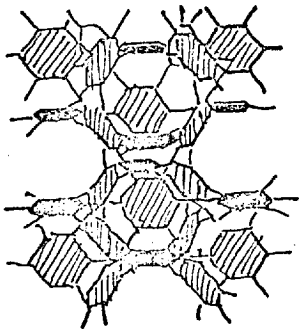
FIGURE--V--1 -VARIOUS STRUCTURES OF CARBON.



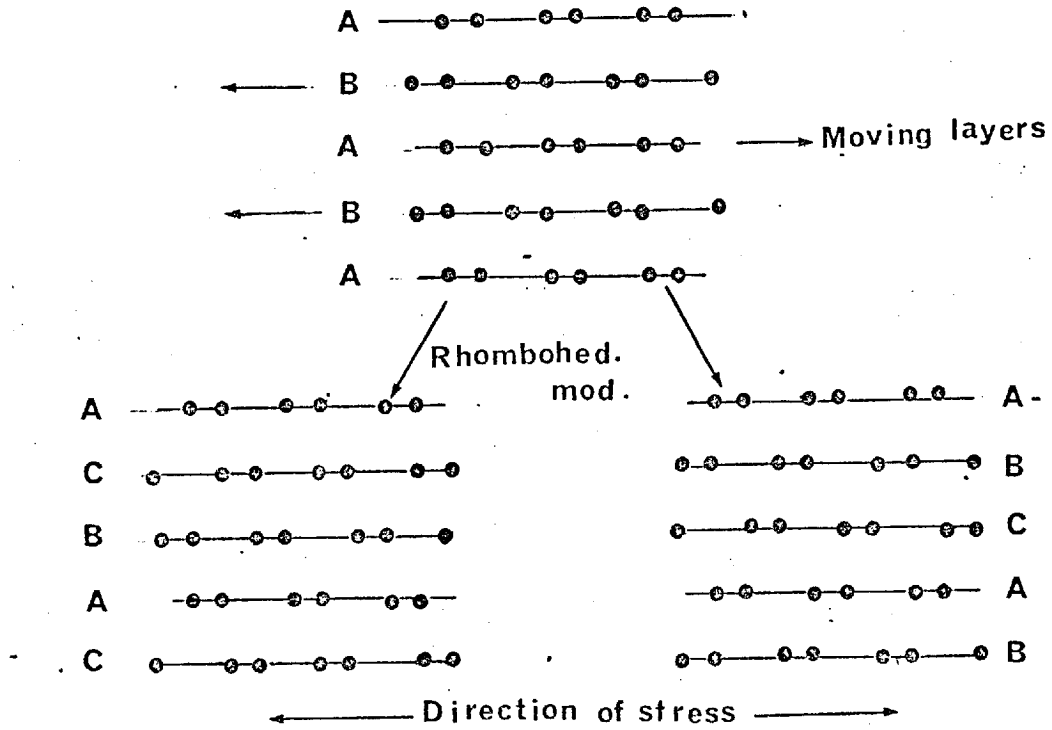
A --HEXAGONAL GRAPHITE



B --RHOMBOHEDRAL GRAPHITE.



C --AMORPHOUS CARBON.



D --MECHANISM FOR LATTICE TRANSFORMATION OF HEXAGONAL TO RHOMBOHEDRAL FORM BY ACTION OF SHEAR.

slide as smear mount and grinding was avoided. The reason for this is that mechanical grinding treatment produces rhombohedral modification as a consequence of translation or gliding of the layer plane.

The hexagonal graphite Figure (V) 1A has carbon layers in sequence AB AB.... and the rhombohedral Figure (V) 1B form has a layer sequence of ABC ABC..... The action of shear due to mechanical grinding brings about a transition AB ----AC in a preferred direction which excludes AAA..... as a possible intermediate state bringing about the rhombohedral modification. Figure (V) 1D shows here that the rhombohedral form can arise from the hexagonal form in this way by the action of shear (Boehm and Coughlin, 1964) Figure (V) 1C structures of amorphous carbon.

Silverman (1964) has shown that when organic matter is heated, evolution of low molecular weight hydrocarbon $(C_{n=1}-C_{n=4})$ occurs, which show enrichment of ^{12}C, leaving the residue depleted in ^{12}C. On the basis of their $^{12}C/^{13}C$ measurements, Oehler et al. (1972) believes the Onverwacht material to be unmetamorphosed, yet the graphite in these samples clearly indicates either high temperature or *shear* stress both of which are metamorphic features.

B-2. Kalgoorlie

PM-1 (Archean) shows a very intense graphite peak associates with rutile. The graphite show a fully developed form (hexagonal).

B-3. South Alligator

X.R.D. indicated ordering of carbon in some samples PM-192, 195, 196, 198, 201 (?) and 202 (?) and all contain a graphite-like component.

These samples also show a characteristic hump between 23^{o}-$34^{o}2\theta$. Some of the samples contain high temperature minerals such as rutile and spinel.

B-4. Insoluble Carbonaceous Matter from Hamersley - W. Australia

It can be seen from Table (II) 3c that insoluble matter from this area was very sparse in many samples. Hence the X.R.D. work was restricted to a few samples. The data show that the insoluble matter from some samples does not show the characteristic hump-like structure peculiar to the Kromberg Formation, which is characteristic of asphaltic material.

However, some samples (PM-13, 14 and 17) do show the hump. A closer look at the lithology of these samples shows that an abundant mineral besides quartz is carbonate (either calcite or dolomite or both). It can be said tentatively that the hump probably represent the hydro-carbon from a carbonate starting material.

One sample (PM-49) shows some ordering of carbon and as noted from Kromberg Formation that when there is graphite, rutile (a high temperature mineral) is associated with it.

C. E.S.R. CHEMICAL ANALYSIS AND X-RAY MICRO-ANALYSIS

In this section the data obtained from above techniques will be discussed together. The data follows from Tables (II) 7,6,8 for E.S.R. C, H analysis and X-ray micro-analysis respectively.

C-1. Kromberg Formation

A typical ESR spectrum consists of a simple symmetrical line, devoid of any fine structure (Fig. (II) 15A). Various ESR parameters together with H/C ratio and crystallite size are shown in Table (V) 1 below.

TABLE (V) 1. ESR Parameters*, H/C ratio and crystallite size

S.No.	Free radicals spin/g x 10^{-15}	Line width ΔH gauss	"g" value	H/C ratio	Crystallite size Å
H1 W/L	1.87	2.4	2.00177	0.17	24.16
H2	2.09	2.7	2.00186	0.15	21.23
K6**	4.76	6.2	2.00166	-	-
K7	5.23	3.6	2.00177	0.32	19.31
KIA	6.78	3.7	2.00174	0.41	480.46
HI	7.14	4.0	2.00201	0.30	530.53
K4	9.43	3.5	2.00192	0.28	310.19
K3	9.47	4.1	2.00195	0.58	1074.43
DPPH(STD)	1.53 x 10^{21}	0.17	2.00237	-	-
PM1	5.28	Very narrow	2.00462	-	304.60

* Average of two determinations

** Sample K6 contaminated with filter paper during filtration.

The table (V) 2 below shows the X.R.D. data on insoluble carbonaceous matter and X.R.D. patterns for insoluble residues are shown for comparison.

TABLE V.2 X-ray Diffraction Data on Insoluble Carbonaceous Matter from Kromberg Formation.

S.No.	Peak Shape	(002) repeat distance $^{o}2\theta$	Å	Remarks
H-1 W/L*	Hump	24.0	4.31	Maximum at 3.42 Å
		36.0	2.90	
H-2*	Hump	24.0	4.35	Maximum at 3.46 Å
		36.0	2.90	
K-6	Bimodal	28.0	3.70	Less intense graphite peak
		30.1	3.46	
K-7	Hump	27.0	3.84	Maximum at 3.58 Å
		32.0	3.25	
K-IA	Broad hump	24.31	4.35-3.35	Graphite peak visible at 3.35 Å
	Bimodal hump	27.0	3.84	
		30.0	3.46	
H-I	Bimodal	30.0	3.06	
		30.7	3.38	
K-3	Bimodal	29.6	3.62	Graphite peak visible
		31.1	3.34	
PM-I		31.1	3.34	Strong graphite peak

* - XRD shows pure concentrate of kerogen although X-ray micro-analysis shows minor amounts of trace elements (transition).

PLATE--V--9

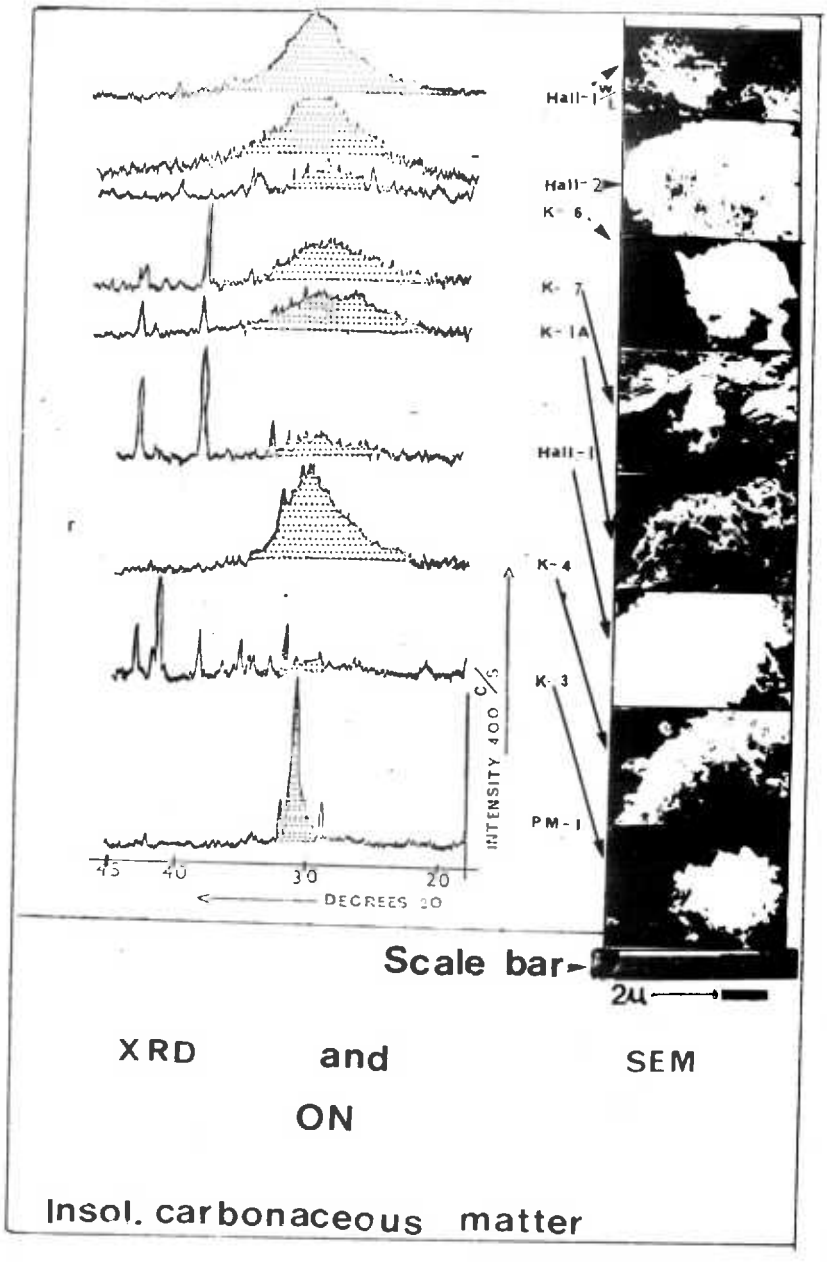


Fig.9: X.R.D. and S.E.M. on insoluble carbonaceous matter from Khaperkheda formation. The shaded area under the peaks were related to the crystallite size.

Sample PM-1 is included here for comparison purposes only (Archean, Bulong, near Kalgoorlie, W. Australia). The sample has graphite in it so it was thought it would complete the rank and be a proper fit. From the data obtained it would seem that most samples from Kromberg Formation have had different thermal histories. The three types of XRD peak shown in Pl. (V) 9 are characterized by:-

1. A diffuse broad peak with maximum near $30^{\circ}2\theta$ indicating non-crystalline material (Samples HALL-2, HALL-1 W/L and K-7)
2. A diffuse broad peak from about 29° to $32^{\circ}2\theta$ with individual peaks at $27^{\circ}2\theta$ and $31.5^{\circ}2\theta$ with repeat distances of 3.84 and 3.34 Å (Samples HALL-1, K-4 and K-6)
3. A broad diffuse peak with a definite graphite peak at $31.1^{\circ}2\theta$ (Samples K-1A, k-3).

The (002) repeat distance decreases from 3.46 Å to 3.35 Å. This corresponds with a shift from 3.6 to 3.8 Å in lignite to high volatile bituminous coal rank to 3.5 Å in metanthracite and graphite first pointed out by Blayden et al. (1940) and Griffin (1967).

Comparison of Table (V) 11 (ESR data) and Table (V) 2 (XRD data) show that spin concentration increases with rank. Retcofsky et al. (1968a and 1968b) have noted change in crystallite dimensions of ESR signals of coals of varying rank. Line width, the other ESR parameter also shows increase with the rank. The g-values are all lower than the free electron value for DPPH (2.00237), but the higher rank material gave a value close to those found for free radicals.

The reasons for increase in line width and the spin concentration could possibly be due to the following reasons.

As the heating proceeds the σ bonds are broken at the periphery of the aromatic skeleton. The un-paired electrons are increased and there are not enough counterparts to go around to pair them off. Because of un-paired electrons, there is an apparent *Spin-Spin inter-action.* And we therefore observe the line broadening and increase in spin concentration as the rank progresses (this is obvious from the data). This is the second reason why during XRD sample preparation, the carbonaceous matter is not subjected to grinding. The other reason is to avoid the lattice transformation of graphite structure.

When the structure reaches the three dimensional structure of graphite (PM-1), the carbon atoms attain s^2p^2 electronic configuration Coulson (1965) and the p_z orbitals of these s^2p^2 atoms serve as efficient traps for π electrons. And we can observe the narrowing of the line width and drop in the spin concentration.

Furthermore there is a systematic change in H/C atomic ratio with increase in rank and Marchand et al. (1966, 1969) measured the spin density of pure kerogens and co-related increase in spin density with H/C ratio.

Following the Scherrer Equation (Eq. (II) 8) an attempt to measure the dimensions of crystallite size was made. This was done by relating the crystallite size to the breadth of the diffraction peaks.

Table (V) 1 shows the crystallite size and shows that the dimension increases from nearly 20 Å to nearly 1100 Å for high rank material and drops to 304.6 Å for PM-1 which has a perfectly developed 3.35 Å peak. This may be because carbon layers can accommodate volatile matter in the interlayer spacing, and collapse of the crystallite lattice could result

from the expulsion of volatiles. Griffin (1967) observed such a lattice contraction in the study of humic materials and showed that volatiles must be eliminated entirely from the interlayer spacing before the layers approach one another and the adjacent carbon layers produce ab plane rotation, resulting in a three dimentional structure.

These studies, therefore, show that there is a striking parallel between carbonisation of coal and organic matter during incipient metamorphism. ESR and XRD studies of insoluble carbonaceous matter could furnish a method for characterizing the degree of alteration of organic matter undergoing diagenesis or low rank metamorphism.

ESR DATA FOR AUSTRALIAN SAMPLES

C-2. Kalgoorlie and Hamersley

PM-1 sample from Kalgoorlie has a three dimensional graphite and has low free radical concentration. This data has previously been discussed with reference to Kromberg ESR data.

The samples from Hamersley are not sufficient in number to warrant detailed discussion. Only certain features of ESR spectra will be discussed. (Refer to Fig. (II) 17 on page 75 for the spectra)

(1) The apparent absence of fine structure, which is peculiar to free radical absorption, appears to be absent for almost every sample analysed except PM-38. This could be the result of super-position of many multiplets. Hence the values for free radial concentration should be treated as relative. This is obvious from the spectra for PM-47, 48 and 49, where one can see the hyperfine splitting of Mn^{2+} at $g \sim 2.0$ (compare with Fig. II 14 for Komati 3 whole rock ESR spectra).

(2) The other feature of these spectra is the resonance line at $g \sim 4.0$ attributed to Fe^{3+}. Extensive literature exists describing resonance close to g = 4.0, which has firmly established as due to Fe^{+3} ions, so occupying a variety of low symmetry crystalline environment in a range of material, Castner et al. (1960), Aasa and Vanngard (1965), Wickmar et al. (1965), and Angel et al. (1974).

(3) The other feature is for PM-49, which has a very high concentration of free radicals (49.12×10^{15}). X-ray micro-analysis of carbonaceous material showed the presence of Uranium in the sample. Friedel & Breger (1959) exposed different varieties of coal to pile-irradiation

and they reported increase in free radial content. Duchesene et al. (1961) put forward the hypothesis for genesis of free radicals encountered in coals, lignite, petroleum etc. as a consequence of natural radio-activity. ESR spectra for PM-47 and 48 also show high concentration of free radials, though the spectrum 48 shows intense peak but has other contributory factors. Incidentally, PM-47 and 48 also show Uranium concentration in their carbonaceous matter.

C-3. South Alligator: Refer to Fig. (II) 18a, b, on pages 76, 77 for ESR spectra.

Almost all the spectra from this area show g = 2.00 absorption, show narrow and intense peak characteristic of organic free radials. g = 4.2 absorption is again common to all the samples probably due to Fe^{3+}. There are a number of additional features and they could be attributed to other para-magnatic ions such as CO^{2+}, Ni^{2+}, Cu^{2+}. It is often difficult to detect any signal from these ions at room temperature, because strong inter-actions between the neighbouring ions are characterized by such *short relaxation* times that the resonances are too broad to be observed (Poole, 1967). This is the reason why some samples be needed to run at liquid nitrogen temperature.

It seems that in practice ESR technique is much more complicated than previously thought. Wakeham and Carpenter (1974) have shown that *g*-value of about 4.2 is due to Fe^{3+} in tetrahedral sites, while Fe^{3+} in octahedral sites has a *g*-value of 2.0. The author feels that the effect of such impurities on these resonances can be studied by synthetically dopping the material under investigation. This is quite possible with the natural material, but with the carbonaceous material that has been isolated, would require quite a bit of thinking.

D:1. SOME ARTIFACTS PRODUCED BY HCl/HF PROCESSING OF SAMPLES FOR MICROPALAEONTOLOGY AND ORGANIC GEOCHEMISTRY (In Press - Precambrian Research, 1976)

For nearly 155 years hydrofluoric acid has been used in preparation for the analysis of inorganic materials. During this time the two main applications have been (as quoted by Langmyhr, 1968).:-

(a) as a decomposing agent for minerals and rocks, particularly for samples used for quantitative determination of sodium and potassium, and,

(b) to remove silica by evaporation.

These original objectives have been extended by including palaeontological applications. The presence of micro-organisms in rocks, both Phanerozoic and Precambrian, requires HF digestion to remove the mineral matrix from organic walled microfossils and where there are no morphological remains, from "Molecular Fossils" - molecular remains in which the intimate molecular architecture is far different from its original form.

Micropalaeontological studies have concentrated on Precambrian sediments that occur within the temperature zones covering incipient metamorphism (diagenesis). The work is extended by examining the acid resistent residue-Kerogen isolated from sediments. The study of this kerogen throws light on i) the redox potential during the early stages of diagenesis and ii) the thermal history of the host rocks. The acid insoluble residue in its metamorphic stages acquires the characteristics of graphite. This graphite is monitores by X-ray diffraction (XRD) and it is imperative that quartz is completely removed from the sample as the quartz peak overlaps the (002) reflection of graphite. This is done by treating the sample

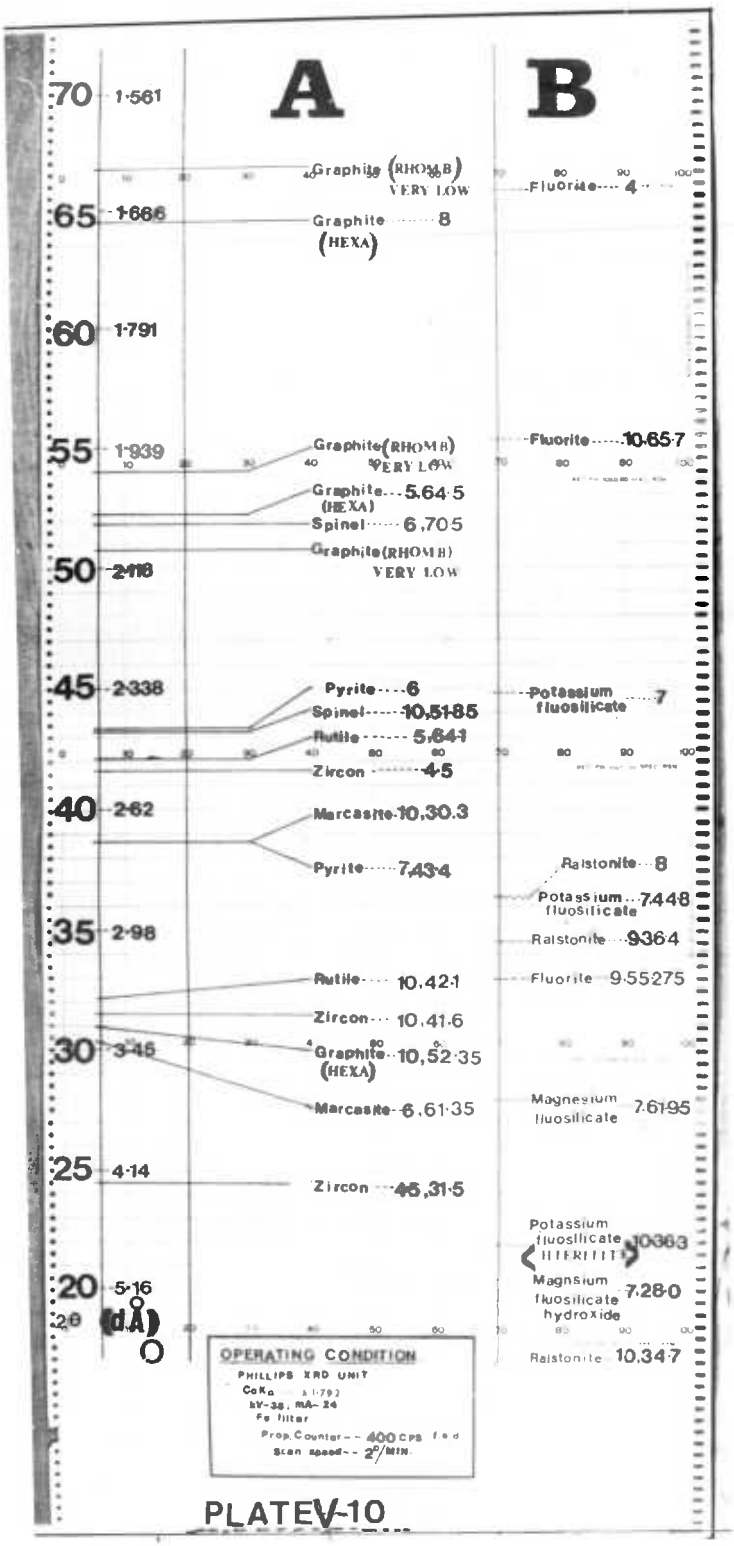

A
B
70 1·561
65 1·666
60 1·791
55 1·939
50 2·118
45 2·338
40 2·62
35 2·98
30 3·45
25 4·14
20 5·16
2θ (D.Å)
Graphite (RHOMB) VERY LOW
Graphite (HEXA) 8
Graphite (RHOMB) VERY LOW
Graphite (HEXA) 5,64·5
Spinel 6,70·5
Graphite (RHOMB) VERY LOW
Pyrite 6
Spinel 10,51·85
Rutile 5,64·1
Zircon 4·5
Marcasite 10,30·3
Pyrite 7,43·4
Rutile 10,42·1
Zircon 10,41·6
Graphite (HEXA) 10,52·35
Marcasite 6,61·35
Zircon 45,31·5
Fluorite 4
Fluorite 10,65·7
Potassium fluosilicate 7
Ralstonite 8
Potassium fluosilicate 7,44·8
Ralstonite 9,36·4
Fluorite 9·55275
Magnesium fluosilicate 7,61·95
Potassium fluosilicate 10,36·3
Magnsium fluosilicate hydroxide 7,28·0
Ralstonite 10,34·7
OPERATING CONDITION
PHILLIPS XRD UNIT
CoKα λ 1·792
kV-38, mA-24
Fe filter
Prop. Counter -- 400 CPS f.s.d
Scan speed -- 2°/MIN.

PLATE V-10

with hydrofluoric acid in a PTFE crucible.

One of the problems that arises in using HF is that with more basic rocks some insoluble fluorides of the type $MgAlF_5 . xH_2O$, $NaAlF_4 . xH_2O$ and occasionally $Fe^{+2}(Al, Fe^{+3})F_5 . XH_2O$ are formed (Langmyhr and Kringstadt, 1966). The formation of insoluble fluorides and fluosilicates can sometimes be prevented by using a strong complexing agent like 2.5% boric acid or hot in HCl treatment for 24 hours.

Complete removal of mineral material is, in practical terms, impossible. The identification of synthetic minerals (artefacts) becomes cumbersome. Furthermore some workers study the same insoluble matter in the Scanning Electron Microscope (S.E.M.) to look for microfossils. During such investigations, the author discovered some structures with a morphology which could have misinterpreted as fossils.

This communication is, therefore, intended to sound a note of caution to those workers who use X.R.D. and S.E.M. techniques in their investigations.

PART I. X.R.D.

A chart has been constructed to simplify and speed up the indentification of HF resistant synthetic material. A portion of this chart is shown in Pl. (V) (10). The chart is drawn on a recording paper of the type used in X.R.D. work for easier use. The chart is reporduced in Table (V) 3.

The original scale of the chart is exactly that of the trace when goniometer and recorder are moving 1^{o}/minute and the positions of the

PLATE - V - 11 - [illegible] sample preparation artifacts.

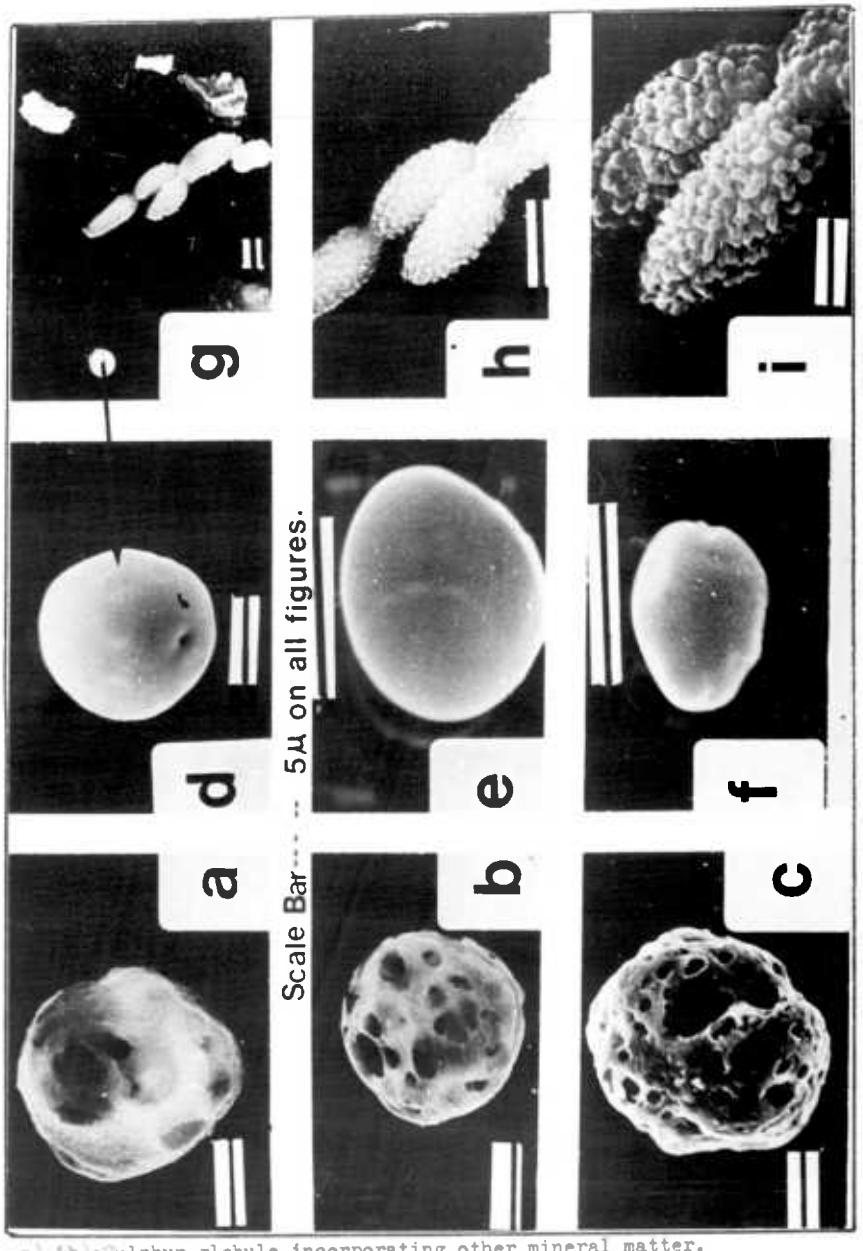


Fig.11--a) & b) :Sulphur globule incorporating other mineral matter.
c) Sulphur globule with etched surface due to acid attack.
d) Sulphur globule in pure form. e) Natural Sulphur (Mining Geology Colle.
g), h) & i) Framboid like structure. Scale Bar :5μon all figures.

Arrow emphasize the globule at higher magnification in(d).

peaks are those obtained when using CoK_{α} radiation at 38 kV, 24mA with the proportional counter running continuously from 5° to $70^{\circ}2\theta$.

The chart is divided into several columns. The first column represents $^{\circ}2\theta$ to define the peak position. The second column represents the corresponding *d* spacing at an interval of $5^{\circ}2\theta$ for reference. Then the chart is divided into two broad areas. The first on the left hand side (A), is for the minerals that survive the INHCl, 40% HF attack. The area on the right-hand side (B) shows the minerals which are formed as insoluble fluorides or fluoro-complexes (artefacts).

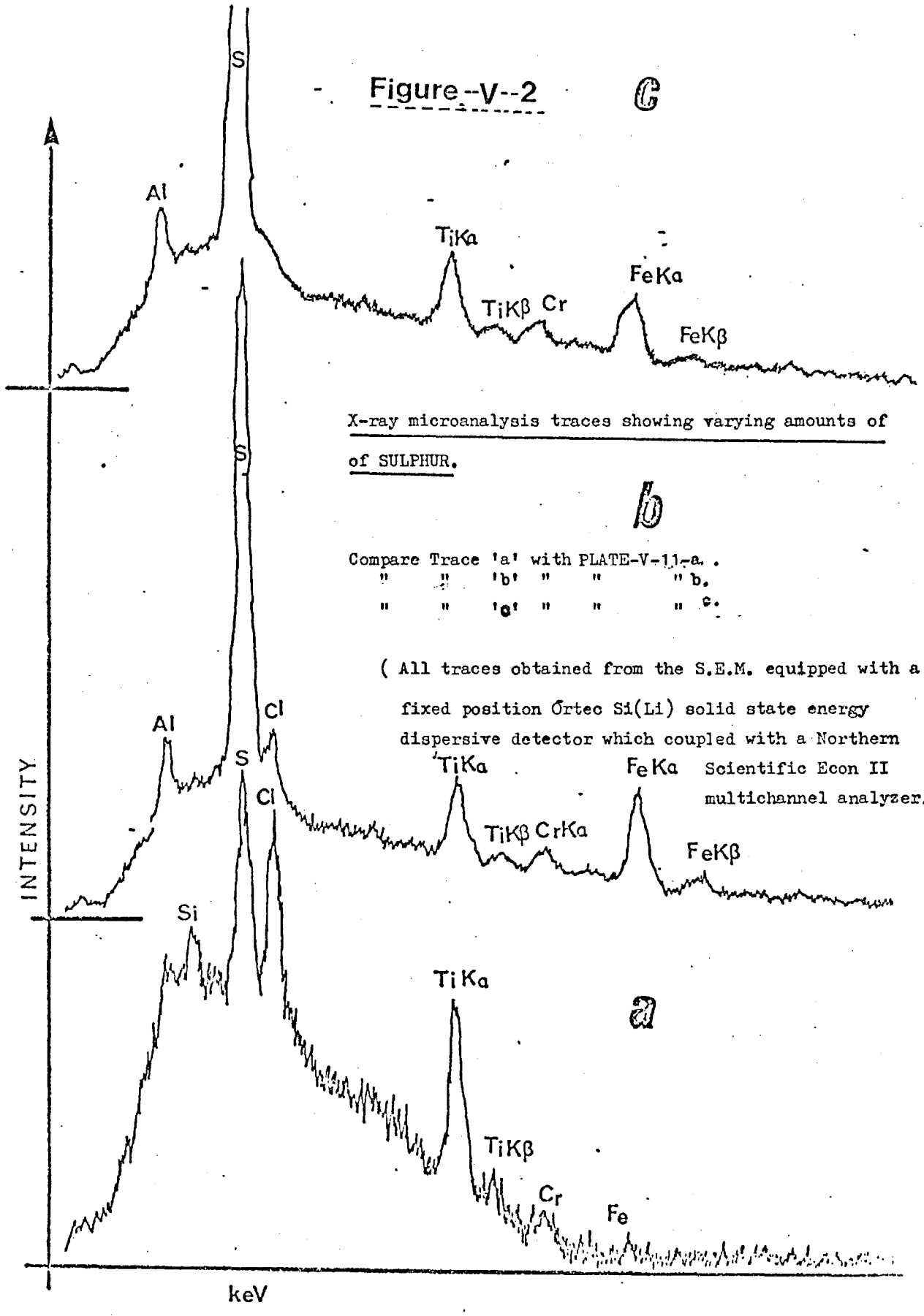
After every mineral name, two other figures are inserted. The first figure is the intensity of the peak and the second figure is the angle at which the next peak for the mineral would occur. For every mineral three peaks are included for identification. Because the peaks will appear in a scan of 5° to $70^{\circ}2\theta$. This chart and Table (V) 3 are by no means complete. Rock samples of varied lithology may give additional artefacts, and this chart could assist workers studying rocks from Precambrian Banded Iron Formation (B.I.F.) and possibly many others too.

PART II. S.E.M.

The insoluble carbonaceous residue obtained after treating rock samples with INHCl and 40% HF (See Karkhanis, 1975) was examined under S.E.M. The residue was mounted on an aluminium stub with "Durafix" glue and vacuum coated with carbon to increase the conductivity between the samples and the stub.

The material analysed showed a structure with a striking morphological resemblance to fungal conidophore (Plate (V) 11 g-i). This seems unlikely

Figure -V--2



X-ray microanalysis traces showing varying amounts of of SULPHUR.

Compare Trace 'a' with PLATE-V-11-a.
" " 'b' " " " b.
" " 'c' " " " c.

(All traces obtained from the S.E.M. equipped with a fixed position Ortec Si(Li) solid state energy dispersive detector which coupled with a Northern Scientific Econ II multichannel analyzer.

as the samples were collected from rocks of Precambrian age where such structures are unknown and stringent precautions were taken to prevent contamination. Further S.E.M. work showed that there were other spherical structures with an average diameter of 10μ, with a different surface texture.

The X-ray micro-analysis of these spherules showed high amounts of sulphur. Three such micro-analysis traces are shown in Fugure (V) 2. X.R.D. analysis of the original rocks showed that it contained pyrite and other iron minerals such as hematite and goethite. It is, therefore, believed that the body (morphologically like a fungus) could be a framboidal structure. This kind of texture is almost exclusive to pyrite and this sulphur pseudomorph is probably an artefact formed during sample preparation.

It has been suggested that framboidal structure is indicative of biogenic activity (Cloud et al., 1975). Berner (1969), Farrand (1970) and Sunegawa et al. (1971) conclusively demonstrated that biological control is *unnecessary* in framboid formation. Rickard (1970) has discussed the origins of franboids in detail.

Possible mechanisms are suggested below by which this texture may have developed in the reaction vessel - *a closed experimental system* - where the physico-chemical conditions are homogeneous and could possibly account for the uniform size of individual framboid.

In the original rock sample X.R.D. showed the presence of pyrite and certain iron minerals like hematite, goethite and some pyrrhotite. The various textures of sulphur spheres (Plate (V) (11) a,b,c) can be explained by analogy with immiscible oil globule sitting at a water interface.

Globules of sulphur (Figue d) could float on the liquid surface in the reaction vessel. Some of the globules would entrap other minerals (silicates) by adsorption and surface effects. As the acid leaching proceeds, the HF would attack the incorporated silicates and will produce the holes from which minerals have been dissolved and removed (Figure b, c). If one compares the X-rays microanalysis traces (Figure a,b,c) with the morphologies of spherules (Figure a,b,c), we can see indications of varions in acid leaching which leads ulimately to pure sulphur sphere (Figue c). Figure e,f are the S.E.M. photographs of natural sulphur (Royal School of Mines, Mining collection) for comparison.

The production of elemental sulphur can be accounted for by the following reaction between sulphide and goethite (Rickard, 1970).

$$2FeO.OH + 3H_2S_{Aq} = 2FeS + S^{o} + OH^{-}_{Aq} + 3H_2O \quad \text{.....} \quad \text{Eq. (V) 1}$$

This reaction is taken further whereby polysulphide ions are formed due to the reaction between sulphide and sulphur.

The production of pyrite then can proceed through the following reaction:-

$$FeS + 2S^{2-}_{Aq} = FeS^{2} + S^{2-}_{Aq} \quad \text{.....} \quad \text{Eq. (V) 2.}$$

Reaction (2) leads to the release of more ions which are rendered free to react with goethite. On the other hand according to condition (2) described by Sweeny and Kaplan (1975) iron sulphide will react with elemental sulphur to form pyrite in an aqueous environment at temperatures of up to $85^{o}C$.

PLATE V-12

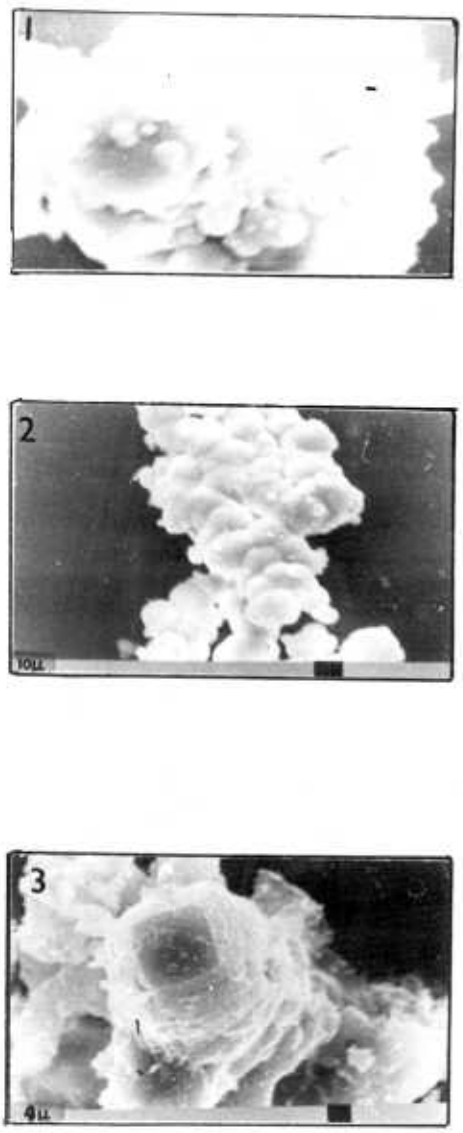


Fig.12:Similar FRAMBOIDAL structures from HM-200(South Alligator), S.E.M. photographs of insoluble carbonaceous matter.

In summary it can be said - in the microenvironment of the laboratory vessel A) some minerals survive HF B) some minerals are produced, and that for siliceous cherty rocks, identification could be made by the chart Pl. (V) 10. C) Strange globules that can easily be misidentified as microfossils can be produced synthetically from samples that had pyrite in the reaction vessel. Although it is claimed that the environment in the laboratory vessel could be represented as homogeneous, care need be taken during batch analysis, when a few samples might have just the conditions to give the above-mentioned artefacts. (Plate (V) 11). These are the artefacts from Pm-24 and PM-200 respectively which contain sulphides and other iron minerals.

It seems the branched morphology of the framboid is determined by the presence of filamentous fossils (Pl.(IV) (8) 2) which act as point of nucleation. Later similar results were obtained for PM-200, from its insoluble carbonaceous matter (Plate (V) 12). It is worth noting that the minerology is identical (contains sulphides and iron minerals).

Because such artefacts are easily produced, S.E.M. studies of organic residues should only be undertaken where genuine organic walled microfossils occur and can be shown to be *in situ* in their sections under light microscope.

It should be noted that these views are presented here to sound a note of caution (Karkhanis. In Press in Precambrian Research, 1976) and should not be taken as implying that either X.R.D. or S.E.M. technique are useless and inapplicable to micropalaeontology and organic geochemistry, just that a few simple checks should be carried out to ensure that, if artefacts are present in the final residues, they can be identified as such and not assumed to be genuine parts ofthe original rock.

During the X.R.D. investigation of carbonaceous matter, it was observed that quite a number of samples from Kromberg Formation and Hamersley group showed graphite, or ordering of carbonaceous matter indicative of high grade metamorphism. On the basis of $^{12}C/^{13}C$ measurements, Oehler et al. (1972) believed that the Onverwacht material to be unmetamorphosed. As with most greenstone belts, the entire Barbarton Mountain Land has suffered only a low grade regional greenschist facies of metamorphism. The experimental data on the stability of greenschist facies minerals is 300-500^{o}C (Fyfe et al., 1958).

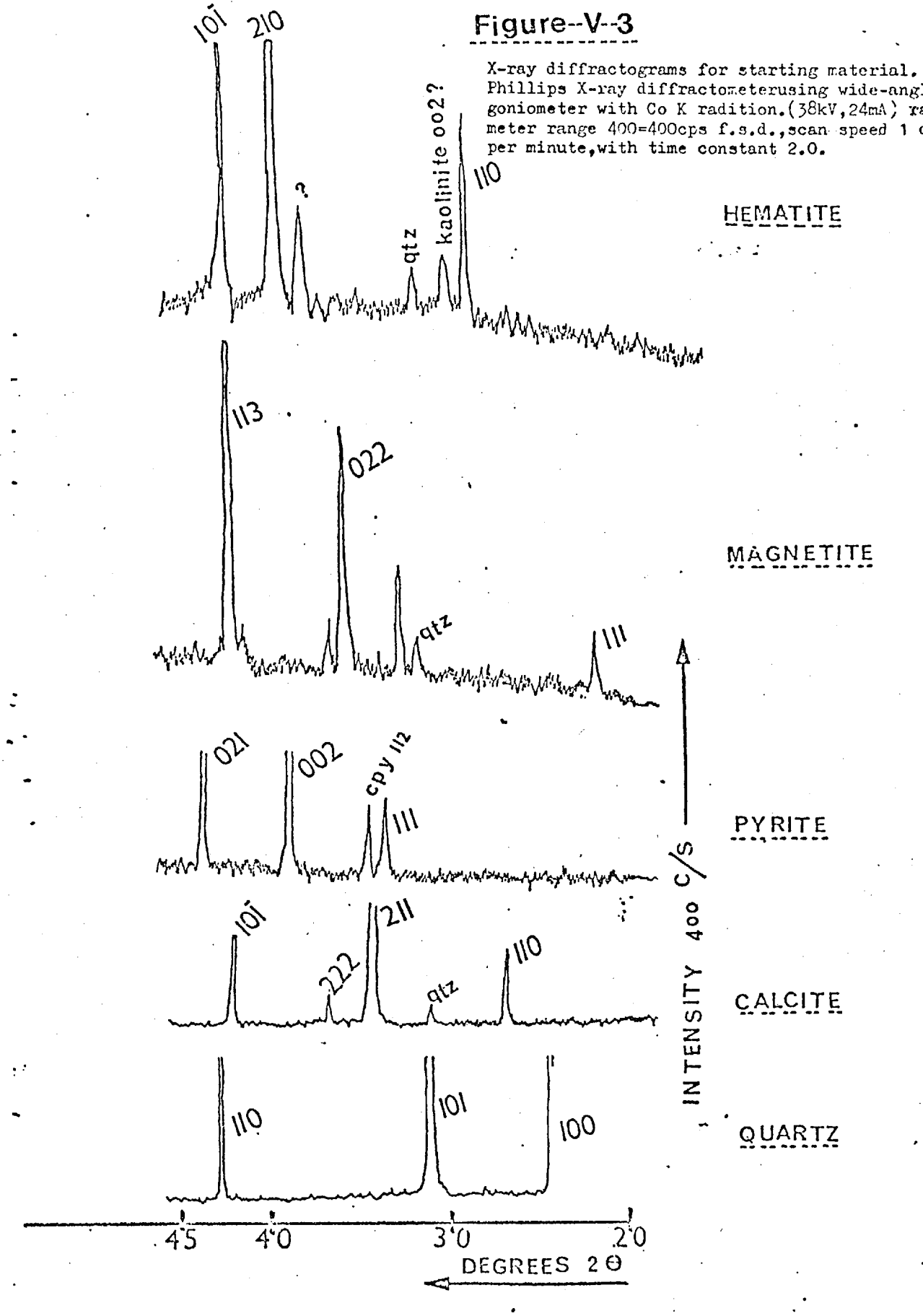
Similarly according to previous belief, the Hamersley Group has nowhere undergone regional metamorphism. According to evidence of Hoering no part of Brockman Iron Formation had reached a temperature above 160^{o}C (Trendal and Blockley, 1970). Incidentally Grubb (1967) was able to synthesize successfully fibrous riebeckite at only 35^{o}C.

In the present work, during optical microscopy, no high temperature minerals were revealed. However, some samples contain high temperature minerals such as rutile zircon and occasionally spinel. It is believed that these minerals were missed during optical microscopy, probably because of their minute quantity and small size and for the same reason they were not detected by whole rock X.R.D. Later they were detected in carbonaceous matter and their X.R.D., because if they were present then they were concentrated during HCl/HF sample preparation, to which they are, anyway, chemically resistant.

Hence an alternative source of origin of graphite was investigated. The experiment described proves that abiogenic graphite or ordering in carbonaceous matter can take place at 600^{o}C with 1Kb pressure.

Figure--V--3

X-ray diffractograms for starting material. Phillips X-ray diffractometerusing wide-angle goniometer with Co K radition.(38kV,24mA) rat meter range 400=400cps f.s.d.,scan speed 1 de per minute,with time constant 2.0.



D:2. SYNTHESIS OF ABIOGENIC GRAPHITE UNDER PRECAMBRIAN CONDITIONS

As stated above, the purpose of this experiment is to examine whether it is possible to graphitize carbonaceous material at geologically reasonable temperatures and pressures. French (1964), Ergun (1968), Kisch (1969), MacMillan et al. (1970), Landis (1971) and Grew (1974) have shown that crystallinity of carbonaceous matter increases with increasing metamorphic grades and ultimately results in well-ordered graphite. This study was designed to reproduce the formation of graphite in the laboratory by simulating pressure and temperature conditions in Precambrian iron formations.

In most occurrences of Precambrian iron formation, James (1959) has distinguished four sedimentary facies: The sulphide, oxide, carbonate and silicate facies. Iron formation of carbonate and silicate facies typically averages 25-30% Fe, whereas the oxide facies (magnetite or hematite) averages 30-35% Fe. In general the amounts of Fe and Si are inversely proportional.

Experimental

Crystals of quartz, magnetite, hematite, pyrite, and calcite (Royal School of Mines Geology Collection) were identified optically, hand-picked and their purity checked by X-ray diffraction (Figure (V) 3).

The bulk composition of charge 1 which was sieved at 200 mesh is shown in Table (V) 4. A simultaneous run was also carried out with charge 2, whose bulk composition was as for charge 1 except that organic matter in the form of the present day stromatolite was omitted.

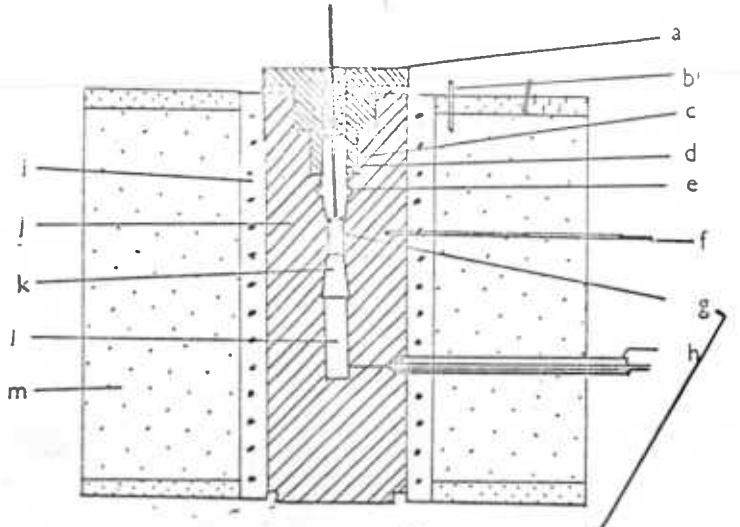
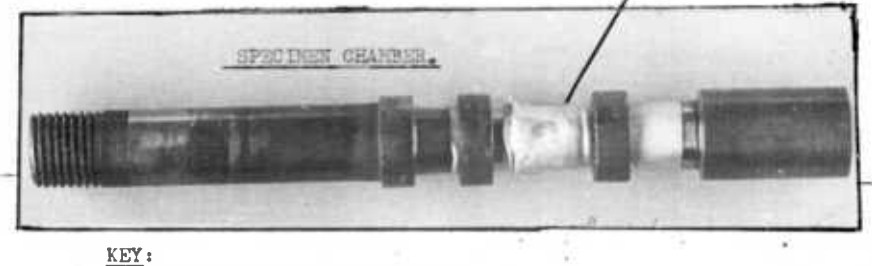


Figure--V--4

Schematic drawing of the furnace(Redrawn from Rutter,1970)Not to scale.



KEY:

a-Upper piston connector.
b-Furnace control thermocouple.
c-Packing ring.
d-Hard steel ring.
e-Upper piston.
f-Reference thermocouple.
g-Powdered specimen chamber(Hollow copper tube-3.8X0.7 cm.)
h-Confining pressure inlet pipe(0.125 inch diameter).
i-Furnace element.
j-Pressure cylinder.
k-Lower piston.
l-Force gauge column.
m-Furnace insulation.

TABLE (V) 4. Bulk Composition of Charges 1 and 2

Component	% by weight
Quartz	70
Magnetite	5
Hematite	5
Pyrite	5
Calcite	10
Stromatolite*	5

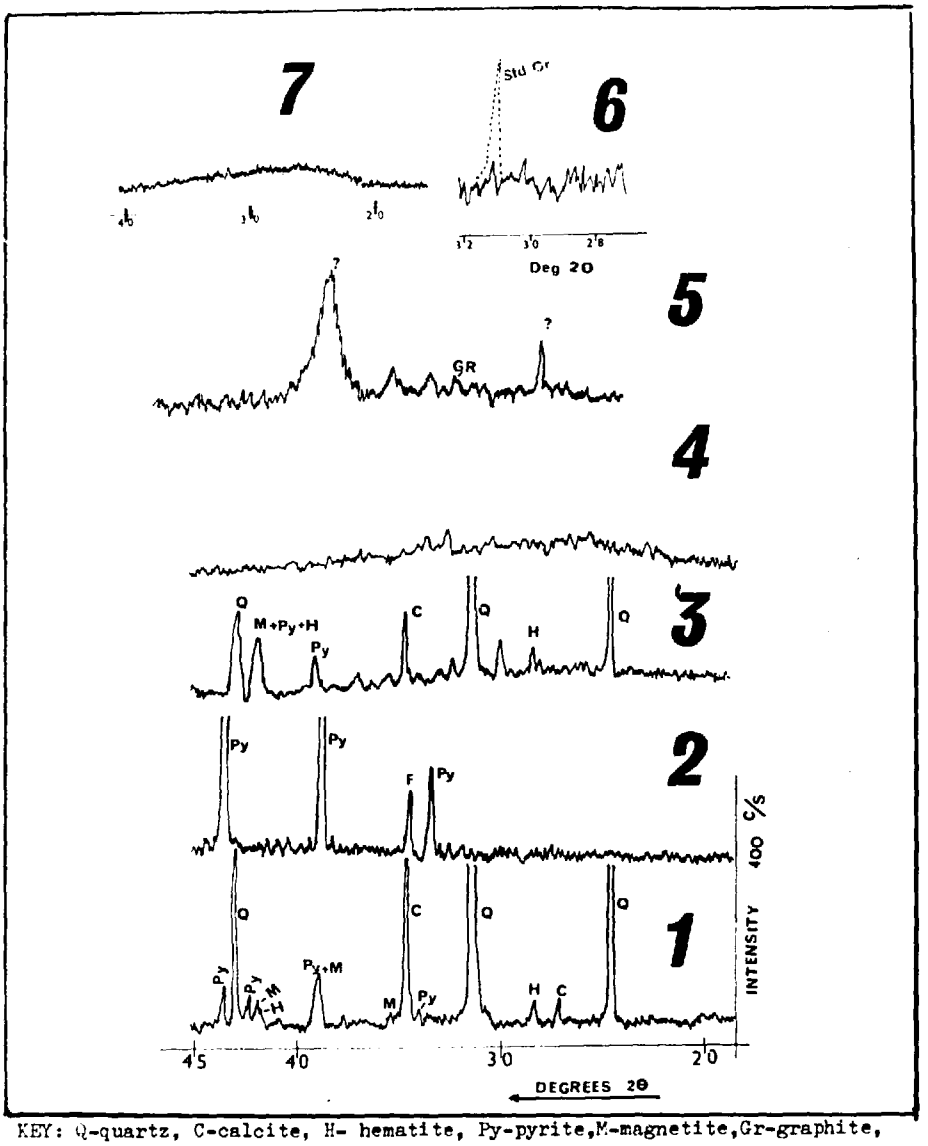
*Persian Gulf Algal mat, omitted in charge 2.

For the high temperature and pressure experiments a modified furnace normally used for *triaxial* rock deformation studies in the Engineering Geology laboratories at Imperial College was commissioned. A sketch of the internally heated pressure vessel is shown in Fig. (V) 4. Included also is the Figure for sample holder.

The temperature measuring device was a chromel-alumel thermocouple and the temperature was regulated by an 'Ether Transistrol' potentiometer. The temperature record was plotted on a 'Honeywell' multipoint strip chart recorder. The hydrostatic pressure was generated by an 'Olinair junior' three stage compressed air-operated hydraulic pump.

The charge is placed inside the sample holder (See inset Fig. (V) 4 which consists of a hollow copper tube of 3.8 x 0.7 cm. The open ends of this tube were sealed by two crystal plugs. Under these conditions the tube can hold 5-7 gm of powdered sample. This tube is dropped inside a steel block where it fits snugly and the block is heated by a nichrome wire resistance furnace.

PLATE-V-13----X-ray diffractogram showing formation of GRAPHITE-abiogenically.



KEY: Q-quartz, C-calcite, H- hematite, Py-pyrite, M-magnetite, Gr-graphite, F-fluoride complex, ?-unidentified.

1: Charge 2(composition as Table (V).4).
2: Charge 2 residue after treating with 1N HCl & 40% HF.
3: Charge 2 heated to 600 deg.C at 1 Kb pressure for 96 hr.
4: Residue from air contaminated portion after treating with 1N HCl & 40% HF.
5: Residue from non-air contaminated portion after treating with 1N HCl & 40% HF showing GRAPHITE peak(ordering of carbon).
6: Residue from 5 + standard graphite (standard addition technique).
7: Glass sample cavity mount (BLANK).

Because of the unadaptability of the apparatus, it was not possible to have simultaneously high pressure and high temperature conditions. However, to approximate the simultaneous application of heat and pressure, the sample holder was kept under pressure (1Kb) for 96 hours at the end of which time the temperature was raised to 600°C and maintained at this temperature for 96 hours. At the end of this period the holder was withdrawn from the furnace, cooled, and small pieces of the resulting material crushed and then treated with 1N HCl and 40% HF in a PTFE beaker. The insoluble residue was then examined by X.R.D., monitoring the (002) reflection peak near 3.4-3.5 Å as French (1964), Griffin (1969), Landis (1971) and Karkhanis (1975) have done for metamorphosed materials.

Results and Discussion

Charges 1 and 2 were heated to a range of temperatures between 200°C and 600°C. At 600°C and 1 Kb pressure all the organic material in charge 1 was oxidized to a soot-like residue which could not be collected for analytical work. When charge 2 was removed from the copper holder half of the 3.8 cm long, rod-like residue had a different colour (buff) from the other half (grey). The buff coloured portion had been oxidised by air which had gained access to this part of the sample tube.

Both portions were treated with 10% HCl and 40% HF separately to remove carbonates and silicates and the oxidised portion had no trace of carbon. However, the unoxidised portion demonstrated a certain degree of ordering of (002) reflection, showing the presence of well-ordered graphite (Pl. (V) 13). The chemical analysis of this material gave 1.12% carbon. This evidence suggests that abiotic graphite can be formed from carbonates at reasonably low laboratory temperatures and that its formation may be due

to a catalytic effect dependent on the minerals present. In the absence of a catalytic agent, graphitization of carbonaceous material in the laboratory requires considerably higher temperatures (1500-2000°C) for the first appearance of ordered layers and well-ordered graphite (2500-3600°C), Ubbelohde and Lewis (1960), Walker (1962), Richards (1968), Noda (1969), Pacault (1971). The relatively low temperatures needed for graphitization during metamorphism as compared with those required for the process in the laboratory are probably the result of the added influence of the factors listed in Table (V) 5 (Grew, 1974).

TABLE (V) 5. Experimental Conditions Promoting Graphitization

Conditions	References
Silica and Sericite impurities	Steward and Cook (1960) Istikwa and Yoshizawa (1963)
Contact with Limestone	Noda (1968) Inagiki et al. (1968)
Preferred orientation of crystallites in starting material	Franklin (1951) Walker (1962) Fischbach (1971)
Plastic deformation	Fischbach (1969)
Hydrostatic pressure (to 10 Kb)	Kamiya et al. (1968) Fischbach (1971)
Use of air or CO_2 instead of N_2 and Ar as ambient gas phase. Increased gas pressure	Noda and Inagaki (1964) Noda et al. (1965)
Use of optical grade of calcite at 500°C, 200 psi PH_2 for 6HR	Salotti et al. (1971)

* Modified after Grew (1974)

In the absence of air as in the presence of a hydrogen atmosphere (it is generally assumed that a reducing atmosphere lacking free oxygen existed early in the history of premordial Earth at a time before the deposition of presently known sedimentary rocks) the graphite could be formed abiotically as a reaction product between carbonate minerals and atmospheric hydrogen at low temperatures. This can be assumed to approximate closely the processes involved in the very early Precambrian. Previous studies based on the concept of limited thermodynamic equilibrium substantiates this assertion Eck et al. (1966), Girardini et al. (1968, 1969).

The 600°C 1 Kb experimental conditions for the first appearance of layering in ordering of carbonaceous matter has been observed by several other workers from naturally occurring samples (Table (V) 6). Salotti et al. (1971) proposed a mechanism for the formation of graphite vein deposits. The simplified reaction they give for the calcite-hydrogen system is:-

$$CaCO_3 + 4H_2 \text{ ..... } CH_4 + H_2O + Ca(OH)_2 \qquad \text{Eq. (V) 3}$$

$$CH_4 \text{ .....} C + 2H_2 \text{ (Pyrolitic dissociation)} \qquad \text{Eq. (V) 4}$$

The experimental conditions were 500°C, 2000 psi PH_2, 6HR, which showed graphite formed on the surface of $Ca(OH)_2$ and 600°C, 2000 psi PH_2, 0.5 HR which showed amorphous carbon formed on $Ca(OH)_2$ surfaces.

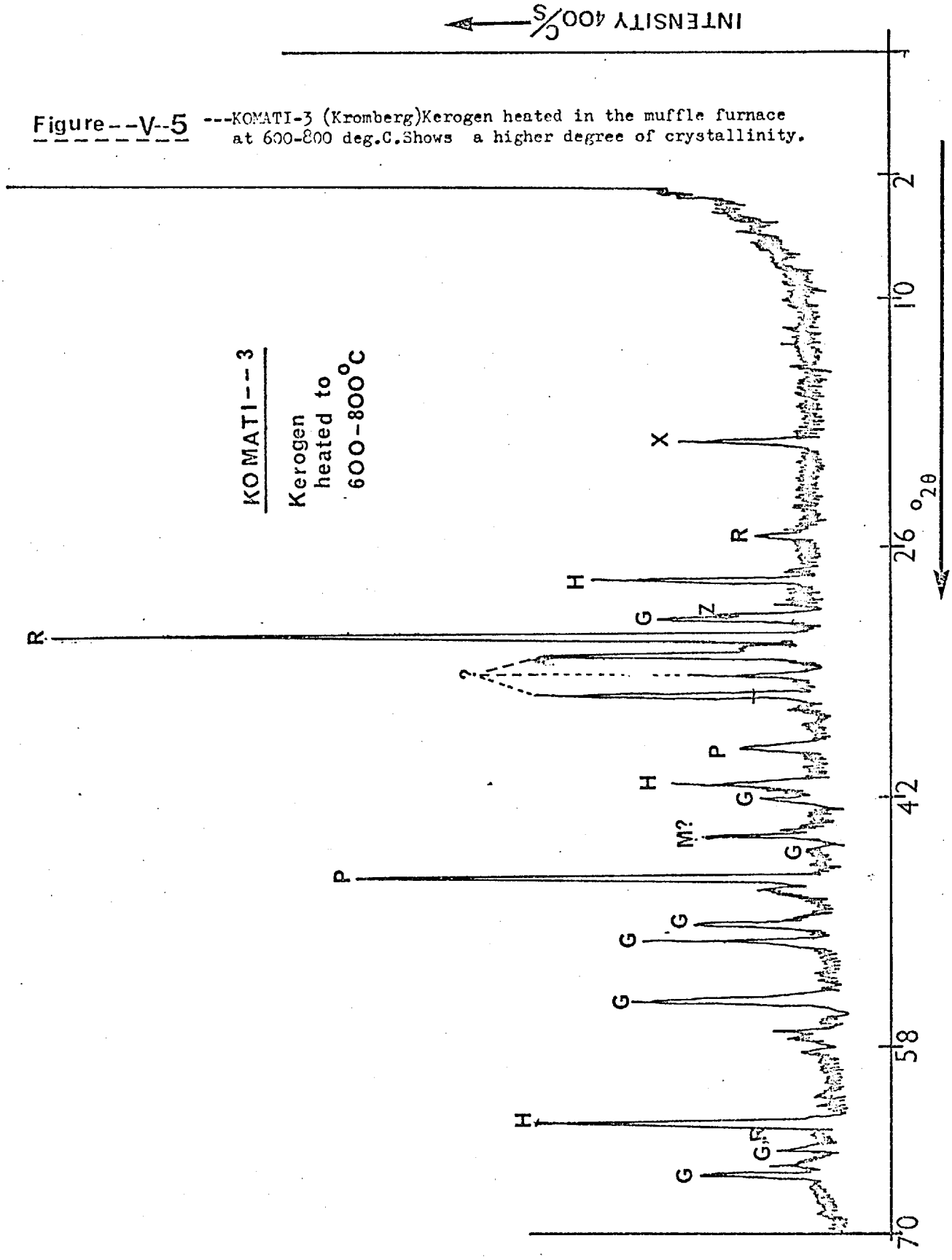
TABLE (V) 6. Pressure and Temperature of Graphitization under Normal Conditions

Locality	Metamorphic type	Temp.	Pressure	Reference
(a) Appearance of layer ordering				
Narragansett basin, Rhode Island	Chlorite facies	400-500°C	3-4 Kb	Grew (1974)
Antartica	Contact	Max. 1000°C at least 600°C for 1000 years	1 Kb	Grew (1974)
(b) Appearance of well-ordered graphite				
Narragansett basin, Rhode Island	Sillimanite Zone	600-690°C	4.5-5.0 Kb	Grew & Day (1972)
Undercliffe Australia	Hornblende hornfels facies	550-700°C	1-3 Kb	Hamilton et al. (1969)
Isua, S.W. Greenland	Greenschist facies	300-500°C	-	Nagy et al. (1975)

It is also noted that when the sample was removed from the holder after heating a peculiar sweet smell resembling ester or amyl alcohol was noted. This indirectly establishes that some kind of organic reaction has proceeded. It will be of further interest to analyze these vapours by Gas chromatographic analysis.

From these results one must conclude that besides graphite a number of number of other intermediate organic compounds could also be formed under these conditions and that there is a need for diagnostic criteria to distinguish between abiogenic and biologically produced organic matter.

Figure--V--5 ---KOMATI-3 (Kromberg)Kerogen heated in the muffle furnace at 600-800 deg.C.Shows a higher degree of crystallinity.



Recent reports by Harrison (1976) who reported laboratory graphitization of modern esturine kerogen, noted a better developed graphite like atomic arrangement after heating modern kerogen for 50 hrs at 300°

The author did similar experiments for kerogen for sample Komati 3 (Fig. (V) 5), which was heated in a muffle furnace in a porcelain silic boat for 600° to 800°C. The graphite peak observed in the original Kero (Fig. (II) 2) was found to be enhanced after this treatment and also the other component showed a higher degree of crystallinity.

D:3. Curtisite? (Poly-cyclic Aromatic Hydro-Carbon, $C_{24}H_{18}$)

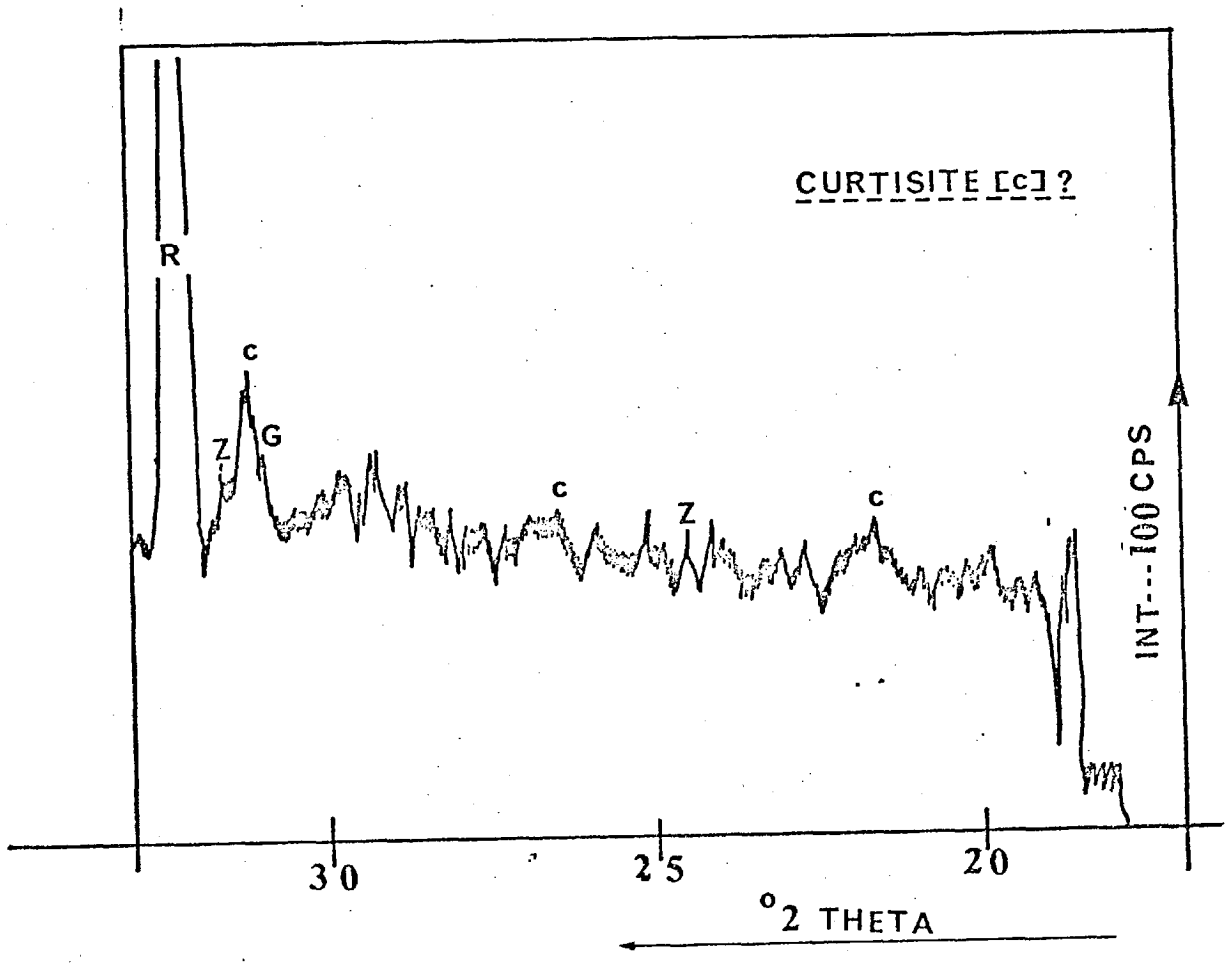
During the slow X.R.D. scan (1 degree 2θ per minute) at a count rate of 100 counts per second f.s.d. (full scale deflection) on some of the acid insoluble carbonaceous residues from the Kromberg Formation, it was observed that some of the peaks suggested the presence of hydrocarbons (Komati 3). Assignment of these peaks suggests that the contributory compound could be Curtisite, Fig. (V) 6, a polycyclic aromatic hydrocarbon mineral. This mineral was first reported by Wright and Allen (1930) and it normally occurs at the surface vents of the hot springs. It has a melting point (M.P. of 272-302°C (Grinsberg and Shimanskii (1954). According to Blumer (1975), the origin of curtisite and its associated compounds are derived from organisms through extended equilibration at elevated temperatures in the sub-surface and final fractionation during migration to the surface.

The same insoluble residue was heated to 600-800°C in a porcelain boat in a muffle furnace. As reported previously, the X.R.D. showed an enhancement in the graphite peak (Fig. (V) 5) and the area in which the curtisite peaks appear were no more to be seen, which probably accounts for the expulsion of this compound at this temperature, (Curtisite M.P. 272-302°C) from the graphite lattice giving the extra sharpness to the graphite peak.

There is a need to confirm this finding by Gas Chromatography and Mass Spectrometry (G.C.M.S.). In the meantime, in the absence of G.C.M.S. data, this conclusion should be regarded with caution.

Figure--V-6

Slow X.R.D. scan on acid insoluble carbonaceous residue from Komati-3(Kromberg) sample, show presence of poly-cyclic aromatic hydrocarbon, identified as CURTISITE?(c). The other peaks are zircon(Z). rutile(R). graphite(G).



It should, however, be remembered here that hydrocarbons have previously been reported in shales 1 billion years old (Meinschein et al. (1964), Eglington et al. (1964), Barghoorn et al. (1965), in cherts 2 billion years old, Oro et al. (1965) and in cherts 3 billion years old, Hoering (1965), Meinchein (1967), Oro and Nooner (1967), Macleod (1968), Hans & Calvin (1969).

D:4. Some Comments on the Use of Carbonaceous Matter as an Indicator of Metamorphic Grade and Palaeo-Temperature

From preceding discussion it appears that there is a similarity between the carbonisation of the insoluble carbonaceous matter (kerogen) and the coal. The minerological studies on these areas have not shown any high temperature mineral assemblages - except in few instances where minerals such as rutile, sphene and zircon appear in some samples. These minerals, however, are detrital minerals. Hence the estimate of temperature from mineral assemblages has been difficult. The rocks of the Onverwacht Group have been subjected to *greenschist facies* metamorphism. The possible temperature range compatible with experimental data on the stability of greenschist facies minerals is 300-500^{o}C (Fyfe et al., 1958). The Hamersley Group has nowhere undergone regional metamorphism, and the Brockman Iron Formation has not reached a temperature above 160^{o}C. (Trendall & Blockley, 1970), although recent work (Smith, 1976) indicates a basinal greenschist grade metamorphism.

During the X.R.D. work on numerous samples, the carbonaceous matter gave patterns of various types. At one end, pattern similar to Ceylon Graphite was obtained on sample PM-1, depicting 3-dimensional crystallite growth of graphite structure, whereas some samples gave the pattern for amorphous carbon.

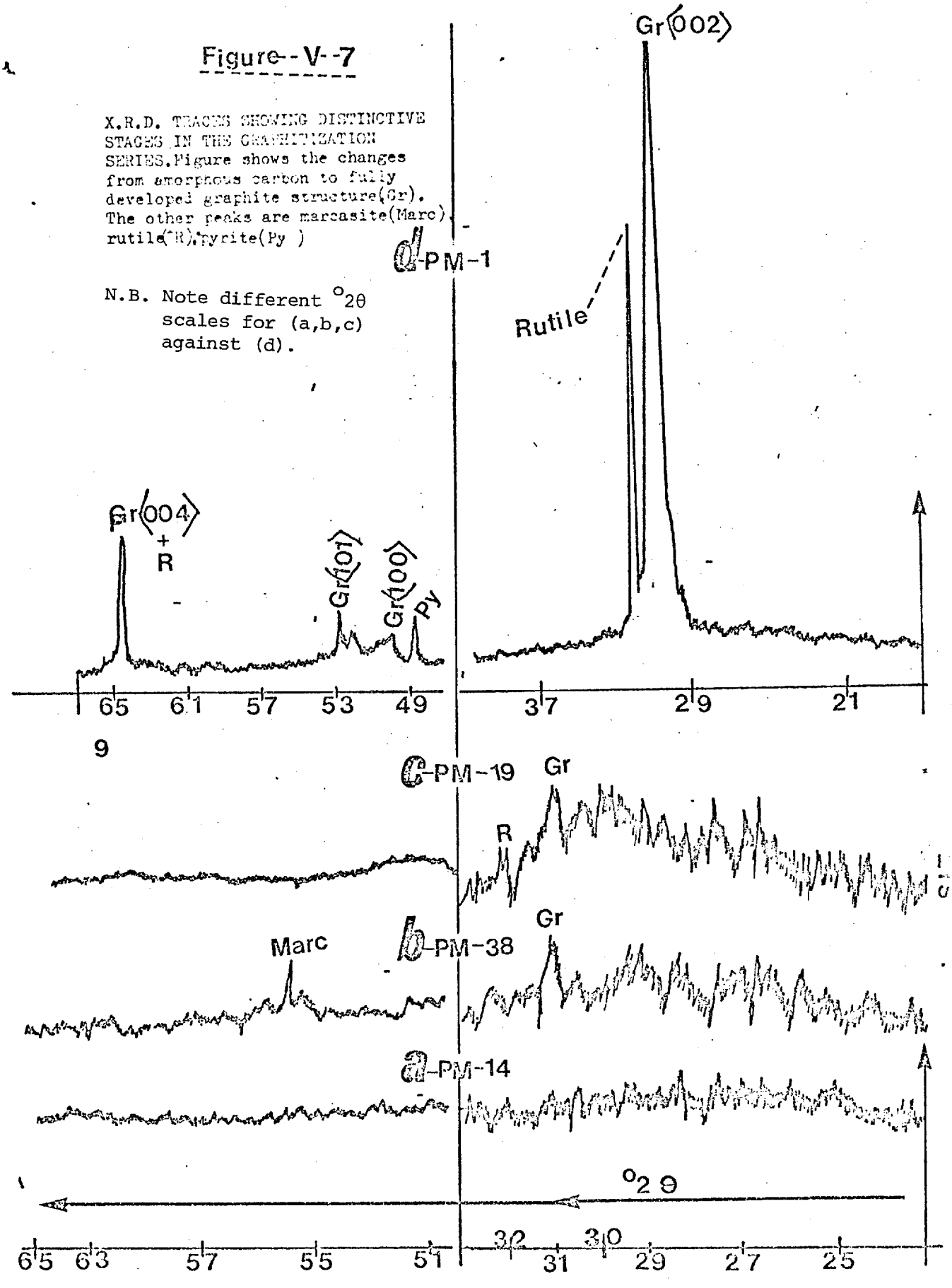
On the basis of diffractograms, the writer recognizes few more distinctive stages in the graphitization series. Fig. (V) 7 shows the changes from amorphous carbon (a) to fully developed graphite structure (d).

The X.R.D. pattern (Fig. (V) 7a) shows a broad hump and no graphite peaks in the sample. The effect of incipient metamorphism or temperature on the carbonaceous matter shows the broadening (hump) in the region

Figure--V--7

X.R.D. TRACES SHOWING DISTINCTIVE STAGES IN THE GRAPHITIZATION SERIES. Figure shows the changes from amorphous carbon to fully developed graphite structure(Gr). The other peaks are marcasite(Marc), rutile(R), pyrite(Py)

N.B. Note different $^{o}2\theta$ scales for (a,b,c) against (d).



29-33°2θ (CO-radiation) corresponding to d spacing of 3.58 Å - 3.15 Å. (Fig. (V) 7b).

By the next pattern (Fig. (V) 7c) where one can see the 'hump' in the region 29-33°2θ, some of the carbon has started graphitizing. Another 'hump' starts appearing in the region 49-53°2θ i.e. 2.16 Å - 2.006 Å. The fourth pattern (Fig. (V) 7d) shows well-ordered graphitic peak in the region 29°-33°2θ, and the 'hump' between 49°-53°2θ being split into (100) and (101) graphite peak and development of (004) and (103) reflections (not shown) towards the larger angles.

Figure (V) 7 a,b,c are examples of partial graphitization. The recognition of these stages and the apparent changes in the interplanar spacing suggests that from the diffused peak to well-ordered graphite there is a gradual change which can be co-related with the grade of incipient metamorphism and/or thermal history of the samples.

When viewed in conjunction with the coalification series of coal rank, the coal changes from Anthracite to graphite through meta-anthracite. This seems to be a very abrupt change (or coalification jump) in relation to (002) reflection. It is possible to fill this gap by monitoring the development of peaks in the region of 49-53°2θ and 64-65°2θ. The appearance of peaks in these regions completes the three dimenstional graphite structure.

It is tentatively possible to summarize the X-ray studies which indicate that carbonaceous matter (Fig. (V) 7b) is possibly made up of graphite layers roughly parallel to one another but with random orientation with layer spacing larger than that found in graphite. With further metamosphism ((heat) the layers start to grow in crystallite size with corresponding increase in the rank. Ultimately the ordered layer decreases to

the graphite value of 3.35 Å and there is a corresponding decrease in crystallite size. This contraction in lattice corresponds to expulsion of volatile content from the *'box'* like graphite structure as proved by Griffin (1967) for Humic sediments and Oberlin et al. (1973).

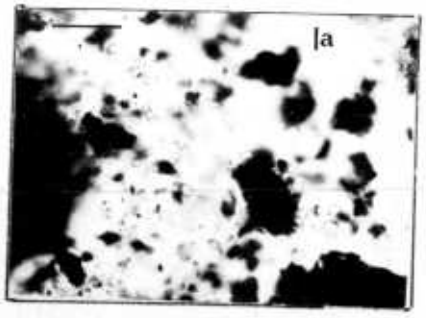
D:5. Environment of Deposition

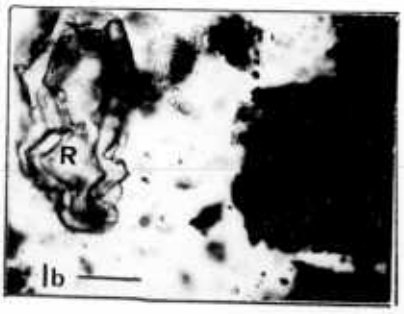
Plate (V) (14A) 1 shows various organic structures found in insoluble carbonaceous matter from PM-48 and PM-47. They may have been developed due to reactions in colloidal or gel precipitates. It is believed that Magadiite or a Sodium silicate gel may have been a precursor (Eugster and Ming Chow, 1973) and such gels could act as a substitute for accumulation and preservation of organic compounds (Govett, 1966). They could also be formed by inorganic osmotic processes. Hawley (1926) working with water glass and ferrous sulphate produced some structures simulating algae and fungi. He also observed a bulb-like membrane or receptacle, which would release a number of these structures on rupturing (Compare Plate (V) (13A), Plate (V) (14A) b with Plate (V) (14B).

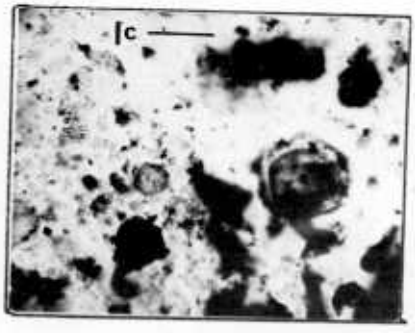
Two simple trial experiments with Sodium Silicate (water glass) were performed. (1) In one experiment, water glass was treated with HCl, HF acid to see if any artefacts are produced through sample preparation. The optical microscopic examination showed negative results. (2) In the second experiment, iron was added in the form of hematite, pyrite, and siderite to simulate B.I.F. minerology. The mixture was treated with HCl, HF. The residue was examined under the optical microscope. Various structures of various sizes and shapes were observed, but the circular form was most abundant. These synthetic circular bodies had smooth outlines as compared with those observed in PM-48 (Compare micro-photograph 2), which have serrated outlines. In some structures, cell-like walls and septae are visible (Pl. (V)(14A) 2d,2e,2f and 2g). Such morphologies have been reported by Leduc (1914).

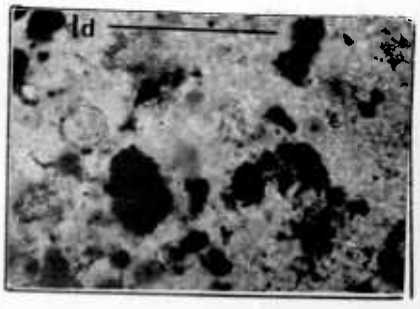
The X.R.D. on the insoluble carbonaceous matter from PM-48 and PM-47 showed the presence of an artifactual fluoride complex of Na, which has a

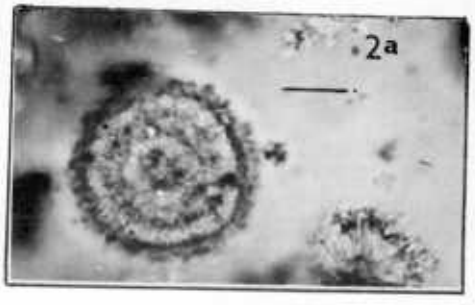
PLATE----V--14A



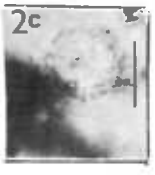














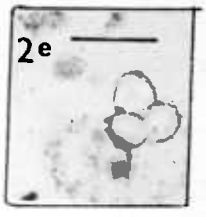






PLATE---V--14B



PLATE--V--14A and PLATE--- V-14B.

A case for ENVIRONMENT of DEPOSITION.(see text).

Fig.14A-1: Various inorganic structures from insoluble carbonaceous matter from PM-47 & 48 (Hamersley). Note a bulb-like membrane or receptacle(R-in fig.1b) which release these structures

1 a,b,c,d: Scale Bar= 100μ.
2 :Circular body with serrated outline.
Scale Bar: 10μ for fig.2a
25μ for fig.2b,c,d ,f &g.
50μ for fig.2e.

Fig.14B :Ferrous silicate osmotic growths from sulphate salt in concentrated water glass.(after Hawley-1926-who observed these synthetic membranes or receptacles in his gel experiments).Compare 14B with 14A-1,especially 1b.

similar *'d'* spacing of the mineral Ralstonite (Na_2(Aℓ, Mg) (F,OH)6.1-Y H_2O) and a similar peak was also observed for the insoluble residue for present day algal mat from the Persian Gulf, which has abundant Na_2CO_3 and NaCl.

Three important inferences can be drawn form these experiments:-

(1) Formation of Ralstonite (during HCl/HF/X.R.D. work) can be used as an index of original Na content in the sample.

(2) These structures can be taken as evidence for the environment of deposition, possibly a *Playa lake complex* with Sodium Silicate as the precursor for chert formation as suggested by Eugster and Ming Chow (1973)

(3) This could be a conceivable pathway for the formation of *"precell"* microspheres through polymerization of gel like substance and concentration of organic matter on spheroid surfaces.

Summary and Conclusions

In the absence of minerological information, the indigenous insoluble carbonaceous matter, which is a minor constituent of most sedimentary and metasedimentary rocks, appears to be a good thermal marker for determining degree of diagenesis. Variation in colour with temperature (thermal metamorphism) is not universally applicable tool, although a colour series (yellow-orange-brown-dark brown-black) is possible at the lower end of the temperature range.

X.R.D. studies on insoluble carbonaceous matter show that there is a gradual transformation from amorphous carbon to three dimensional graphite, that the change is not reversible and that it, therefore, leaves an imprint.

In the study of coal rank, there is a gradual change from peat to lignite and thence to anthracite. However, from anthracite to graphite there is an abrupt change. This gap - or *coalification jump* - can be bridged by monitoring *(110)* and *(112)* bands. These bands do not appear in lower rank material, but as the rank increases, they appear first as a single broad band, ultimately resolving into the three dimensional *(hkl)* reflections of graphite.

Separation of insoluble organic matter (kerogen) is still a difficult problem. Use of HCl/HF acid treatment is preferred for two reasons:-

(i) to remove the quartz *(101)* reflection (to be able to see the graphite *(002)* reflection).

(ii) to reduce as far as possible alteration to the original kerogen structure. Benzene sulphonic acid can be used instead of HCl to give a less severe treatment with the added advantage of less formation of insoluble flurocomplexes.

After numerous X.R.D. analyses had been carried out, only one sample (Komati-3) was found to contain *rhombohedral* form of graphite, which was concluded to have resulted from a *shear* in the rocks. Rhombohedral graphite is practically never found under natural conditions. The isothermal calometer experiment conducted by Boehm and Coghlin (1964) to measure the heat of formation of potassium graphite -C_8K- showed that:-

(1) The heat of reaction of -84 ± 0.3 cal/g C using pure hexagonal graphite.

(2) -88.1 ± 1.1 cal/g C using 33% rhombohedral modification.

Thus there is very little difference in the conditions needed to form C_8K and both forms react similarly.

It is, however, quite easy to bring about lattice modification by simple mechanical treatment e.g. grinding (Boehm and Hofmann (1955), Lares and Baskin (1956)). Thus for X.R.D. work (to avoid lattice deformation) and for ESR work (to avoid creating broken σ bonds at the periphery of crystallites) on carbonaceous matter, during sample preparation, grinding ought to be avoided.

During minerological investigations, the technique of staining was of immense value for identifying the various carbonate minerals. During staining some fossils were identified as possibly filamentous iron bacteria, which were preserved as casts or moulds. This technique could be applied to all carbonate rocks (especially Ferroan type) to look for micropalaeontological information, which might have been otherwise lost.

The estimation of temperature still remains difficult. Most of the rocks investigated are of gree-schist facies and the experimental temperature range for mineral assemblages in this facies is bout 300-500^{o}C.

Most of the rocks have α-quartz (low temperature) as their major component. This sets an upper limite of 867°C (above 867°C β quartz is a stable phase).

The writer carried out an experiment to attempt to synthesize graphite and from the experiment a temperature deduced for the appearance of layered ordering, of around 600°C at a pressure of 1 Kb. Well-ordered graphite was developed when one of the samples containing insoluble carbonaceous matter (K-3) was heated to 800°C in a muffle furnace.

Therefore in the natural formation of graphite the estimated upper limit is 867°C and the lower limit to 600°C. Graphite ordering seems to start at considerably lower temperatures in nature compared with laboratory requirements (1500°-2000°C) and it may be that some minerals act as catalysts in promoting graphitization. In conclusion it may be said:-

(1) Carbonaceous matter might be used as an indicator of metamorphic grade.

(2) The existence of *"Free Radicals"* has been shown in the insoluble carbonaceous matter. These radicals appear to be exceptionally stable with respect to geological time and the *'g'* values approach the free radical value of 2.0037 characteristic of organic free radicals.

(3) A regular increase in *'free radical'* content with increase in rank is observed. (1.87 to 9.47 x 10^{15} spin/g). A similar correlation exists between ESR line width, crystallite size and rank.

(4) The possible use of free radical content and the measurement of other E.S.R. parameters can be used to follow the course of diagenesis or incipient metamorphism.

(5) The X.R.D. technique can also be used, hand in hand, to monitor the crystallinity of the carbonaceous matter.

(6) Isolation of pure *'kerogen'* for this type of investigation is after all not absolutely necessary. Much information can still be obtained by present methods.

(7) Application of staining technique should be made as a routine method particularly for carbonate rocks.

(8) Lastly the X.R.D. and E.S.R. techniques would render valuable information if applied to a carefully selected suite of samples rather then scattered samples.

(9) The grinding of carbonaceous matter should be avoided if the X.R.D. and E.S.R. Techniques are applied.

APPENDIX

APPENDIX I

(A). SOUTH AFRICAN SAMPLES

ONVERWACHT GROUP, SWAZILAND SUPERGROUP

Sample No.	Age (years)	Age (Stratigraphic)	Locality
K 1 A	3.4×10^9	Archaean Kromberg Formation, Onverwacht Group.	Komati River, Scaapbrug, near the old JC1 mining Camp.
K 3	3.4×10^9	" "	" " "
K 4	3.4×10^9	" "	" " "
K 5	3.4×10^9	" "	" " "
K 6	3.4×10^9	" "	" " "
K 7	3.4×10^9	" "	" " "
HALL 1	3.4×10^9	" "	" " "
HALL 2	3.4×10^9	" "	" " "
HALL 1 W/L	3.4×10^9	" "	" " "

(B). AUSTRALIAN SAMPLES

KALGOORLIE, WESTERN AUSTRALIA

Sample No.	Age (years)	Age (stratigraphic)	Locality
PM 1	2.7×10^9	Archaean Kalgoorlie System.	approx. 17m E. of Kalgoorlie W.A.
PM 3	2.7×10^9	" "	" " "
PM 5	2.7×10^9	" "	approx. 12m S. of Southern Cross W.A.

(C). SOUTH ALLIGATOR RIVER GROUP

NORTHERN TERRITORY, AUSTRALIA

Sample No.	Age (years)	Age (Stratigraphic)	Locality
PM 192	2.2×10^9	Lower Proterozoic, Koolpin Formation	El Sherana Mine, South Alligator River N. About 50m E.N.E. of Pine Creek.
PM 193	2.2×10^9	" " "	" "
PM 194	2.2×10^9	" " "	" "
PM 195	2.2×10^9	" " "	" "
PM 196	2.2×10^9	" " "	" "
PM 197	2.2×10^9	" " "	" "
PM 198	2.2×10^9	" " "	" "
PM 199	2.2×10^9	" " "	O'Dwyers Mine tip, about 50m E.N.E. of Pine Creek, N.T.
PM 200	2.2×10^9	" " "	" "
PM 201	2.2×10^9	" "	" "
PM 202	2.2×10^9	" " "	Rockhole Mine about 50m. E.N.E. of Pine Creek, N.
PM 203	2.2×10^9	" " "	" "

(D). HAMERSLEY RANGE, WESTERN AUSTRALIA

Sample No.	Age (years)	Age (Stratigraphic)	Locality
PM 9	2.0×10^9	Lower Proterozoic, Dales Gorge Member, Hamersley Group.	Approx. 4m S. of Wittenoonm W.A.
PM 11	2.0×10^9	" " "	" "
PM 12	2.0×10^9	" " "	Side Creek on E. side of Wittenoom Gorge, 4m S. of Wittenoom, W.A.

cont'd.....

(D). HAMERSLEY RANGE, WESTERN AUSTRALIA

Sample No.	Age (years)	Age (Stratigraphic)	Locality
PM 13	2.0×10^9	Lower Proterozoic, Dales Gorge Member, Hamersley Group.	Side Creek on E. side of Wittenoom Gorge, 4m S. of Wittenoom, W.A.
PM 14	2.0×10^9	" " "	" " "
PM 15	2.0×10^9	" " "	" " "
		PM 9 - 15 occur in the S15 Shale of Trendall.	
PM 17	2.0×10^9	Lower Proterozoic, Dales Gorge Member, Hammersley Group, BIF 15	Same as PM 12
PM 19	2.0×10^9	Lower Proterozoic, Dales Gorge Member, Hamersley Group.	" "
PM 21	2.0×10^9	" " "	" "
		PM 19 - 21 occur in the S16 Shale of Trendall.	
PM 23	2.0×10^9	Lower Proterozoic, Dales, Gorge Member, Hamersley Group, BIF 16	Same loc. as PM 12
PM 24	2.0×10^9	Lower Proterozoic, Whaleback Shale Mbr, Hamersley Group, WS 1	" " "
PM 25	2.0×10^9	Lower Proterozoic, Whaleback Shale Mbr, Hamersley Group, WS 2.	" " "
PM 28	2.0×10^9	Lower Proterozoic, Whaleback Shale Mbr, Hamersley Group WS 3.	" " "
PM 30b	2.0×10^9	Lower Proterozoic, Whaleback Shale Mbr, Hamersley Group WS 3.	" " "
PM 31	2.0×10^9	Lower Proterozoic, Whaleback Shale Mbr, Hamersley Group, WS 3	" " "

cont'd.....

(D). HAMERSLEY RANGE, WESTERN AUSTRALIA

Sample No.	Age (years)	Age (Stratigraphic)	Locality
PM 36	2.0×10^9	Lower Proterozoic, Dales Gorge Member, Hamersley Group, BIF 12 base.	4m S. of Wittenoom WA.
PM 38	2.0×10^9	Lower Proterozoic, McRae Shale, Hamersley Group.	approx. 3m S. of Wittenoom, W.A.
PM 39	2.0×10^9	" " "	" " "
PM 40	2.0×10^9	Lower Proterozoic, Mt. Sylvia Formation, Hamersley Group.	" " "
PM 43	2.0×10^9	Lower Proterozoic, Dales Gorge Member, Hamersley Group.	ABA (Australian Blue Asbestos Pty Ltd.) drill core Locality uncertain but probably between Bee Gorge &
PM 44	2.0×10^9	" " "	Wittenoom Gorge. W.A.
PM 45	2.0×10^9	" " "	" " "
PM 46	2.0×10^9	" " "	" " "
PM 47	2.0×10^9	Lower Proterozoic, Roy Hill Member, Jeerinah Formation, Fortescue Group.	Tom Price-Paraburdoo Railway cutting at 181.2m mark, WA.
PM 48	2.0×10^9	" " "	" " "
PM 49	2.0×10^9	" " "	" " "
PM 50	2.0×10^9	" " "	" " "
PM 51	2.0×10^9	" " "	" " "
PM 52	2.0×10^9	Lower Proterozoic, Wittenoom Dolomite, Hamersley Group	Hill above Water Tank for Tom Price Mine Supply, WA.

APPENDIX II

(A). CARBON ISOTOPES STUDIES BY INFRA-RED SPECTROSCOPY

Part of this work was carried out when the author did one year (1973) Post graduate research in the Laboratory of Chemical Evolution, Department of Chemistry, University of Maryland, College Park, U.S.A. under the direction of Dr. Raj Khanna, under the overall supervision of Prof. Cyril Ponnamperuma.

The preliminary results were encouraging and the approach to the problem appeared to be valid, hence the need to report here. I do not intend to go into detail and only a brief introduction to the subject will be given. As the work was left unfinished, this information should be regarded as a proposal for future work.

Introduction

Why is it necessary to study isotope fractionation?

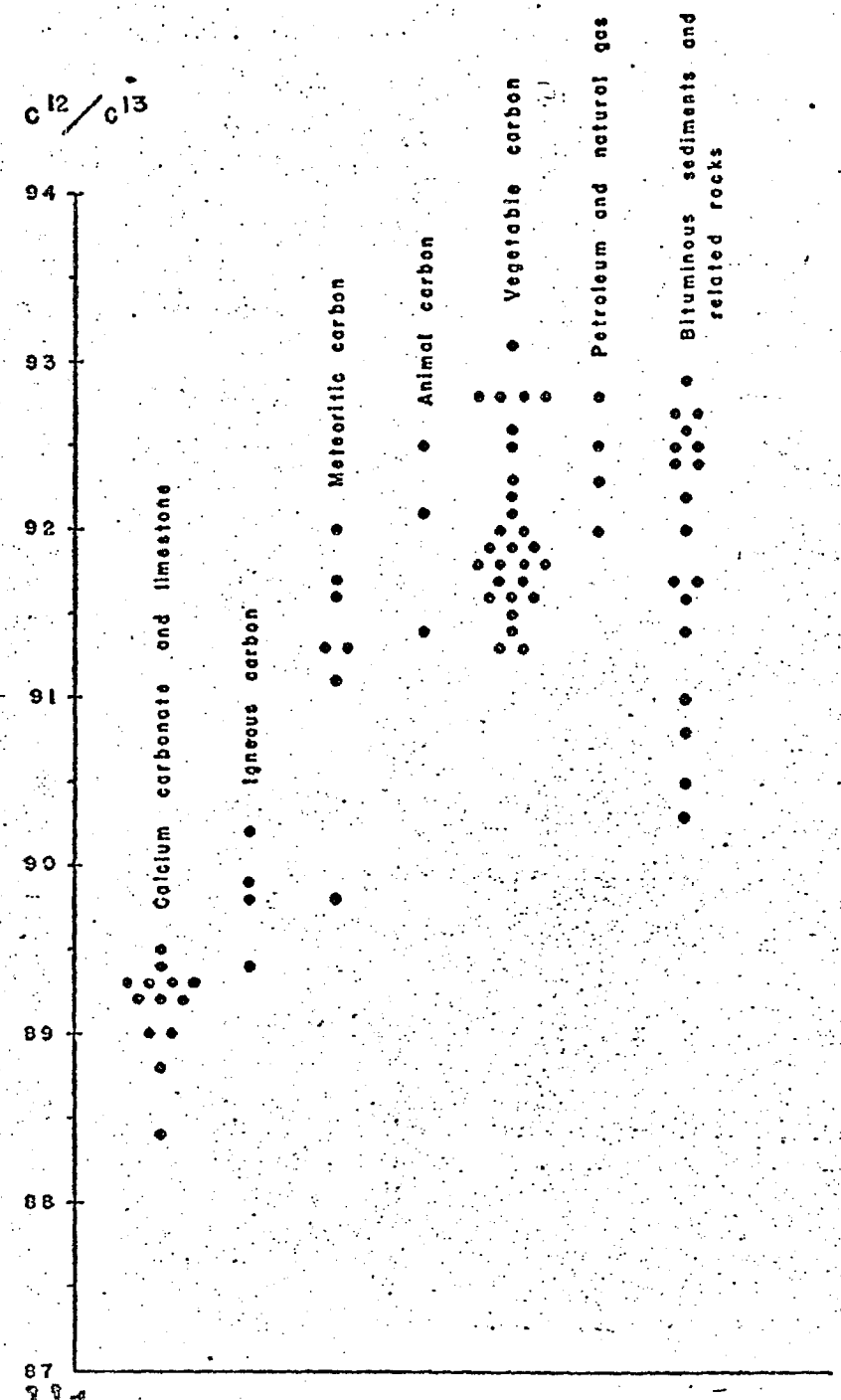
(1). In geology, we are dealing with two major problems (Degens, 1969)

(a) Diagenetic fate of organic matter through geological time.

(b) To try to get more insight into the nature of prebiological carbon in terrestrial and extra-terrestrial bodies.

(2). In biology, the problem lies in the delineation of bio-synthetic pathways through using and comparing isotope ratios in discrete biochemicals.

(3). Therefore, using (1) and (2) it may be possible to establish some relation between carbon containing compounds from living and fossil organism and thereby understand the complex Bio-chemical cycle of carbon through time and space.



Appex-III-C^{12}/C^{13} ratios in carbonaceous materials, classified according to their origin

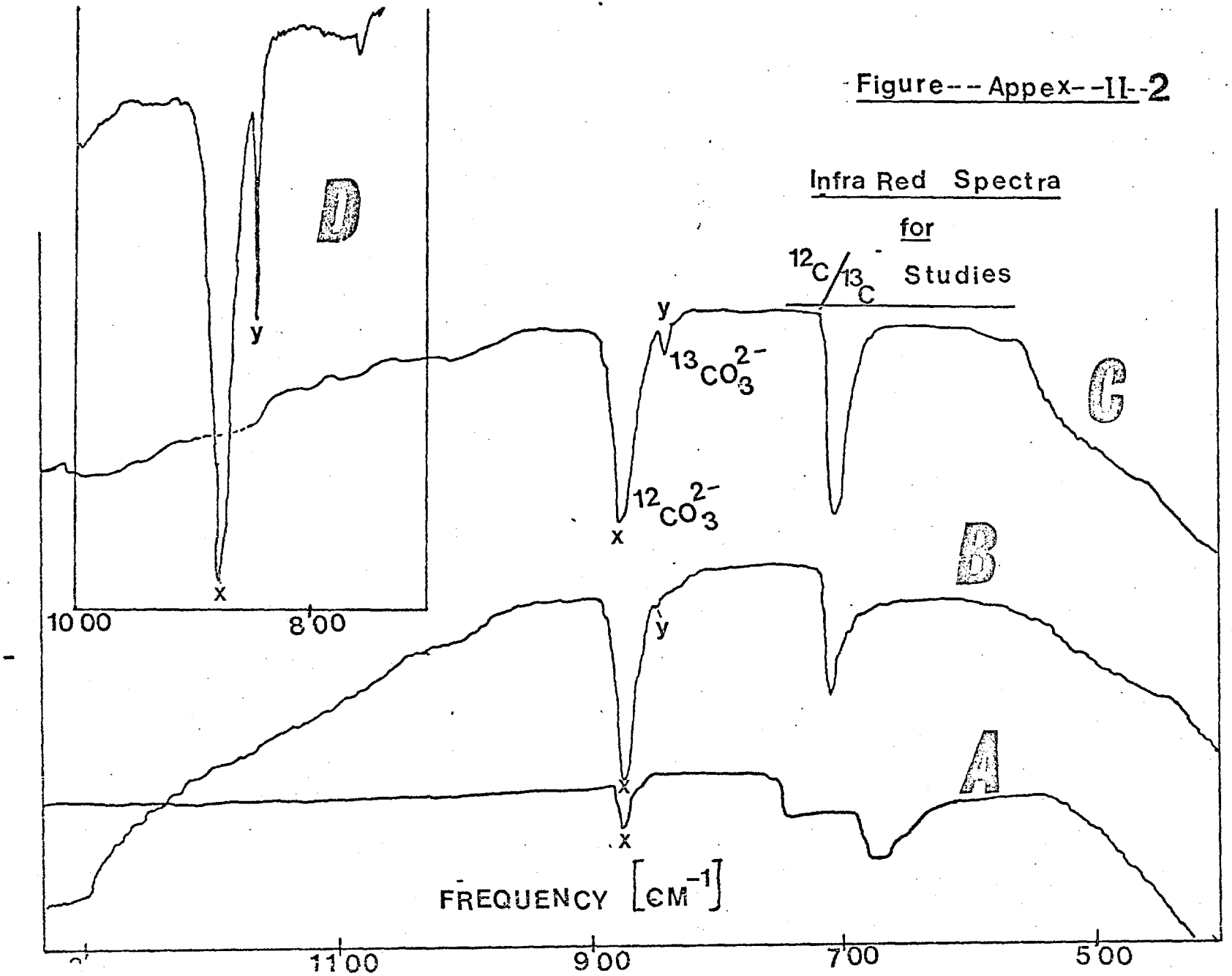
The stable carbon isotopic composition data from modern and ancient materials can be used to give information about the origin and evolution of life. Fig. (Appendix II) 1 is a plot of $^{12}C/^{13}C$ ratios in carbonaceous materials according to their origin. We can see a distinct trend for inorganic carbon is around 88 to 90, and the organic carbon group has a ration 90-93. It is probably reasonable to assume meteoritic carbon does show the primordial isotopic composition (Rankama, 1948). The general picture of fractionation of carbon isotopes shows that there are two series of processes viz: the inorganic process and oxidized compounds bringing about the enrichment of C^{13} and lowering of C^{12}/C^{13} ratio, and the organic processes and reduced compounds which accumulate C^{12} and increase the isotope ratio.

Now, if we assume that at the time of the origin of the Earth no geological or biological processes were active which could otherwise alter the primordial isotopic composition of carbon, it is, therefore, safe to assume that the original isotopic composition cannot be found in the present day carbon of inorganic or organic origin. This indirectly gives us a hypothesis saying that somewhere during geological time there should be a discontinuity which can be correlated with the Origin of Life.

The use of isotopic constitution indicates the biogenic or non-biogenic origin of carbon in ancient rocks and is based on the following (true or false) assumptions Rankama (1954):-

(1) It is assumed that ancient organisms were able to fractionate the carbon isotopes in a way similar to their present counter-parts.
(2) It is assumed that the isotopic constitution, once established, does not materially change with physical and chemical conditions of the surroundings. It remains unaffected by geological processes.

Figure---Appex--II--2



(3) It is also assumed that the isotopic constitution of carbon in the exchange reservoir has not materially changed during the geological history of the Earth.

Analytical Technique

Way of reporting isotpic data:-Three ways are used in reporting isotopic data of carbon.

(i) Absolute numerical ration $^{12}C/^{13}C$ or $^{13}C/^{12}C$ known as 'R'.

(ii) The results are sometimes reported as difference between absolute ratios in a simple and standard R sample - R standard (Dansgaard, 1953).

(iii) If very small difference in the isotopic constitution is to be determined, the $\delta^{13}C$ values, in per mil, with respect to arbitrary standard is used thus,

$$\delta^{13}C^{o}/oo = 1000 \frac{R \text{ sample}}{R \text{ std}} - 1$$

with correction for ^{17}O contribution to mass 45. Thus a-ve value for δ indicates the sample is 'lighter' i.e. contains less C^{13} than the standard and is enriched in C^{12}, and if at value, then the sample is enriched in C^{13} with respect to the standard. The standard used most commonly is a sample of belemnite, *Belemnitella americana* from the cretaceous Peedee formation in South Carolina. Normally the isotopic

analysis is performed a by Mass spectrometry and there is an extensive literature on this subject (Hayes and Biemann, 1968).

The alternative method is based on Infra-Red spectroscopy (I.R.). It is based on the following principle.

The stretching frequency (υ in CM^{-1}) of a band is related to the masses of two atoms (M_x and M_y, in grams) according to the relation.

$$\upsilon = \frac{1}{2\pi C} \sqrt{\frac{K}{M_x M_y / (M_x + M_y}}$$

$$= \frac{1}{2\pi C} \sqrt{\frac{K}{\mu}}$$

where K = force constant (dynes/cm)

e = velocity of light

μ = reduced mass $= \frac{M_x \times M_y}{M_x + M_y}$

Since 'μ' is different, the vibrational frequency is different i.e. the heavier molecule will have a smaller vibrational frequency. This is known as the *ISOTOPE EFFECT*, which was first observed by Loomis (1920) and independently by Kratzer (1920) in rotation vibration spectrum of HCl.

In a particular spectrum the band belonging to higher mass is shifted a small amount towards longer wavelength with respect to the lower mass. This kind of shift is prominent in the case of heavy hydrogen. Here the difference is nearly ½ and hence the isotope shift is very great in molecules

such as H^1Cl^{35}, H^2Cl^{35} or H^1Cl^{37} and H^2Cl^{37}. And therefore the bands Cℓ appear in different spectral region Hardy et al. (1932)。 The vibrational isotope effect is prominent compared to the rotational isotope effect。

The accurate measurement of the isotope effect could be used to obtain precise values for ratio of the masses of two kinds of isotopic atoms。 Under favourable conditions, the accuracy of the data so obtained is comparable with mass spectrographic values, Herzberg (1939).

Sampling Technique for I.R. measurements

The ionic solids such as alkali halides the Cℓ (R = 0。99 Å) ion could be replaced by CO_3^{2-} because of a *Schottky defect* in the crystal lattice Fyfe (1964)。 In doing so, the overall lattice will still maintain stoichiometric balance and charge neutrality.

This kind of solution could be brought about by -

(1) freeze drying

(2) crystal growth

Brief description of these techniques follows:-

(1) Freeze drying: $CaCO_3$ (calcite) has a very low solubility in water (0.0014% @ 25°C). Hence an intermediate solvent could be used。 NH_4Cl was used for that purpose. The mixture of the following composition was freeze dried。

5 g KCℓ in 50 ml H_2O

0。25 g $NH_4Cℓ$

100 mg $CaCO_3$

The I.R. spectra in Fig. (Appex II) 2 confirms that CO_3^{2-} transformation to KCl lattice, and $^{13}CO_3^{2-}$ shoulder peak is visible. Further development of this technique is needed to achieve better separation of CO_3^{2-} broad absorption peak (870 CM^{-1}).

(2) Through Crystal Growth:- In this technique, a mixture of $CaCO_3$ and KCl was prepared (10g KCl + 500 mg $CaCO_3$). The mixture was poured into 14 mm AG.81 Vycor tube. This tube was lowered into a vertical furnace at a very very slow rate (approx. 2 ft/24 Hrs.) by means of a mechanical (clock) device. The furnace was made up of high temperature quartz tube wound with heating element controlled by rheostat to maintain the temperature of 898°C (M.Ps of calcite 898°C, and KCl 776°C). The melt thus formed is mixed on its own due to the convection current in the melt. As the dropping of the fusion tube continues, the tube emerges out of the hot spot of the furnace, the cooling proceeds at a very slow rate. At this the crystal starts growing. At the end of 24 hours, the tube is cooled and the crystal thus formed is subjected to I.R. analysis. The I.R. spectrum C shows a strong peak @ 870 CM^{-1} (x) due to symmetrical bending of $^{12}CO_3^{2-}$ and other weak absorption band near 850 CM^{-1} (y) due to $^{13}CO_3^{2-}$.

The sample pallet was run at liquid N_2 temperature. At low temperature, the vibration of molecules are minimised and one can see a good separation in the isotope and the parent peak. (See I.R. spectrum Fig. D). The spectrum A is for direct KCl, $CaCO_3$ pellet for comparison.

This high temperature application has its merits if one has to work on the siliate rock types.

(B). POSSIBLE USE OF BENZENE SULPHONIC ACID (BSA)

I would like to introduce the use of new acid for attacking the rock samples. The investigations are still incomplete. But the initial results are encouraging.

I recommend the use of Benzene Sulphonic acid (BSA) instead of HCl, HF combination for the dissolution of rocks.

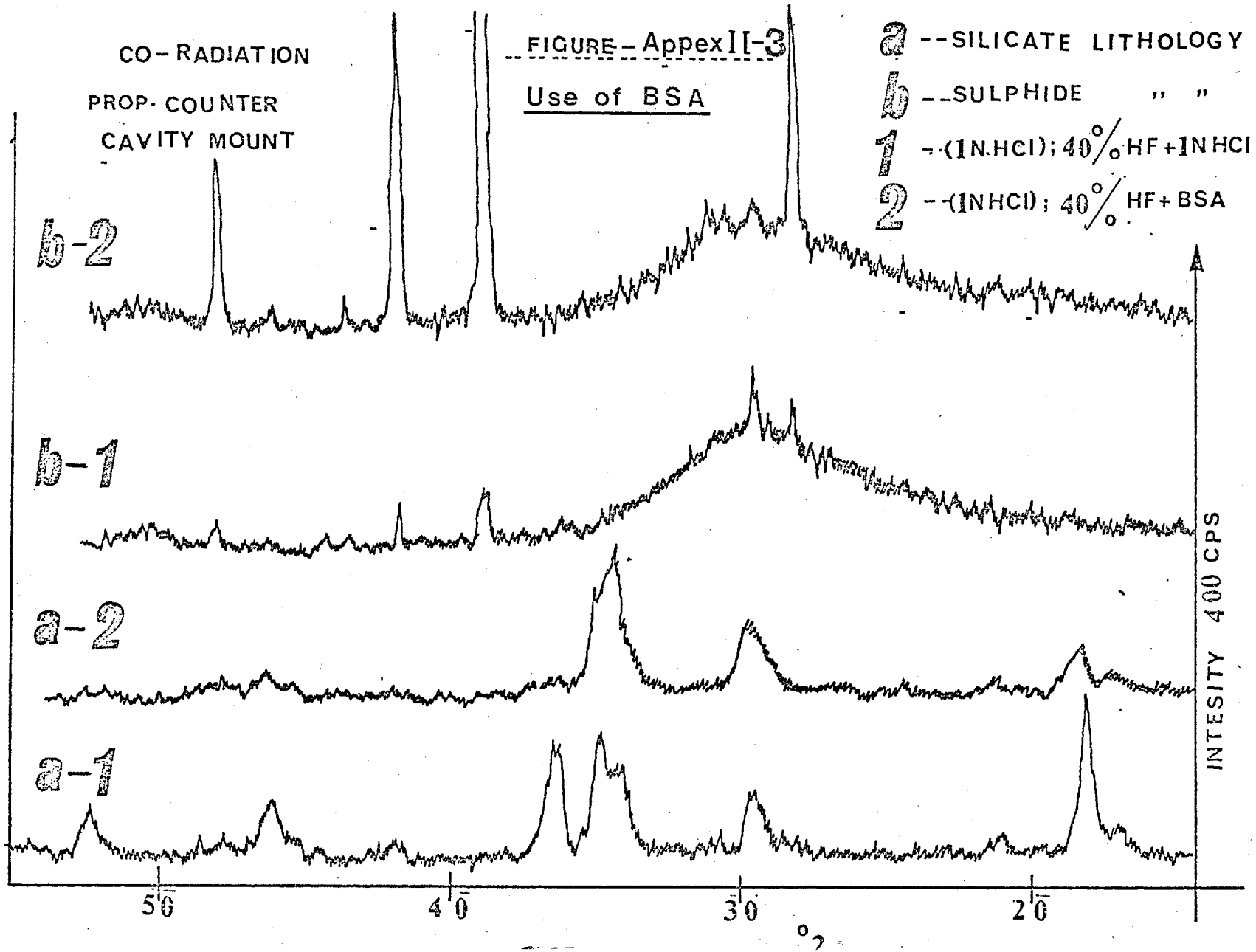
Number of insoluble fluorides are formed during HCl, HF attack. The prevention of insoluble fluorides complexes can be achieved by effectively removing SiF_4 and the excess of fluorine. This would be achieved by raising the boiling point of HF-HCl azeotrope mixture (B.P. 120° C). Here where the HCl fails and therefore in few instances we obtain insoluble fluorides. BSA has a high boiling point (130° C) and has a high solubility for its salts.

The random portion was chosen for this experiment (1:5, 30% BSA:40% HF) and samples of two different lithologies - one sulphide and the other siliate - were chosen.

Fig. (Appex. II) 3 shows the XRD monitoring of the carbonaceous matter and are compared against the conventional acid attack.

It is clearly obvious that HCl/HF attack is superior for sulphide lithology but for siliate sample the BSA attack is better.

The other advantage I visualize is that if one is trying to determine the structure of kerogen, one would know at least the reaction products of BSA. Preparation of sulphonate does not involve breaking of C-O bond. When we carry out reaction this reaction, we know exactly what we are starting with.


CO-RADIATION
PROP. COUNTER
CAVITY MOUNT
FIGURE - AppexII-3
Use of BSA
a --SILICATE LITHOLOGY
b --SULPHIDE " "
1 -(1N.HCl); 40% HF+1N HCl
2 -(1N HCl); 40% HF+BSA
b-2
b-1
a-2
a-1
INTESITY 400 CPS
5°
4°
3°
2°
θ

But in the case of HCl, there are a number of reactions that can occur with various functional groups, which could possibly alter the original kerogen. The possible reactions are (Saxby, 1970) (1) hydrolysis, (2) addition, (3) Quaternization, (4) alkylhalide formation.

APPENDIX III

Publications:-

1) Evidence for graphite from the Onverwacht Series Precambrian cherts, Swaziland System of South Africa.

   Chemical Geology (1975), 16, pp. 233-238.

2) Fossil iron bacteria may be preserved in Precambrian ferroan carbonate.

   Nature (1976) 261, pp. 406-407.

3) Artifacts produced by chemical processes of samples for micropalaeontology and organic geochemistry: A note of caution.

   Precambrian Research (1976) in Press.

4) Chemical studies on insoluble carbonaceous matter from Precambrian sediments by Electron spin resonance and X-ray diffraction techniques.

   Chemical Geology - submitted 25.11.1975.

5) Synthesis of abiogenic graphite under Precambrian conditions.

   Jour. of Geol. Soc. of India - submitted 14.5.1976.

6) Scanning electron microscopy of fossil iron bacteria.

   Jour. of Microscopy - In preparation

7) Microscopical and chemical studies on organic matter from early Precambrian Rocks. Paper presented at the Microscopy of organic sediments, coal and coke meeting held at Wadham College, Oxford, 5-6 April, 1976. Abstracts Royal Microscopical Society - Proceedings V. 11, Pt. 2 (1976). pp. 87-88

REFERENCES

REFERENCES

ABELSON, P.H. (1959). Geochemistry of organic substances *in* P.H. Abelson (ed) Researches in Geochemistry, Wiley, New York pp. 79-103.

ALEXANDROV, E.A. (1955). Contribution to studies of Origin of Precambrian Banded Iron Ores. Eco. Geology, 50 (5). pp. 459-468.

ANHEUSSER, C.R., ROERING, C., VILJOEN, M.J. and VILJOEN, R.P. (1968). The Barberton Mountainland: a model of the elements and evolution of Archaean fold belt. Annex. Geol. Soc. S. Africa, 71 pp. 225-255.

AYSCOUGH, P.B. (1967). Electron Spin Resonance *in* Chemistry. Methuen and Co. Ltd., London, 451p.

BARGHOORN, E.S., MEINSCHEIN, V.G. & SCHOPF, J.V. (1965). Palaeobiology of a Precambrian Shale Science 148 (3669). pp. 461-472.

BARGHOORN, E.S. and SCHOP , J.W. (1966). Microorganisms 3 billion years old from the Precambrian of South Africa Science 152, pp. 758-763.

BARGHOORN, E.S. and TYLER,.A. (1965). Microorganisms from the Gunflint chert Science. 147 pp. 563-575.

BERKNER, L.V. and MARSHALL, L.C. (1965). History of major atmospheric components. Proc. Nat. Acad. Sci. (U.S.) 53, pp. 1215-1225.

BERNER, R.A. (1969). The synthesis of framboidal pyrite. Eco. Geol. 64. pp. 383-384.

BERRY, L.G. and THOMPSON, R.M. (1962). X-ray powder data for ore minerals. The peacock Atlas. Geo. Soc. of Am. Mem. 85.

BINDER, C.R. (1965). Electron spin resonance. Its application to the study of thermal and natural histories of organic sediments: Ph.D. Thesis Penn. State University, University Park, Pa., 129p.

BITTERLI, P. (1963a): Classification of Bitumenous rocks of Western Europe: Reprint, 6th World Petroleum Congr., Frankfurt/Main, Scc. 1, Paper 30, 11p.

BITTERLI, P. (1963b). Aspects of genesis of bitumenous rock sequences: Geol. en Mijnb., Jaarg. 42, no. 6, pp.183-201.

BLAYDEN, H.E., RILEY, H.L. and TAYLOR, A. (1940). Crystalline growth during carbonisation. J. Am. Chem. Soc. 62, 180-186.

BLUMER, M. (1975). Curtisite, Idrialite and Pendletonite, polycyclic aromatic hydrocarbon minerals, their components and origin. Chem. Geol. 16. pp. 245-256.

BOEHM, H.P. and COUGHLIN, R.W. (1964). Enthalpy difference of hexagonal and rhombohedral graphite. Carbon, 2, pp. 1-6.

BRANDTH, R.T., GROSS, G.A., GRUBB, H., SEMENKO, N.P., DORR II, J.W.N. (1972). Problems of nomenclature for banded ferruginous-cherty sedimentary rocks and their metamorphic equivalents. Eco. Geol. 67, pp. 682-684.

BREED, R.S. (1975). *In* Bergey's Manual of determinative Bacteriology (Baltimore). The William and Wilkins Co. pp. 4-14.

BROOKS, J. and MUIR, M.D. (1971). Morphology and chemistry of the organic insoluble matter from the Onverwacht Series, Precambrian chert and the Orgueil and Murray carbonaceous meteorities. Grana, 11, pp. 9-14.

BROOKS, J. Muir, M.D. and SHAW, G. (1973). Chemistry and morphology of Precambrian Microorganisms. Nature 244, No. 5413, pp. 215-217.

CELLIERS, J.J. le R. and GENIS, J.H. (1964). Crocidolite asbestos in the Cape Province, in the Geology of some ore deposits of South Africa, II: Geol. Soc. South Africa. pp. 543-570.

CLOUD, P.E. (Jr.) (1965). Significance of Gunflint (Precambrian) microflora, Science, 148. pp. 27-35.

CLOUD, P.E. (Jr.) (1968). Pre-metazoan evolution and the origins of the metazoa, pp. 1-72 *in* E.T. Drake (ed.) evolution and environment. Yale University Press, New Haven.

CLOUD, P. (Jr.) (1972). A working model of primitive earth. Am. Jour. Science, 272. pp. 537-548.

CLOUD, P. (Jr.) (1973). Palaeoecological significance of the banded iron formation, Eco. Geol. 68. pp. 1135-1143.

CLOUD, P. (Jr.) and Lecari, G.R. (1968). Microbiotas of the banded iron formation. (U.S.). Nat. Acad. Sci. Proc. 61. pp. 779-786.

CLOUD, P. (Jr.), MOORMAN, M., PIERCE, D. (1975). Sporulation and ultra structure in late proterozoic cyanophyte: some implications for taxonomy and plant phylogeny. Quart. Rev. Biol. 50. No. 2, pp. 131-150.

COMPSTON, W. and ARRIENS, P.A. (1968). The Precambrian geochronology of Australia. Can. J. Earth Sci. 5, pp. 561-583.

CONVEY, D. and LIBBY, W.F. (1958). The measurement of very slow reaction rates: decarboxication of alanine. J. Am. Chem. Soc. 80, pp. 1077-1084.

COOPER, D.H.N. (1935). Iron in the sea and marine plankton. Royal Soc. London Proc. Ser. B. 118, pp. 414-439.

COOPER, D.H.N. (1937-38). Oxidation-reduction potential *in* sea-water. U.K. Marine Biol. Assoc. Jour. 20, pp. 167-176.

CORREIA, M. (1967). Relations possibles entre l'état de conservation des élements figures de la matière organique (microfossiles palynoplactologiques) et l'existenee de gisements d'hydrocarbures. Revue de l'institut français du petrole V. XXII, No. 9. pp. 1285-1306 (in French).

CORRENS, C.W. (1949). Einführung in die Minerologie. Spring-Verlag, Berlin. 414p.

CRELLING, J.C. and DUTCHER, R.R. (1968). A petrographic study of a thermally altered coal from Pergatoire River valley of Colorado. Geol. Soc. Am. Bull. 79, No. 10. pp. 1375-76.

DANSGAARD, W. (1953). Comparative measurements of standards for carbon isotopes. Geochimica et cosmochimica. Acta 3. pp. 253-256.

DEGENS, E.T. (1965). A brief Survey Geochemistry of sediments. Prentice-Hall. Inc. Englewood Cliff, N.J. 352p.

DEGENS, E.T. (1967). Diagenesis of organic matter *in* G. Larsen and G.V. Chillinger (ed.). Diagenesis of sediments. Developments in Sedimentology 8. Elsevier Publ. Co. Amsterdam, Lond., N.Y. 1967.

DEGENS, E.T. (1969). *In* Organic Geochemistry (ed.) G. Eglington and M.T.J. Murphy, Spring-Verlag, N.Y. Heidelberg Berlin.

DESIKACHARY, T.V. (1959). Cyanophyta (Indian Council of Agricultural Research, New Delhi. pp. 420-423).

DICKSON, J.A.D. (1965). A modified staining technique for carbonates in thin sections. Nature. 205, No. 497, p. 587.

DICKSON, J.A.D. (1966). Carbonate identification and genesis as revealed by staining. Jour. Sed. petrology. 36, No. 2. pp. 491-505.

DORR, J.V.N. (1964). Supergene iron ores of Minas Grais, Brazil. Eco. Geol. 59, pp. 1203-1240.

DREVER, J.I. (1974). Geochemical model for the origin of Precambrian Banded iron formation. Geol. Soc. Am. Bull. 85, pp. 1099-1106.

DUCHENE, J., DEPIREUX, J. and van der KAA, J.M. (1961). Origin of free radicals in carbonaceous matter. Geochimica et cosmochimica. Acta. 23, pp. 207-218.

DUNGWORTH, G. and SWARTZ, A.W. (1972). Kerogen isolates from Precambrian of South Africa and Australia for Carbonised microorganisms and Pyrolysis gas liquid chromotography. Advances in Organic Geo-chemistry 1971 (ed.). H.R. v. Gaertner and H. Wehner. pp. 699-706.

ECK, R.V., LIPPINCOTT, E.R., DAYOFF, M.O. and Pratt, Y.I. (1966). Thermo-dynamic Equilibrium and Inorganic origin of organic components. Science, 153, pp. 628-635.

EDGELL, H.J. (1964). Precambrian fossils from Hamersley Range, Western Australia and their use in stratigraphic co-relation. Jour. Geol. Soc. of Australia, XI, PART 2, pp. 236-261.

EGLINGTON, G., SCOTT, P.M., BELSKY, T., BURLINGAME, A.L. and CALVIN, M. (1964). Hydrocarbons of Biological origin from one-billion-year-old sediment. Science. 145 pp. 263-264.

EGLINGTON, G., SCOTT, P.M., BELSKY, T., BURLINGAME, A.L. RICHTER, W. and CALVIN, M. (1966). Occurrences of isoprenoid alkenes in Precambrian sediments. Advances in Organic Geochemistry (Ed.). G.D. Hobson and M.C. Lovis. Pergamon, London, pp. 41-47.

ENGEL, A.E.J., ENGEL, C., HAVENS, R.G. (1965). Chemical characteristics of oceanic basalts and the upper mantle. Bull. Geol. Soc. Amer. 76, pp. 719-736.

ENGEL, A.E.J., NAGY, B., NAGY, L.A., ENGEL, C.G., KREMP, G.O.W., and DREW, C.M. (1968). Alga-like forms in Onverwacht Series, South Africa; Oldest recognized Life-like forms on Earth. Science 161, pp. 1005-1008.

ERGUN, S. (1968). X-ray studies of coals and carbonaceous materials. U.S. Bureau of Mines Bull. 648, 38p.

EVANS, S.R. and STAPLIN, F.C. (1969). Regional facies of organic metamorphism. Geochemical exploration 1970. Boyle, R.W. and J.I. McGerr (ed.). Can. Inst. Min. & Met. Spec. 2, pp. 517-520.

EUGSTER, H.P. (1969). Inorganic bedded cherts from Magadi area, Kenya. Contr. Minerology Petrology. 22. pp. 1-31.

EUGSTER, H.P. and J-MING CHOU (1973). The depositional environments of Precambrian Banded Iron Formation. Eco. Geol. 68, pp. 1144-68.

FARRAND, M. (1970). Framboidal sulphides precipitated synthetically Mineralium Deposita 5, pp. 237-247.

FISCHBACH, D.B. (1969). The influence of high temperature plastic deformation on the kinetics of graphitization of pyrolitic carbons, *IN* Aspects fondamentaux de la carbonisation et de la graphitization. J. Chim. Phys. et Physico-chemie Biol. Special No. April 1969. pp. 121-127.

FISCHBACH, D.B. (1971). The kinetics and mechanisms of graphitization *IN* Walker, P.L. (Jr.) (ed.). Chemistry & Physics of Carbon. Marcel Dekker, New York V. 7. p. 105.

FORSMAN, J.P. (1963). Geochemistry of kerogen *IN* I.A. Breger (ed.). Organic geochemistry, Pergamon, London. pp. 148-182.

FRANKLIN, R.E. (1951). Crystallite growth in graphitizing and non-graphitizing carbons; Proc. Roy. Soc. Lond. Sec. A: 209, pp. 196-210.

FREISE, E.J. and KELLY, A. (1963). The deformation of graphite crystals and the production of rhombohedral form. Philos. Mag. 8 (93). pp. 1519-1533.

FRENCH, B.M. (1964). Graphitization of org. material in a progressively metamorphosed Precambrian iron formation. Science, 146 (3646) pp. 917-918.

FRENCH, B.M. (1968). Progressive contact metamorphism of the Biwabik Iron Formation, Masabi Range, Minnesota. Minn. Geol. Sur. Bull. 45.103p.

FYFE, W.S. (1964). Geochemistry of Solids. Mc Graw-Hill Book Co., New-York.

FYFE, W.S., TURNER, F.J. and VERHOOGEN, J. (1958). Metamorphic reactions and metamorphic facies. Geol. Soc. Am. Mem. 73. 259p.

GARRELS, R.M. and CHRIST, C.L. (1965). Solutions, Minerals and equilibria. New York, Harper and Row, 450 p.

GEHMAN, H.M. (1962). Organic matter in limestones. Geochimica et Cosmochimica Acta. 26. pp. 885-897.

GIARDINI, A.A. and SALOTTI, C.A. (1969). Kinetics and relations in calcite-hydrogen reaction and relation in dolomite-hydrogen and siderite-hydrogen systems. Am. Mineral, 54, pp. 1151-1172.

GIARDINI, A.A. and SALOTTI, C.A., LAKNER, J.F. (1968). Synthesis of graphite and hydrocarbons by reaction between calcite and hydrogen. Science 159. pp. 317-319.

GLAESSNER, M.F. (1962). Precambrian fossils. Biol. Rev. 37, 467-94.

GLAESSNER, M.F. (1969). Trace fossils from the Precambrian and basal Cambrian. Lethaia, 2 (4), pp. 369-393.

GLIKSON, A.Y. (1971). Archaen geosynclinal sedimentation near Kalgoorlie, Western Australia. Reprinted from sp. pub.: No. 3. Geol. Soc. of Australia. pp. 443-460.

GOLDICH, S.S. (1973). Ages of Precambrian Banded iron formation. Eco. Geol. 68, pp. 1126-1134.

GOVETT, G.J.S. (1966). Origin of banded iron formations: Geol. Soc. Am. Bull. 77, pp. 1191-1212.

GRAY, J. and BOUCOT, A.S. (1975). Colour changes in pollen and spores. A review G.S.A. Bull. 86. pp. 1019-1033.

GREW, E.S. (1974). Carbonaceous material in some metamorphic rocks of New England and other areas. J. Geol. 82 (1). pp. 50-73.

GREW, E.S. and DAY, H.W. (1972). Staurolite, kyanite and sillimanite from Narrgansett basin of Rhode Island. U.S. Geol. Sur. Prof. Paper 800-D D151-157.

GRIFFIN, G.M. (1967). X-ray diffraction techniques applicable to studies of diagenesis and low rank metamorphism in humic sediments. J. Sed. Petrol. 37, pp. 1006-1011.

GRINBERG, I.V. and SHIMANSKII, V.M. (1954). Study of chemical nature of the coloured organic mineral curtisite and its associates. Mineral, Sb., L'VOV Geol. Ova., 1954. No. 8. pp. 95-108.

GROSS, G.A. (1961). Metamorphism of iron formations and its bearing on the beneficiation. Can. Min. and Met. Bull. 54, No. 545, pp. 30-37.

GRUBB, P.L. C. (1971). Silicates and their paragenesis in the Brockman iron formation of Wittanoom Gorge, W. Australia. Ecol. Geol. 66, pp. 281- 292.

GUNDERSEN, J.N. and SCHWARTZ, G.M. (1962). The geology of the metamorphosed Biwabik Iron Formation, Eastern Masabi dist. Minnesota. Minn. Geol. Sur. Bull. 43, 139p.

GUTJAHR, C.C.M. (1966). Carbonization measurements of pollen grains and spores and their application. Leidse Geol. Meded., 38. pp. 1-29.

HAMILTON, L., RAMSDEN, A.R., and STEPHEN, J.F. (1970. Fossiliferrous graphite from Undercliff, New South Wales. J. Geol. Soc. Aust. 117 (1). pp. 31-36.

HAN, J. and CALVIN, M. (1969). Occurrence of fatty acids and aliphatic hydrocarbons in a 3.4 billion-year-old sediment. Nature. 161. pp. 1005-1008.

HARDY, J.D., BARKER, E.F., DENNISON, D.M. (1932). The Infra-red spectra of H^2Cl. Physical Rev. 42. pp. 279-289.

HAWLEY, J.E. (1926). An evaluation of the evidence of life in the Archaen J. of Geology. 34. pp. 441-461.

HAYES, J.M. and BIEMANN, K. (1968). High resolution mass spectrometers investigation of the organic constituents of the Murray & Holbrook Chondrites. Geochimica et cosmochimica acta. 32. pp. 239-267.

HERZBERG, G. (1939). Molecular Spectra and Molecular Structure. Prentice Hall in corp.

HOERING, T.C. (1965). The extractable organic matter in Precambrian rocks and the problem of contamination. Carnegie Inst. Year Book, 64. pp. 215- 218.

HOOD, A. and CASTAÑO, (1974). Organic metamorphism. Its relation to petroleum generation and application to studies of authegenic minerals: Reprinted from United Nations ESCAP, COOP Technical Bulletin 8, p. 85-118.

HOUGH, J.L. (1958). Fresh water environment of deposition of Precambrian banded iron formation. Jour. of Sed. Petrol. 28, No. 4, pp. 414-430.

HUNT, J.M. (1962). Some observations on organic matter in sediments. Paper presented at Oil Scientific Session "25 years of Hungarian Oil". 8-13th October 1962. Budapest.

HURLEY, P.M., PINSON, W.H., NAGY, B., and TESKA, T.M. (1972). Ancient age of the middle marker horizon, Onverwacht Group, Swaziland Sequence, South Africa. Earth Plan. Sci. Lett. 14, pp. 360-366.

ILER, R.K. (1955). Colloidal chemistry of silica and siliates. Cornell Univ,Press, Ithaeca 324p.

INGRAM, D.J.E., TAPLEY, J.G., JACKSON, R., BAND, R.L. and MURNAHGAN, A.R. (1954). Paramagnetic resonance in carbonaceous solids. Nature. 174, pp. 797-798.

ISHIKAWA, T. and YOSHIZAWA, S. (1963). Manufacture of high purity artificial graphite-III, catalytic action of sericite on graphitization of carbon. J. Chem. Soc. Japan and Indus. Chem. Soc. Sec. 66, pp. 929-933.

JAMES, H.L. (1954). Sedimentary facies of iron formation. Eco. Geol. 49, No. 3, pp. 235-239.

JAMES, H.L. (1955). Zones of regional metamorphism in the Precambrian of North Michigan. Geol. Soc. Am. Bull. 66, pp. 1455-1488.

JAMES, H.L. and SIMS, P.K. (1973). Precambrian Iron Formation of the World. Econ. Geol. 69, pp. 913-914.

KAMIYA, K., INAGAKI, M., MIZUTANI, M. and NODA, T. (1968). Effect of pressure on graphitization of Carbon IV. Abrupt graphitization of hard carbon under 5 Kbar. Chem. Soc. Soc. Japan Bull., 41, pp. 2169-217

KARKHANIS, S.N. (1975). Evidence of graphite from the Onverwacht series Precambrian cherts, Swaziland System of South Africa. Chemical Geology, 16, pp. 233-238.

KARKHANIS, S.N. (1976). Fossil iron Bacteria may be preserved in Precambrian Ferroan Carbonate. Nature 261. No. 5559. pp. 406-407.

KARKHANIS, S.N. (1976). Artifacts produced by chemical processing of samples for micropalaeontology and organic geochemistry. A note of caution. Precambrian Research - in Press.

KISCH, H.J. (1969). Coal rank and burial metamorphic mineral facies. In Schenk, P.A. and Haveneer, I. (eds.). Advances in organic geochemistry, 1968. Proc. 4th Int. Meeting Org. Geochem. Amsterdam, Sept. 16-18, 1968. Pergamon, Oxford, pp. 407-425.

KISCH, H.J. (1971). Anthracite and meta-anthracite coal ranks associated with 'anchimetamorphic' pyrophyllite and high illite crystallinites: Abstracts VIII. Internat. Sedimentological Congress 1971, Heidelberg, Germany (BDR), p. 51.

KLEIN, C. (1964). Minerology and petrology of Wabush Iron Formation, Labrador City Area, New Foundland. Ph.D. Thesis, Harvard Univ. 154p.

KLEIN, C. (1973). Changes in mineral assemblages with metamorphism of some banded Precambrian iron formation. Eco. Geol. 68, pp. 1075-88.

KRATZER, van A. (1920). Eine spektroskopische Bestätigung der Isotopen des Chlors. 2. Physik 3. pp. 460-465. (in German).

KRAUSKOPF, K.B. (1969). The Geochemistry of silica in sedimentary environments. p. 4-19. *IN* Ireland, H.A. (ed.). Silica in sediments. Soc. Eco. Palaeontologists and minerologists. Sp. Pub. No. 7. 185p.

KRAUSKOPF, K.B. (1965). Dissolution and precipitation of silica at low temperature. Geochimica et Cosmochimica acta 10. pp. 1-26.

KRUMBEIN, W.C. and GARRELS,M. (1952). Origin and classification of chemical sediments in terms of pH and oxidation-reduction potentials. Jour. of Geol. 60, No. 1, pp. 1. 33.

La BERGE, G.L. (1964). Development of magnetite in Iron Formations of the Lake Superior region. Eco. Geol. 59, pp. 1313-1342.

La BERGE, G.L. (1967). Microfossils and Precambrian iron formations. Geol. Soc. Am. Bull. 78, pp. 331-342.

LANDIS, C.A. (1971). Graphitization of dispersed carbonaceous material in metamorphic rocks. Contr. Mineral Petro. 30, pp. 34-45.

LANGMYHR, F.J. (1968). Recent developments in the use of hydrofluoric acid as a decomposing agent for inorganic materials. Acta Geologica et Geographica Universitatis Comenianae Geologica 15, pp. 23-33.

LANGMYHR, F.J. and KRINGSTADT, K. (1966). An investigation of the precipitates formed by the decomposition of siliate rocks in 38-40% hydrofluoric acid. Anal. Chim. Acta. 35, pp. 131-135.

LEDUC, S. (1914). The mechanism of Life, New York, Rehman Co.

LEPP, H. and Goldisch, S.S. (1964). Origin of Precambrian iron formations. Eco. Feol. 59, pp. 1025-1060.

LEWIN, J.C. (1961). The dissolution of silica from diatom wells. Geochimica et cosmochimica acta. 21, pp. 182-198.

LIPSON, H. and STOCKES, A.R. (1942-43). The structure of graphite. Proc. Roy. Soc. Lond. Ser. A. pp. 101-105.

LOOMIS, F.W. (1920). Infra-red spectra of isotopes. Astrophys. J. 52. p. 248-256.

MACLEOD, W.D. (1968). Combined gas chromatography-mass spectrometry of complex hydrocarbon trace residues in sediments. J. Gas Chrom. 6, pp. 591-594.

MARCHAND, A., LIBERT, P.A. and COMBAZ, A. (1968). Physicochemical criteria of the diagenesis of kerogen. Compt Rend. Ser. D, 266 (25) pp. 2316-2319 (in French).

MARCHAND, A., LIBERT, P.A. and COMBAZ, A. (1969). Physicochemical characterization tests of the diagenesis of several biologically homogeneous organic rocks. Rev. Inst. Pet. Ann. Combust. Liquides 24(1), pp. 3-20 (in French).

MARSHALL, C.G.A., MAY, J.W. and PERRET, C.J. (1964). Fossil Microorganisms: Possible presence in Precambrian shield of Western Australia. Science. 144, pp. 290-292.

McINTYRE, D.J. (1972). Effect of experimental metamorphism on pollen in lignite. Geoscience and Man, 4, pp. 111-117.

McKIRDY, D.M., SUMARTOJO, J., TUCKER, D.H. and GOSTIN, V. (1975). Organic, minerological and magnetic indications of metamorphism in the Tapley Hill formation. Adelaide Geosyncline, Precambrian Research. 2. pp. 345-373.

MEINSCHEIN, W.G. (1967). Palaeobiochemistry - 1967. McGraw Hill Year book of Science and Technology. pp. 283-285.

MEINSCHEIN, W.G., BARGHOORN, E.S. and SCHOPF, J.W. (1964). Biological remnants in a Precambrian sediment. Science 145, pp. 262-263.

MOORE, E.S. and MAYNARD, J.E. (1929). Solution, transport and precipitation of iron and silica. Eco. Geol. 24, No. 3,4,5. p. 272-303, 365-402 and 506-621.

MUIR, M.D. and GRANT, P.R. (1976). Micropaleontological evidence from Onverwacht Group, South Africa. *In* "Early History of Earth" (ed.) B.F. Windley, Wiley/London.

MUIR, M.D., GRANT, P.R., BLISS, G.M., DIVER, W.L. and HALL, D.O. (1976). A discussion of biogenecity criteria in Geological context with examples from a very old greenstone Belt. A late Precambrian deformed zone, and tectonised Phanerozoic rock.

MUIR, M.D. and HALL, D.O. (1974). Diverse microfossils in the Precambrian Onverwacht group rocks of South Africa. Nature. 252, No. 5482, pp. 376-378.

MUIR, M.D., HAMILTON, L.H., GRANT, P.R. and SPICER, R.A. (1974). A comparative study of modern and fossil microbes using X-ray microanalysis and cathode luminescence *IN* Microprobe Analysis as applied to cells and tissues (eds.) Hall, T., Echlin, P. and Kaufmann, R. Acad. Press, London and New York, pp. 33-58.

MUIR, M.D., SPICER, R.A., GRANT, P.R. and GIDDENS, R. (1974). X-ray microanalysis in the SEM for the determination of elements in Modern and Fossil Microorganisms. 8th International Congress on Electron Microscopy, Canberra, 2, p. 104-105.

NAGY, L.A. (1974). Transvaal Stromatolite: First evidence for the diversification of cells about 2.2×10^9 years ago. Science 183. pp. 514-516.

NAGY, B. and NAGY, L.A. (1968). Investigation of the early Precambrian Onverwacht sedimentary rocks in South Africa. Proc. Int. Meeting Org. Geochem., Amsterdam, pp. 209-215.

NAGY, B. and NAGY, L.A. (1969). Early Precambrian Onverwacht microstructures possibly the oldest fossils on Earth. Nature (Lond.) 223, pp. 1226-1229.

NAGY, B., ZUMBERGE, J.E. and NAGY, L.A. (1975). Abiotic, graphitic microstructures in micaceous metaquartzite about 3760 million years old South-Western Greenland: Implications for early Precambrian Microfossils. Proc. Natl. Acad. Sci. U.S.A. 72, pp. 1206-1209.

NODA, T. (1969). Influence of different factors on graphitization in Aspects fondamentaux de la carbonisation et de la graphitization S. Chimie. Phys. et Physicochemie Biol., Special No. April, 1969, pp. 151-159.

NODA, T. and INEGAKI, M. (1964). Effect of gas phase on graphitization of carbon. 2, pp. 127-130.

NODA, T., INAGAKI, M., HIRANO, S. and ANANUMA, K. (1968). Effect of co-existing minerals on graphitization of carbon I. Heat treatment of carbon under 3 Kbar in the presence of limestone. Chem. Soc. Japan Bull. 41, pp. 1245-1248.

NODA, T., INAGAKI, M. and SEKIYA, T. (1965). Kinetic studies of graphitization process-I. Effect of Ambient gas phase on the rate of graphitization. Carbon 3, pp. 175-180.

NOONER, D.W. and ORO, J. (1967). Organic compounds in Meteorites, Geochimica et Cosmochimica acta. 31. pp. 1359-1394.

O'BERLIN, A., BOULMIER, J.L. and DURAND, B. (1973). Natural evolution (catagenesis) related to carbonization (as studied by High resolution electron microscopy, *IN* Advances in Organic Geochemistry. ed. by Tissot, B. and Bienner, F. Proceeding of the 6th International meeting on Organic Geochemistry Sept. 18-21, 1973. Rueil-Melmison, France.

OEHLER, D.Z., SCHOPF, J.W. and KVENVOLDEN, K.B. (1972). Carbon isotope

OFTEDAHL, C. (1958). A theory of exalative sedimentary ores. S. Geologiska, Foeningens I. Stockholm Forhandlinger. Bd. 80, H. 1, p. 1-19.

ORO', J. and NOONER, D.W. (1967). Aliphatic hydrocarbons in Precambrian rocks. Nature, 213, pp. 1082-1085.

ORO', J. and NOONER, D.W., ZLATKIS, A., WILKINSTROOM, S.A. and BARGHOORN, E.S. (1965). Hydrocarbons of Biological origin in sediments about two billion years old. Science. 148 (3666). pp. 777-779.

PACAULT, A. (1971). Kinetics of graphitization *IN* Walker, P.L. (ed.). Chemistry & Physics of Carbon. Marcel Dekker, New York, 7, pp. 107-154.

PALACAS, J.G. (1959). Geochemistry of Carbohydrates. Thesis of University of Minnesota, Minnepolis. 103 pp.

PERRAULT, G. (1955). Geology of Western margin of the Labrador trough. Unpubl. Ph.D. Thesis of the Univ. of Toronto, p. 302.

PERRY, E.C. (Jr.), TAN, F.C. and MORAY, G.B. (1973). Stable isotopes geochemistry of the Biwabik iron formation. Eco. Geol. 68, pp. 1110-25.

PHILIPI, G.T. (1957). Identification of oil source beds by chemical means: Section III Geologia del Petroleo: Congreso Geologico International XX Sesion, Ciudad de Mexico, 1956. pp. 25-38.

PHILLIPI, G.T. (1965). On the depth, time and mechanism of petroleum generation. Geochimica et cosmochimica acta. 29. pp. 1021-1049.

PIRIE, N.W. (1965). Discussion *in* S.W. Fox (editor). The origins of prebiological systems. Acad. Press, New York, N.Y. p. 33.

PUSEY III, E.W.C. (1973). Palaeotemperatures in the Gulf Coast using ESR-Kerogen method. Reprinted from Transactions-Gulf Coast Assoc. of Geologist societies. 33, pp. 195-202.

RANKAMA, K. (1948). A note on the original isotopic composition of terrestrial carbon. J. Geol. 56. pp. 199-209.

RANKAMA, K. (1954). The isotopic constitution of carbon in ancient rocks as indicator of its biogenic or non-biogenic origin. Geochimica et Cosmochimica. Acta 5. p. 142.

RETCOFSKY, H.L. and FRIEDEL, R.A. (1968). Room temperature proton magnetic relaxation times in bituminous coal. Fuel. 47, pp. 391-395.

RETCOFSKY, H.L., STARK, J.M. and FRIEDEL, R.A. (1968). Electron Spin resonance in American coals. Anal. Chem. 40, pp. 1699-1704.

REX, R.W. (1960). Electron paramagnetic resonance studies of stable free radicals in lignins and humic acids. Nature. 188, pp. 1185-1186.

RICHARD, D.T. (1970). The Origin of Framboids. Lithos. 3, pp. 269-293.

RICHARDS,,B.P. (1970). Relationship between interlayer spacing, stacking order and crystallinity in carbon materials. J. Appl. Crystallogr. 1, pp. 35-48.

ROBINSON, W.G. (1969). Isolation procedures for kerogens and associated soluble organic materials. *IN* Eglington & Murphy (ed.) Organic Geochemistry. Springer-Varlaj, Berlin-Heidelberg, New York, pp. 181-195.

ROSCOE, S.M. (1969). Huronian Rocks and Uraniferrous conglomerate in the Canadian Shields. Geo. Sur. Canada Paper 68-40, 205 p.

RULAND, W. (1968). X-ray diffraction studies on carbon and graphite. *IN* Chemistry and Physics of carbon, Vol. 4. (ed. P.L. Waller, Jr.) Marcel and Dekker: New York.

RUTTER, E.H. (1970). An experimental study of the factors affecting the rheological properties of rocks in simulated geological environments. Unpubl. thesis submitted for D.I.C. Imperial College, Sept. 1970.

SAKAMOTO, T. (1950). The origin of the Precambrian banded iron ores. Am. Jour. Sci. 248, pp. 449-474.

SALOTTI, C.A., HEINRICH, E., Wm., and GIARDINI, A.A. (1971). Abiotic carbon and the formation of graphitic deposits. Eco. Geol. 66, pp. 929-932.

SAXBY, J.D. (1970). Isolation of kerogen in sediments by chemical methods. Chem. Geol. 6, No. 3, pp. 173-184.

SCHERRER, P. (1918). Gotlinger Nachsichten. 2. p. 98.

SCHOPF, J.M. (1975). Modes of fossil preservation. Review Palaeobotany & Palynol., 20, pp. 27-53.

SCHOPF, J.W. (1968). Microflora of the Bitter Springs Formation, Late Precambrian, central Australia. J. Paleonto. 42. pp. 651-88.

SCHOPF, J.W. (1975). Precambrian Palaeobiology: Problems and perspectives reprint from Ann. Rev. of Earth and Planetary Sciences. 3. pp. 213-249.

SCHOPF, J.W. and BARGHOORN, E.S. (1967). Algalike fossils from the Early Precambrian of South Africa. Science, 156, No. 3774, pp. 508-512.

SENGUPTA, S. (1975). Experimental alterations of spores of Lycopodium Clavatum as related to diagenesis. Review of Palaeobotany and Palynology. 19. pp. 173-192.

SILVERMAN, J.R. (1964). *IN* H. Craig (Editor) Isotopic and Cosmic Chemistry. North Holland, Amsterdam.

SMITH, R.E. (1975). Metamorphism of the Protorozoic Fortescue Group Western Australia - A reconnaissance study. Pt. 2 of a conceptional approach to mineralization potential of the Fortesque Group. C.S.I.R.O., Div. of Minerology Reprint No. FP9.

STAPLIN, F.L. (1969). Sedimentary organic matter, organic metamorphism, and oil and gas occurrence. Bull. Can. Pet. Geol.; 17, No. 1. pp. 47-66.

STAPLIN, F.L., BAILEY, N.J.L., POCOCK, S.A.J. and EVANS, C.R.(1973). Diagenesis and metamorphism of sedimentary organic matter. A.A.P.G. Symposium-1973.

STEWARD, E.G. and COOK, B.P. (1960). Graphitization in oriented carbons. Zeitschr. Kristalogr. 114, pp. 245-245.

SUNAGAWA, I, ENDO, Y. and NAKAI, W. (1971). Hydrothermal synthesis of framboidal pyrite. Soc. Mining Geologists, Japan, Spec. issue 2, pp. 10-14.

SURDAM, R.C., EUGSTER, H.P. and MARINER, R.H. (1972). Magadi type chert in Jurassic and Eocene to Pleistocene rocks, Wyoming. Geol. Soc. Am. Bull. 83, pp. 2261-2266.

SWEENEY, R.E. and KAPLAN, I.R. (1973). Pyrite framboidal formation. Laboratory synthesis and marine sediments. Eco. Geol. 68, pp. 618-634.

TANAKA, M. (1953). Etude Chimique sur le matabolisme mineral dan les lacs. Jour. Earth Sci. Nagoya Univ. 1. pp. 119-134.

TEICHMULLER, M. and TEICHMULLER, R. (1966). Geological causes of coalification. *IN:* R.F. GOULD (editor), Coal, Science, A in Chemistry, 55, Am. Chem. Soc., Washington, D.C. pp. 133-155.

TEICHMULLER, M. and TEICHMULLER, R. (1968). Geological Aspects of coal metamorphism *IN* Murchison, D. and Westall, T.S. (editors) Coal and Coal bearing strata, New York, Elsevier, pp. 233-267.

THENIUS, E. (1973). Fossils and the Life of the Past. Heidelberg Science Library. 14. The English Universities Press Ltd., London, Springer-Verlag, New York, Heidelberg, Berlin, p. 194.

TISSET, B.B., DURAND, J. ESPITALIE, and COMBAZ, A. (1974). Influence of nature and diagenesis of organic matter in formation of petroleum. A.A.P.G. Bull. 58, pp. 499-506.

TRENDALL, A.F. (1965). Progress Report in Brockman Iron Formation in Wittenoom-Yampire area. Rec. W. Aust. Geol. Sur. Annual Report for 1965, pp. 75-87.

TRENDALL, A.F. (1970). Iron formations of the Hamersley Group of W. Australia, type examples of Varved Precambrian Evaporites. Unesco (1973). Genesis of Precambrian and manganese deposits. Proc. Kiev. Symp. 1970 (Earth Science, 9).

TRENDALL, A.F. and BLOCKLEY, J.G. (1970). The Iron Formation of the Precambrian Hamersley Group, W. Australia. W. Aust. Geol. Sur. Bull. 119, 366p.

TURNER, F.S and VERHOOGEN, J. (1960). Igneous and Metamorphic Petrology (2nd. ed.). McGraw Hill Book Company, New York 694p.

TYLER, S.A. and TWENHOFEL, W.H. (1952). Sedimentation and Stratigraphy of Huronian of Upper Michigan. Am. Jour. Sci. 250, p. 1-27, 118-151.

TYLER, S.A. and BARGHOORN, E.S. (1954). Occurrence of structurally preserved plants in Precambrian rocks of the Canadian Shield. Science 119, pp. 608-8.

UBBELOHDE, A.R. and LEWIS, F.A. (1960). Graphite and its crystal components. Clarendon, Oxford.

UEBERSFELD, J., ETIENNE, A. and COMBRISSON, J. (1954). Paramagnetic resonance, a new property of coal-like material. Nature 174, p. 614.

VALLENTYNE, J.R. (1957). Thermal degradation of amino-acids. Carnegie Inst. Year Book, 56, pp. 185-186.

van HISE and LEITH, C.K. (1911). Geology of Lake Superior Region. U.S. Geol. Sur. Mem. 52, 641p.

van KREVELEN, D.W. (1961). Coal: Topology, Chemistry, Physics and constitution. Elsevier, New York.

VILJOEN, M.S., VILJOEN, R.P. (1969a). In African Magnetism and tectonics (ed.) by T.N. Clifford & I. Gass. Oliver & Boyd.

VILJOEN, M.S., VILJOEN, R.P. (1969b). The Geology of Barberton area. S. African Geol. Sur. Bull. Spec. Pub. No. 15.

VISSER, D.J.L. (compiler (1956). The Geology of Barberton area. S. African Geol. Sur. Bull. Spec. Pub. No. 15

WALKER, P.L. (1962). Carbon - an old but new material. Am. Scientist, 50, pp. 259-293.

WALPOLE, B.P., CROHN, P.W., DUNN, P.R. and RANDALL, M.A. (1968). Geology of the Katerine-Darwin Region, Norther Territory, Bur. Min. Resource, Aust. Bul. 82.

WALTER, M.R. (1972). A hot spring analog for the depositional Environment of Precambrian iron formation of Lake Superior. Eco. Geol. 67, 965-980.

WALTER, M.R. (1975). Abstr. First. Australian Geol. Convention, Proterozoic Geology, Adelaid. pp. 15-16.

WEEKS, L.G. (1958). Habitat of Oil and factors that control it. *IN* L.G. Weeks. (ed.) Habitat of Oil. Am. Ass. Pet. Geol. Tulsa, Okla p. 1-61.

WILSON, H.D.B., ANDREWS, P., MOXHAM, R.L. and RAMLAL, K. (1965). Archaean volcanism in Canadian Shield. Can. J. Earth Sci. 2, pp. 161-175.

WILEY, J.F. (1963). *IN* Chemistry of coal utilization. Supplementary Volume (ed.) Lowry, H., Wiley, H.

WOOLNOUGH, W.G. (1941). Origin of banded deposits - a suggestion. Eco. Geol. 36, p. 465.

WRIGHT, F.E. and ALLEN, E.T. (1970). Curtisite: A new organic mineral from Skaggs Springs, Sonoma County, California. Am. Mineral. 15, pp. 169-173.

YEN, T.F. (1972). Terrestrial and extra-terrestrial stable organic molecules. *IN* Landel, R.F. and Rembaum, A. (editors). Chemistry in Space Research. Elsevier. pp. 105-153.

ZOBELL, C.E. (1955). Occurrence and activity of bacteria in marine sediments p. 416-427. *IN* Trask, P.D. (ed.). Recent marine sediments. Soc. Eco. Palaeontologists & Minerologists, Sp. Publ. No. 4. 736 p.

